University of Strathclyde
Department of Naval Architecture, Ocean and Marine Engineering

Development of Automatic Time-Domain Simulation Programme of Berthing Operation of Ships

by

Kwang Sic Chung

A thesis presented in fulfilment of the requirements for the degree of Doctor of Philosophy

2023

Signed: *Date:*

Dedicated to my father, Won Tag Chung, and my mother, Shindeuk Kang

For their love and support

Abstract

As the world trade has increased significantly over the past 50 years, safe and effective management of harbour system is becoming an important issue. In particular, due to the increased complexity of harbour environment with various harbour facilities, berthing operation of ships takes much time and requires various technical supports from harbour masters, pilots and engineers. In this point of view, precise prediction and practice of berthing operation are required and development of automatic simulation tool is requested for planning and managing effective harbour system.

In this study, a novel methodology to control the heading angle and the speed of ships on the simulation of berthing operation is presented. Particularly under the low advance speed of a ship, the simulation of ship movement and the application of mathematical models are challengeable objectives in the current research field. Through this study, the development of two different time-domain simulation programs using the PD (Proportional Derivative) control and the MPC (Model Predictive Control) is performed with two different mathematical models which are the normal MMG model and Kose's model. Furthermore, the model simulation is performed and the result is compared with previous works in different berthing conditions. With various cases of simulation result, the statistical analysis is performed for defining the initial environment of efficient berthing operation. This study is expected to provide an efficient time-domain simulation tool to harbour designers for planning and managing a harbour system cost-effectively and an opportunity to harbour masters and pilots for practicing and understanding the berthing operation in various harbour situations.

To increase the accuracy on prediction of ship berthing operation, it is needed to analyse ship movement, in particular, with low advance speed and to develop an effective algorithm and controller for simulating the berthing operation accordingly.

Acknowledgements

Above all, I would like to express my deepest gratitude to my supervisor, Dr Zhiming Yuan, for his invaluable patience and feedback. I am also deeply indebted to Professor Mehmet Atlar and the examining committee, Professor Noriyuki Sasaki, Dr Zafer Ayaz and Professor Evangelos Boulougouris, who generously provided knowledge and expertise. Furthermore, words cannot express my gratitude to Professor Byung-Suh Kang of Kyung Hee University and Dr Jakub Cichowicz of DNV for their invaluable advice. Also, I could not have undertaken this journey without Professor Chul Hee Jo and Professor Kisung Kim of Inha University who guided me to the PhD study. I am also extremely grateful to Dr Choong Heum Park, the former CEO of Samsung Engineering for his encouragement. Additionally, I would like to express my deepest appreciation to Blue Korea Innovation Ltd. for the generous support.

I am also grateful to Professor Iraklis Lazakis and Professor Chengi Kuo for their encouragement and to Dr B. S. Lee, Professor Shan Huang, Professor Dimitrios Konovessis, Professor Atilla Incecik, Dr Panagiotis Kaklis and Dr Byoungug Jeong for their support. Thanks should also go to the administrative staffs, Mrs Susan Pawson, Miss Lynne Samson, Mr Stephen Gallagher, Mrs Fiona MacKie and Mr Alex Watterson, for their assistance and special thanks to Mrs Thelma Will. I would also like to acknowledge Professor Young-Sub Kwon of Chosun University and Professor Seung-Keon Lee and Professor Sun-Hong Kwon of Pusan National University for their support. Furthermore, I am thankful to my friends, Dr Neil Harper and Miss Alison Thompson, for their encouragement and to Edward Lobb, Honorary Associate Minister of the Tron Church, and his wife, Catherine Lobb, for their generous support.

Lastly, this endeavour would not have been possible without my father, Won Tag Chung, my mother, Shindeuk Kang, my brother, Eunsic Chung, my sister-in-law, Sookjin Kim, and my nephews, Daehyun Chung and Kyuhyun Chung. Also, I would like to extend my sincere thanks to Miss Minjung Sohn for her encouragement and support.

Table of Contents

Abstract iii
Acknowledgements iv
Table of Contents v
List of Figures vii
List of Tables xxi
1. Introduction 1
1.1 Preamble 1
1.2 Background and Motivation 1
1.3 Research Aim and Objectives 2
1.4 Structure of the Thesis 2
2. Critical Review 4
2.1 Preamble 4
2.2 Berthing Operation 4
2.3 Shallow Water Manoeuvring 8
2.4 Manoeuvring Control 9
2.5 Summary 19
2.6 Research Gaps and Challenges 20
3. Mathematical Model of Ship Berthing Manoeuvre 21
3.1 Preamble 21
3.2 Outline of the Approach 22
3.3 Modelling of Berthing Operation 23
3.4 Coordinate System and Motion Equation 24
3.5 Hull 25
3.6 Propeller 26
3.7 Rudder 27
3.8 Manoeuvring Equation of Low Advance Speed 28
3.9 PD Control Algorithm 29
3.10 Model Predictive Control (MPC) 30
3.11 Kose’s Mathematical Model in Model Predictive Control 30
4. Methodology 33
4.1 Preamble 33
4.2 Initial Simulation Programme 34
4.2.1 Comparison of Numerical and Analytical Solutions 34

4.2.2 Ship Turning Circle 35
4.3 Experimental Design of Simulation Programme Using PD Controller 37
4.3.1 The Scheme of Simulation 37
4.3.2 Design of the Numerical Experiments 40
4.3.3 Hypotheses Test 41
4.4 Comparison of PD and ANN Controllers 41
4.5 Simulation using Model Predictive Control 42
4.6 Closure 42
5. Time-Domain Simulations of Ship Berthing Operation 43
5.1 Preamble 43
5.2 Berthing Simulation using Proportional Derivative (PD) Control 44
5.2.1 Application of Kose's Mathematical Model 46
5.2.2 Application of MMG Model 58
5.2.3 Comparative Analysis for Kose's Model and MMG Model 70
5.3 Comparative Analysis for Proportional Derivative (PD) Control and Artificial Neural Network (ANN) 82
5.4 Statistical Analysis 84
5.4.1 Simulation Time 550 seconds 84
5.4.2 Simulation Time 650 seconds 86
5.5 Berthing Simulation using Model Predictive Control 89
5.6 Closure 93
6. Discussion 94
6.1 Preamble 94
6.2 Own Contribution 94
6.3 Recommendations for Further Research 95
6.4 Closure 96
7. Conclusion 97
8. References 98
A. Appendix. Simulation Result 103
A.1 Application of Kose's Mathematical Model 103
A.2 Application of MMG Model 122
A.3 Comparative Analysis for Kose's Model and MMG Model 141
A.4 Comparative Analysis for Proportional Derivative (PD) Control and Artificial Neural Network (ANN) 155
A.5 Berthing Simulation using Model Predictive Control 159

List of Figures

Figure 3.1 Coordinate system 24

Figure 3.2 PD control algorithm 29

Figure 4.1 Harmonic vibration of 1 DOF (a) Analytical result (time step: 0.3 seconds) (b) Numerical result (ode 45, time step: default) (c) Numerical result (oderk, time step 0.3 seconds).. 35

Figure 4.2 Trajectory of ship turning circle 36

Figure 4.3 Yaw rate and speed for Mariner class vessel.. 36

Figure 4.4 Berthing simulation with 20 random cases of initial heading angle of ship (range of heading angle from -180 to +180 degrees, simulation time 550 seconds, initial position of ship (-3L, 5L), initial speed of ship 3 m/s, model ship: tanker, Kose's model)... 38

Figure 5.1 Trajectory for berthing simulation of tanker ship using PD controller with Kose's mathematical model: initial posision of ship (-5L, 4L), initial heading angle of ship -40 degrees and initial speed of ship 3 m/s... 46

Figure 5.2 RPS and δr for berthing simulation of tanker ship using PD controller with Kose’s mathematical model: initial position of ship (-5L, 4L), initial heading angle of ship -40 degrees and initial speed of ship 3 m/s... 47

Figure 5.3 Heading angle ψ for berthing simulation of tanker ship using PD controller with Kose’s mathematical model: initial position of ship (-5L, 4L), initial heading angle of ship -40 degrees and initial speed of ship 3 m/s............................ 48

Figure 5.4 X and Y variation for berthing simulation of tanker ship using PD controller with Kose’s mathematical model: initial position of ship (-5L, 4L), initial heading angle of ship -40 degrees and initial speed of ship 3 m/s............................ 49

Figure 5.5 Trajectory for berthing simulation of tanker ship using PD controller with Kose's mathematical model: initial posision of ship (-5L, 4L), initial heading angle of ship -40 degrees and initial speed of ship 4 m/s... 50

Figure 5.6 RPS and δr for berthing simulation of tanker ship using PD controller with Kose’s mathematical model: initial position of ship (-5L, 4L), initial heading angle of ship -40 degrees and initial speed of ship 4 m/s... 51

Figure 5.7 Heading angle ψ for berthing simulation of tanker ship using PD controller with Kose’s mathematical model: initial position of ship (-5L, 4L), initial heading angle of ship -40 degrees and initial speed of ship 4 m/s............................ 52

Figure 5.8 X and Y variation for berthing simulation of tanker ship using PD controller with Kose’s mathematical model: initial position of ship (-5L, 4L), initial heading angle of ship -40 degrees and initial speed of ship 4 m/s............................ 53

Figure 5.9 Trajectory for berthing simulation of tanker ship using PD controller with Kose's mathematical model: initial posision of ship (-5L, 4L), initial heading angle of ship -40 degrees, initial speed of ship 4 m/s, rudder height 15 m and rudder area 131.66 m^2 54

Figure 5.10 RPS and δr for berthing simulation of tanker ship using PD controller with Kose's mathematical model: initial position of ship (-5L, 4L), initial heading angle of ship -40 degrees, initial speed of ship 4 m/s, rudder height 15 m and rudder area 131.66 m^2........ 55

Figure 5.11 Heading ψ for berthing simulation of tanker ship using PD controller with Kose's mathematical model: initial position of ship (-5L, 4L), initial heading angle of ship -40 degrees, initial speed of ship 4 m/s, rudder height 15 m and rudder area 131.66 m^2........ 56

Figure 5.12 XY for berthing simulation of tanker ship using PD controller with Kose's mathematical model: initial position of ship (-5L, 4L), initial heading angle of ship -40 degrees, initial speed of ship 4 m/s, rudder height 15 m and rudder area 131.66 m^2 57

Figure 5.13 Trajectory for berthing simulation of tanker ship using PD controller with normal MMG model: initial position of ship (-5L, 4L), initial heading angle of ship -40 degrees and initial speed of ship 3 m/s........ 58

Figure 5.14 RPS and δr for berthing simulation of tanker ship using PD controller with normal MMG model: initial position of ship (-5L, 4L), initial heading angle of ship -40 degrees and initial speed of ship 3 m/s........ 59

Figure 5.15 Heading angle ψ for berthing simulation of tanker ship using PD controller with normal MMG model: initial position of ship (-5L, 4L), initial heading angle of ship -40 degrees and initial speed of ship 3 m/s........ 60

Figure 5.16 X, Y variation for berthing simulation of tanker ship using PD controller with normal MMG model: initial position of ship (-5L, 4L), initial heading angle of ship -40 degrees and initial speed of ship 3 m/s........ 61

Figure 5.17 Trajectory for berthing simulation of tanker ship using PD controller with normal MMG model: initial position of ship (-5L, 4L), initial heading angle of ship -40 degrees and initial speed of ship 4 m/s........ 62

Figure 5.18 RPS and δr for berthing simulation of tanker ship using PD controller with normal MMG model: initial position of ship (-5L, 4L), initial heading angle of ship -40 degrees and initial speed of ship 4 m/s........ 63

Figure 5.19 Heading angle ψ for berthing simulation of tanker ship using PD controller with normal MMG model: initial position of ship (-5L, 4L), initial heading angle of ship -40 degrees and initial speed of ship 4 m/s........ 64

Figure 5.20 X, Y variation for berthing simulation of tanker ship using PD controller with normal MMG model: initial position of ship (-5L, 4L), initial heading angle of ship -40 degrees and initial speed of ship 4 m/s........ 65

Figure 5.21 Trajectory for berthing simulation of tanker ship using PD controller with normal MMG model: initial posision of ship (-5L, 4L), initial heading angle of ship -40 degrees, initial speed of ship 4 m/s, rudder height 15 m and rudder area 131.66 m^2 66

Figure 5.22 RPS and δr for berthing simulation of tanker ship using PD controller with normal MMG model: initial position of ship (-5L, 4L), initial heading angle of ship -40 degrees, initial speed of ship 4 m/s, rudder height 15 m and rudder area 131.66 m^2 67

Figure 5.23 Heading ψ for berthing simulation of tanker ship using PD controller with normal MMG model: initial position of ship (-5L, 4L), initial heading angle of ship -40 degrees, initial speed of ship 4 m/s, rudder height 15 m and rudder area 131.66 m^2 68

Figure 5.24 XY for berthing simulation of tanker ship using PD controller with normal MMG model: initial position of ship (-5L, 4L), initial heading angle of ship -40 degrees, initial speed of ship 4 m/s, rudder height 15 m and rudder area 131.66 m^2 69

Figure 5.25 Trajectory for berthing simulation of tanker ship using PD controller with (a) Kose's mathematical model and (b) normal MMG model: initial position of ship (-5L, 4L), initial heading angle of ship -40 degrees and initial speed of ship 3 m/s 70

Figure 5.26 RPS and δr for berthing simulation of tanker ship using PD controller with (a) Kose's mathematical model and (b) normal MMG model: initial position of ship (-5L, 4L), initial heading angle of ship -40 degrees and initial speed of ship 3 m/s 71

Figure 5.27 Heading angle ψ for berthing simulation of tanker ship using PD controller with (a) Kose's mathematical model and (b) normal MMG model: initial position of ship (-5L, 4L), initial heading angle of ship -40 degrees and initial speed of ship 3 m/s 71

Figure 5.28 X and Y variation for berthing simulation of tanker ship using PD controller with (a) Kose's mathematical model and (b) normal MMG model: initial position of ship (-5L, 4L), initial heading angle of ship -40 degrees and initial speed of ship 3 m/s 72

Figure 5.29 Trajectory for berthing simulation of tanker ship using PD controller with (a) Kose's mathematical model and (b) normal MMG model: initial position of ship (-5L, 4L), initial heading angle of ship -40 degrees and initial speed of ship 4 m/s 74

Figure 5.30 RPS and δr for berthing simulation of tanker ship using PD controller with (a) Kose's mathematical model and (b) normal MMG model: initial position of ship (-5L, 4L), initial heading angle of ship -40 degrees and initial speed of ship 4 m/s 75

Figure 5.31 Heading angle ψ for berthing simulation of tanker ship using PD controller with (a) Kose's mathematical model and (b) normal MMG model: initial position of ship (-5L, 4L), initial heading angle of ship -40 degrees and initial speed of ship 4 m/s 75

Figure 5.32 X and Y variation for berthing simulation of tanker ship using PD controller with (a) Kose's mathematical model and (b) normal MMG model: initial position of ship (-5L, 4L), initial heading angle of ship -40 degrees and initial speed of ship 4 m/s 76

Figure 5.33 Trajectory for simulation of tanker ship using PD controller with (a) Kose's model and (b) MMG: initial position of ship (-5L, 4L), initial heading angle of ship -40 degrees, initial speed of ship 4 m/s, rudder height 15 m and rudder area 131.66 m^2 77

Figure 5.34 RPS and δr for simulation of tanker ship using PD controller with (a) Kose's model and (b) MMG: initial position of ship (-5L, 4L), initial heading angle of ship -40 degrees, initial speed of ship 4 m/s, rudder height 15 m and rudder area 131.66 m^2 78

Figure 5.35 Heading ψ for simulation of tanker ship using PD controller with (a) Kose's model and (b) MMG: initial position of ship (-5L, 4L), initial heading angle of ship -40 degrees, initial speed of ship 4 m/s, rudder height 15 m and rudder area 131.66 m^2 78

Figure 5.36 XY for simulation of tanker ship using PD controller with (a) Kose's model and (b) MMG: initial position of ship (-5L, 4L), initial heading angle of ship -40 degrees, initial speed of ship 4 m/s, rudder height 15 m and rudder area 131.66 m^2 79

Figure 5.37 RPS and δr for simulation of tanker ship, PD controller with Kose's model (a) h 12.94 m, A_r 98 m^2 (b) h 15 m, A_r 131.66 m^2: initial position of ship (-5L, 4L), initial heading angle of ship -40 degrees, initial speed of ship 4 m/s........ 80

Figure 5.38 RPS and δr for simulation of tanker ship, PD controller with MMG (a) h 12.94 m, A_r 98 m^2 (b) h 15 m, A_r 131.66 m^2: initial position of ship (-5L, 4L), initial heading angle of ship -40 degrees, initial speed of ship 4 m/s........ 81

Figure 5.39 Trajectory for berthing simulation of tanker ship using (a) PD controller and (b) ANN controller (Hasegawa and Kitera, 1993) with Kose's mathematical model: initial position of ship (-5L, 4L), initial heading angle -40 degrees and initial speed 3 m/s 82

Figure 5.40 RPS and δr for berthing simulation of tanker ship using (a) PD controller and (b) ANN controller (Hasegawa and Kitera, 1993) with Kose's mathematical model: initial position of ship (-5L, 4L), initial heading angle -40 degrees and initial speed 3 m/s 83

Figure 5.41 Trajectory for berthing simulation of tanker ship using MPC with Kose's mathematical model: initial position of ship (-5L, 4L), initial heading angle of ship -40 degrees and initial speed of ship 3 m/s........ 89

Figure 5.42 X position XG, Y position YG, heading angle psi, surge velocity u, sway velocity v and yaw rate r for berthing simulation of tanker using MPC with Kose's model: initial position of ship (-5L, 4L), initial heading angle -40 degrees and initial speed 3 m/s 90

Figure 5.43 Actual and optimal trajectories for berthing simulation of tanker ship using MPC with Kose’s mathematical model: initial position of ship (-5L, 4L), initial heading angle of ship -40 degrees and initial speed of ship 3 m/s 91

Figure 5.44 Diagram for berthing simulation of tanker ship using MPC with Kose’s mathematical model: initial position of ship (-5L, 4L), initial heading angle of ship -40 degrees and initial speed of ship 3 m/s 92

Figure A.1 Yaw rate r for berthing simulation of tanker ship using PD controller with Kose’s mathematical model: initial position of ship (-5L, 4L), initial heading angle of ship -40 degrees and initial speed of ship 3 m/s 103

Figure A.2 Surge (u) and sway (v) velocity for berthing simulation of tanker ship using PD controller with Kose’s mathematical model: initial position of ship (-5L, 4L), initial heading angle of ship -40 degrees and initial speed of ship 3 m/s 104

Figure A.3 Trajectory for berthing simulation of tanker ship using PD controller with Kose’s mathematical model: initial position of ship (-5L, 4L), initial heading angle of ship -70 degrees and initial speed of ship 3 m/s 105

Figure A.4 RPS and δr for berthing simulation of tanker ship using PD controller with Kose’s mathematical model: initial position of ship (-5L, 4L), initial heading angle of ship -70 degrees and initial speed of ship 3 m/s 105

Figure A.5 Heading angle ψ for berthing simulation of tanker ship using PD controller with Kose’s mathematical model: initial position of ship (-5L, 4L), initial heading angle of ship -70 degrees and initial speed of ship 3 m/s 106

Figure A.6 Yaw rate r for berthing simulation of tanker ship using PD controller with Kose’s mathematical model: initial position of ship (-5L, 4L), initial heading angle of ship -70 degrees and initial speed of ship 3 m/s 106

Figure A.7 Surge (u) and sway (v) velocity for berthing simulation of tanker ship using PD controller with Kose’s mathematical model: initial position of ship (-5L, 4L), initial heading angle of ship -70 degrees and initial speed of ship 3 m/s 107

Figure A.8 X, Y variation for berthing simulation of tanker ship using PD controller with Kose’s mathematical model: initial position of ship (-5L, 4L), initial heading angle of ship -70 degrees and initial speed of ship 3 m/s 107

Figure A.9 Trajectory for berthing simulation of tanker ship using PD controller with Kose’s mathematical model: initial position of ship (-5L, 3L), initial heading angle of ship -40 degrees and initial speed of ship 3 m/s 108

Figure A.10 RPS and δr for berthing simulation of tanker ship using PD controller with Kose’s mathematical model: initial position of ship (-5L, 3L), initial heading angle of ship -40 degrees and initial speed of ship 3 m/s 108

Figure A.11 Heading angle ψ for berthing simulation of tanker ship using PD controller with Kose's mathematical model: initial position of ship (-5L, 3L), initial heading angle of ship -40 degrees and initial speed of ship 3 m/s 109

Figure A.12 Yaw rate r for berthing simulation of tanker ship using PD controller with Kose's mathematical model: initial position of ship (-5L, 3L), initial heading angle of ship -40 degrees and initial speed of ship 3 m/s.. 109

Figure A.13 Surge (u) and sway (v) velocity for berthing simulation of tanker ship using PD controller with Kose's mathematical model: initial position of ship (-5L, 3L), initial heading angle of ship -40 degrees and initial speed of ship 3 m/s......... 110

Figure A.14 X, Y variation for berthing simulation of tanker ship using PD controller with Kose's mathematical model: initial position of ship (-5L, 3L), initial heading angle of ship -40 degrees and initial speed of ship 3 m/s.. 110

Figure A.15 Trajectory for berthing simulation of tanker ship using PD controller with Kose's mathematical model: initial position of ship (-6L, 2L), initial heading angle of ship -30 degrees and initial speed of ship 3 m/s.. 111

Figure A.16 RPS and δr for berthing simulation of tanker ship using PD controller with Kose's mathematical model: initial position of ship (-6L, 2L), initial heading angle of ship -30 degrees and initial speed of ship 3 m/s.. 111

Figure A.17 Heading angle ψ for berthing simulation of tanker ship using PD controller with Kose's mathematical model: initial position of ship (-6L, 2L), initial heading angle of ship -30 degrees and initial speed of ship 3 m/s 112

Figure A.18 Yaw rate r for berthing simulation of tanker ship using PD controller with Kose's mathematical model: initial position of ship (-6L, 2L), initial heading angle of ship -30 degrees and initial speed of ship 3 m/s.. 112

Figure A.19 Surge (u) and sway (v) velocity for berthing simulation of tanker ship using PD controller with Kose's mathematical model: initial position of ship (-6L, 2L), initial heading angle of ship -30 degrees and initial speed of ship 3 m/s......... 113

Figure A.20 X, Y variation for berthing simulation of tanker ship using PD controller with Kose's mathematical model: initial position of ship (-6L, 2L), initial heading angle of ship -30 degrees and initial speed of ship 3 m/s.. 113

Figure A.21 Yaw rate r for berthing simulation of tanker ship using PD controller with Kose's mathematical model: initial position of ship (-5L, 4L), initial heading angle of ship -40 degrees and initial speed of ship 4 m/s.. 114

Figure A.22 Surge (u) and sway (v) velocity for berthing simulation of tanker ship using PD controller with Kose's mathematical model: initial position of ship (-5L, 4L), initial heading angle of ship -40 degrees and initial speed of ship 4 m/s......... 115

Figure A.23 Trajectory for berthing simulation of tanker ship using PD controller with Kose's mathematical model: initial position of ship (-5L, 4L), initial heading angle of ship -70 degrees and initial speed of ship 4 m/s.. 116

Figure A.24 RPS and δr for berthing simulation of tanker ship using PD controller with Kose's mathematical model: initial position of ship (-5L, 4L), initial heading angle of ship -70 degrees and initial speed of ship 4 m/s.. 116

Figure A.25 Heading angle ψ for berthing simulation of tanker ship using PD controller with Kose's mathematical model: initial position of ship (-5L, 4L), initial heading angle of ship -70 degrees and initial speed of ship 4 m/s........................... 117

Figure A.26 Yaw rate r for berthing simulation of tanker ship using PD controller with Kose's mathematical model: initial position of ship (-5L, 4L), initial heading angle of ship -70 degrees and initial speed of ship 4 m/s.. 117

Figure A.27 Surge (u) and sway (v) velocity for berthing simulation of tanker ship using PD controller with Kose's mathematical model: initial position of ship (-5L, 4L), initial heading angle of ship -70 degrees and initial speed of ship 4 m/s......... 118

Figure A.28 X, Y variation for berthing simulation of tanker ship using PD controller with Kose's mathematical model: initial position of ship (-5L, 4L), initial heading angle of ship -70 degrees and initial speed of ship 4 m/s.. 118

Figure A.29 Trajectory for berthing simulation of tanker ship using PD controller with Kose's mathematical model: initial position of ship (-5L, 3L), initial heading angle of ship -40 degrees and initial speed of ship 4 m/s.. 119

Figure A.30 RPS and δr for berthing simulation of tanker ship using PD controller with Kose's mathematical model: initial position of ship (-5L, 3L), initial heading angle of ship -40 degrees and initial speed of ship 4 m/s.. 119

Figure A.31 Heading angle ψ for berthing simulation of tanker ship using PD controller with Kose's mathematical model: initial position of ship (-5L, 3L), initial heading angle of ship -40 degrees and initial speed of ship 4 m/s........................... 120

Figure A.32 Yaw rate r for berthing simulation of tanker ship using PD controller with Kose's mathematical model: initial position of ship (-5L, 3L), initial heading angle of ship -40 degrees and initial speed of ship 4 m/s.. 120

Figure A.33 Surge (u) and sway (v) velocity for berthing simulation of tanker ship using PD controller with Kose's mathematical model: initial position of ship (-5L, 3L), initial heading angle of ship -40 degrees and initial speed of ship 4 m/s......... 121

Figure A.34 X, Y variation for berthing simulation of tanker ship using PD controller with Kose's mathematical model: initial position of ship (-5L, 3L), initial heading angle of ship -40 degrees and initial speed of ship 4 m/s.. 121

Figure A.35 Yaw rate r for berthing simulation of tanker ship using PD controller with normal MMG model: initial position of ship (-5L, 4L), initial heading angle of ship -40 degrees and initial speed of ship 3 m/s.. 122

Figure A.36 Surge (u) and sway (v) velocity for berthing simulation of tanker ship using PD controller with normal MMG model: initial position of ship (-5L, 4L), initial heading angle of ship -40 degrees and initial speed of ship 3 m/s................. 123

Figure A.37 Trajectory for berthing simulation of tanker ship using PD controller with normal MMG model: initial position of ship (-5L, 4L), initial heading angle of ship -70 degrees and initial speed of ship 3 m/s.. 124

Figure A.38 RPS and δr for berthing simulation of tanker ship using PD controller with normal MMG model: initial position of ship (-5L, 4L), initial heading angle of ship -70 degrees and initial speed of ship 3 m/s.. 124

Figure A.39 Heading angle ψ for berthing simulation of tanker ship using PD controller with normal MMG model: initial position of ship (-5L, 4L), initial heading angle of ship -70 degrees and initial speed of ship 3 m/s.. 125

Figure A.40 Yaw rate r for berthing simulation of tanker ship using PD controller with normal MMG model: initial position of ship (-5L, 4L), initial heading angle of ship -70 degrees and initial speed of ship 3 m/s.. 125

Figure A.41 Surge (u) and sway (v) velocity for berthing simulation of tanker ship using PD controller with normal MMG model: initial position of ship (-5L, 4L), initial heading angle of ship -70 degrees and initial speed of ship 3 m/s................. 126

Figure A.42 X, Y variation for berthing simulation of tanker ship using PD controller with normal MMG model: initial position of ship (-5L, 4L), initial heading angle of ship -70 degrees and initial speed of ship 3 m/s.. 126

Figure A.43 Trajectory for berthing simulation of tanker ship using PD controller with normal MMG model: initial position of ship (-5L, 3L), initial heading angle of ship -40 degrees and initial speed of ship 3 m/s.. 127

Figure A.44 RPS and δr for berthing simulation of tanker ship using PD controller with normal MMG model: initial position of ship (-5L, 3L), initial heading angle of ship -40 degrees and initial speed of ship 3 m/s.. 127

Figure A.45 Heading angle ψ for berthing simulation of tanker ship using PD controller with normal MMG model: initial position of ship (-5L, 3L), initial heading angle of ship -40 degrees and initial speed of ship 3 m/s.. 128

Figure A.46 Yaw rate r for berthing simulation of tanker ship using PD controller with normal MMG model: initial position of ship (-5L, 3L), initial heading angle of ship -40 degrees and initial speed of ship 3 m/s.. 128

Figure A.47 Surge (u) and sway (v) velocity for berthing simulation of tanker ship using PD controller with normal MMG model: initial position of ship (-5L, 3L), initial heading angle of ship -40 degrees and initial speed of ship 3 m/s................. 129

Figure A.48 X, Y variation for berthing simulation of tanker ship using PD controller with normal MMG model: initial position of ship (-5L, 3L), initial heading angle of ship -40 degrees and initial speed of ship 3 m/s.. 129

Figure A.49 Trajectory for berthing simulation of tanker ship using PD controller with normal MMG model: initial position of ship (-6L, 2L), initial heading angle of ship -30 degrees and initial speed of ship 3 m/s.. 130

Figure A.50 RPS and δr for berthing simulation of tanker ship using PD controller with normal MMG model: initial position of ship (-6L, 2L), initial heading angle of ship -30 degrees and initial speed of ship 3 m/s.. 130

Figure A.51 Heading angle ψ for berthing simulation of tanker ship using PD controller with normal MMG model: initial position of ship (-6L, 2L), initial heading angle of ship -30 degrees and initial speed of ship 3 m/s.. 131

Figure A.52 Yaw rate r for berthing simulation of tanker ship using PD controller with normal MMG model: initial position of ship (-6L, 2L), initial heading angle of ship -30 degrees and initial speed of ship 3 m/s.. 131

Figure A.53 Surge (u) and sway (v) velocity for berthing simulation of tanker ship using PD controller with normal MMG model: initial position of ship (-6L, 2L), initial heading angle of ship -30 degrees and initial speed of ship 3 m/s................. 132

Figure A.54 X, Y variation for berthing simulation of tanker ship using PD controller with normal MMG model: initial position of ship (-6L, 2L), initial heading angle of ship -30 degrees and initial speed of ship 3 m/s.. 132

Figure A.55 Yaw rate r for berthing simulation of tanker ship using PD controller with normal MMG model: initial position of ship (-5L, 4L), initial heading angle of ship -40 degrees and initial speed of ship 4 m/s.. 133

Figure A.56 Surge (u) and sway (v) velocity for berthing simulation of tanker ship using PD controller with normal MMG model: initial position of ship (-5L, 4L), initial heading angle of ship -40 degrees and initial speed of ship 4 m/s................. 134

Figure A.57 Trajectory for berthing simulation of tanker ship using PD controller with normal MMG model: initial position of ship (-5L, 4L), initial heading angle of ship -70 degrees and initial speed of ship 4 m/s.. 135

Figure A.58 RPS and δr for berthing simulation of tanker ship using PD controller with normal MMG model: initial position of ship (-5L, 4L), initial heading angle of ship -70 degrees and initial speed of ship 4 m/s.. 135

Figure A.59 Heading angle ψ for berthing simulation of tanker ship using PD controller with normal MMG model: initial position of ship (-5L, 4L), initial heading angle of ship -70 degrees and initial speed of ship 4 m/s.. 136

Figure A.60 Yaw rate r for berthing simulation of tanker ship using PD controller with normal MMG model: initial position of ship (-5L, 4L), initial heading angle of ship -70 degrees and initial speed of ship 4 m/s.. 136

Figure A.61 Surge (u) and sway (v) velocity for berthing simulation of tanker ship using PD controller with normal MMG model: initial position of ship (-5L, 4L), initial heading angle of ship -70 degrees and initial speed of ship 4 m/s................. 137

Figure A.62 X, Y variation for berthing simulation of tanker ship using PD controller with normal MMG model: initial position of ship (-5L, 4L), initial heading angle of ship -70 degrees and initial speed of ship 4 m/s.. 137

Figure A.63 Trajectory for berthing simulation of tanker ship using PD controller with normal MMG model: initial position of ship (-5L, 3L), initial heading angle of ship -40 degrees and initial speed of ship 4 m/s.. 138

Figure A.64 RPS and δr for berthing simulation of tanker ship using PD controller with normal MMG model: initial position of ship (-5L, 3L), initial heading angle of ship -40 degrees and initial speed of ship 4 m/s.. 138

Figure A.65 Heading angle ψ for berthing simulation of tanker ship using PD controller with normal MMG model: initial position of ship (-5L, 3L), initial heading angle of ship -40 degrees and initial speed of ship 4 m/s....................................... 139

Figure A.66 Yaw rate r for berthing simulation of tanker ship using PD controller with normal MMG model: initial position of ship (-5L, 3L), initial heading angle of ship -40 degrees and initial speed of ship 4 m/s.. 139

Figure A.67 Surge (u) and sway (v) velocity for berthing simulation of tanker ship using PD controller with normal MMG model: initial position of ship (-5L, 3L), initial heading angle of ship -40 degrees and initial speed of ship 4 m/s................ 140

Figure A.68 X, Y variation for berthing simulation of tanker ship using PD controller with normal MMG model: initial position of ship (-5L, 3L), initial heading angle of ship -40 degrees and initial speed of ship 4 m/s.. 140

Figure A.69 Yaw rate r for berthing simulation of tanker ship using PD controller with (a) Kose's mathematical model and (b) normal MMG model: initial position of ship (-5L, 4L), initial heading angle of ship -40 degrees and initial speed of ship 3 m/s 141

Figure A.70 Surge (u) and sway (v) velocity for berthing simulation of tanker ship using PD controller with (a) Kose's mathematical model and (b) normal MMG model: initial position of ship (-5L, 4L), initial heading angle -40 degrees and initial speed 3 m/s 141

Figure A.71 Trajectory for berthing simulation of tanker ship using PD controller with (a) Kose's mathematical model and (b) normal MMG model: initial position of ship (-5L, 4L), initial heading angle -70 degrees and initial speed 3 m/s 142

Figure A.72 RPS and δr for berthing simulation of tanker ship using PD controller with (a) Kose's mathematical model and (b) normal MMG model: initial position of ship (-5L, 4L), initial heading angle -70 degrees and initial speed 3 m/s 142

Figure A.73 Heading angle ψ for berthing simulation of tanker ship using PD controller with (a) Kose's mathematical model and (b) normal MMG model: initial position of ship (-5L, 4L), initial heading angle -70 degrees and initial speed 3 m/s 143

Figure A.74 Yaw rate r for berthing simulation of tanker ship using PD controller with (a) Kose's mathematical model and (b) normal MMG model: initial position of ship (-5L, 4L), initial heading angle -70 degrees and initial speed 3 m/s 143

Figure A.75 Surge (u) and sway (v) velocity for berthing simulation of tanker ship using PD controller with (a) Kose's mathematical model and (b) normal MMG model: initial position of ship (-5L, 4L), initial heading angle -70 degrees and initial speed 3 m/s 144

Figure A.76 X, Y variation for berthing simulation of tanker ship using PD controller with (a) Kose's mathematical model and (b) normal MMG model: initial position of ship (-5L, 4L), initial heading angle -70 degrees and initial speed 3 m/s 144

Figure A.77 Trajectory for berthing simulation of tanker ship using PD controller with (a) Kose's mathematical model and (b) normal MMG model: initial position of ship (-5L, 3L), initial heading angle -40 degrees and initial speed 3 m/s 145

Figure A.78 RPS and δr for berthing simulation of tanker ship using PD controller with (a) Kose's mathematical model and (b) normal MMG model: initial position of ship (-5L, 3L), initial heading angle -40 degrees and initial speed 3 m/s 145

Figure A.79 Heading angle ψ for berthing simulation of tanker ship using PD controller with (a) Kose's mathematical model and (b) normal MMG model: initial position of ship (-5L, 3L), initial heading angle -40 degrees and initial speed 3 m/s 146

Figure A.80 Yaw rate r for berthing simulation of tanker ship using PD controller with (a) Kose's mathematical model and (b) normal MMG model: initial position of ship (-5L, 3L), initial heading angle -40 degrees and initial speed 3 m/s 146

Figure A.81 Surge (u) and sway (v) velocity for berthing simulation of tanker ship using PD controller with (a) Kose's mathematical model and (b) normal MMG model: initial position of ship (-5L, 3L), initial heading angle -40 degrees and initial speed 3 m/s 147

Figure A.82 X, Y variation for berthing simulation of tanker ship using PD controller with (a) Kose's mathematical model and (b) normal MMG model: initial position of ship (-5L, 3L), initial heading angle -40 degrees and initial speed 3 m/s 147

Figure A.83 Yaw rate r for berthing simulation of tanker ship using PD controller with (a) Kose's mathematical model and (b) normal MMG model: initial position of ship (-5L, 4L), initial heading angle of ship -40 degrees and initial speed of ship 4 m/s 148

Figure A.84 Surge (u) and sway (v) velocity for berthing simulation of tanker ship using PD controller with (a) Kose's mathematical model and (b) normal MMG model: initial position of ship (-5L, 4L), initial heading angle -40 degrees and initial speed 4 m/s 148

Figure A.85 Trajectory for berthing simulation of tanker ship using PD controller with (a) Kose's mathematical model and (b) normal MMG model: initial position of ship (-5L, 4L), initial heading angle -70 degrees and initial speed 4 m/s 149

Figure A.86 RPS and δr for berthing simulation of tanker ship using PD controller with (a) Kose's mathematical model and (b) normal MMG model: initial position of ship (-5L, 4L), initial heading angle -70 degrees and initial speed 4 m/s 149

Figure A.87 Heading angle ψ for berthing simulation of tanker ship using PD controller with (a) Kose's mathematical model and (b) normal MMG model: initial

position of ship (-5L, 4L), initial heading angle -70 degrees and initial speed 4 m/s 150
Figure A.88 Yaw rate r for berthing simulation of tanker ship using PD controller with (a) Kose's mathematical model and (b) normal MMG model: initial position of ship (-5L, 4L), initial heading angle -70 degrees and initial speed 4 m/s 150
Figure A.89 Surge (u) and sway (v) velocity for berthing simulation of tanker ship using PD controller with (a) Kose's mathematical model and (b) normal MMG model: initial position of ship (-5L, 4L), initial heading angle -70 degrees and initial speed 4 m/s 151
Figure A.90 X, Y variation for berthing simulation of tanker ship using PD controller with (a) Kose's mathematical model and (b) normal MMG model: initial position of ship (-5L, 4L), initial heading angle -70 degrees and initial speed 4 m/s 151
Figure A.91 Trajectory for berthing simulation of tanker ship using PD controller with (a) Kose's mathematical model and (b) normal MMG model: initial position of ship (-5L, 3L), initial heading angle -40 degrees and initial speed 4 m/s 152
Figure A.92 RPS and δr for berthing simulation of tanker ship using PD controller with (a) Kose's mathematical model and (b) normal MMG model: initial position of ship (-5L, 3L), initial heading angle -40 degrees and initial speed 4 m/s 152
Figure A.93 Heading angle ψ for berthing simulation of tanker ship using PD controller with (a) Kose's mathematical model and (b) normal MMG model: initial position of ship (-5L, 3L), initial heading angle -40 degrees and initial speed 4 m/s 153
Figure A.94 Yaw rate r for berthing simulation of tanker ship using PD controller with (a) Kose's mathematical model and (b) normal MMG model: initial position of ship (-5L, 3L), initial heading angle -40 degrees and initial speed 4 m/s 153
Figure A.95 Surge (u) and sway (v) velocity for berthing simulation of tanker ship using PD controller with (a) Kose's mathematical model and (b) normal MMG model: initial position of ship (-5L, 3L), initial heading angle -40 degrees and initial speed 4 m/s 154
Figure A.96 X, Y variation for berthing simulation of tanker ship using PD controller with (a) Kose's mathematical model and (b) normal MMG model: initial position of ship (-5L, 3L), initial heading angle -40 degrees and initial speed 4 m/s 154
Figure A.97 Trajectory for berthing simulation of tanker ship using (a) PD controller and (b) ANN controller (Hasegawa and Kitera, 1993) with Kose's mathematical model: initial position of ship (-5L, 4L), initial heading angle -70 degrees and initial speed 3 m/s 155
Figure A.98 RPS and δr for berthing simulation of tanker ship using (a) PD controller and (b) ANN controller (Hasegawa and Kitera, 1993) with Kose's mathematical model: initial position of ship (-5L, 4L), initial heading angle -70 degrees and initial speed 3 m/s 156

Figure A.99 Trajectory for berthing simulation of tanker ship using (a) PD controller and (b) ANN controller (Hasegawa and Kitera, 1993) with Kose's mathematical model: initial position of ship (-5L, 3L), initial heading angle -40 degrees and initial speed 3 m/s 156

Figure A.100 RPS and δr for berthing simulation of tanker ship using (a) PD controller and (b) ANN controller (Hasegawa and Kitera, 1993) with Kose's mathematical model: initial position of ship (-5L, 3L), initial heading angle -40 degrees and initial speed 3 m/s 157

Figure A.101 Trajectory for berthing simulation of tanker ship using (a) PD controller and (b) ANN controller (Hasegawa and Kitera, 1993) with Kose's mathematical model: initial position of ship (-6L, 2L), initial heading angle -30 degrees and initial speed 3 m/s 157

Figure A.102 RPS and δr for berthing simulation of tanker ship using (a) PD controller and (b) ANN controller (Hasegawa and Kitera, 1993) with Kose's mathematical model: initial position of ship (-6L, 2L), initial heading angle -30 degrees and initial speed 3 m/s 158

Figure A.103 Trajectory for berthing simulation of tanker ship using MPC with Kose's mathematical model: initial position of ship (-5L, 4L), initial heading angle of ship -70 degrees and initial speed of ship 3 m/s 159

Figure A.104 X position XG, Y position YG, heading angle psi, surge velocity u, sway velocity v and yaw rate r for berthing simulation of tanker using MPC with Kose's model: initial position of ship (-5L, 4L), initial heading angle -70 degrees and initial speed 3 m/s 160

Figure A.105 Actual and optimal trajectories for berthing simulation of tanker ship using MPC with Kose's mathematical model: initial position of ship (-5L, 4L), initial heading angle of ship -70 degrees and initial speed of ship 3 m/s 161

Figure A.106 Diagram for berthing simulation of tanker ship using MPC with Kose's mathematical model: initial position of ship (-5L, 4L), initial heading angle of ship -70 degrees and initial speed of ship 3 m/s 161

Figure A.107 Trajectory for berthing simulation of tanker ship using MPC with Kose's mathematical model: initial position of ship (-5L, 3L), initial heading angle of ship -40 degrees and initial speed of ship 3 m/s 162

Figure A.108 X position XG, Y position YG, heading angle psi, surge velocity u, sway velocity v and yaw rate r for berthing simulation of tanker using MPC with Kose's model: initial position of ship (-5L, 3L), initial heading angle -40 degrees and initial speed 3 m/s 162

Figure A.109 Actual and optimal trajectories for berthing simulation of tanker ship using MPC with Kose's mathematical model: initial position of ship (-5L, 3L), initial heading angle of ship -40 degrees and initial speed of ship 3 m/s 163

Figure A.110 Diagram for berthing simulation of tanker ship using MPC with Kose's mathematical model: initial position of ship (-5L, 3L), initial heading angle of ship -40 degrees and initial speed of ship 3 m/s.. 163

List of Tables

Table 3.1 Coefficients related to propeller reversing forces and moment 27
Table 4.1 Ship particulars 37
Table 4.2 Experimental level of the factors 39
Table 4.3 Layout of the experimental design for the two models.............................. 40
Table 4.4 Results of Kose's model of 10 vectors under the simulation time of 550 seconds 41
Table 5.1 Simulation case and condition 44
Table 5.2 Hydrodynamic derivatives of Kose's mathematical model......................... 45
Table 5.3 Derivatives of surge equation in mathematical models 73
Table 5.4 Derivatives of sway equation in mathematical models.............................. 73
Table 5.5 Derivatives of yaw equation in mathematical models 73
Table 5.6 Kose (heading step: 30 degrees, random initial heading: 10 cases for each) 85
Table 5.7 MMG (heading step: 30 degrees, random initial heading: 10 cases for each) 85
Table 5.8 Kose (heading step: 30 degrees, random initial heading: 10 cases for each) 87
Table 5.9 Kose (heading step: 30 degrees, random initial heading: 30 cases for each) 88
Table 5.10 Kose (heading step: 15 degrees, random initial heading: 30 cases for each) 88

1. Introduction

1.1 Preamble

In this study, the methodology to control the heading angle and speed of ships on the simulation of berthing operation is presented. Furthermore, it is studied to consider ship manoeuvring in low advance speed of a ship for simulation of berthing operation.

Through this research, the development of time-domain simulation tool and the model simulation are performed, and the result is compared with previous works in different situations. Furthermore, the statistical analysis is performed for defining the initial environment of efficient berthing operation. This study is expected to provide an efficient simulation tool to harbour designers for planning and managing a harbour system cost-effectively and an opportunity to harbour masters and pilots for practicing and understanding the berthing operation in various harbour situations.

1.2 Background and Motivation

As world trade has been increasing these days, effective management of harbour system is becoming an important issue. In particular, due to the increased complexity of harbour environment with various harbour facilities, berthing operation of ships takes much time and requires various technical supports from harbour masters, pilots and engineers. In this point of view, precise prediction and practice of berthing operation are required and development of automatic simulation tool is requested for planning and managing effective harbour system.

For increasing accuracy on prediction of berthing operation, it is needed to analyse ship movement particularly with low advance speed and to develop an effective algorithm and controller for simulating the berthing operation accordingly.

1.3 Research Aim and Objectives

The present study aims to develop a fast and reliable numerical tool to simulate the manoeuvrability of ships during berthing operations in low advance speed of ships. To achieve this goal, the following objectives will be conducted in this study:

a) To undertake a critical review of the relevant literature, aiming to understand the state-of-the-art in ship berthing operation and identify the research gaps;

b) To propose a methodology for ship berthing control, with highlight on manoeuvring in low advance speed of a ship;

c) To develop a fast and reliable numerical tool which can be widely used to simulate berthing operation of ships in various initial conditions including initial position, initial heading angle and initial speed of ships;

d) To validate the developed numerical tool by using the result from Im and Hasegawa (2001);

e) To conduct parametric study and to investigate the factors (mathematical model, control algorithm, manoeuvring speed, etc.) which will affect the simulation for berthing operation of ships;

1.4 Structure of the Thesis

The thesis is structured in seven chapters and a number of associated appendices. A brief outline of the content of each chapter is given below:

- Chapter 1 (Introduction), the current chapter, provides the background to the research described in the thesis and states the overall aim and specific objectives that constitute the focus of the research work.

- Chapter 2 (Critical Review), contains a critical review of current and emerging concepts for simulation of ship berthing operation with the key merits and drawbacks of each and concludes with the need to develop an integrated new approach.
- Chapter 3 (Mathematical Model of Ship Berthing Manoeuvre) presents two different mathematical models for ship manoeuvring and explains how to apply the mathematical models for ship berthing operation.
- Chapter 4 (Methodology), presents the methodological procedures and the complete design of the numerical experiments employed in this study.
- Chapter 5 (Time-Domain Simulations of Ship Berthing Operation), presents the simulation results and analysis.
- Chapter 6 (Discussion), contains an account of the contribution of the thesis to the field, critically discusses the outcome of the thesis on the basis of the objectives stated in Chapter 2, outlines the difficulties encountered and the manner in which these were handled, and based upon the discussion, provides recommendations for further research.
- Chapter 7 (Conclusions), summarises the main conclusions of the research presented in the thesis.

2. Critical Review

2.1 Preamble

The berthing operation has been highlighted as the most important procedure in ship manoeuvring and various approaches have been tried to improve safety and efficiency of ship berthing performance. In this chapter, review of the previous work and the current methodologies of ship berthing operation and simulation are presented, based on the four categories as follows.

a) Berthing operation
b) Shallow water manoeuvring
c) Manoeuvring control
d) Summary

2.2 Berthing Operation

The research by Kasasbeh et al. (1993) was aimed to provide a complete simulation of a vessel automatically berthing in a generic port and to carry out a feasibility study of the hardware and software for a system to be installed on a small vessel for physical trial tests.

It is a very difficult and complicated procedure, even for experienced ship mariners, to approach or leave a berth in a harbour. In general, in the case of a large ship, such manoeuvres are achieved by appropriate assistance received from tugs, whereas the master of a small ship must control it without tugs.

Automatic berthing was achieved in a series of stages. In all but the final stage, the process consisted of steering towards an intermediate destination point determined by the program. In the final stage, the ship's thrusters were used to move it sideways against the berth. It was presumed that the berthing mechanism was activated when the ship arrived within a predetermined distance from the port, at which time control was handed over to the software. The program, therefore, started with the ship at a typical start position. The validity of the software could be further tested by moving the initial position of the ship and the ship's initial heading (Kasasbeh et al., 1993) which is done in this thesis for more elaborate study.

In the paper by Im and Hasegawa (2001), a parallel ANN (artificial neural networks) for the automatic berthing was discussed. The controller had separated hidden layers and each controls an engine and a rudder respectively. Simulations using MATLAB were performed with different initial conditions and the performance of separated hidden layer was compared with that of united hidden layer. This paper shows some successful simulation cases with the newly designed ANN. However, it does not explain exactly what is the problem caused by traditional approaches for berthing operation and how the new controller could make the improvement of berthing simulation in the point of naval architect and control. A 260,000 tons of tanker was adopted for the paper, of which dynamics and details were explained in the research by Kose et al. in 1986.

Furthermore, in the study by Ahmed and Kazuhiko (2015), the minimum time course changing manoeuvre was utilised to ensure consistency and a new concept named 'virtual window' was introduced. Such consistent teaching data were used to train two separate multi-layered feed forward neural networks for commanding rudder and propeller revolution output.

On the other hand, a quasi-real-time method applicable to minimum-time approaching control for automatic berthing was proposed in the study by Mizuno et al. (2015). The proposed system was composed of a multiple shooting algorithm based optimal berthing solution generator and a nonlinear model predictive controller for tracking to the optimal trajectory. The multiple shooting algorithm was expected to generate the approximate optimal solution considering the wind disturbance at the start point of the berthing, in a few minutes.

On the other hand, the interest for automating ship berthing operation have made different trials even in the same base of controller. In the study by Qiang et al. (2019), a robust neural network (NN) adaptive approach based on the navigation dynamic deep-rooted information (Papadimitrakis et al.) was proposed to reconstruct the lumped uncertainties caused by unknown ship dynamics and external disturbances. Meanwhile, the dynamic surface control (DSC) and the minimum learning parameter (MLP) techniques were used to reduce the computational load of the adaptive NN control scheme. Considering the input saturation effects of control actuator, such as a rudder and a propeller, and the coupling characteristics of uncertainties, the approach integrated neural network weights, approximation errors and external disturbance term as the composite uncertain parameters, which was estimated online by parameter adaptive technique.

In the recent study by Maki et al. (2019), the off-line automatic berthing problem was counted for the first step of study. The optimal control problem was modelled as minimum-time problem and the collision risk with the berth was considered. In the study, it was performed to apply the covariance matrix adaption evolution strategy (CMA-ES), which was considered state-of-the-art in evolutionary computation approaches for optimization of real-valued variables. In the study, a propeller and a rudder were used only as control inputs and therefore, the degree of difficulty was significantly high. It was noteworthy that preparation of a feasible initial control input was not required in the calculation process, which made the proposed procedure robust.

As computer technology and programming tools are developed, ship manoeuvring is analysed more accurately and presented with simulation for understanding whole or part of ship movement. In particular, the need of accurate prediction for ship moving in the harbour gives motivation for developing the simulation programme reflecting real sea and harbour conditions. In this point of view, there have been various approaches for simulating ship movement to be used not only in effective harbour management but also in safety improvement on channel design etc.

2.3 Shallow Water Manoeuvring

In recent years, it is observed that the dimensions of ships, particularly for container ships, Ro-Ro vessels and LNG carriers, have been increased continuously to improve the cost-efficiency and the flow and the ship manoeuvring in harbours come to be influenced more and more by waterways restrictions. A phenomenon that occurs on vessels in the area is ship squat, which may be defined as the sinkage and trimming of the ship due to the pressure changes along the ship length in shallow waters. The trim change can be explained by hydrodynamic interactions between the ship and the bottom due to speed and pressure distribution change. Large and fuller ships such as tankers and bulk carriers should pay extra attention when navigating in restricted waters. The squat effect is directly related to ship dimensions, its speed and water depth (Serban and Panaitescu, 2015). A case study of ship for shore interaction when a bulk carrier passes at different speeds through a narrow waterway in Suez Canal was performed using NTPRO 5000 navigational simulator by Serban and Panaitescu (2015) and the shore interaction and ship squat phenomenon were analysed.

Furthermore, a case study through a novel test for ship manoeuvring in modern inland waterway was performed for provision of reference data for benchmarking of numerical methods by Mucha et al. (2017). Hull geometry, main particulars and appendages for propulsion and manoeuvring were introduced and the results of resistance and propulsion model tests in shallow water condition were discussed in the study.

For the berthing manoeuvre in shallow water, Lee et al. showed that the strength and position of the separated vortices are affected significantly by the water depth, which directly affects the hydrodynamic forces acting on the berthing ship. The bad-executed berthing condition could seriously damage the structure of the quay as well as the ship itself. Therefore, the accurate prediction of the hydrodynamic performance of the ship in berthing procedure is a prior requirement for the safety and the design of fender facility.

The prediction of hydrodynamic forces acting on the berthing ship is traditionally carried out by experimental method, which has a merit of accuracy. However, the experiment needs to take long time and high cost. Previously, a various of experiments were performed by Huang et al. to collect essential data for transient flow field encountered during the berthing operations. Furthermore, the towing tests were performed by Gerigk to investigate the effects of a distance to the berth and water depth on the performance of propellers.

In the study by Wang et al. (2017), numerical simulation of the berthing manoeuvre of ship taking account of quay wall was performed. Furthermore, the results were compared with the data from the computational fluid dynamics (CFD) analysed by Toda.

On the other hand, the noise levels of the ship were recorded from different types of ship in four heavily ship-trafficked marine areas in Denmark by Hermannsen et al. (2014). In the study, ship noise levels in shallow water in light of the potential impacts were evaluated.

2.4 Manoeuvring Control

The control Methodologies are reviewed with the following categories;

- Proportional Integral Derivative (PID) control
- Fuzzy control
- Fuzzy PID control (FPID)
- Neural Network control
- Model Predictive Control (MPC)

(1) Proportional Integral Derivative (PID) Controller

The design of the PID control system depends on the choice of the three control constants K_p, K_d and K_i. The control will be effective with the simultaneous use of all three constants with differential values. If seen individually these constants have various effects on the system. K_p reduces the time taken to reach the desired output, but it shows an overshoot. Convergence is never achieved due to the presence of a steady error or an offset. K_i is found useful in reducing the steady error or offset. K_i sometimes pushes the transient response to unstable region. K_d improves the stability by reducing the overshoot. But the applicability of high frequency noise in hydrodynamics that a differentiator will amplify the noise and an integrator will suppress it is yet to be ascertained. It may be assumed that in water high frequency signals will be attenuated to lower frequency range.

There are some practical limitations in opting for certain values of the abovementioned constants. It is difficult to turn the rudder to affect the immediate turning of the ship at a very fast rate because of the heavy damping provided by the surrounding fluid and inertia due to self-weight. The rudder has a projected surface area, in proportion to the ships lateral area underwater, and its own inertia. At the same time, a fin can be turned at faster rate than a rudder since the fin area is smaller compared to rudder. Ship motion control by Perez (2005) can be referred for understanding fin actions to control roll motion. But rudder turning rate can be improved by high power electro-hydraulic system of the steering gear. In such case the installation cost becomes a bigger financial burden to the ship owner (Lee et al., 2009).

Through the study by Lee et al. (2009), a good similarity between fuzzy and PID controls was seen from the simulation results and it means control based on fuzzy logic and PID are comparable excepting the fact that the linear acceleration in the lateral direction was twice the value in case of fuzzy logic control. PID can be taken as a standard result as the fuzzy logic can be easily manipulated in its algorithm. Algorithm based on PID is a proven technique in engineering.

PID seems to be more successful method compared to fuzzy logic if the respective constants are chosen. For tune-invariant cases they are chosen by trial and error methods. The accuracy of fuzzy logic control can be improved using more membership functions. There is possibility for combining the two algorithms so that a new approach is feasible for ship motion control. Such an algorithm can be useful for all new generation single hull ships (Lee et al., 2009).

(2) Fuzzy Controller

In seaway, the path or trajectory is constructed by using a set of way-points, which can be generated according to sail plan and weather data (minimum resistance or energy approach), or given manually as autopilot inputs. In way-point tracking control problem, it is assumed that the ship is moving at a constant forward speed, and only the rudder is controllable. The way-point tracking control problem is how to make the ship follow the path planned with the way-points by controlling the rudder.

The way-point tracking controller has been improved over several years. A tracking controller for special ship applications such as mine hunting and dredging has been developed, which is based on adaptive course controller. LQG feedback combined with feed forward control approach to keep the ship to a desired trajectory was proposed by Holzhüter (1997). The paper by Pettersen and Lefeber (2001) gave a yaw torque control law for ship way point tracking control problem based on a full state feedback control approach.

Cheng et al. (2006) proposed a new approach to design the ship autopilot for the way-point tracking control problem with fuzzy control method. Intuitive comprehension of the ship behaviour and manipulations of human were used in designing of the fuzzy autopilot. The human operator, the most successful intelligent controller available until now, is able to control the complicated process without knowledge of the process mathematical model. Also, the human operator can learn to control many systems without prior knowledge of system response behaviour. Based on human operator's manipulating experience, the control rules for tracking control and turning control were developed.

Since only one control loop is needed, the fuzzy control algorithm greatly reduces the control parameters number, and also simplifies the control design process, and can be easily put into practical applications. Simulation performed by Cheng et al. (2006) was implemented based on a warship model. Way-point tracking results showed that the fuzzy autopilot implemented the way-point tracking control effectively and had satisfactory performance.

When a ship passes dense traffic areas, narrow straits, harbour entrances, etc. economic factors are not as important as safety ones. Therefore, in these cases the manoeuvring control and trajectory tracking strategies are employed to ensure the precise control of the ship's motions. The reference trajectory is usually defined by a supervisory guidance system or a human operator. The control system used for tracking usually works in one of the two forms (Fossen, 1994):

- Manoeuvring control (geometric and dynamic task) is performed with the small lateral velocities (crab movements). In this condition, the rudder is almost ineffective. Therefore, the vessel is controlled by the thrusters and the main engine working on small rpm set-points. The regulator controls not only the geometrical position of the ship in relation to the reference trajectory but also the velocities of the hull. In this case, the ship can move along the trajectory with the arbitrary heading angle and usually the difference between the longitudinal and the transversal velocities is not significant.

- Trajectory tracking (geometric task) is using forward thrust of the main propeller for speed control and the rudder deflection to minimize cross tracking error. In this case, the ship moves between the way-points with the heading as close as possible to the direction of the local segment of the reference trajectory. The longitudinal velocity of the ship is high in relation to the transversal one and is commonly close to the cruise speed of the vessel.

In the study presented by Gierusz et al. (2007), the regulator devoted to manoeuvring control was based on a robust systems technology and the fuzzy logic control system applied to solve a trajectory tracking problem. The simulation model of the ship built with acceptable accuracy gave possibilities for creating the manoeuvring velocities controller based on the simulation trials instead of cost and time-consuming full-scale experiments. The drawback of D-K iteration algorithm was the high order of the obtained controller, even after the order reduction procedure. Therefore, it was difficult (or impossible) to give the physical interpretation of its coefficients. In the case of a fuzzy logic system, the regulator controls the vessel on the basis of the knowledge of a human operator (experienced helmsman) and not on the basis of the mathematical model of the process. Therefore, this regulator is more flexible to adapt its behaviour to the different vessels or vessel operating under different work conditions.

While fuzzy control has emerged as an alternative to some conventional control schemes since it has shown success in some application areas (e.g., in train control and camera auto-focusing), there are several drawbacks to this approach: a) the design of fuzzy controllers is usually performed in an ad hoc manner where it is hard to justify the choice of some controller parameters (e.g., the membership functions), and b) the fuzzy controller constructed for the nominal plant may later perform inadequately if significant and unpredictable plant parameter variations occur.

However, Layne and Passino (1993) presented a comparative analysis of the “fuzzy model reference learning controller” (FMRLC) and conventional “model reference adaptive control” (MRAC) for a cargo ship steering application through their paper. For the cargo ship steering application, the simulation results showed that the FMRLC has several potential advantages over MRAC including a) improved convergence rates, b) use of less control energy, c) enhanced disturbance rejection properties, and d) lack of dependence on a mathematical model (Layne and Passino, 1993).

(3) Fuzzy PID Controller (FPID)

Fuzzy logic controllers (FLCs) have good characteristics in zones with large errors of control, where the controllers can produce quick dynamic responses due to nonlinear characteristics. When controllers work near stable points, the role of FLC is not sufficient, and a PID controller may have better effectiveness.

A new method for constructing ship autopilots based on the combination of fuzzy logic control (FLC) and linear control theory (PID control) was presented by Le et al. (2004). Through the study it was clearly seen that, in comparison with the PID autopilot, the new FPID (Fuzzy PID) autopilot had several important features:

- in general, ship heading error (or deflection of the ship heading angle from reference values) of the FPID autopilot was smaller than that of the PID autopilot;
- times of over-correction and maximum values of overshoot of heading angle for the FPID autopilot were much more smaller than those of the PID autopilot.

The new ship autopilot had the advantages of both the PID and FLC control methodologies: easy to construct, and optimal control laws could be established based on ship master knowledge. The new autopilot was much more effective than the PID autopilot in course-keeping and course-changing manoeuvres.

However, in order to be able to use the FPID autopilot in practice, several problems need to be solved. Among them are: determination of the most suitable form for membership functions of the FPID controller, how to automatically design the membership functions and defuzzification laws for the autopilot, criteria for the optimal autopilot, and consideration of real aspects of the autopilot (Le et al., 2004).

(4) Neural Network Controller

In the past, researchers have developed adaptive algorithms that cater for varying ship dynamic characteristics, the self-tuning regulator designed by Astrom and Wittenmark being a prime example (Åström and Wittenmark, 1973) (Burns, 1995). Through the paper, Burns (1995) presented the study using an alternative approach, namely that of the multi-layered perceptron, a technique becoming widely used in artificial neural network architecture. The main objective of the work was to see if a trained network can perform over a range of forward speeds as well as an optimal guidance system, whose parameters need to be re-calculated for each forward speed.

The optimal guidance of a ship, say into the approaches of a port, may be considered as a multivariable control problem (Burns, 1989). The deviation from the desired position, course, and speed must be corrected for by operation of the rudder(s) and main engine(s). A feature of an optimal system was that it would seek to minimize a global parameter J, called the cost function or performance index. This was based upon the summation of the weighted errors over some time intervals, say, the time to complete the pilotage phase of the voyage. In addition to minimizing the errors in the output parameters, the optimal controller attempted to minimize also the control effort, i.e., to keep to a minimum the rudder and engine activity.

The results of this initial study demonstrated that a neural network may be trained from data provided by an optimal guidance system. The trained network performed in a slightly sub-optimal manner—but had the advantage that it did not have to re-compute controller parameters for different forward speeds. At this stage it was not known how the network would cope with another way-point configuration.

The properties of multi-layer neural networks were not yet fully understood. It would appear, however, that a ship guidance system was a potential application of the technique. There is extensive scope for further research in this field, particularly in the design of unsupervised learning networks that adapt in an on-line manner.

Such a scheme could integrate the features of both the optimal control policy back propagation approach, whereby incremental changes in weightings were designed to produce a global minimum in a selected cost function, in this case linked to errors in position, heading, and speed.

Furthermore, as already mentioned in the literature review, a discussion about a parallel ANN (artificial neural networks) for the automatic berthing was presented by Im and Hasegawa (2001).

(5) Model Predictive Control

Model Predictive Control (MPC) is an advanced method of process control to control a process while satisfying a set of constraints. In particular, it has been used for process industries in chemical plants and oil refineries since the 1980s. In recent years, various research works have been performed for MPC to be applied in different fields including manoeuvring control of cars and robots. Although the MPC has not been used widely for ship manoeuvring yet, there have been efforts to find feasibility of application for ship control.

Mizuno et al. (2015) presented a quasi real-time optimal control scheme for automatic berthing. For having an optimal ship trajectory, minimum-time approaching control was used on ship manoeuvring and nonlinear MPC was employed for tracking to the optimal trajectory.

On the other hand, a propeller and a rudder were used as control inputs to address an automatic berthing by Maki et al. (2020). In the research, the optimal control problem was modelled as minimum-time problem and the collision risk with the berth was considered.

Furthermore, Model Predictive Control has been tried to solve the collision avoidance of ships. Sun et al. (2018) presented a method that is based on finite control set model predictive control (FCS-MPC). A finite control set is generated by more practical control commands: the thruster speed and propulsion angle of the unmanned surface vehicles (USV).

Eriksen et al. (2019) presented a new algorithm for short-term maritime collision avoidance (COLAV) named the branching-course model predictive control (BC-MPC) algorithm. The algorithm is designed to be robust with respect to noise on obstacle estimates, which is a significant source of disturbance when using exteroceptive sensors such as, for example, radars for obstacle detection and tracking. Exteroceptive sensors do not require vessel-to-vessel communication, which enables COLAV toward vessels not equipped with, for example, automatic identification system transponders, in addition to increasing the robustness with respect to faulty information which may be provided by other vessels.

Papadimitrakis et al. (2021) studied the multi-ship control problem using a model predictive controller that makes use of obstacle ship trajectory prediction models built on the RBF framework and is trained on real AIS data sourced from an open-source database.

Zhao et al. (2018) presented an extensive analysis of the properties of different control horizon sets in an Extended Prediction Self-Adaptive Control (EPSAC) model predictive control framework. Analysis was performed on the linear multivariable model of the steam/ water loop in large-scale watercraft/ ships. The results indicated that larger control horizon values leaded to better loop performance, at the cost of computational complexity. Hence, it was necessary to find a good trade-off between the performance of the system and allocated or available computational complexity. In the paper, this problem was explicitly treated as an optimization task, leading to the optimal control horizon sets for the steam/ water loop example. Based on simulation results, it was concluded that specific tuning of control horizons outperformed the case when only a single valued control horizon was used for all the loops.

Multi Input and Multi Output (MIMO) control is one of the advantages which can be achieved by MPC. Gierusz and Rybczak (2020) presented synthesis methods for a multidimensional Robust controller and a multidimensional LMI controller. From their research, the experiments were performed on the lake and examples useful for examining both controller's performance were presented.

Liu et al. (2021) applied Model Predictive Control to synchronization control of dynamic positioning ships. In their paper, a novel synchronization controller on account of model predictive control (MPC) for dynamic positioning (DP) ships was devised to achieve underway replenishment. The underway replenishment was formulated into a leader-follower configuration. A quasi-infinite horizon technique was employed to guarantee stability by designing an appropriate terminal cost function based on the Lyapunov theorem. The simulation results showed that the follower could move along with the leader ship automatically from different initial points under disturbances, and the synchronization of velocities could be achieved; then, the key parameter of the MPC was investigated.

2.5 Summary

The fundamental concepts and methodologies for simulation of ship berthing operation have been critically reviewed and analysed. In particular, control methodologies for berthing procedure have been focused considering development of effective simulation programme and the main conclusions are as follows:

a) Speed and heading control of ships is the critical issues to be addressed on berthing operation.

b) In particular, rudder control in slow ship speed has been discussed as a main control problem to be overcome.

c) Analysis of different mathematical models is needed.

d) Various researches have been being performed with Fuzzy controller and Neural Network controller for replacing the traditional PID controller. However, both controllers are still unstable in certain conditions and also need to be verified with many different cases.

From the review shown above, the control algorithm with considering different control methodologies needs to be found and the time-domain simulation programme of ship berthing operation presented in this thesis would contribute to the berthing simulation field with improving safety and effectiveness of berthing performance. Furthermore, the ideal conditions to start berthing procedure of ships would be proposed through the simulation results with the statistical approach as well as kinematic analysis.

2.6 Research Gaps and Challenges

As described above, PD controller has been used for simulating ship manoeuvring in many years. However, in particular, berthing operation of ship is still very difficult part to predict and development of simulation programme with new controller is needed to predict ship berthing operation accurately. Recent years, MPC controller has been used to simulate manoeuvring cars and robots but has not been tried for ships yet. In this research, the simulation programmes have been developed with MPC controller in addition to PD controller and simulation results have been compared for having improved solution in simulating ship berthing operation.

3. Mathematical Model of Ship Berthing Manoeuvre

3.1 Preamble

In Chapter 3, a critical review of the mathematical models in berthing operation and simulation has been undertaken with the aim of highlighting deficient areas within the current methodologies. In particular, various approaches with different controllers have been reviewed for recognising the drawbacks as well as the merits of each control system and providing the improved approach.

The objective of this chapter is to explain the approach that has been followed in this thesis with reference to the mathematical model and application. Through this chapter, the mathematical models for developing time-domain simulation programme of ship berthing operation are explained in detail.

3.2 Outline of the Approach

There have been various trials to develop simulation tools for ship manoeuvring with different approaches. The current approaches are mostly using human experience for ship berthing operation and a traditional PID controller for ship heading control. However, as ship speed must be decreasing and rudder angle is also changing to perform berthing procedure, development of effective control system and algorithm for ship speed and heading control has been one of the key issues which need to be solved.

On this background, the approach adopted in this thesis has the following principal characteristics;

- Improvement of simulation algorithm
- Analysis of mathematical models for accurate simulation of berthing performance
- Development of an improved time-domain simulation tools using two different controllers: PD control and Model Predictive Control
- Providing data with comparative analysis
- Providing statistical analyses to suggest initial positions and heading angles of a ship for safe and effective berthing operation

Through this approach, berthing operation is simulated with accurate control of ship speed and heading angle and the time-domain simulation programme will provide useful data for effective and safe berthing operation as well as for pilot-training. Furthermore, this procedure can provide useful information for designing an effective harbour system.

3.3 Modelling of Berthing Operation

The ship is considered to be a rigid body with the three horizontal degrees of freedom of surge, sway, and yaw (Roseman, 1987). Ship motions in the three vertical degrees of freedom of heave, roll, and pitch are assumed to be negligible in common with most manoeuvring studies. The ship motions are measured with respect to the right-handed coordinate system (x_s, y_s, z_s), fixed on the ship, with its origin O located at the intersection of the longitudinal plane of symmetry and the midship section (Zhang et al., 1997).

Abkowitz (1964) makes the following assumptions:

(1) Most ship manoeuvres can be described with a 3rd-order truncated Taylor expansion about the steady state condition $u=u_0$.
(2) Only 1st-order acceleration terms are considered.
(3) Standard port/starboard symmetry simplifications except terms describing the constant force and moment arising from single-screw propeller.
(4) The coupling between the acceleration and velocity terms is negligible.

3.4 Coordinate System and Motion Equation

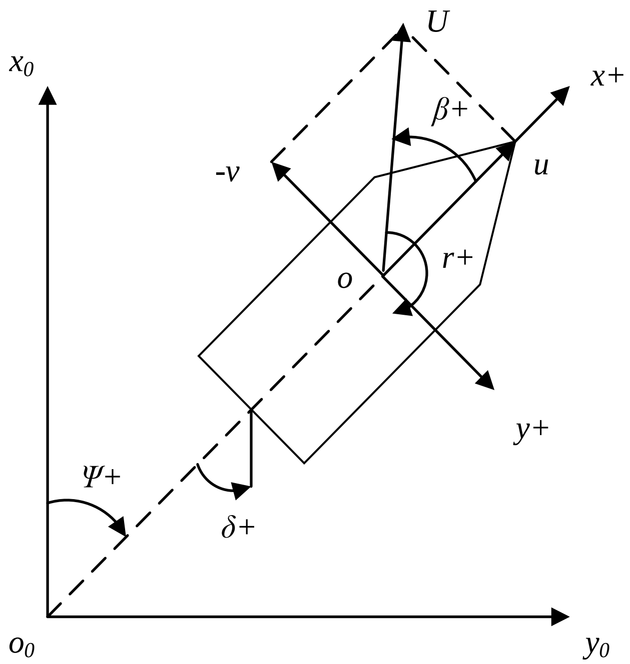

Figure 3.1 Coordinate system

The coordinate system for the mathematical model of ship manoeuvring is shown in Fig 3.1. The Earth-fixed frame is $o_0 x_0 y_0$ and the local coordinate frame is fixed on the ship with positive x-axis pointing towards the bow and y-axis pointing towards the starboard. Furthermore, three degrees of freedom (DOF) for surge, sway and yaw motion of manoeuvring model in calm water is as follows.

$$\mathrm{m}(\dot{\mathrm{u}}_{\mathrm{G}} - \mathrm{v}_{\mathrm{G}}\mathrm{r}_{\mathrm{G}}) = \mathrm{X}_{\mathrm{G}} \tag{3.1}$$

$$\mathrm{m}(\dot{\mathrm{v}}_{\mathrm{G}} + \mathrm{u}_{\mathrm{G}}\mathrm{r}_{\mathrm{G}}) = \mathrm{Y}_{\mathrm{G}} \tag{3.2}$$

$$\mathrm{I}_{\mathrm{zz}} \cdot \dot{\mathrm{r}}_{\mathrm{G}} = \mathrm{N}_{\mathrm{G}} \tag{3.3}$$

$$(\mathrm{m} + \mathrm{m}_{\mathrm{x}})\dot{\mathrm{u}} - \left(\mathrm{m} - \mathrm{m}_{\mathrm{y}}\right)\mathrm{vr} = \mathrm{X} \tag{3.4}$$

$$\left(\mathrm{m} + \mathrm{m}_{\mathrm{y}}\right)\dot{\mathrm{v}} + (\mathrm{m} + \mathrm{m}_{\mathrm{x}})\mathrm{ur} = \mathrm{Y} \tag{3.5}$$

$$(\mathrm{I}_{\mathrm{zz}} + \mathrm{J}_{\mathrm{zz}})\dot{\mathrm{r}} = \mathrm{N} \tag{3.6}$$

Where m is mass of the vessel. u, v and r are the surge, sway and yaw velocity respectively. I_{zz} is the moment of inertia in the horizontal plane. The superscript dot indicates the derivative with respect to the time of the corresponding quantities. X, Y and N are the external forces in surge, sway and yaw directions. In order to solve the above equation system, it is essential to find the external forces (moments) in the right-hand side of the above equations. The external force consists of three components, namely the ship hull hydrodynamic force, propeller force and rudder force, which are expressed as

$$X = X_H + X_P + X_R \tag{3.7}$$

$$Y = Y_H + Y_P + Y_R \tag{3.8}$$

$$N = N_H + N_P + N_R \tag{3.9}$$

In which the subscripts H, P and R represent the ship hull, propeller and rudder.

3.5 Hull

(1) Kose's model for low advance speed of ships

$$X_H^* = X_{vr}^* v^* r^* + X_{uu}^* |u^*| u^* + X_{uvv}^* u^* v^{*2}/U^* + X_{vvr}^* |v^*| v^* r^*/U^* \tag{3.10}$$

$$Y_H^* = Y_v^* v^* U^* + Y_{vv}^* |v^*| v^* + Y_{vvvvv}^* v^{*5} U^{*3} + Y_r^* r^* + Y_{ur}^* u^* r^* \tag{3.11}$$

$$+ Y_{uvvr} u^* v^{*2} r^*/U^{*2} + Y_{vrr}^* v^* r^{*2}/U^*$$

$$N_H^* = N_{uv}^* u^* v^* + N_r^* r^* + N_{rrr}^* r^{*3} + N_{ur}^* u^* r^* + N_{vvr}^* v^{*2} r^* \tag{3.12}$$

Where,

$$X^*, Y^* = X, Y/\left(\frac{\rho}{2} L^3 g\right),\ N^* = N/\frac{\rho}{2} L^4 g \tag{3.13}$$

$$m^* = m/\left(\frac{\rho}{2} L^3\right),\ I_{zz}^* = I_{zz}/\left(\frac{\rho}{2} L^5\right) \tag{3.14}$$

$$u^*, v^* = u, v/\sqrt{Lg},\ r^* = r/\sqrt{L/g} \tag{3.15}$$

$$\dot{u}^*, \dot{v}^* = \dot{u}, \dot{v}/g,\ \dot{r}^* = \dot{r} L/g \tag{3.16}$$

(2) MMG model

$$X_H = X_{\dot{u}}\dot{u} + X_u u + (X_{vr} - Y_{\dot{v}})vr + X_{vv}v^2 + X_{rr}r^2 \tag{3.17}$$

$$\begin{aligned} Y_H = {} & Y_{\dot{v}}\dot{v} + Y_{\dot{r}}\dot{r} + Y_v v + Y_r r + Y_{vvv}v^3 \\ & + Y_{vvr}v^2 r + Y_{vrr}vr^2 + Y_{rrr}r^3 \end{aligned} \tag{3.18}$$

$$\begin{aligned} N_H = {} & N_{\dot{v}}\dot{v} + N_{\dot{r}}\dot{r} + N_v v + N_r r + N_{vvv}v^3 \\ & + N_{vvr}v^2 r + N_{vrr}vr^2 + N_{rrr}r^3 \end{aligned} \tag{3.19}$$

Where $X_{\dot{u}}, X_u, X_{vv}, X_{vr}, Y_{\dot{v}}, X_{rr}, Y_{\dot{v}}, Y_v, Y_r, X_{\dot{u}}, Y_{vvv}, Y_{vvr}, Y_{vrr}, N_{\dot{r}}, N_v, N_r, N_{vvr}, N_{vrr}, N_{rrr}$ are the hydrodynamic derivatives, $\dot{u}, \dot{v}$ and $\dot{r}$ are derivatives of u, v and r with respect to the time.

3.6 Propeller

Propeller forces are estimated by the propeller rotation speed. When propelling ahead, the propeller force can be written as

$$X_P^* = \begin{cases} C_1 + C_2 J_s \;\; (J_s \geq C_{10} \text{ and } n > 0) \\ C_8 + C_9 J_s \;\; (J_{st} < J_s < C_{10} \text{ and } n > 0) \\ C_6 + C_7 J_s \;\; (J_s \geq C_{10} \text{ and } n < 0) \\ C_3 \;\; (J_{st} < J_s < C_{10} \text{ and } n < 0) \end{cases} \tag{3.20}$$

$$Y_P^* = \begin{cases} A_1 + A_2 J_s \;\; (J_{syn} \leq J_s < J_{syn0}) \\ A_3 + A_4 J_s (J_s < J_{syn}) \\ A_5 \;\; (J_{syn0} \leq J_s) \end{cases} \tag{3.21}$$

$$N_P^* = \begin{cases} B_1 + B_2 J_s \;\; (J_{syn} \leq J_s < J_{syn0}) \\ B_3 + B_4 J_s (J_s < J_{syn}) \\ B_5 \;\; (J_{syn0} \leq J_s) \end{cases} \tag{3.22}$$

$$J_s = \frac{U}{nD_P} \tag{3.23}$$

Table 3.1 Coefficients related to propeller reversing forces and moment

A_1	-0.079×10^{-3}	C_2	-0.200
A_2	7.99×10^{-3}	C_3	-0.251
A_3	-4.93×10^{-3}	C_6	-0.175
A_4	-5.87×10^{-3}	C_7	0.330
A_5	-0.558×10^{-3}	C_8	0.457
B_1	0.035×10^{-3}	C_9	0.408
B_2	0.035×10^{-3}	C_{10}	-0.233
B_3	-3.17×10^{-3}	J_{st}	-0.64
B_4	1.96×10^{-3}	S_{syn}	-0.35
B_5	2.33×10^{-3}	J_{syn0}	0.225×10^{-3}
C_1	0.315		

$$X_P^* = X_P/(\rho n^2 D_P^2) \tag{3.24}$$

$$Y_P^* = Y_P/\left(\frac{\rho}{2} Ld(nD_P)^2\right) \tag{3.25}$$

$$N_P^* = N_P/\left(\frac{\rho}{2} L^2 d(nD_P)^2\right) \tag{3.26}$$

3.7 Rudder

The rudder forces can be derived from the normal force acting on the rudder surface as

$$X_R = -(1 - t_R)F_N \sin\delta \tag{3.27}$$

$$Y_R = -(1 + a_H)F_N \cos\delta \tag{3.28}$$

$$N_R = -(x_R + a_H x_H)F_N \cos\delta \tag{3.29}$$

Where δ is the rudder angle, x_H is the distance between the pressure center of the rudder and the yaw center of the hull, t_R, α_H and x_R are the reduction parameters. F_N is the normal force acting on the rudder which is calculated as

$$F_N = \begin{cases} \frac{\rho}{2} A_R f_\alpha U_R^2 \sin\alpha_R \quad (n \geq 0) \\ 0 \quad (n < 0) \end{cases} \tag{3.30}$$

$$f_\alpha = \frac{6.13\Lambda}{2.25+\Lambda} \tag{3.31}$$

$$U_R \fallingdotseq U \tag{3.32}$$

3.8 Manoeuvring Equation of Low Advance Speed

$$\begin{aligned}(m + m_x)\dot{u} = {} & \left(m + m_y + X_{vr}\right)vr + X_{uu}|u|u + X_{uvv}uv^2/U \\ & +X_{vvr}|v|vr/U + X_P - (1 - t_R)F_N \sin\delta - R\end{aligned} \tag{3.33}$$

$$\begin{aligned}\left(m + m_y\right)\dot{v} - Y_{\dot{r}}\dot{r} = {} & Y_v vU + Y_{vv}|v|v + Y_{vvvvv}v^5U^3 + Y_r r \\ & +Y_{ur}ur + Y_{uvvr}uv^2r/U^2 + Y_{vrr}vr^2/U \\ & +Y_P - (1 + a_H)F_N \cos\delta\end{aligned} \tag{3.34}$$

$$\begin{aligned}(I_{zz} + J_{zz})\dot{r} - N_{\dot{v}}\dot{v} = {} & N_{uv}uv + N_r r + N_{rrr}r^3 + N_{ur}ur \\ & +N_{vvr}v^2r + N_P - (x_R + a_H x_H)F_N \cos\delta\end{aligned} \tag{3.35}$$

Where R is resistance

$$m_y^* = m_y/\left(\frac{\rho}{2}L^2d\right) = \pi\left(\frac{d}{L}\right)^2\left(1 + 0.16C_b\frac{B}{d} - 5.1\left(\frac{B}{L}\right)^2\right) \tag{3.36}$$

$$J_{zz}^* = J_{zz}/\left(\frac{\rho}{2}L^4d\right) = \pi\left(\frac{d}{L}\right)^2\left(\frac{1}{12} + 0.017C_b\frac{B}{d} - 0.33\left(\frac{B}{L}\right)\right) \tag{3.37}$$

$$Y_{\dot{r}}^* = Y_{\dot{r}}/\left(\frac{\rho}{2}L^3d\right) = -\pi\left(\frac{d}{L}\right)^2\left(0.67\frac{B}{L} - 0.033\left(\frac{B}{L}\right)^2\right) \tag{3.38}$$

$$N_{\dot{v}}^* = N_{\dot{v}}/\left(\frac{\rho}{2}L^3d\right) = -\pi\left(\frac{d}{L}\right)^2\left(1.1\left(\frac{B}{L}\right) - 0.041\left(\frac{B}{L}\right)\right) \tag{3.39}$$

3.9 PD Control Algorithm

The traditional PD controller is used in this simulation programme and the algorithm is as follows.

$$\psi_{LOS} = a\tan\left(\frac{y_t - y}{x_t - x}\right) \tag{3.40}$$

$$\delta_{CTE} = K_{p1}(\psi_{CTE} - \psi) + K_{d1}(0 - r) \tag{3.41}$$

$$\delta_{LOS} = K_{p2}(\psi_{LOS} - \psi) + K_{d2}(0 - r) \tag{3.42}$$

$$d_{LOS} = \sqrt{(x_t - x)^2 + (y_t - y)^2} \tag{3.43}$$

$$d_{CTE} = y - y_t \tag{3.44}$$

$$\lambda = \frac{d_{CTE}}{\|y_0 - y_t\|} \tag{3.45}$$

$$\delta_r = \lambda\delta_{CTE} + (1 - \lambda) \cdot \delta_{LOS} \tag{3.46}$$

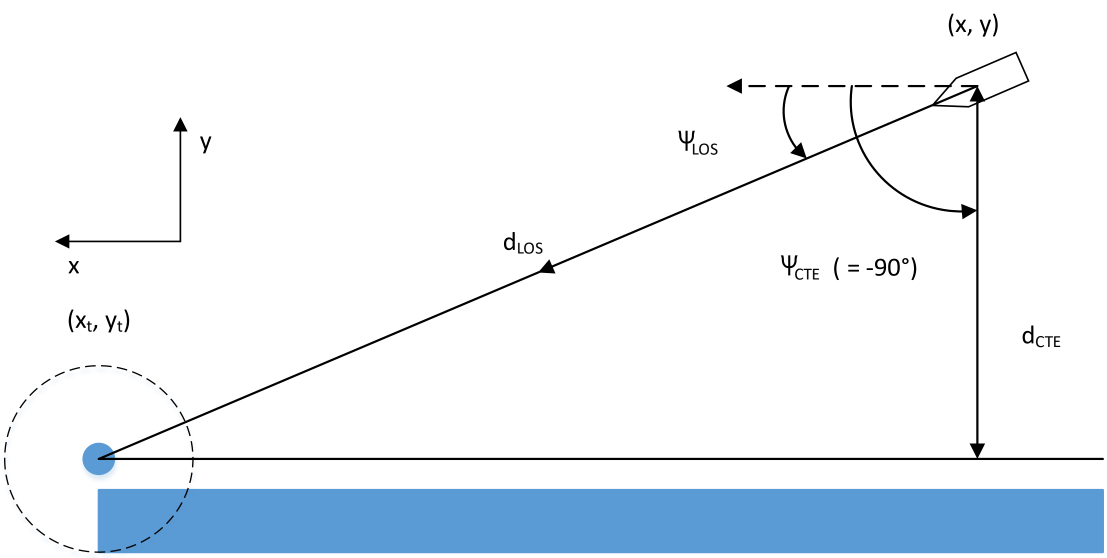

Figure 3.2 PD control algorithm

3.10 Model Predictive Control (MPC)

As introduced in the previous chapter, Model Predictive Control has been used in process industries successfully as an advanced method of process control. In this project, the MPC is used for developing an automatic time-domain simulation program for ship berthing operation along with the PD control and performs for generating optimal trajectory of a ship and following the path.

3.11 Kose's Mathematical Model in Model Predictive Control

In the application of MPC for ship berthing operation, Kose's mathematical model with vehicle speed U is as follows.

$$U = \sqrt{u^2 + v^2} \tag{3.47}$$

(1) Surge

$$\begin{aligned} X = (m + mY) \times v \times r + \left(\frac{\rho}{2} \times L^2 \times g\right) \times X_{vr} \times v \times r + \left(\frac{\rho}{2} \times L^2\right) \times X_{uu} \times |u| \times u \\ + \left(\frac{\rho}{2} \times L^2\right) \times X_{uvv} \times u \times \frac{v^2}{U} + \left(\frac{\rho}{2} \times L^2 \times g\right) \times X_{vvr} \times |v| \times v \times \frac{r}{U} \\ + X_r + X_p \end{aligned} \tag{3.48}$$

(2) Sway

$$\begin{aligned} Y = \left(\frac{\rho}{2} \times L^2\right) \times Y_v \times v \times U + \left(\frac{\rho}{2} \times L^2\right) \times Y_{vv} \times |v| \times v + \left(\frac{\rho}{2 \times L \times g^3}\right) \times Y_{vvvvv} \times v^5 \times \\ U^3 + \left(\frac{\rho}{2} \times L^{\frac{5}{2}} \times g^{\frac{3}{2}}\right) \times Y_r \times r \\ + \left(\frac{\rho}{2} \times L^2 \times g\right) \times Y_{ur} \times u \times r + \left(\frac{\rho}{2} \times L^2 \times g\right) \times Y_{uvvr} \times u \times v^2 \times \frac{r}{U^2} + \\ \left(\frac{\rho}{2} \times L^2 \times g^2\right) \times Y_{vrr} \times v \times \frac{r^2}{u} \\ + Y_r + Y_p \end{aligned} \tag{3.49}$$

(3) Yaw

$$N = \left(\frac{\rho}{2} \times L^3\right) \times N_{uv} \times u \times v + \left(\frac{\rho}{2} \times L^{\frac{7}{2}} \times g^{\frac{3}{2}}\right) \times N_r \times r + \left(\frac{\rho}{2} \times L^{\frac{5}{2}} \times g^{\frac{5}{2}}\right) \times N_{rrr} \times r^3$$

$$+ \left(\frac{\rho}{2} \times L^3 \times g\right) \times N_{ur} \times u \times r + \left(\frac{\rho}{2} \times L^{\frac{5}{2}} \times g^{\frac{1}{2}}\right) \times N_{vvr} \times v^2 \times r$$

$$+N_r + N_p \tag{3.50}$$

(4) State-space

Equations of motion for a manoeuvring at low advance speed are given as the following system of three scalar equations:

$$(m + m_x)\dot{u} - \left(m - m_y\right)vr = X \tag{3.51}$$

$$\left(m + m_y\right)\dot{v} + (m + m_x)ur = Y \tag{3.52}$$

$$(I_{zz} + J_{zz})\dot{r} = N \tag{3.53}$$

Where,

m: mass of the ship

m_x, m_y: added mass in surge and sway, respectively

I_{zz}: ship's moment of inertia

J_{zz}: propeller's moment of inertia

X: sum of the hydrodynamic (hull), propeller and rudder forces along the x-axis (inertial system of reference)

Y: sum of the hydrodynamic (hull), propeller and rudder forces along the y-axis (inertial system of reference)

N: sum of the hydrodynamic (hull), propeller and rudder moments about the z-axis (inertial system of reference)

u: velocity along the x-axis (inertial system of reference)

v: velocity along the y-axis (inertial system of reference)

r: angular velocity about z-axis (inertial system of reference)

The above system of scalar equations can be written in a matrix form $M\ddot{q} = f$, where M is an inertia matrix, $M = \begin{bmatrix} m+m_x & 0 & 0 \\ 0 & m+m_y & 0 \\ 0 & 0 & I_{zz}+J_{zz} \end{bmatrix}$,

$\ddot{q} = [\dot{u} \quad \dot{v} \quad \dot{r}]^T$ is a vector of generalised accelerations and

$f = \left[X + \left(m - m_y\right)vr \quad Y - (m + m_x)ur \quad N\right]$ is a vector of the external forces

$$\begin{bmatrix} m+m_x & 0 & 0 \\ 0 & m+m_y & 0 \\ 0 & 0 & I_{zz}+J_{zz} \end{bmatrix} \begin{bmatrix} \dot{u} \\ \dot{v} \\ \dot{r} \end{bmatrix} = \begin{bmatrix} X + \left(m - m_y\right)vr \\ Y - (m + m_x)ur \\ N \end{bmatrix} \tag{3.54}$$

Multiplying both sides of the above equation by the inverse of the inertia matrix, M^{-1} allows to express the accelerations as

$$\begin{bmatrix} \dot{u} \\ \dot{v} \\ \dot{r} \end{bmatrix} = \begin{bmatrix} \left(X + \left(m - m_y\right)vr\right)(m + m_x)^{-1} \\ (Y - (m + m_x)ur)\left(m + m_y\right)^{-1} \\ N(I_{zz} + J_{zz})^{-1} \end{bmatrix} \tag{3.55}$$

Taking into account that $[\dot{x} \quad \dot{y} \quad \dot{\psi}]^T = [u \quad v \quad r]^T$ it is possible to express the time-derivative of the state vector $X = [u \quad v \quad r \quad x_0 \quad y_0 \quad \psi]^T$ as

$$\dot{X} = \begin{bmatrix} \dot{u} \\ \dot{v} \\ \dot{r} \\ \dot{x_0} \\ \dot{y_0} \\ \dot{\psi} \end{bmatrix} = \begin{bmatrix} \left(X_H + X_P + X_R + \alpha_1 u + \alpha_2 u^2 + \left(m - m_y\right)vr\right)(m + m_x)^{-1} \\ (Y_H + Y_R - (m + m_x)ur)\left(m + m_y\right)^{-1} \\ (N_H + N_R)(I_{zz} + J_{zz})^{-1} \\ u\cos\psi - v\sin\psi \\ u\sin\psi + v\cos\psi \\ r \end{bmatrix} \tag{3.56}$$

Where x_0 and y_0 are coordinates of the centre of gravity of the ship within the Earth-fixed coordinate system and ψ is the yaw angle.

4. Methodology

4.1 Preamble

This chapter presents the methodology employed in this study, including collection of information on berthing operation, development of simulation programmes, and data analyses based on experimental design. Firstly, wide range of subjects related with berthing operation were collected and discussed in the previous chapters, with purpose of solving the stated problems in this study. Most of information was retrieved in the literature such as Journal of Ocean Engineering, Journal of Navigation, etc. Further, ship berthing operation was observed in Aberdeen Harbour, Scotland. And Korea Maritime University in the Republic of Korea was visited to meet and discuss with professors who had been engaged in the berthing operation job.

Secondly, simulation programmes are verified by comparing the numerical and analytical solutions and by testing the trajectory of ship turning circle, and yaw rate and speed of the model ship. And PD control algorithm is developed to compare the two mathematical models of Kose and normal MMG. In addition, the PD control algorithm is compared with the ANN of Hasegawa. This process was primarily done in the computer laboratory of the department of naval architecture and ocean engineering in Busan National University, located in south coast of the Republic of Korea, as the computer was utilized for performing simulation and analysing the output.

Thirdly, the complete design of the experiment is illustrated to get proper output. Research hypotheses are also postulated for the purpose of investigating the comparative performance of the two mathematical models which were deeply discussed in the previous chapter. In order to conduct the statistical analyses of the simulation data, this research employs formal statistical procedures including the analysis of variance.

4.2 Initial Simulation Programme

The initial simulation programme is developed, using Matlab which is proper in this study. This language is characterised by stability to give experimental output such as graphical and numerical data. Under Kose's mathematical model, the PD control algorithm is compared with the ANN algorithm from Hasegawa.

4.2.1 Comparison of Numerical and Analytical Solutions

As the first step for developing the programme of ship berthing operation, the basic formula of motion equation has been programmed with both of the analytical way and the numerical way and the results have been compared. In particular, for the numerical calculation, two different programme codes for integration have been used and compared. Through the comparison and analysis of the results in this stage, it is verified that the initial programming for simple motion equation is working properly.

The initial equation is given as follows.

$$f(t) = F_0 \cos 0.8t \tag{4.1}$$

where,

$$F_0 = 1, w = 0.8$$
$$m = 1, c = 1, k = 1$$

The coefficient, m is mass coefficient, c is damping coefficient and k is spring coefficient, and the initial condition is $x(0) = 1, \dot{x}_0 = 10$. The simulation period is 30 seconds with starting time of 0 second, and finishing time of 30 seconds with time interval of 0.3 second.

As integration codes, the two modules of 'ode 45' and 'oderk' have been used in Matlab programming for verification purpose. Figure 4.1 shows the simulation results for harmonic vibration of 1 DOF (degree of freedom) system with Runge-Kutta 4th-order method.

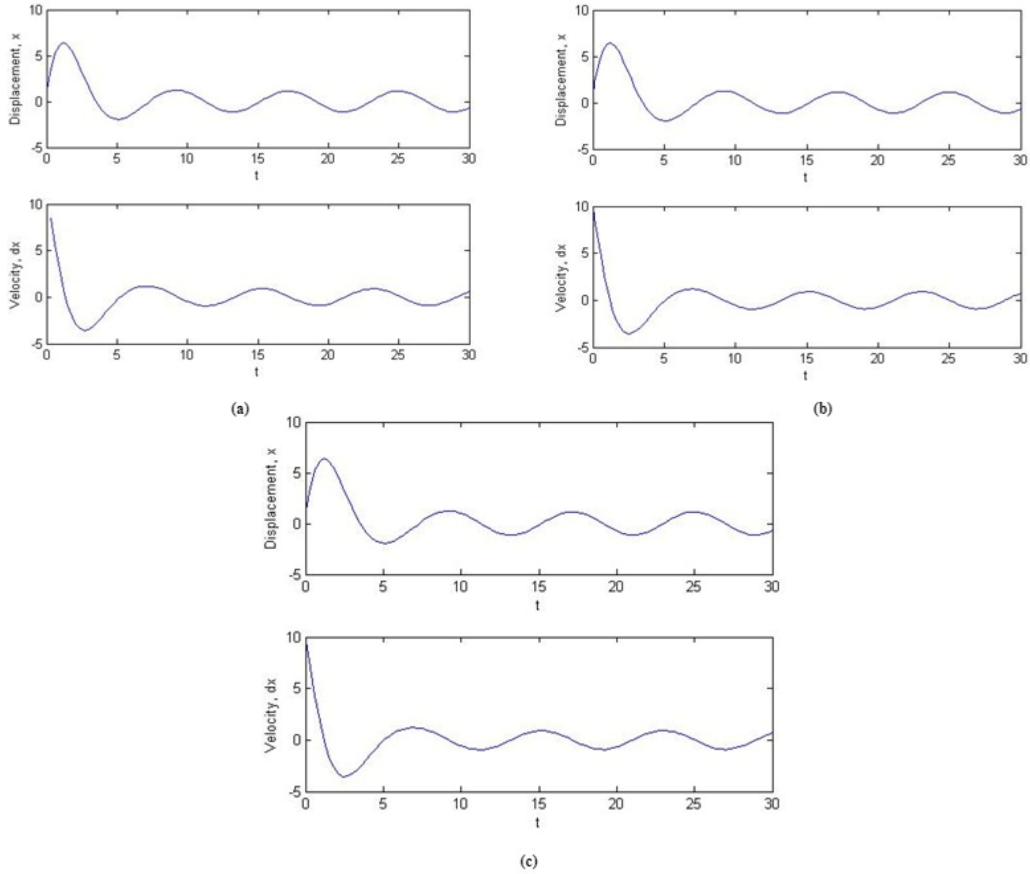

Figure 4.1 Harmonic vibration of 1 DOF (a) Analytical result (time step: 0.3 seconds) (b) Numerical result (ode 45, time step: default) (c) Numerical result (oderk, time step 0.3 seconds)

As shown in figure 4.1, the numerical programming presents good performance and the results of (b) and (c) are well-matched with the analytical result of (a).

4.2.2 Ship Turning Circle

As the second step, ship turning circle test is one of the most important and basic procedures for checking the manoeuvring performance. In particular, this simulation shows rudder performance with heading angle clearly. The simulation test has been performed with the mariner class vessel with the constant rudder angle $\delta_R = -35\deg$ applied at t = 50 sec.

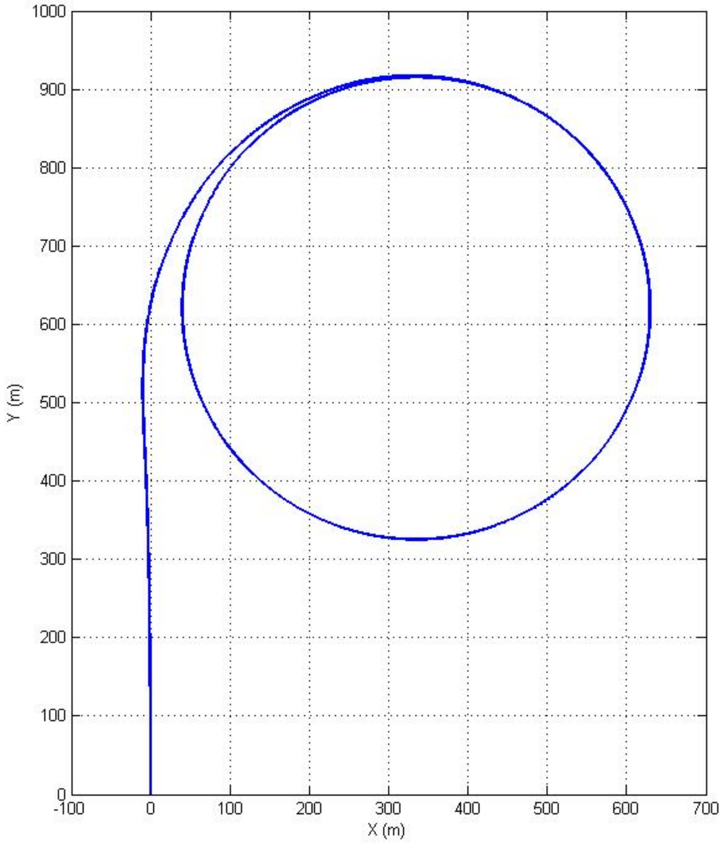

Figure 4.2 Trajectory of ship turning circle

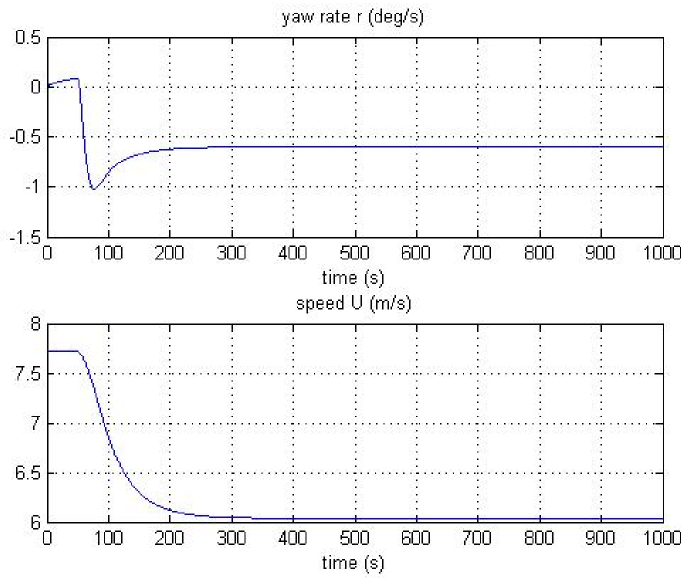

Figure 4.3 Yaw rate and speed for Mariner class vessel

As shown in figure 4.2, the trajectory of ship turning circle test is successfully simulated, and yaw rate and speed of the model ship are found valid as presented in figure 4.3.

4.3 Experimental Design of Simulation Programme Using PD Controller

The design for numerical experiment of simulation program using PD controller is explained. For this study, simulations have been performed with a model of tanker ship and the ship particulars are presented in table 4.1.

Table 4.1 Ship particulars

Length	L	304.0 m
Breadth	B	52.5 m
Mean draught	d	17.4 m
Block coefficient	C_b	0.827
Mass	m	2.350×10^8 kg
Moment of inertia	I_{zz}	1.018×10^{12} kgm^2
Wetted surface area	S	2.259×10^4 m^2
Propeller diameter	D_P	8.5 m
Rudder area	A_R	98.0 m^2
Rudder height	h	12.94 m
Rudder aspect ratio	Λ_R	1.709

4.3.1 The Scheme of Simulation

Based on the initial programme, the simulation programme using PD controller is developed, considering the two mathematical models of Kose and MMG. As stated in the first chapter, the three constituent elements were considered in the experimental design as follows: problem factors, measure of performance evaluation and simulation time.

Firstly, the two problem factors were considered such as starting point and initial heading angle in the experimental design. The combination of the two factors obviously influences the quality of the performance. In order to find the proper range of heading angles, 20 cases of initial heading angle were randomly chosen between -180 degrees and +180 degrees. As a result, this study could determine the range from 0 to -90 degrees and divide it into three areas as shown in Figure 4.4.

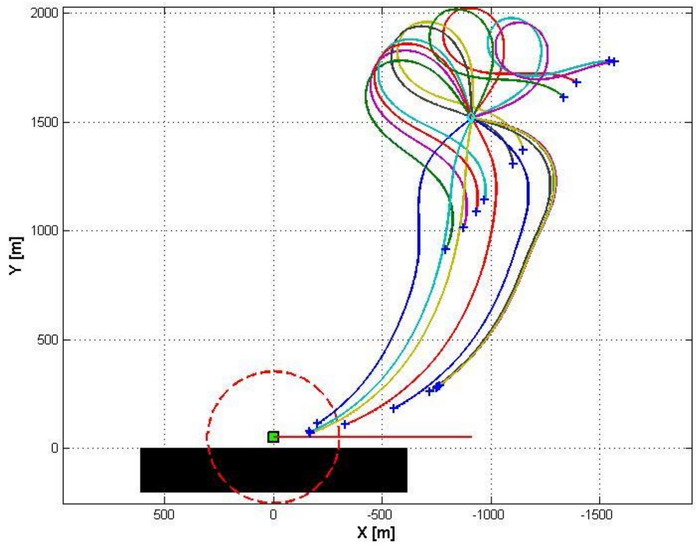

Figure 4.4 Berthing simulation with 20 random cases of initial heading angle of ship (range of heading angle from -180 to +180 degrees, simulation time 550 seconds, initial position of ship (-3L, 5L), initial speed of ship 3 m/s, model ship: tanker, Kose's model)

Based on the observation of practical berthing operations, the starting point was defined in terms of the length of tanker ship from the point of berthing place. The experimental levels were designated as (-3L, 5L), (-5L, 3L), (-5L, 4L), and (-6L, 2L) in the coordinate system. Further, the initial heading angles included three factor levels such as [0 ~ -30], [-30 ~ -60], and [-60 ~ -90]. Thus, the experimental levels of the two factors were determined as follows in table 4.2.

Table 4.2 Experimental level of the factors

Factor	Level
Starting point [1)]	(-3L, 5L), (-5L, 3L), (-5L, 4L), (-6L,2L)
Initial heading angles[2)]	[0 ~ -30], [-30 ~ -60], [-60 ~ -90]

1) L denotes the length of ship.

2) tangent degrees

A fixed set of 12 (4×3) treatments was obtained by determining all combinations of the factor levels of the two ways.

Secondly, in order to compare the quality of algorithm performance, the simulation results of berthing operation were analysed in the experimental design. As the arrival point targeted by the ship, a circle was depicted, its radius being a length of the model ship. If the simulated ship was judged to arrive within the circle, the result was considered successful within given simulation time. If not, unsuccessful.

Thirdly, the berthing problem is concerned with the 'safe landing' to be operated under the time efficiency. Practically, the solution of such problems requires a reasonable amount of computational time. Simulation time was firstly limited to 550 seconds and then extended to 650 seconds in order to find successful operations.

Considering the three constituents, a simulation program is developed by the researcher using Matlab language which is widely employed in engineering fields. Assuming uniform distribution, random number was generated in the range of the heading angles.

Test data was generated using an IBM computer. The simulation program was developed to introduce Kose and MMG model, respectively. The two mathematical programming models were implemented onto the simulator. The program was found to be able to solve optimization problems in the above-mentioned simulation times.

4.3.2 Design of the Numerical Experiments

The complete experimental design is illustrated in table 4.3, which describes the experimental design for evaluating the quality of the two mathematical models producing success of berthing operation under the two types of simulation time of 550 and 650 seconds, respectively.

Table 4.3 Layout of the experimental design for the two models

Starting Point	Initial Heading Angles	Simulation time (550 seconds)		Simulation time (650 seconds)	
		Kose (10 vectors for each cell)	MMG (10 vectors for each cell)	Kose (30 vectors for each cell)	Kose (30 vectors for each cell)
(-3L, 5L)	[0 ~ -30]				
(-3L, 5L)	[-30 ~ -60]				
(-3L, 5L)	[-60 ~ -90]				
(-5L, 3L)	[0 ~ -30]				
(-5L, 3L)	[-30 ~ -60]				
(-5L, 3L)	[-60 ~ -90]				
(-5L, 4L)	[0 ~ -30]				
(-5L, 4L)	[-30 ~ -60]				
(-5L, 4L)	[-60 ~ -90]				
(-6L, 2L)	[0 ~ -30]				
(-6L, 2L)	[-30 ~ -60]				
(-6L, 2L)	[-60 ~ -90]				

As an initial step, the resulting performance was deliberately analysed to make judgement on its successful berthing operation. That is, the number of successful cases was counted for each cell to allow easy comparisons under the two types of time. As an example, table 4.4 shows the case of Kose's model of 10 vectors under the simulation time of 550 seconds.

The Kose’s model shows that the total number of successes is 21 of 120 cases, explaining only 17.5 % success rate. The performance was not good enough in all cases except the initial heading angles of [-30 ~ -60] and [-60 ~ -90] when the starting point was set at (-3L, 5L). Full version of results is to be indicated in the next chapter.

Table 4.4 Results of Kose's model of 10 vectors under the simulation time of 550 seconds

Starting Point	Initial Heading Angles			
	[0 ~ -30]	[-30 ~ -60]	[-60 ~ -90]	Sum
(-3L, 5L)	1	10	10	21
(-5L, 3L)	0	0	0	0
(-5L, 4L)	0	0	0	0
(-6L, 2L)	0	0	0	0
Sum	1	10	10	21

4.3.3 Hypotheses Test

The two-factor analysis of variance (ANOVA) tool was employed to make mean comparison by testing the following research hypothesis: there are differences in mean successful operations between the two models. Its purpose is to statistically investigate the comparative abilities of the two models. The hypothesis test was done for the 10 vectors and 30 vectors, respectively. Accepting or rejecting the hypothesis depends on the critical value of t statistic. In the test, a significance level of 0.05 was used.

4.4 Comparison of PD and ANN Controllers

To propose the reference of the simulation program, the PD control algorithm is compared with the ANN of Hasegawa under the Kose’s mathematical model in terms of trajectory, rudder angle and speed of the model ship. The detailed comparison and result will be discussed in the next chapter.

4.5 Simulation using Model Predictive Control

To extend the development of a simulation program with a different control algorithm and to study the feasibility on the simulation of ship berthing operation, the Model Predictive Control is used with Kose's mathematical model and simulations are performed. Through the simulations, generating optimal trajectory and following the path will be analysed in the next chapter.

4.6 Closure

This chapter presents the research methodology utilised in conducting the investigation. It specifies the experimental design in terms of problem factors, performance and success rate. Next, two types of simulation times were set to compare of effectiveness of Kose's and MMG models. Furthermore, the PD control algorithm was compared with the ANN of Hasegawa. The methodological data collection and testing techniques were explained in this chapter.

5. Time-Domain Simulations of Ship Berthing Operation

5.1 Preamble

With the methodologies mentioned above, time-domain simulation programs have been developed and simulations have been performed with the following steps:

(1) Simulating and comparing berthing operations using Proportional Derivative (PD) control

- Application of Kose's mathematical model
- Application of MMG model

(2) Comparing project analysis with the result from Artificial Neural Network

(3) Performing statistical analysis

- Simulation time 550 seconds
- Simulation time 650 seconds

(4) Simulating berthing operations using Model Predictive Control (MPC)

5.2 Berthing Simulation using Proportional Derivative (PD) Control

The simulation results using PD control algorithm are presented in this chapter. As described in the previous chapter, the simulations have been performed in four different cases with different initial positions, heading angles and speed for a tanker ship and the coordinates of the initial positions for each case are (-5L, 4L), (-5L, 3L) and (-6L, 2L), where L denotes the length of the model ship. Through this chapter, the simulation case for the initial position of (-5L, 4L) is analysed and Kose's mathematical model for low advance speed of ships and the MMG model for normal advance speed are applied for comparative analysis. Table 5.1 shows the simulation cases and conditions in this study and table 5.2 presents the hydrodynamic derivatives of Kose's mathematical model. For the simulation using PD control, simulation time is set to 2000 seconds and sampling time is set to 0.1 seconds.

Through the simulation, the ship trajectory of berthing operation is presented for showing the entire movement of the model ship. And also, the variations of RPS and δ_r are shown in figures to be analysed for the control of speed and rudder angle of the ship. Furthermore, the variation of heading angle is presented to be analysed in accordance with the control algorithm.

Table 5.1 Simulation case and condition

Case	Ship Position (L: Ship Length)	Heading Angle of Ship (Degree)	Ship Speed (m/s)	Rudder Height h (m)	Rudder Area A_r (m^2)	Rudder Aspect Ratio λ_r	Simulation Time (Sec)
(a)	(-5L,4L)	-40	3.0, 4.0	12.94, 15	98, 131.66	1.709	2000
(b)	(-5L,4L)	-70	3.0, 4.0	12.94, 15	98, 131.66	1.709	2000
(c)	(-5L,3L)	-40	3.0, 4.0	12.94, 15	98, 131.66	1.709	2000
(d)	(-6L,2L)	-30	3.0	12.94	98	1.709	2000

Table 5.2 Hydrodynamic derivatives of Kose's mathematical model

X^*_{vr}	-0.310×10^{-2}	N^*_{vvr}	-0.981×10^{-2}
X^*_{uu}	-0.457×10^{-3}	Y^*_{v}	-2.222×10^{-2}
X^*_{uvv}	2.927×10^{-3}	Y^*_{vv}	-2.173×10^{-2}
X^*_{vvr}	-0.558×10^{-2}	Y^*_{vvvvv}	0.0
N^*_{uv}	-7.910×10^{-3}	Y^*_{r}	1.287×10^{-5}
N^*_{r}	-1.632×10^{-4}	Y^*_{ur}	0.510×10^{-2}
N^*_{rrr}	-0.776×10^{-2}	Y^*_{uvvr}	-0.851×10^{-2}
N^*_{ur}	-1.584×10^{-3}	Y^*_{vrr}	-0.874×10^{-2}

5.2.1 Application of Kose's Mathematical Model

(1) Initial speed of ship 3 m/s in Kose's model

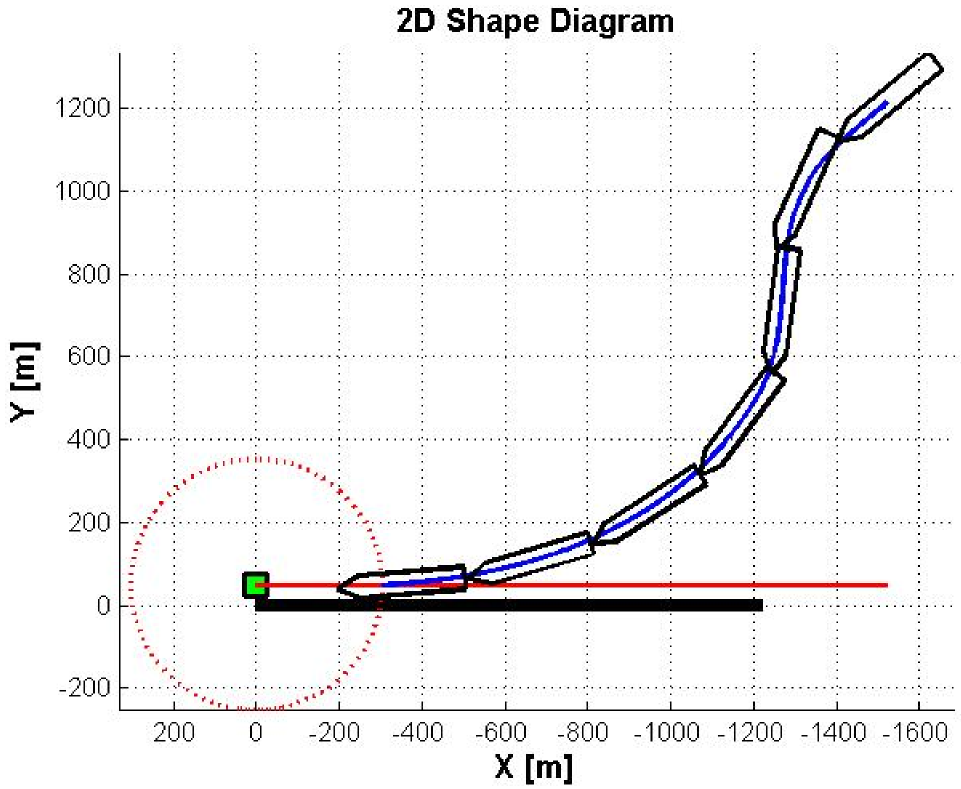

Figure 5.1 Trajectory for berthing simulation of tanker ship using PD controller with Kose's mathematical model: initial posision of ship (-5L, 4L), initial heading angle of ship -40 degrees and initial speed of ship 3 m/s

Figure 5.1 shows the trajectory for berthing operation of the model ship using PD controller with the Kose's mathematical model in case where the initial position of the model ship is (-5L, 4L), the initial heading angle is -40 degrees and the initial ship speed is 3 m/s. Also, 12.94 m of rudder height and 98 m^2 of rudder area are applied in this case. As shown in figure 5.1, the model ship is approaching parallel to the quay in the end of simulation.

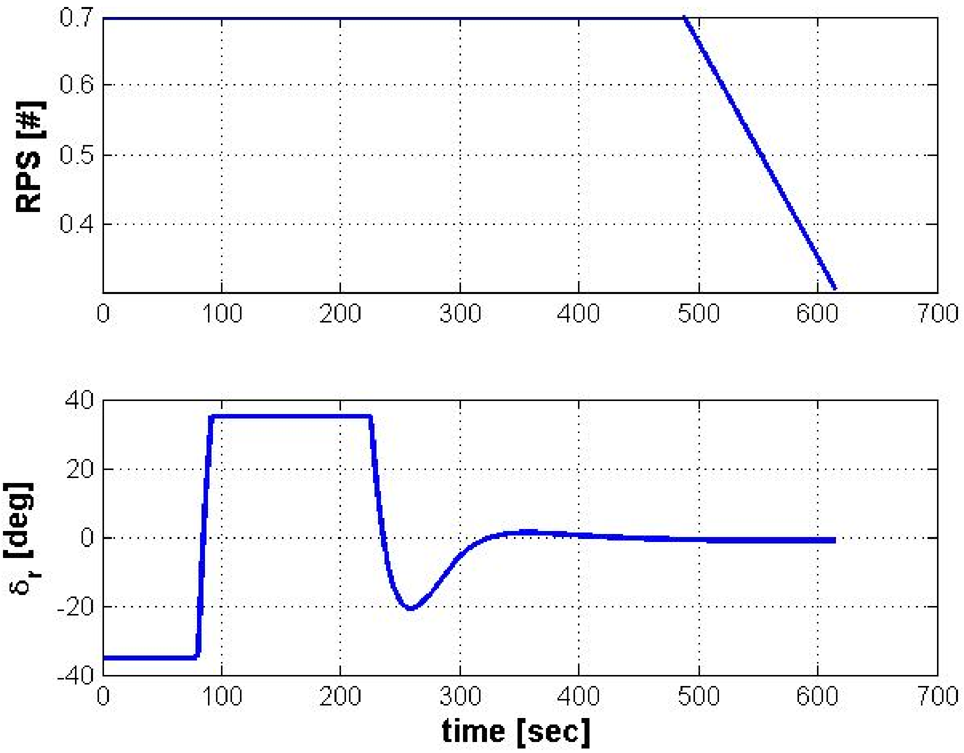

Figure 5.2 RPS and δr for berthing simulation of tanker ship using PD controller with Kose's mathematical model: initial position of ship (-5L, 4L), initial heading angle of ship -40 degrees and initial speed of ship 3 m/s

Figure 5.2 shows the variation of RPS and rudder angle, δ_r, during the simulation. As shown in figure 5.2, the variation of rudder angle is stable after movement between -35 degrees and +35 degrees for about 330 seconds from the beginning of simulation. However, the RPS starts to decrease rapidly from about 480 seconds of simulation time to stop the model ship and to complete the berthing operation.

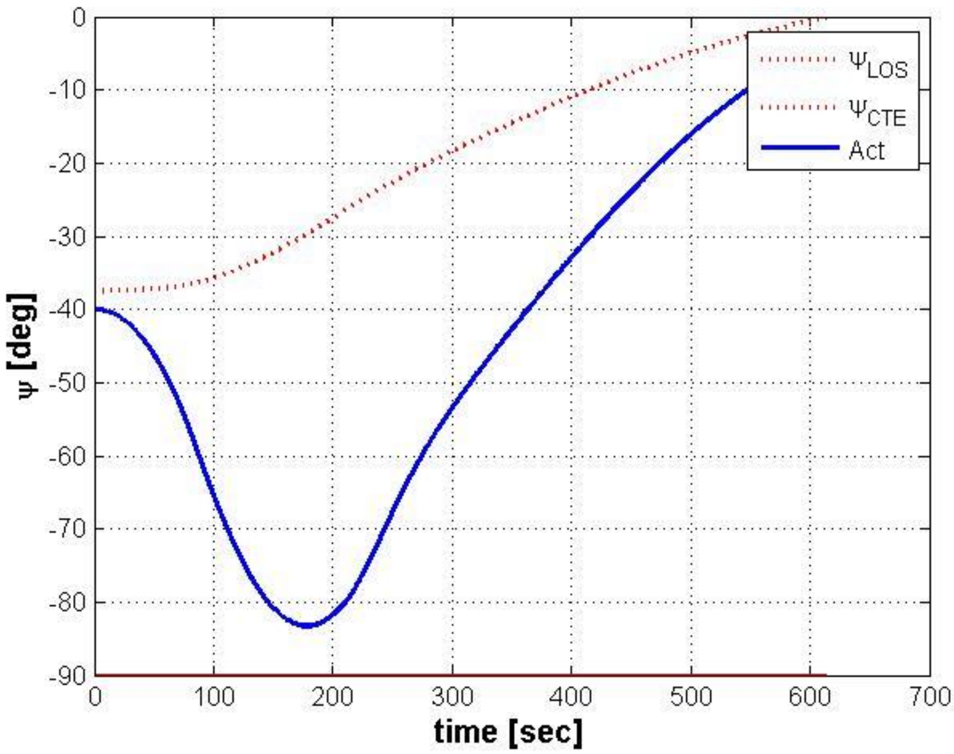

Figure 5.3 Heading angle ψ for berthing simulation of tanker ship using PD controller with Kose's mathematical model: initial position of ship (-5L, 4L), initial heading angle of ship -40 degrees and initial speed of ship 3 m/s

Figure 5.3 shows the variation of heading angle ψ with ψ_{LOS} and ψ_{CTE} during the berthing operation. As presented above, actual heading angle ψ is changed with large variation from -40 degrees to about -83 degrees at the beginning of the berthing process and starts to increase into 0 degree from about 180 seconds of simulation time.

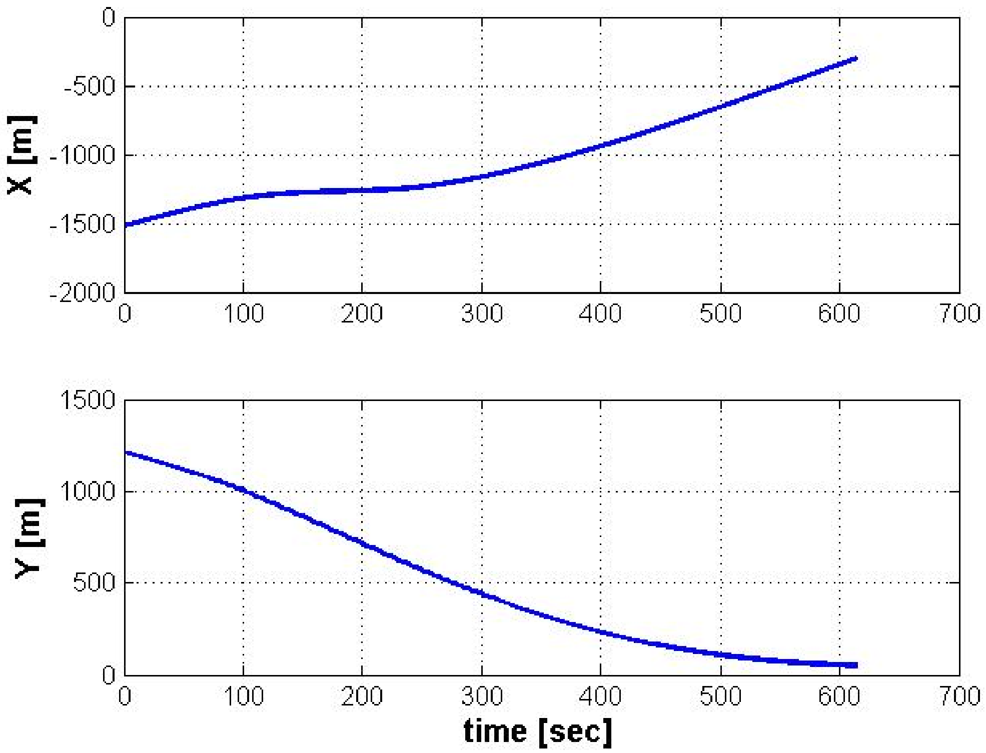

Figure 5.4 X and Y variation for berthing simulation of tanker ship using PD controller with Kose's mathematical model: initial position of ship (-5L, 4L), initial heading angle of ship -40 degrees and initial speed of ship 3 m/s

Figure 5.4 shows X and Y variations of the model ship during berthing process. Under the Kose's mathematical model, the model ship approaches to the target point (0, 0) smoothly in X and Y directions and completes the berthing operation successfully in about 610 seconds of simulation time.

(2) Initial speed of ship 4 m/s in Kose’s model

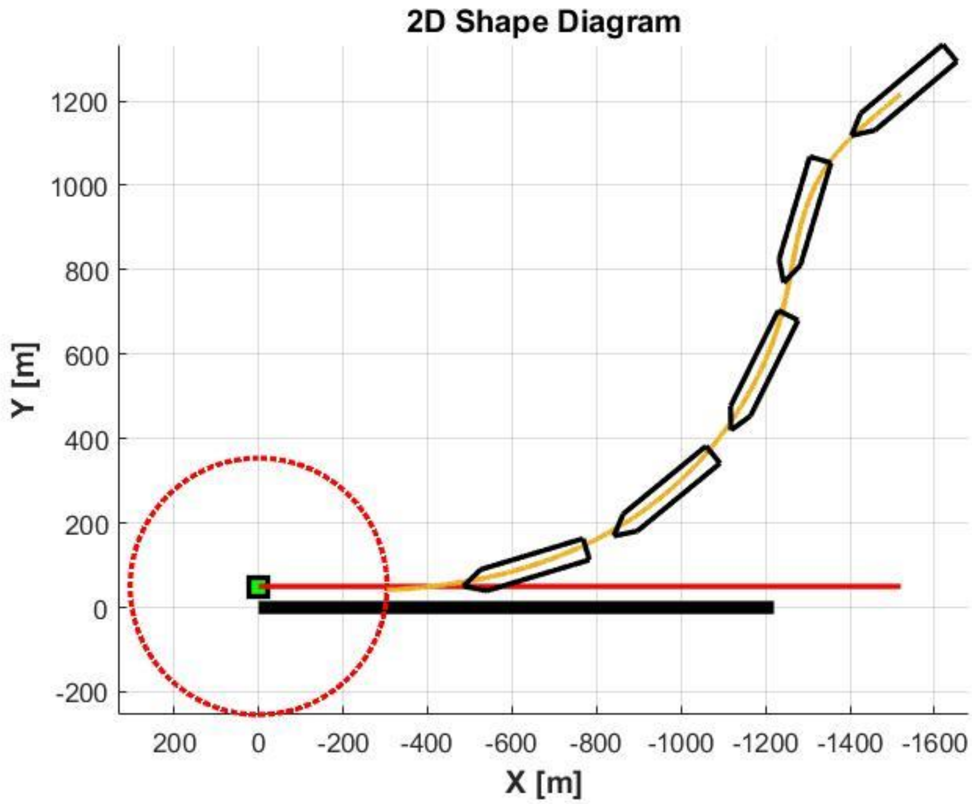

Figure 5.5 Trajectory for berthing simulation of tanker ship using PD controller with Kose's mathematical model: initial posision of ship (-5L, 4L), initial heading angle of ship -40 degrees and initial speed of ship 4 m/s

Figure 5.5 shows the trajectory for berthing operation of the model ship using PD controller with the Kose’s mathematical model in case where the initial position of the model ship is (-5L, 4L), the initial heading angle is -40 degrees and the initial ship speed is 4 m/s. Also, 12.94 m of rudder height and 98 m^2 of rudder area are applied in this case. As shown in figure 5.5, the berthing operation has been performed successfully from the starting point to the target point. However, the model ship is approaching to the line of 50 m above from the quay with about - 4 degrees of heading angle.

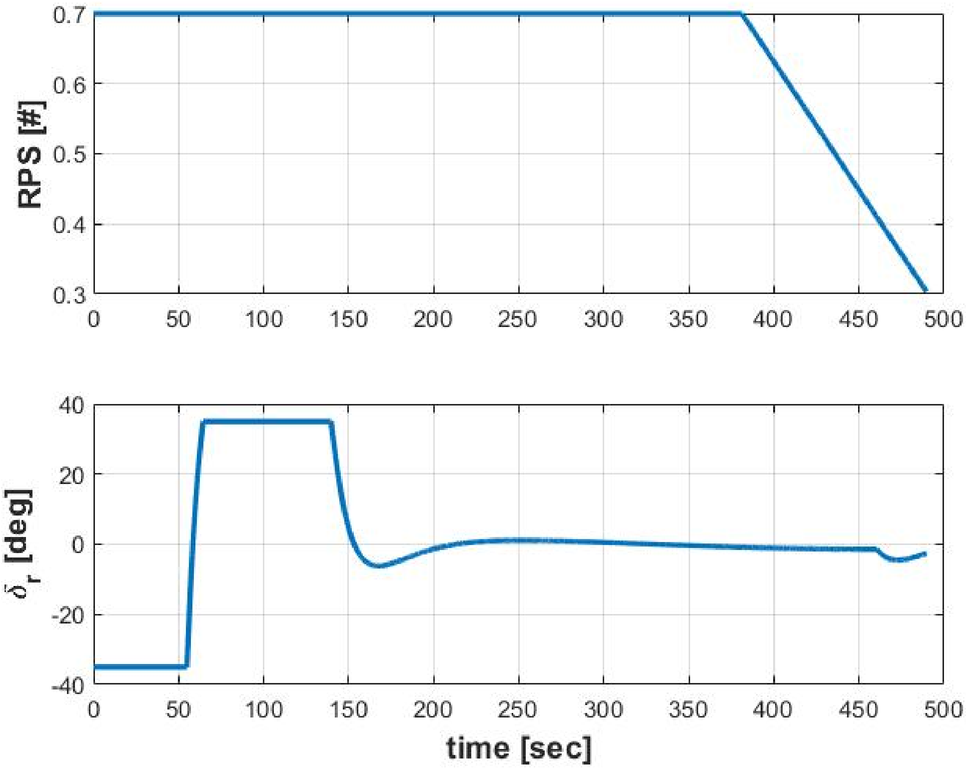

Figure 5.6 RPS and δr for berthing simulation of tanker ship using PD controller with Kose's mathematical model: initial position of ship (-5L, 4L), initial heading angle of ship -40 degrees and initial speed of ship 4 m/s

Figure 5.6 shows the variation of RPS and rudder angle, δ_r, during the simulation. As shown in figure 5.6, the variation of rudder angle becomes stable after movement between about -35 degrees and +35 degrees for about 230 seconds from the beginning of simulation. However, the RPS starts to decrease rapidly from about 380 seconds of simulation time to stop the model ship and to complete the berthing operation.

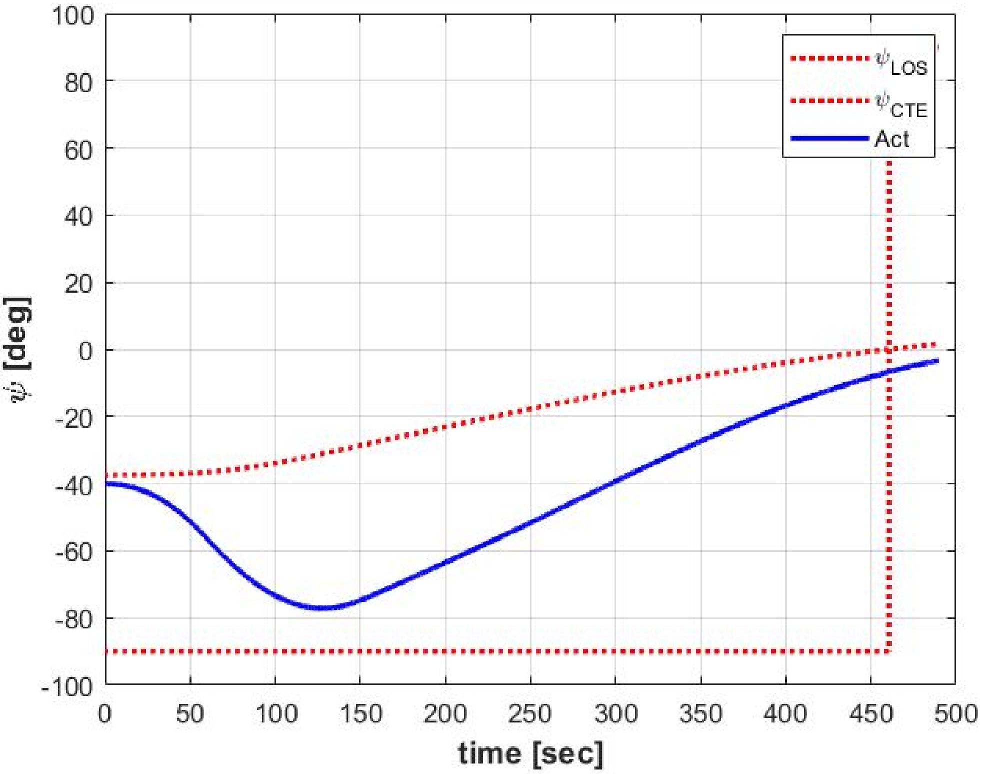

Figure 5.7 Heading angle ψ for berthing simulation of tanker ship using PD controller with Kose's mathematical model: initial position of ship (-5L, 4L), initial heading angle of ship -40 degrees and initial speed of ship 4 m/s

Figure 5.7 shows the variation of heading angle ψ with ψ_{LOS} and ψ_{CTE} during the berthing operation. As presented above, actual heading angle ψ is changed with large variation from -40 degrees to about -78 degrees at the beginning of the berthing process and starts to increase into 0 degree from about 125 seconds of simulation time.

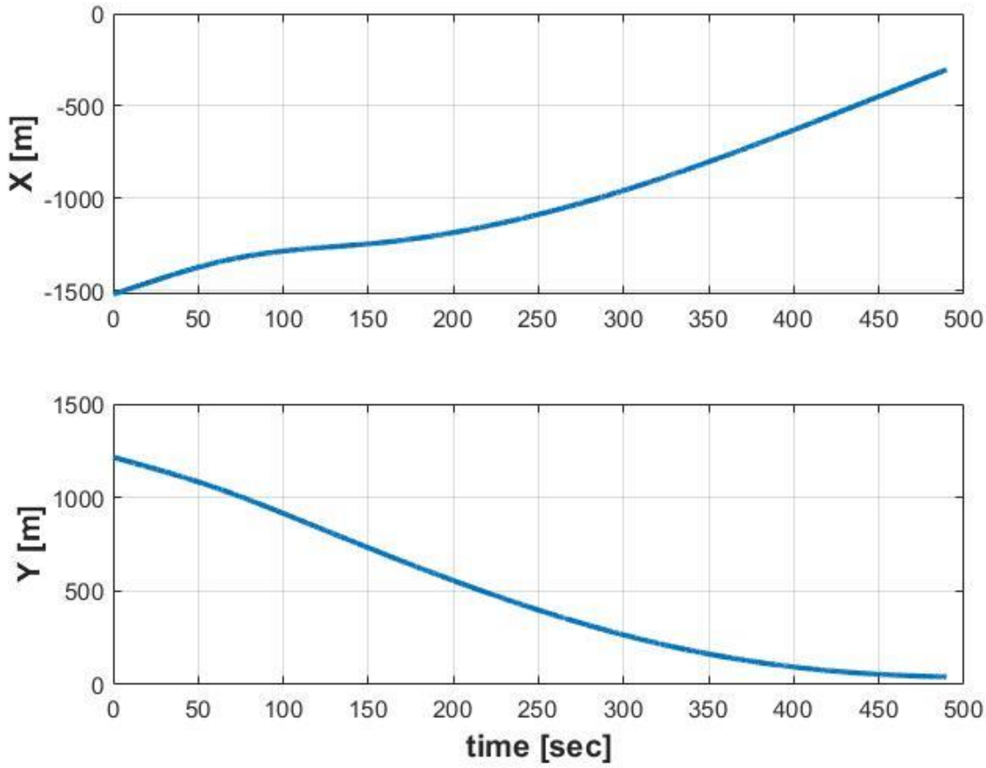

Figure 5.8 X and Y variation for berthing simulation of tanker ship using PD controller with Kose's mathematical model: initial position of ship (-5L, 4L), initial heading angle of ship -40 degrees and initial speed of ship 4 m/s

Figure 5.8 shows X and Y variations of the model ship during berthing process. Under the Kose's mathematical model, the model ship approaches to the target point (0, 0) smoothly in X and Y directions and completes the berthing operation successfully in about 490 seconds of simulation time.

(3) Increased rudder area with initial speed of ship 4 m/s in Kose’s model

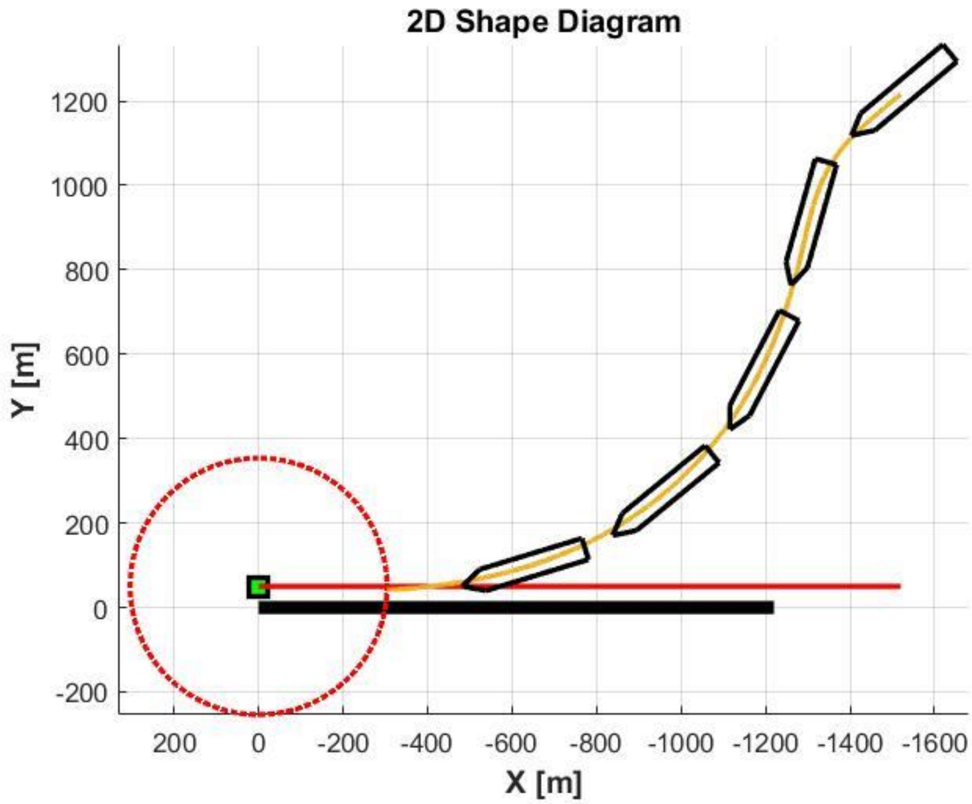

Figure 5.9 Trajectory for berthing simulation of tanker ship using PD controller with Kose's mathematical model: initial posision of ship (-5L, 4L), initial heading angle of ship -40 degrees, initial speed of ship 4 m/s, rudder height 15 m and rudder area 131.66 m^2

Figure 5.9 shows the trajectory for berthing operation of the model ship using PD controller with the Kose’s mathematical model in case where the initial position of the model ship is (-5L, 4L), the initial heading angle is -40 degrees, the initial ship speed is 4 m/s and the rudder area is 131.66 m^2 with rudder height 15 m. As shown in figure 5.9, the berthing operation has been performed successfully from the starting point to the target point. However, the model ship is approaching to the line of 50 m above from the quay with about - 4 degrees of heading angle.

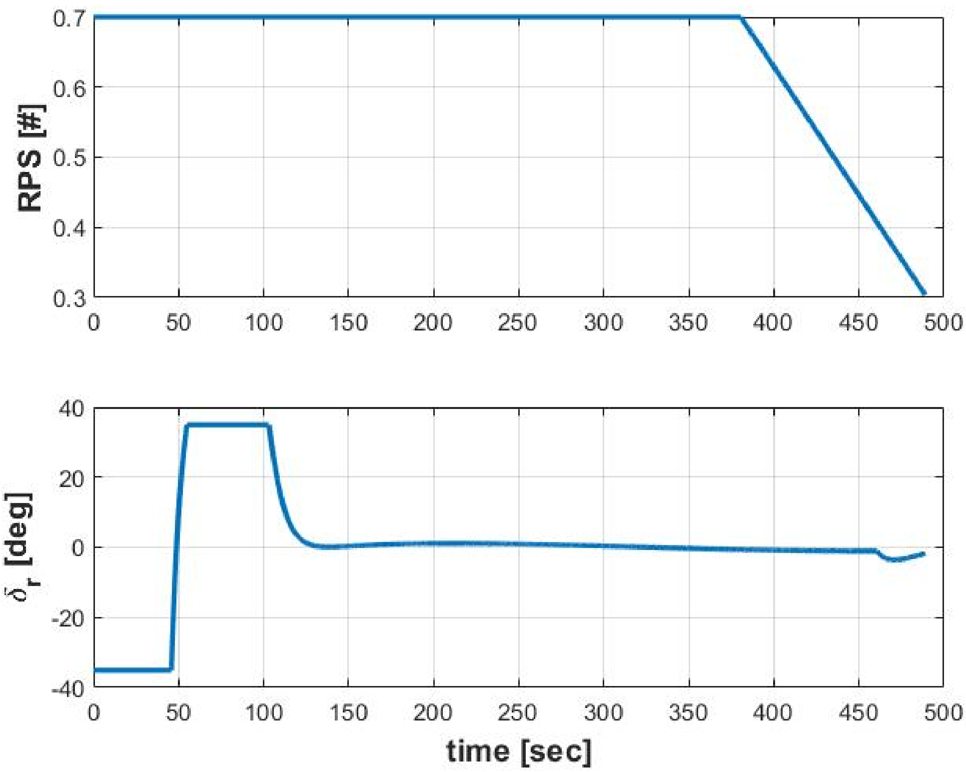

Figure 5.10 RPS and δr for berthing simulation of tanker ship using PD controller with Kose's mathematical model: initial position of ship (-5L, 4L), initial heading angle of ship -40 degrees, initial speed of ship 4 m/s, rudder height 15 m and rudder area 131.66 m^2

Figure 5.10 shows the variation of RPS and rudder angle, δ_r, during the simulation. As shown in figure 5.10, the variation of rudder angle becomes stable after movement between about -35 degrees and +35 degrees for about 130 seconds from the beginning of simulation. However, the RPS starts to decrease rapidly from about 380 seconds of simulation time to stop the model ship and to complete the berthing operation.

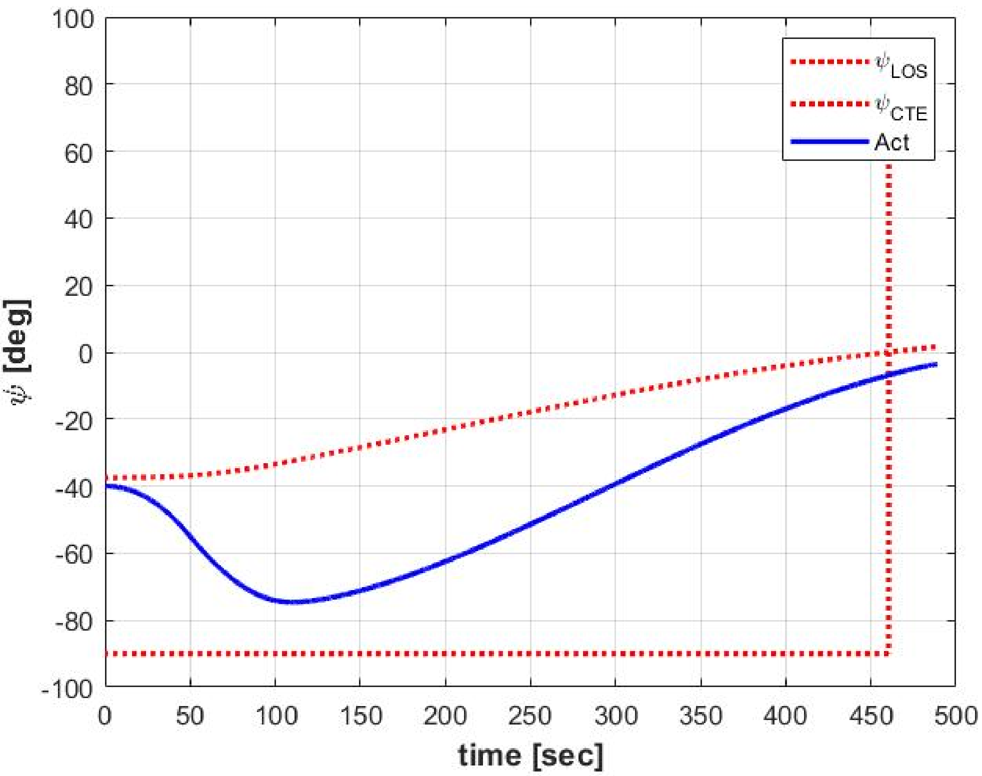

Figure 5.11 Heading ψ for berthing simulation of tanker ship using PD controller with Kose's mathematical model: initial position of ship (-5L, 4L), initial heading angle of ship -40 degrees, initial speed of ship 4 m/s, rudder height 15 m and rudder area 131.66 m^2

Figure 5.11 shows the variation of heading angle ψ with ψ_{LOS} and ψ_{CTE} during the berthing operation. As presented above, actual heading angle ψ is changed with large variation from -40 degrees to about -74 degrees at the beginning of the berthing process and starts to increase into 0 degree from about 110 seconds of simulation time.

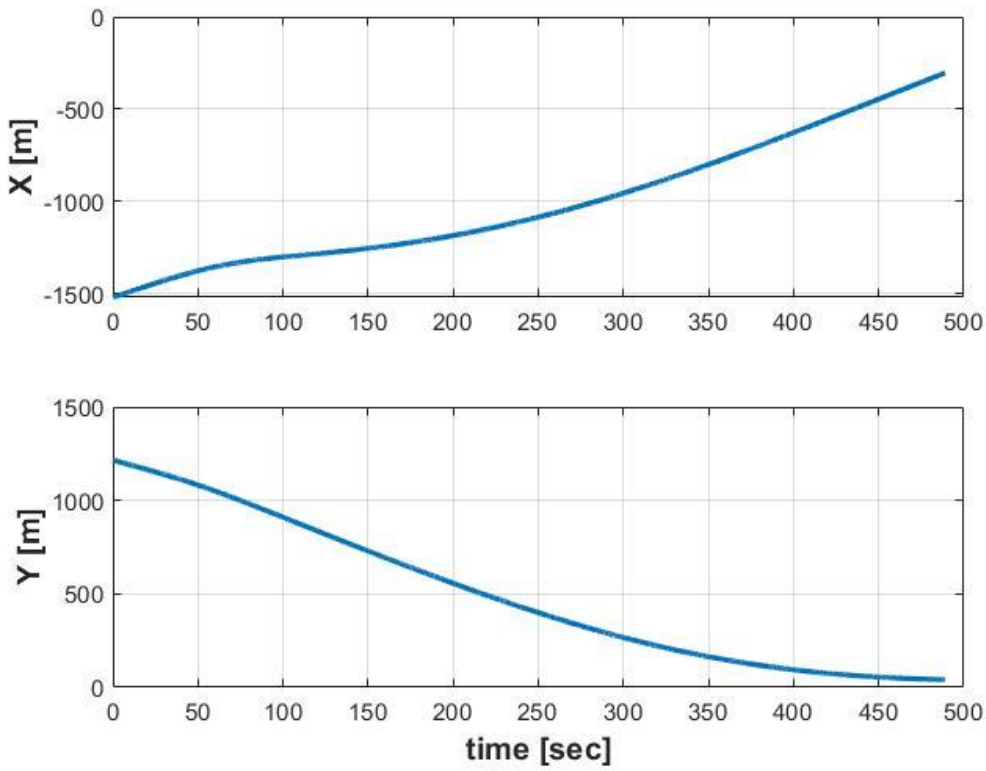

Figure 5.12 XY for berthing simulation of tanker ship using PD controller with Kose's mathematical model: initial position of ship (-5L, 4L), initial heading angle of ship -40 degrees, initial speed of ship 4 m/s, rudder height 15 m and rudder area 131.66 m^2

Figure 5.12 shows X and Y variations of the model ship during berthing process. Under the Kose's mathematical model, the model ship approaches to the target point (0, 0) smoothly in X and Y directions and completes the berthing operation successfully in about 490 seconds of simulation time.

5.2.2 Application of MMG Model

(1) Initial speed of ship 3 m/s in MMG model

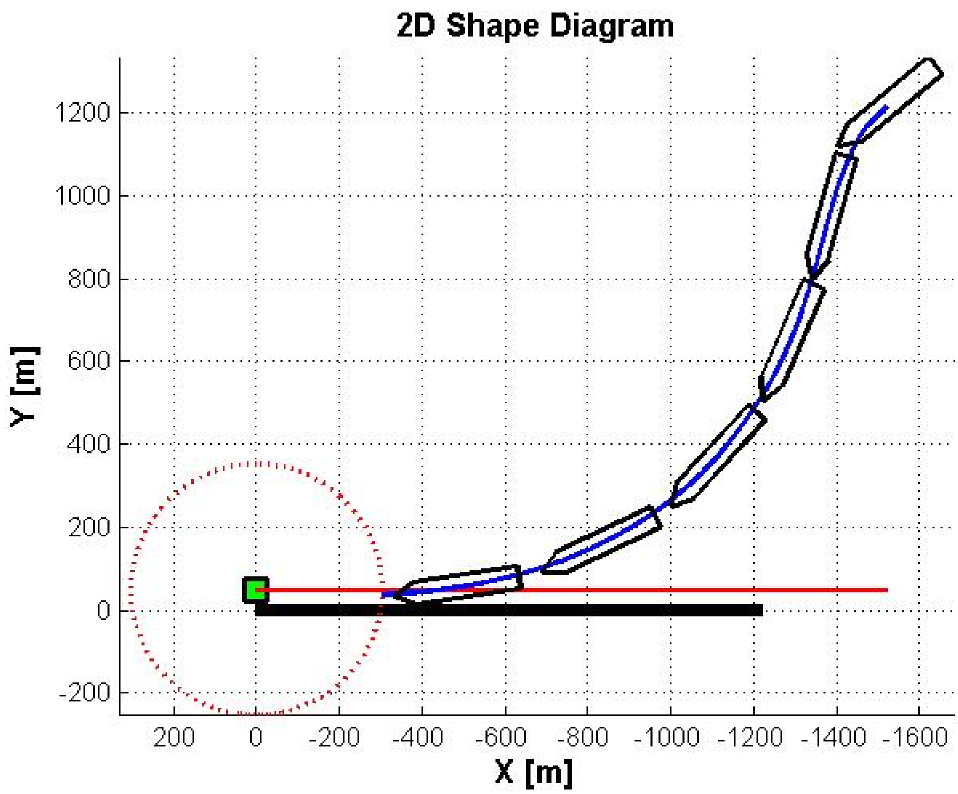

Figure 5.13 Trajectory for berthing simulation of tanker ship using PD controller with normal MMG model: initial position of ship (-5L, 4L), initial heading angle of ship -40 degrees and initial speed of ship 3 m/s

Figure 5.13 shows the trajectory for berthing operation of the model ship using PD controller with normal MMG model in the case where the initial position of the model ship is (-5L, 4L), the initial heading angle is -40 degrees and the initial ship speed is 3 m/s. Also, 12.94 m of rudder height and 98 m^2 of rudder area are applied in this case. As shown in figure 5.13, the model ship is changing its heading smoothly during the whole operation and approaching parallel to the quay in the end of simulation.

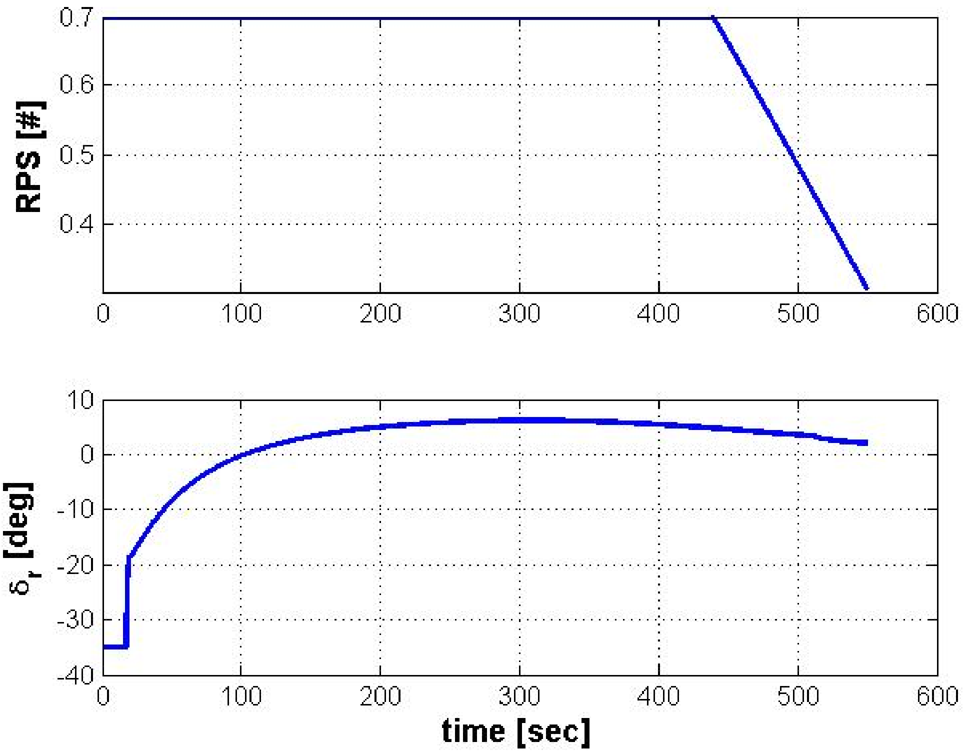

Figure 5.14 RPS and δr for berthing simulation of tanker ship using PD controller with normal MMG model: initial position of ship (-5L, 4L), initial heading angle of ship -40 degrees and initial speed of ship 3 m/s

Figure 5.14 shows the variation of RPS and rudder angle, δ_r, during the simulation. As shown in figure 5.14, the variation of rudder angle is stable between -35 degrees and +7 degrees. However, the RPS starts to decrease rapidly from about 440 seconds of simulation time to stop the model ship and to complete the berthing operation.

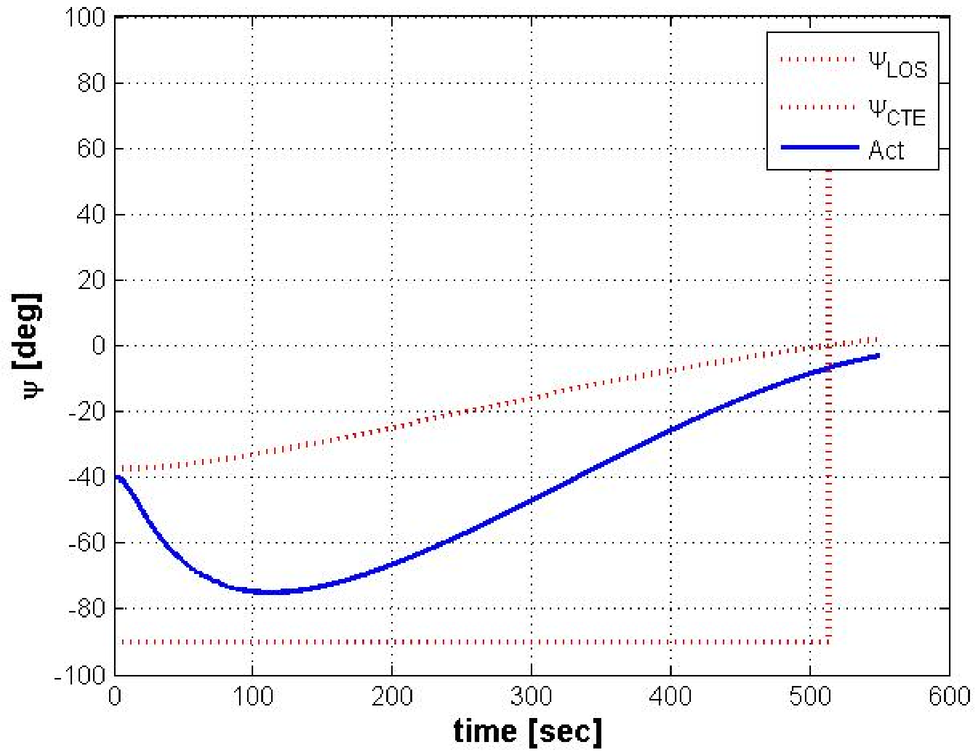

Figure 5.15 Heading angle ψ for berthing simulation of tanker ship using PD controller with normal MMG model: initial position of ship (-5L, 4L), initial heading angle of ship -40 degrees and initial speed of ship 3 m/s

Figure 5.15 shows the variation of heading angle ψ with ψ_{LOS} and ψ_{CTE} during the berthing operation. As presented above, actual heading angle ψ is changed with large variation from -40 degrees to about -75 degrees at the beginning of the berthing process and starts to increase into 0 degree from about 110 seconds of simulation time.

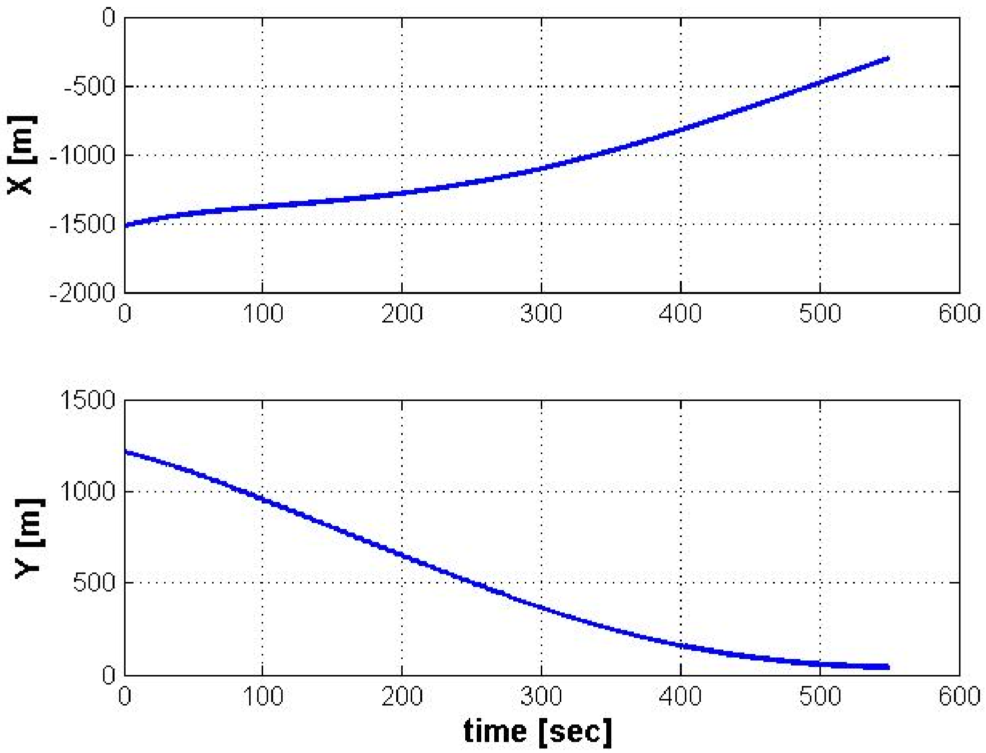

Figure 5.16 X, Y variation for berthing simulation of tanker ship using PD controller with normal MMG model: initial position of ship (-5L, 4L), initial heading angle of ship -40 degrees and initial speed of ship 3 m/s

Figure 5.16 shows X and Y variations of the model ship during berthing process. Under the normal MMG model, the model ship approaches to the target point (0, 0) smoothly in X and Y directions and completes the berthing operation successfully in about 550 seconds of simulation time.

(2) Initial speed of ship 4 m/s in MMG model

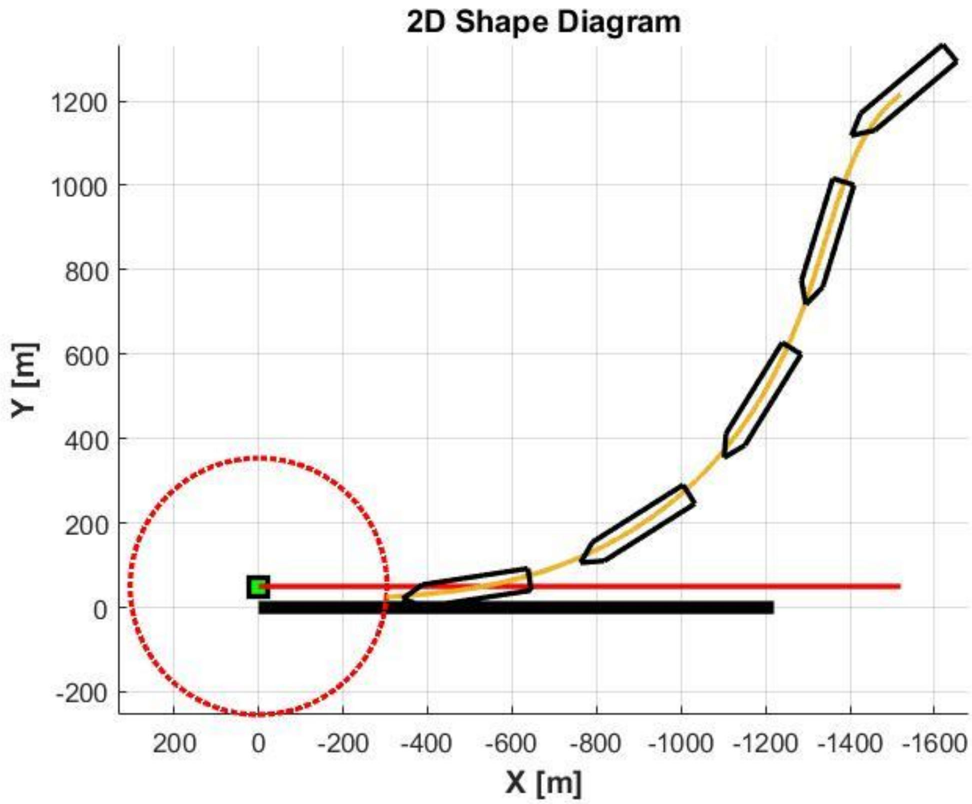

Figure 5.17 Trajectory for berthing simulation of tanker ship using PD controller with normal MMG model: initial position of ship (-5L, 4L), initial heading angle of ship -40 degrees and initial speed of ship 4 m/s

Figure 5.17 shows the trajectory for berthing operation of the model ship using PD controller with normal MMG model in the case where the initial position of the model ship is (-5L, 4L), the initial heading angle is -40 degrees and the initial ship speed is 4 m/s. Also, 12.94 m of rudder height and 98 m^2 of rudder area are applied in this case. As shown in figure 5.17, the model ship is changing its heading smoothly during the whole operation. However, it is approaching not enough parallel to the quay at the end of the simulation and cannot decrease its speed enough before it crashes into the quay.

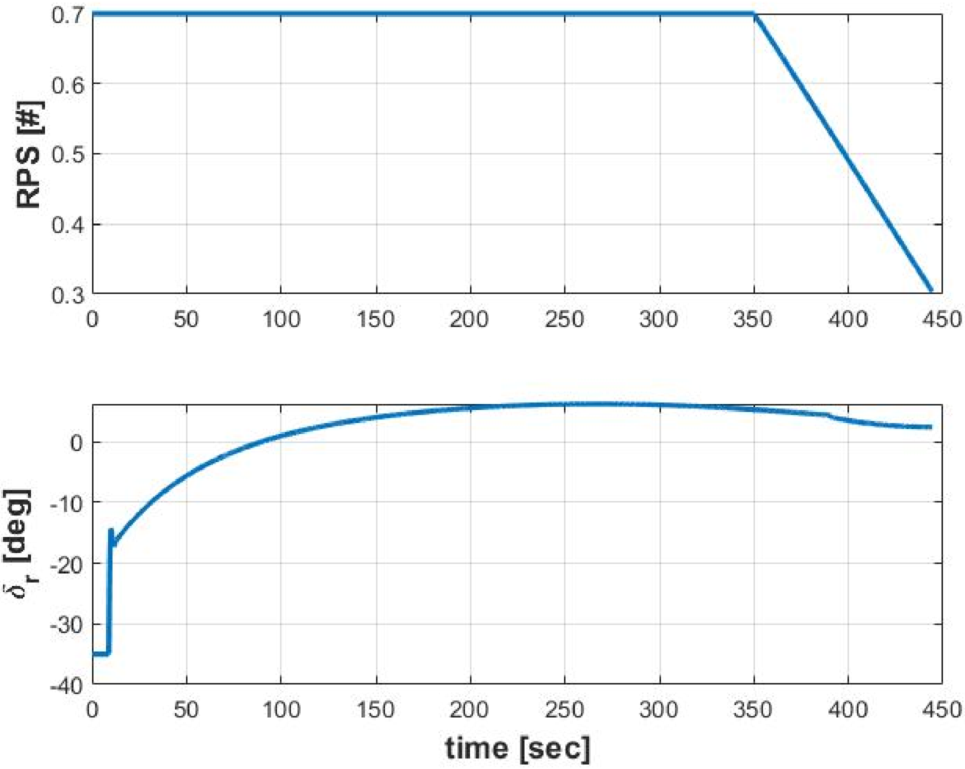

Figure 5.18 RPS and δr for berthing simulation of tanker ship using PD controller with normal MMG model: initial position of ship (-5L, 4L), initial heading angle of ship -40 degrees and initial speed of ship 4 m/s

Figure 5.18 shows the variation of RPS and rudder angle, δ_r, during the simulation. As shown in figure 5.18, the variation of rudder angle is stable between -35 degrees and +5 degrees. However, the RPS starts to decrease rapidly from about 350 seconds of simulation time to stop the model ship and to complete the berthing operation.

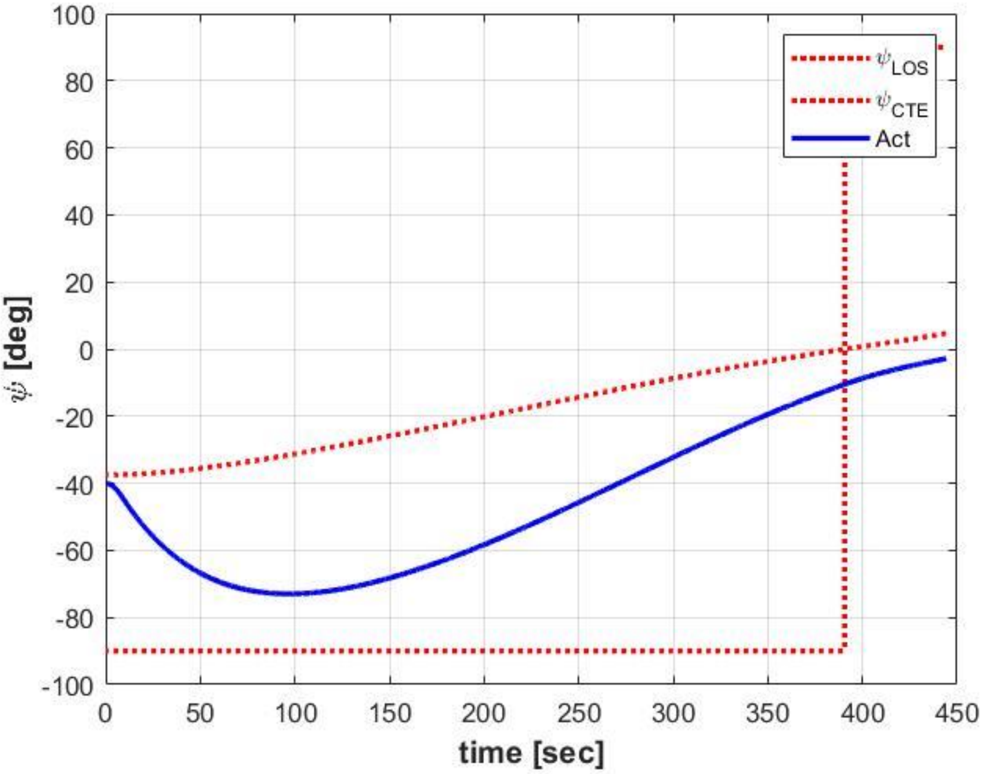

Figure 5.19 Heading angle ψ for berthing simulation of tanker ship using PD controller with normal MMG model: initial position of ship (-5L, 4L), initial heading angle of ship -40 degrees and initial speed of ship 4 m/s

Figure 5.19 shows the variation of heading angle ψ with ψ_{LOS} and ψ_{CTE} during the berthing operation. As presented above, actual heading angle ψ is changed with large variation from -40 degrees to about -73 degrees at the beginning of the berthing process and starts to increase into 0 degree from about 90 seconds of simulation time.

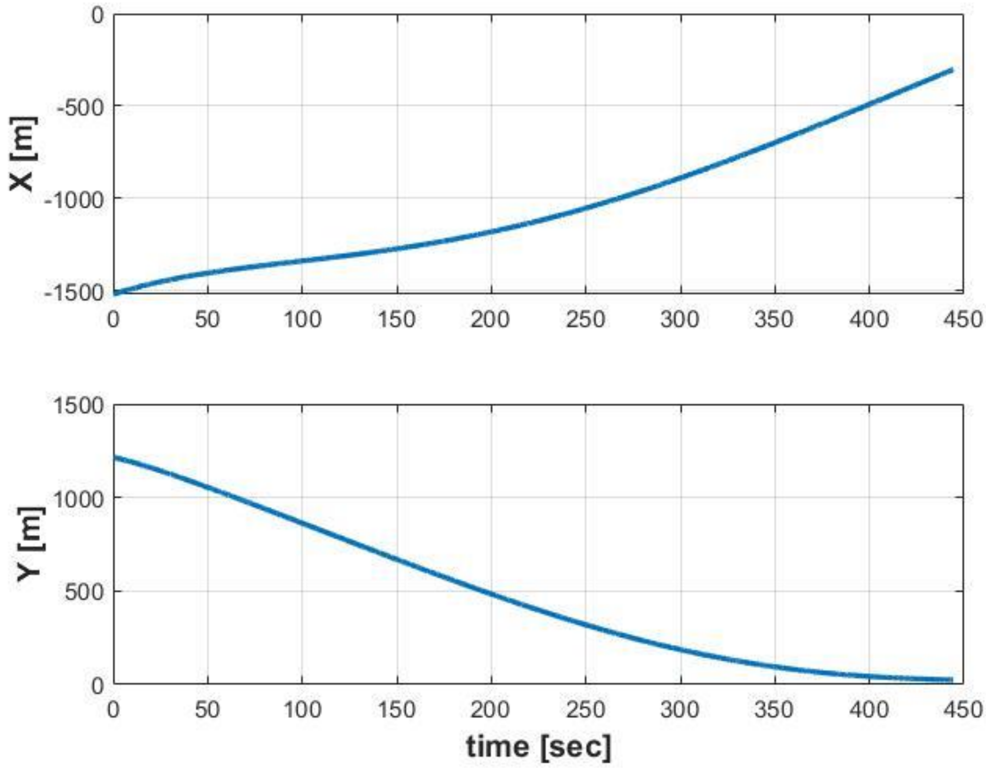

Figure 5.20 X, Y variation for berthing simulation of tanker ship using PD controller with normal MMG model: initial position of ship (-5L, 4L), initial heading angle of ship -40 degrees and initial speed of ship 4 m/s

Figure 5.20 shows X and Y variations of the model ship during berthing process. Under the normal MMG model, the model ship approaches to the target point (0, 0) smoothly in X and Y directions. However, it approaches 0 in Y direction already at 450 seconds of simulation time when it is still -250 m in X direction.

(3) Increased rudder area with initial speed of ship 4 m/s in MMG model

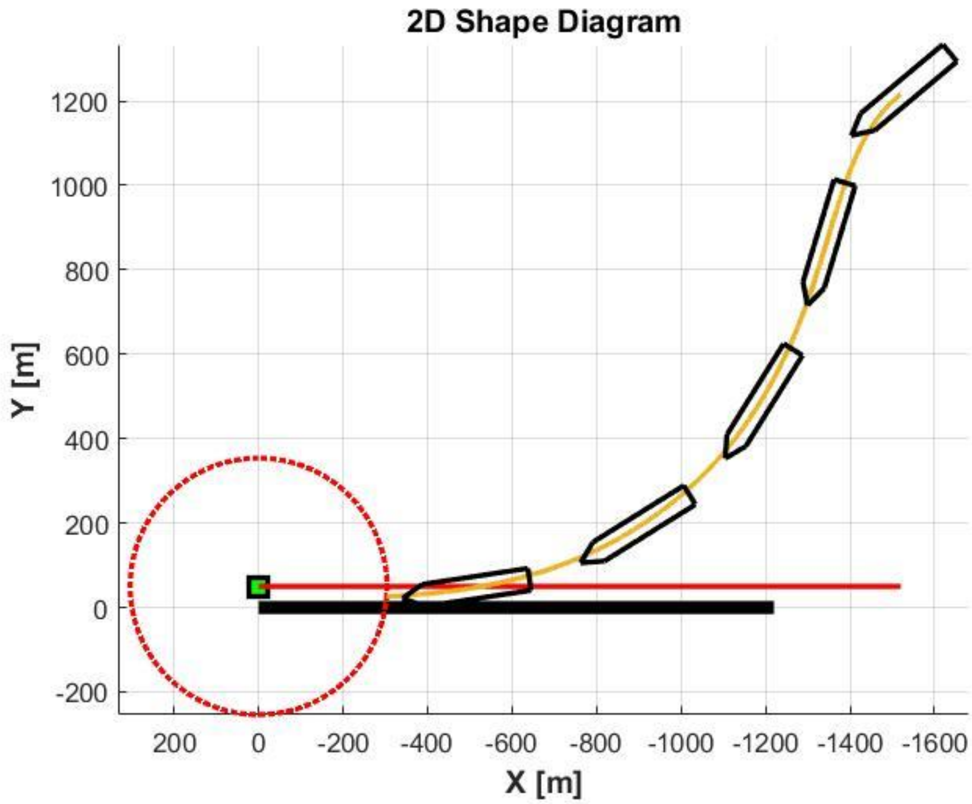

Figure 5.21 Trajectory for berthing simulation of tanker ship using PD controller with normal MMG model: initial posision of ship (-5L, 4L), initial heading angle of ship -40 degrees, initial speed of ship 4 m/s, rudder height 15 m and rudder area 131.66 m^2

Figure 5.21 shows the trajectory for berthing operation of the model ship using PD controller with normal MMG model in the case where the initial position of the model ship is (-5L, 4L), the initial heading angle is -40 degrees, the initial ship speed is 4 m/s and rudder area is 131.66 m^2 with rudder height 15 m. As shown in figure 5.21, the model ship is changing its heading smoothly during the whole operation. However, it is approaching not enough parallel to the quay at the end of the simulation and cannot decrease its speed enough before it crashes into the quay.

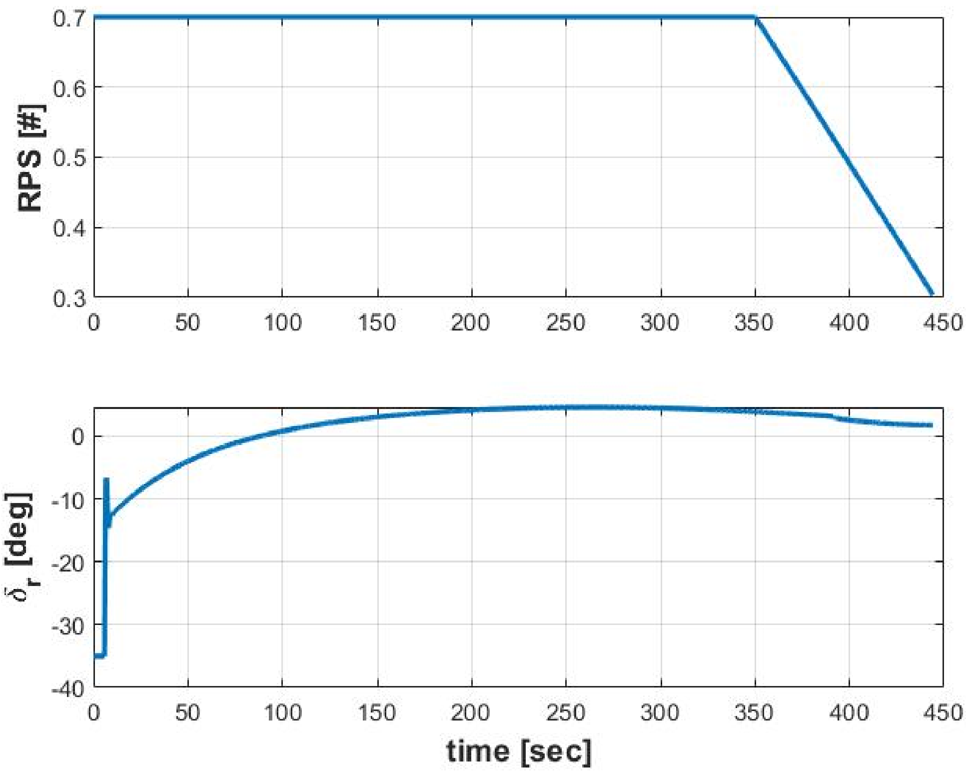

Figure 5.22 RPS and δr for berthing simulation of tanker ship using PD controller with normal MMG model: initial position of ship (-5L, 4L), initial heading angle of ship -40 degrees, initial speed of ship 4 m/s, rudder height 15 m and rudder area 131.66 m^2

Figure 5.22 shows the variation of RPS and rudder angle, δ_r, during the simulation. As shown in figure 5.22, the variation of rudder angle is stable between -35 degrees and +5 degrees. However, the RPS starts to decrease rapidly from about 350 seconds of simulation time to stop the model ship and to complete the berthing operation.

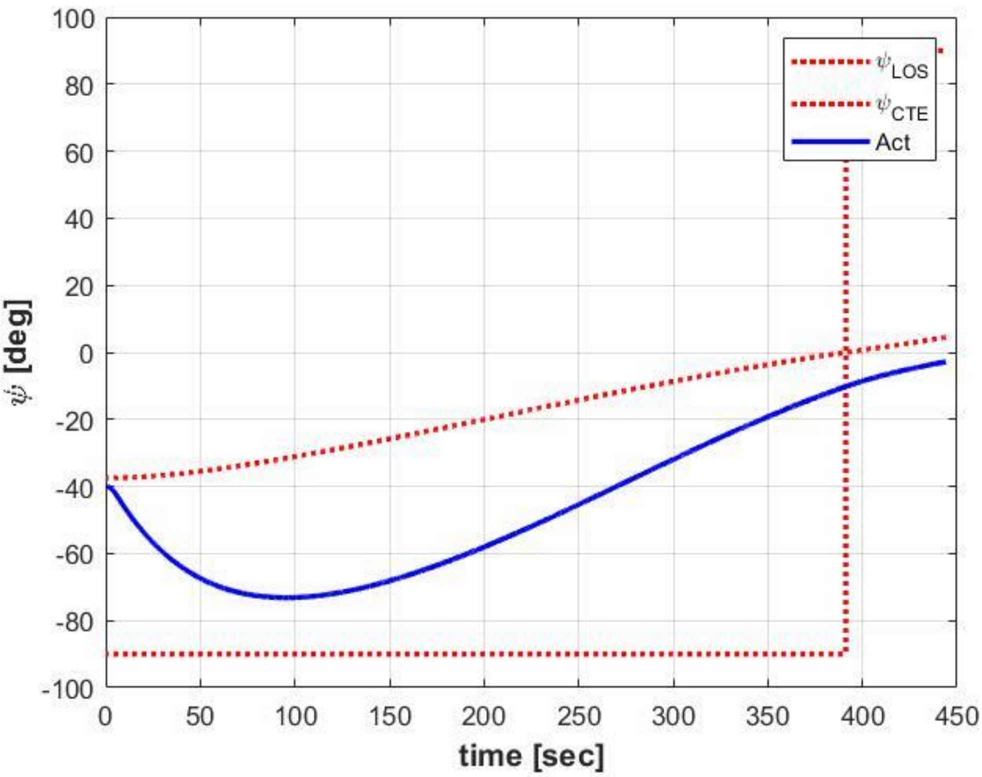

Figure 5.23 Heading ψ for berthing simulation of tanker ship using PD controller with normal MMG model: initial position of ship (-5L, 4L), initial heading angle of ship -40 degrees, initial speed of ship 4 m/s, rudder height 15 m and rudder area 131.66 m^2

Figure 5.23 shows the variation of heading angle ψ with ψ_{LOS} and ψ_{CTE} during the berthing operation. As presented above, actual heading angle ψ is changed with large variation from -40 degrees to about -73 degrees at the beginning of the berthing process and starts to increase into 0 degree from about 90 seconds of simulation time.

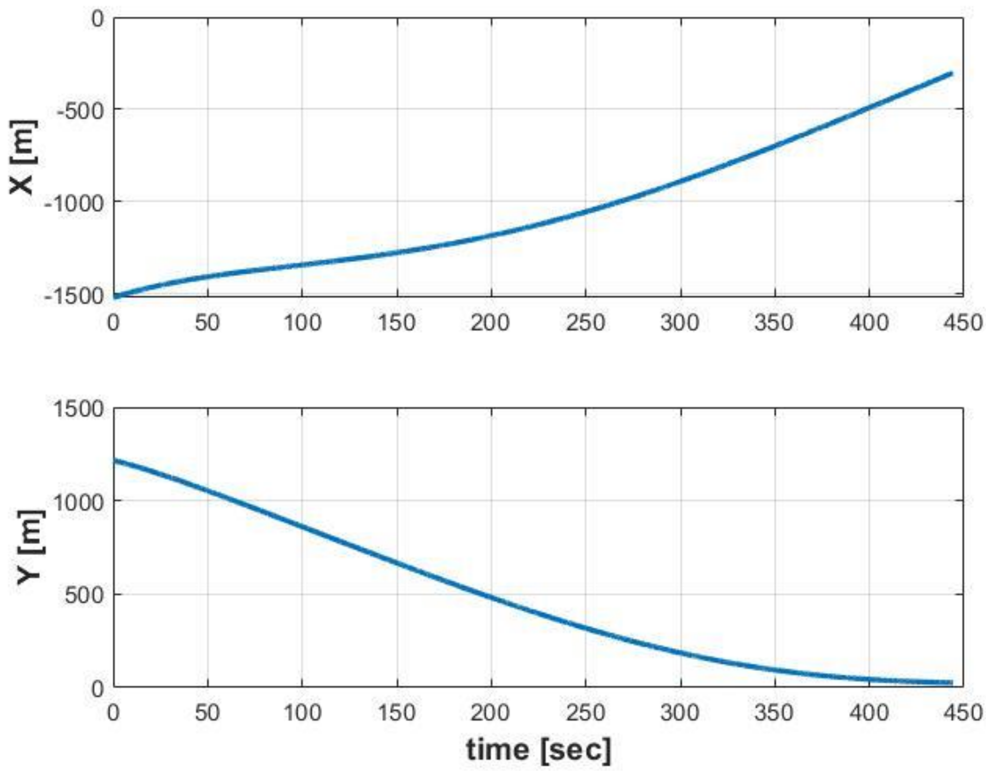

Figure 5.24 XY for berthing simulation of tanker ship using PD controller with normal MMG model: initial position of ship (-5L, 4L), initial heading angle of ship -40 degrees, initial speed of ship 4 m/s, rudder height 15 m and rudder area 131.66 m^2

Figure 5.24 shows X and Y variations of the model ship during berthing process. Under the normal MMG model, the model ship approaches to the target point (0, 0) smoothly in X and Y directions. However, it approaches 0 in Y direction already at 450 seconds of simulation time when it is still -250 m in X direction.

5.2.3 Comparative Analysis for Kose's Model and MMG Model

(1) Initial speed of ship 3 m/s

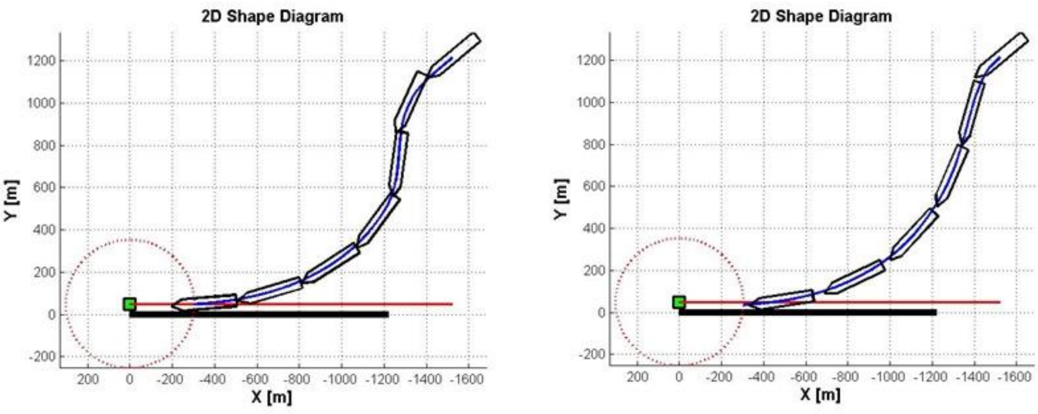

(a) (b)

Figure 5.25 Trajectory for berthing simulation of tanker ship using PD controller with (a) Kose's mathematical model and (b) normal MMG model: initial position of ship (-5L, 4L), initial heading angle of ship -40 degrees and initial speed of ship 3 m/s

Figure 5.25 shows the trajectories for berthing operation of the model ship using PD controller with Kose's mathematical model and the normal MMG model in the case where the initial position of the ship is (-5L, 4L) and the initial heading angle is -40 degrees. For the simulation cases of this study, the initial speed of ship is set up with 3 m/s and also, 12.94 m of rudder height and 98 m^2 of rudder area are applied. Under both mathematical models, the model ships approach to the quay with the angles less than 10 degrees at the end of the simulation. However, under Kose's mathematical model, the heading angle of the model ship is changed more largely compared with that under the normal MMG model during the simulation. Figure 5.26 shows the variations of RPS and rudder angle δ_r during the simulation and also, figure 5.27 shows variations of the actual heading angle ψ with ψ_{LOS} and ψ_{CTE}. As presented from figure 5.26, δ_r is changed largely and rapidly between about -35 and +35 degrees under Kose's mathematical model though it is changed rather gradually only between about -35 and +10 degrees under the normal MMG model. Furthermore, the RPS keeps 0.7 constantly and starts to decrease rapidly from about 490 seconds of simulation time and reach to 0 at around 610 seconds in the case of Kose's mathematical model. However, it starts to decrease already from about 440 seconds and get to 0 at about 550 seconds in the case of the normal MMG model.

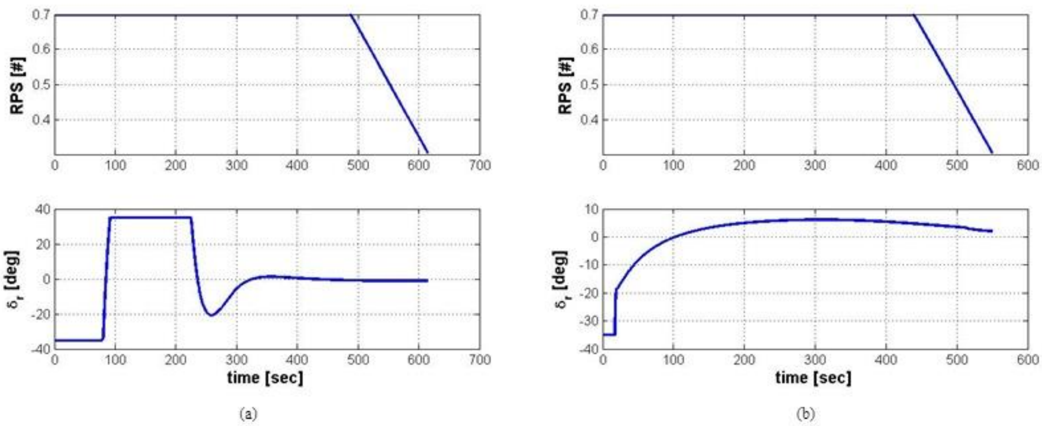

Figure 5.26 RPS and δr for berthing simulation of tanker ship using PD controller with (a) Kose's mathematical model and (b) normal MMG model: initial position of ship (-5L, 4L), initial heading angle of ship -40 degrees and initial speed of ship 3 m/s

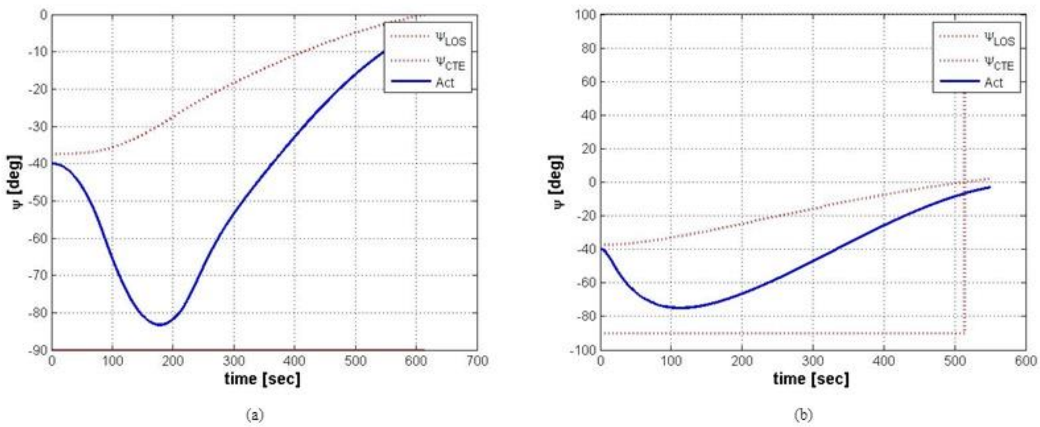

Figure 5.27 Heading angle ψ for berthing simulation of tanker ship using PD controller with (a) Kose's mathematical model and (b) normal MMG model: initial position of ship (-5L, 4L), initial heading angle of ship -40 degrees and initial speed of ship 3 m/s

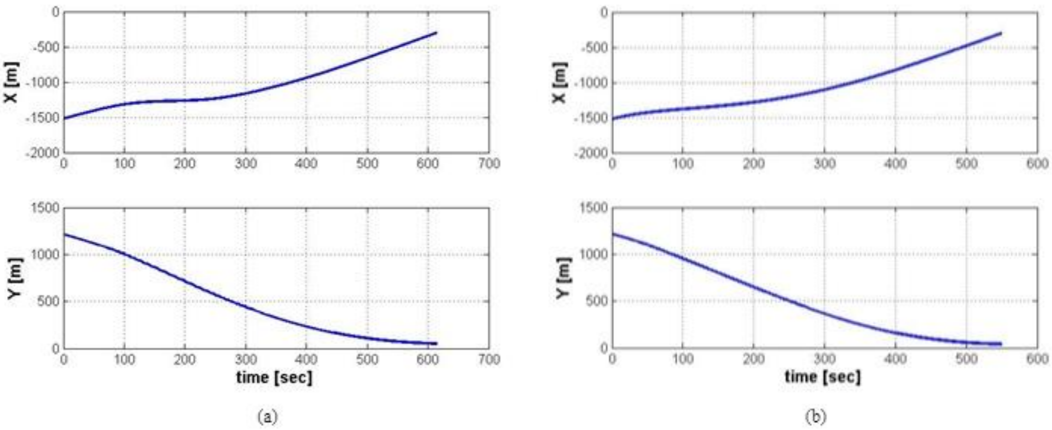

Figure 5.28 X and Y variation for berthing simulation of tanker ship using PD controller with (a) Kose's mathematical model and (b) normal MMG model: initial position of ship (-5L, 4L), initial heading angle of ship -40 degrees and initial speed of ship 3 m/s

Figure 5.28 shows comparison of the two mathematical models for X and Y variations of the model ship during berthing process and the model ship approaches to the target point (0, 0) more smoothly and also, in shorter time of simulation under the normal MMG model compared with the Kose's mathematical model.

According to the mathematical models presented in Chapter 3, it is considered that the difference of rudder movement and speed of ship between Kose's model and normal MMG could be caused by the terms derived by accelerations and it would have an effect on the difference of ship movement and trajectories between the two different mathematical models. As presented in table 5.3, table 5.4 and table 5.5, there are the derivatives by acceleration only in normal MMG model but in Kose's model. Table 5.3 shows the derivatives of surge equation in the mathematical models and table 5.4 shows the derivatives of sway equation. Also, table 5.5 shows the derivatives of yaw equation in the two mathematical models.

Table 5.3 Derivatives of surge equation in mathematical models

Surge Derivative	$X_{\dot{u}}$	X_u	$Y_{\dot{v}}$	X_{vv}	X_{rr}	X_{vr}	X_{uu}	X_{uvv}	X_{vvr}
Kose						●	●	●	●
MMG	●	●	●	●	●	●			

Table 5.4 Derivatives of sway equation in mathematical models

Sway Derivative	$Y_{\dot{v}}$	$Y_{\dot{r}}$	Y_v	Y_r	Y_{vvv}	Y_{rrr}	Y_{vvr}	Y_{vrr}	Y_{vv}	Y_{vvvv}	Y_{ur}	Y_{uvvr}
Kose			●	●				●	●	●	●	●
MMG	●	●	●	●	●	●	●	●				

Table 5.5 Derivatives of yaw equation in mathematical models

Yaw Derivative	$N_{\dot{v}}$	$N_{\dot{r}}$	N_v	N_r	N_{vvv}	N_{vvr}	N_{vrr}	N_{rrr}	N_{uv}	N_{ur}
Kose				●		●		●	●	●
MMG	●	●	●	●	●	●	●	●		

(2) Initial speed of ship 4 m/s

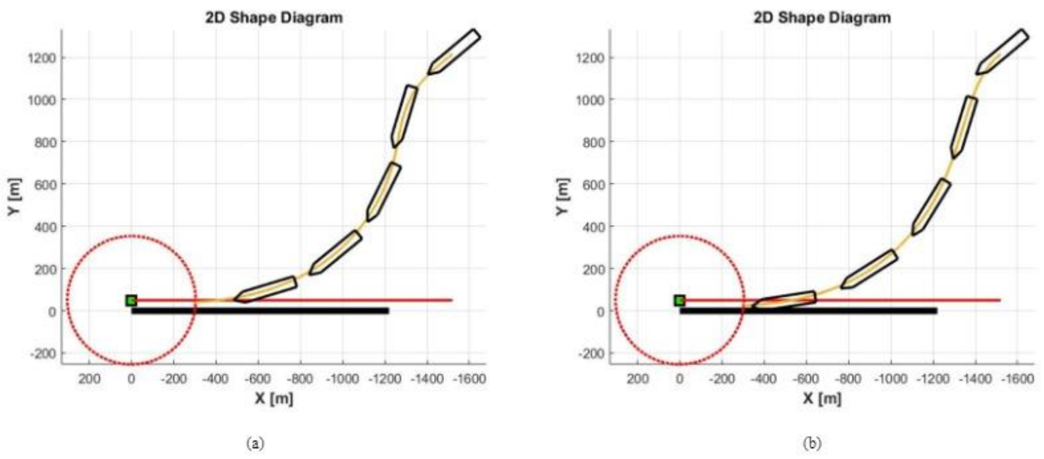

Figure 5.29 Trajectory for berthing simulation of tanker ship using PD controller with (a) Kose's mathematical model and (b) normal MMG model: initial position of ship (-5L, 4L), initial heading angle of ship -40 degrees and initial speed of ship 4 m/s

Figure 5.29 shows the trajectories for berthing operation of the model ship using PD controller with Kose's mathematical model and the normal MMG model in the case where the initial position of the ship is (-5L, 4L) and the initial heading angle is -40 degrees. For the simulation cases of this study, the initial speed of ship is set up with 4 m/s and also, 12.94 m of rudder height and 98 m^2 of rudder area are applied. With both mathematical models, the model ship approaches to the quay along with a smooth path. Under the Kose's mathematical model, the heading angle of the model ship is changed more largely compared with that under the normal MMG model during the simulation and the berthing operation is completed successfully. However, under the normal MMG model, the heading angle is not changed enough for having successful berthing operation. Figure 5.30 shows the variations of RPS and rudder angle δ_r during the simulation and also, figure 5.31 shows variations of the actual heading angle ψ with ψ_{LOS} and ψ_{CTE}. As presented from figure 5.30, δ_r is changed largely and rapidly between about -35 and +35 degrees under Kose's mathematical model though it is changed rather gradually only between about -35 and +5 degrees under the normal MMG model. Furthermore, the RPS keeps 0.7 constantly and starts to decrease rapidly from about 380 seconds of simulation time and reach to 0.3 at around 490 seconds in the case of Kose's mathematical model. However, it starts to decrease already from about 350 seconds and get to 0.3 at about 445 seconds in the case of the normal MMG model.

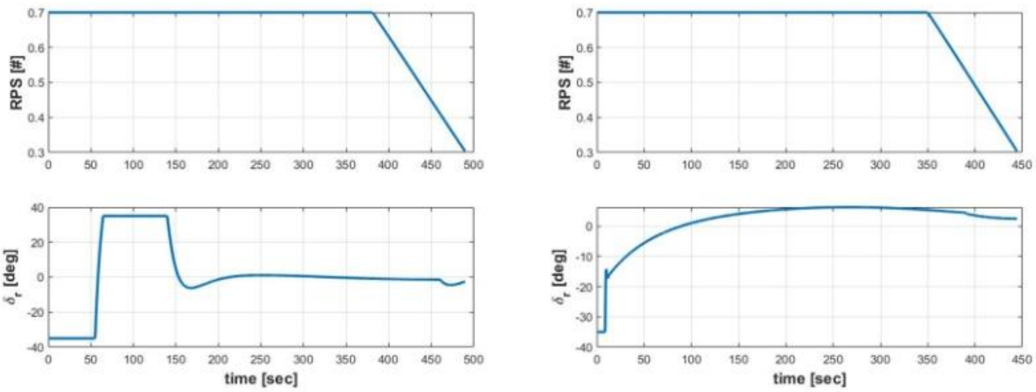

(a) (b)

Figure 5.30 RPS and δr for berthing simulation of tanker ship using PD controller with (a) Kose's mathematical model and (b) normal MMG model: initial position of ship (-5L, 4L), initial heading angle of ship -40 degrees and initial speed of ship 4 m/s

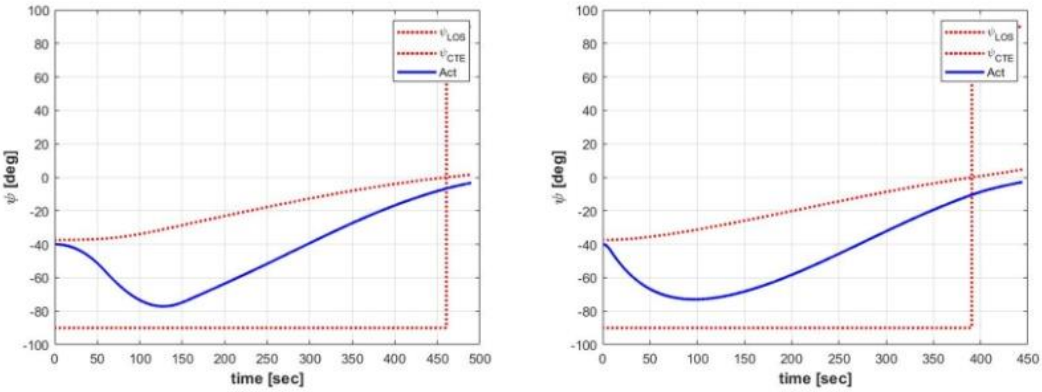

(a) (b)

Figure 5.31 Heading angle ψ for berthing simulation of tanker ship using PD controller with (a) Kose's mathematical model and (b) normal MMG model: initial position of ship (-5L, 4L), initial heading angle of ship -40 degrees and initial speed of ship 4 m/s

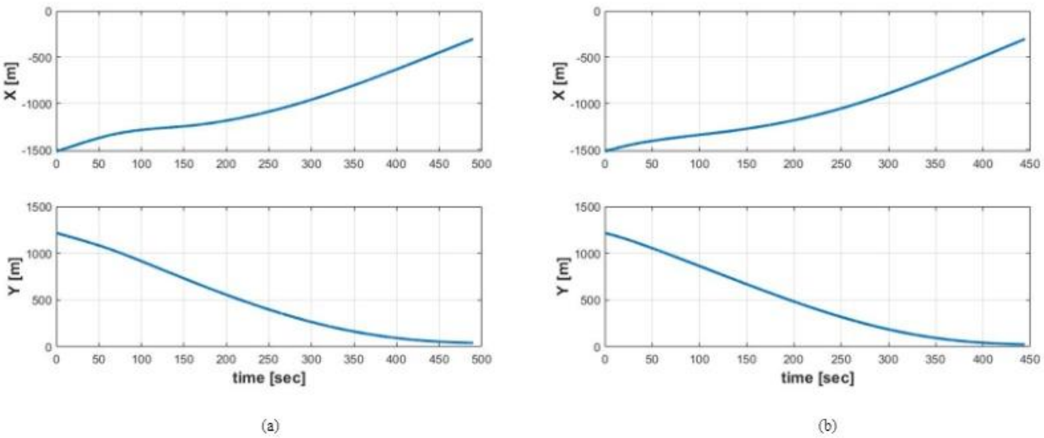

Figure 5.32 X and Y variation for berthing simulation of tanker ship using PD controller with (a) Kose’s mathematical model and (b) normal MMG model: initial position of ship (-5L, 4L), initial heading angle of ship -40 degrees and initial speed of ship 4 m/s

Figure 5.32 shows comparison of the two mathematical models for X and Y variations of the model ship during berthing process and the model ship approaches to the target point (0, 0) more smoothly and also, in shorter time of simulation under the normal MMG model compared with the Kose’s mathematical model. However, the model ship arrives nearly 0 m in Y direction already with about -300 m in X direction at about 500 seconds of simulation time under the Kose’s mathematical model and also, arrives 0 m in Y direction with about -280 m in X direction at about 450 seconds of simulation time under the normal MMG model.

(3) Increased rudder area with initial speed of ship 4 m/s

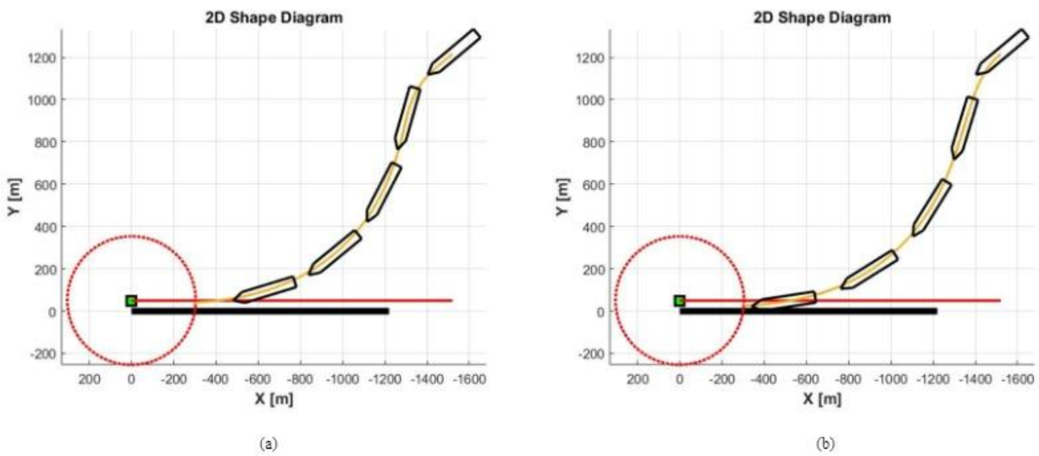

Figure 5.33 Trajectory for simulation of tanker ship using PD controller with (a) Kose's model and (b) MMG: initial position of ship (-5L, 4L), initial heading angle of ship -40 degrees, initial speed of ship 4 m/s, rudder height 15 m and rudder area 131.66 m^2

Figure 5.33 shows the trajectories for berthing operation of the model ship using PD controller with Kose's mathematical model and the normal MMG model in the case where the initial position of the ship is (-5L, 4L) and the initial heading angle is -40 degrees. For the simulation cases of this study, the initial speed of ship is set up with 4 m/s and rudder area is 131.66 m^2 with rudder height 15 m. With both mathematical models, the model ship approaches to the quay along with a smooth path. Under the Kose's mathematical model, the heading angle of the model ship is changed more largely compared with that under the normal MMG model during the simulation and the berthing operation is completed successfully. However, under the normal MMG model, the heading angle is not changed enough for having successful berthing operation. Figure 5.34 shows the variations of RPS and rudder angle δ_r during the simulation and also, figure 5.35 shows variations of the actual heading angle ψ with ψ_{LOS} and ψ_{CTE}. As presented in figure 5.34, δ_r is changed largely and rapidly between about -35 and +35 degrees under Kose's mathematical model though it is changed rather gradually only between about -35 and +5 degrees under the normal MMG model. Furthermore, the RPS keeps 0.7 constantly and starts to decrease rapidly from about 380 seconds of simulation time and reach to 0.3 at around 490 seconds in the case of Kose’s mathematical model. However, it starts to decrease already from about 350 seconds and get to 0.3 at about 445 seconds in the case of the normal MMG model.

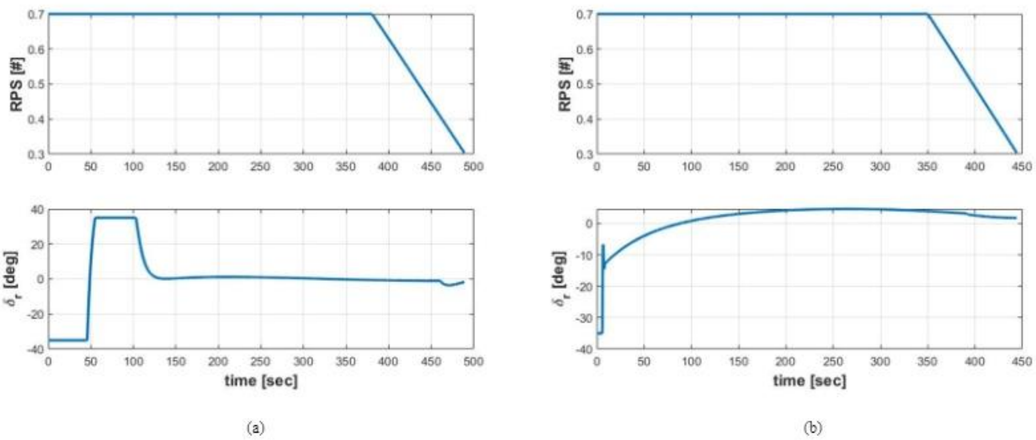

Figure 5.34 RPS and δr for simulation of tanker ship using PD controller with (a) Kose’s model and (b) MMG: initial position of ship (-5L, 4L), initial heading angle of ship -40 degrees, initial speed of ship 4 m/s, rudder height 15 m and rudder area 131.66 m²

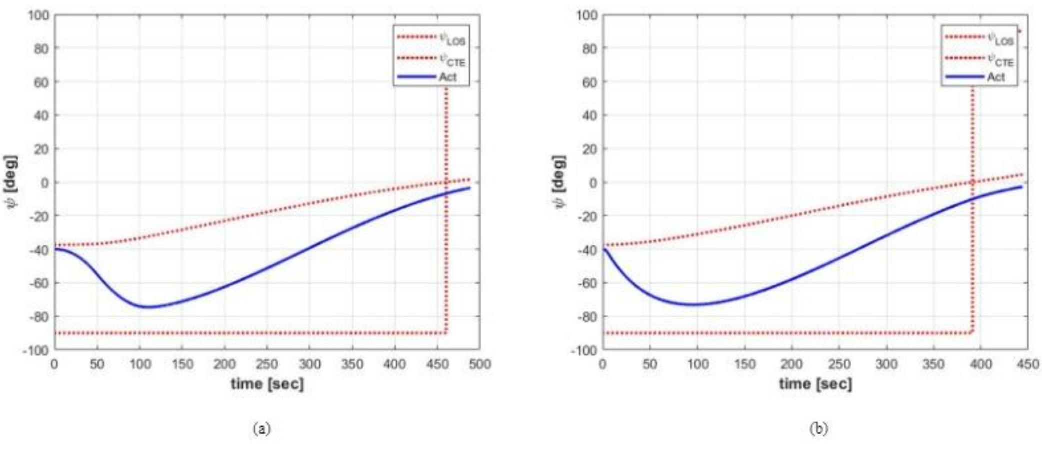

Figure 5.35 Heading ψ for simulation of tanker ship using PD controller with (a) Kose’s model and (b) MMG: initial position of ship (-5L, 4L), initial heading angle of ship -40 degrees, initial speed of ship 4 m/s, rudder height 15 m and rudder area 131.66 m²

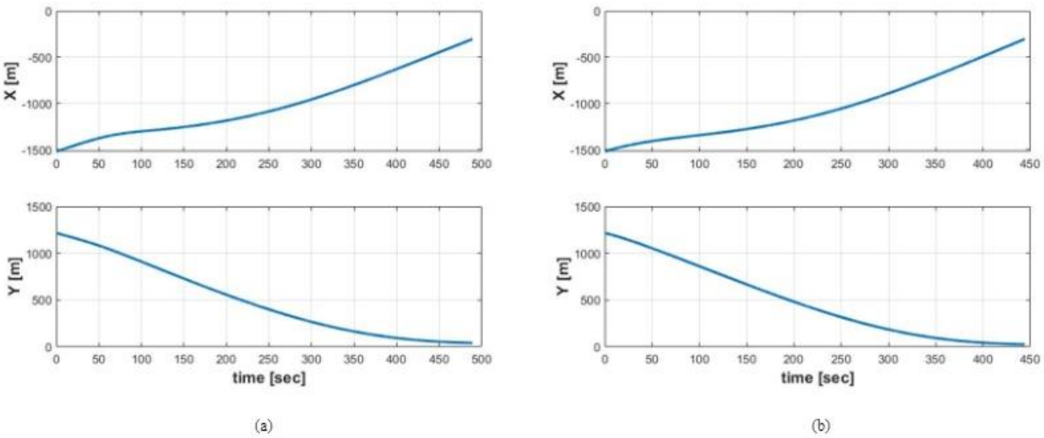

Figure 5.36 XY for simulation of tanker ship using PD controller with (a) Kose's model and (b) MMG: initial position of ship (-5L, 4L), initial heading angle of ship -40 degrees, initial speed of ship 4 m/s, rudder height 15 m and rudder area 131.66 m^2

Figure 5.36 shows comparison of the two mathematical models for X and Y variations of the model ship during berthing process and the model ship approaches to the target point (0, 0) more smoothly and also, in shorter time of simulation under the normal MMG model compared with the Kose's mathematical model. However, the model ship arrives nearly 0 m in Y direction already with about -300 m in X direction at about 500 seconds of simulation time under the Kose's mathematical model and also, arrives 0 m in Y direction with about -280 m in X direction at about 450 seconds of simulation time under the normal MMG model.

(4) Comparative analysis for different rudder areas in initial speed of ship 4 m/s

As presented above, berthing simulations have been performed for two different rudder heights and areas in the initial ship speed 4 m/s. In this study, rudder aspect ratio, λ_r is set for 1.709 as presented in ship particulars in table 4.1 and particularly RPS and rudder angle δ_r are compared in different rudder conditions to see the effect on control of rudder movement and ship speed. Figure 5.37 shows the comparison between the results for rudder area 98 m^2 and 131.66 m^2 in Kose's model and figure 5.38 shows the comparison of results in the normal MMG model. As shown in the results, the rudder angle is kept in large for shorter time with the increased rudder area to change the ship heading for berthing operation in both of Kose's model and normal MMG model.

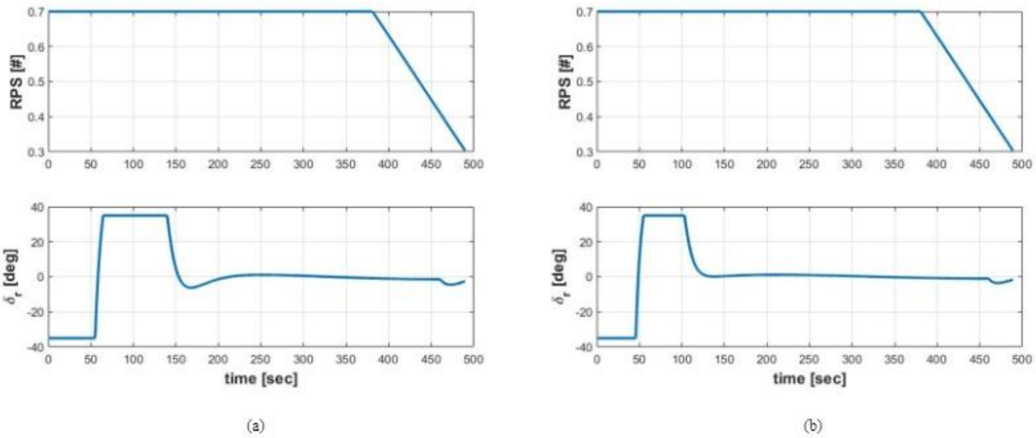

Figure 5.37 RPS and δr for simulation of tanker ship, PD controller with Kose's model (a) h 12.94 m, A_r 98 m^2 (b) h 15 m, A_r 131.66 m^2: initial position of ship (-5L, 4L), initial heading angle of ship -40 degrees, initial speed of ship 4 m/s

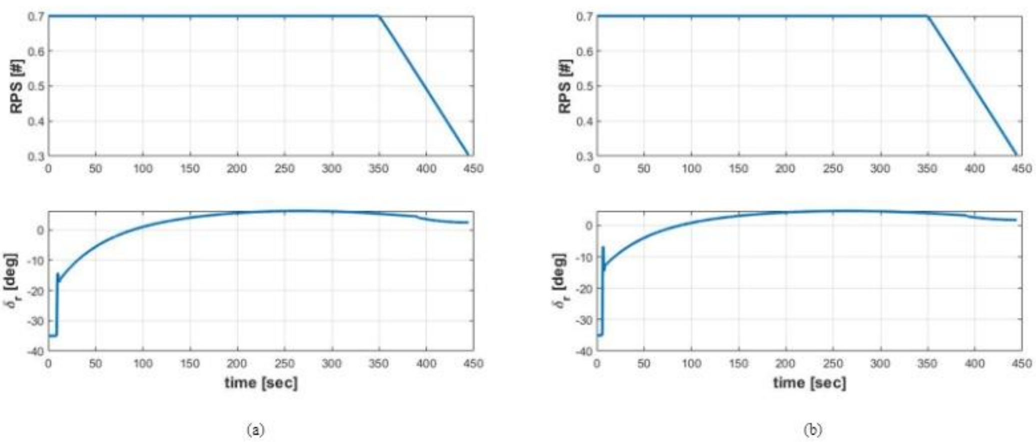

Figure 5.38 RPS and δr for simulation of tanker ship, PD controller with MMG (a) h 12.94 m, A_r 98 m^2 (b) h 15 m, A_r 131.66 m^2: initial position of ship (-5L, 4L), initial heading angle of ship -40 degrees, initial speed of ship 4 m/s

5.3 Comparative Analysis for Proportional Derivative (PD) Control and Artificial Neural Network (ANN)

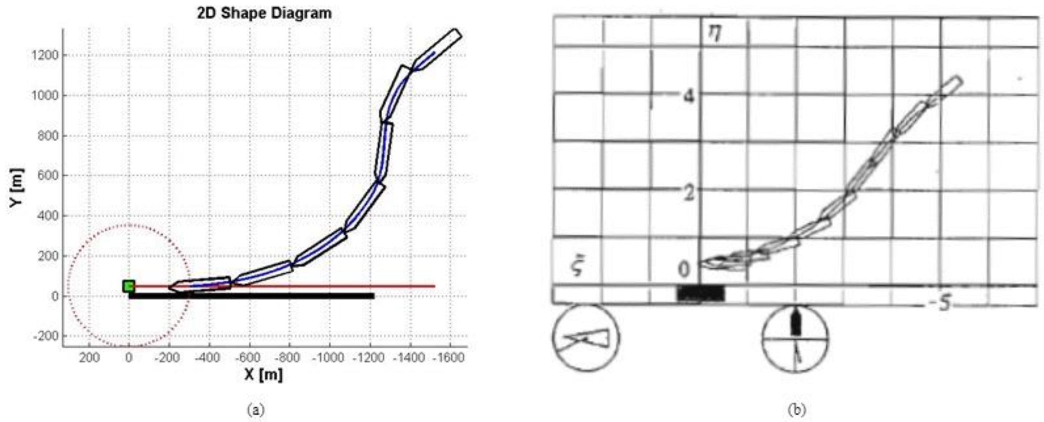

Figure 5.39 Trajectory for berthing simulation of tanker ship using (a) PD controller and (b) ANN controller (Hasegawa and Kitera, 1993) with Kose's mathematical model: initial position of ship (-5L, 4L), initial heading angle -40 degrees and initial speed 3 m/s

Figure 5.39 shows the trajectories of the tanker ship for berthing simulations using PD control algorithm and ANN algorithm with Kose's mathematical model in the case where the initial position of the ship is (-5L, 4L) and the initial heading angle is -40 degrees. For the simulation cases of this study, the initial speed of ship is also set up with 3 m/s. In the case of PD control algorithm, the heading angle of the model ship changes more largely during the simulation compared with the case of ANN algorithm. However, in the case of PD control algorithm, the ship approaches to the quay more in parallel during the end period of simulation compared with the case of ANN algorithm. Figure 5.40 shows the variations of RPS and the rudder angle δ_r during the simulations of both cases and δ_r shows stabler variation in the case of PD control algorithm compared with the case of ANN control algorithm.

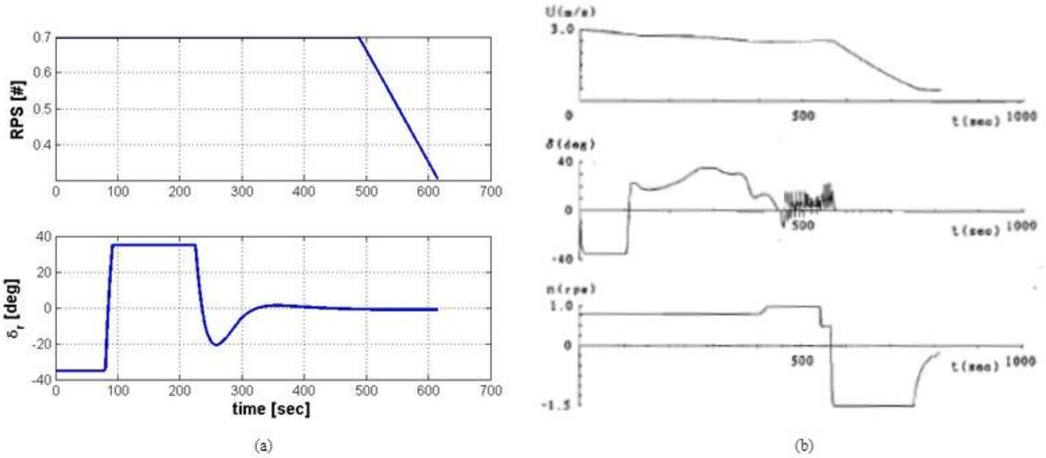

Figure 5.40 RPS and δr for berthing simulation of tanker ship using (a) PD controller and (b) ANN controller (Hasegawa and Kitera, 1993) with Kose's mathematical model: initial position of ship (-5L, 4L), initial heading angle -40 degrees and initial speed 3 m/s

5.4 Statistical Analysis

Statistical analysis for berthing operation has been designed to obtain valuable data about initial conditions of a ship for having successful berthing and it has been performed in two different simulation times which include 550 seconds and 650 seconds. The four different starting points for the simulation of ship berthing operation have been selected as introduced in the previous chapter. Firstly, twenty cases of initial heading angle have been chosen randomly between -180 degrees and +180 degrees on the starting points of berthing operation to find the range of heading angles for having effective simulation of berthing operation and the range from -90 degrees to 0 degree has been selected. For having accuracy of the analysis, the procedure and the results have been reviewed by Prof. B. S. Kang in college of business administration of Kyung Hee University in Republic of Korea.

5.4.1 Simulation Time 550 seconds

The range of heading angles has been divided to three steps and each step is 30 degrees. For the cases of 550 seconds of simulation time, the two mathematical models have been applied and ten cases of initial heading angle have been chosen randomly for each step of heading angles. As shown in table 5.6, only 21 cases from the starting point (-3L, 5L) are successful among the whole trials of 120 cases from four starting points and, in particular, only one case on the heading step, -30 degrees to 0 degree, is successful for the berthing simulation.

Under the MMG model, all cases for the starting point (-3L, 5L) are successful, however, there is no other successful case from the other starting points as presented in table 5.7. Totally, 30 cases among all trials from the four starting points are successful.

Table 5.6 Kose (heading step: 30 degrees, random initial heading: 10 cases for each)

Range of Initial Heading Angle (degree) Initial Position (L=Length of the ship)	[0, -30]	[-30, -60]	[-60, -90]	Sum
(-3L, 5L)	1	10	10	21
(-5L, 3L)	0	0	0	0
(-5L, 4L)	0	0	0	0
(-6L, 2L)	0	0	0	0
Sum	1	10	10	21

Table 5.7 MMG (heading step: 30 degrees, random initial heading: 10 cases for each)

Range of Initial Heading Angle (degree) Initial Position (L=Length of the ship)	[0, -30]	[-30, -60]	[-60, -90]	Sum
(-3L, 5L)	10	10	10	30
(-5L, 3L)	0	0	0	0
(-5L, 4L)	0	0	0	0
(-6L, 2L)	0	0	0	0
Sum	10	10	10	30

5.4.2 Simulation Time 650 seconds

The simulation time has been extended to 650 seconds for finding further performance of berthing operation in the longer simulation time. For the cases of 650 seconds of simulation time, only Kose's mathematical model has been applied since it has been found that many simulation cases with MMG model have not presented successful berthing operation in the extended simulation time.

For the first step, as done in the cases of 550 seconds, the range of heading angles has been divided to three steps and each step is 30 degrees. Also, ten cases of initial heading angle have been chosen randomly for each step of heading angles. As shown in table 5.8, all cases from the starting points (-3L, 5L), (-5L, 3L) and (-5L, 4L) with the heading angles between -90 and -60 degrees and between -60 and -30 degrees are successful for berthing operation, however, there is not any successful case from the starting point (-6L, 2L) with any step of heading angles. With heading angles between -30 to 0 degrees, only 7 cases and 4 cases are successful from the starting points (-5L, -3L) and (-5L, 4L) accordingly. From the starting point (-3L, 5L), all cases are successful with heading angles between -30 and 0 degrees as well as between -90 and -60 degrees and between -60 and -30 degrees.

For the next step, the number of random cases of initial heading angle has been increased to 30 to get the valuable numbers of data for analysing statistically. In this simulation, all cases from the starting points (-3L, 5L), (-5L, 3L) and (-5L, 4L) with the heading angles between -90 and -60 degrees and between -60 and -30 degrees are successful for berthing operation and, with the heading angles between -30 and 0 degrees, 30, 19 and 12 cases from the starting points (-3L, 5L), (-5L, 3L) and (-5L, 4L) are successful accordingly. Furthermore, there is no successful case from the starting point (-6L, 2L) with any step of heading angles between -90 and 0 degrees as shown in table 5.9.

Lastly, the range of heading angles has been divided more minutely for the detailed analysis. The number of heading steps is 6 and each step is 15 degrees accordingly.

In this case, simulation has been performed only from the starting points (-3L, 5L), (-5L, 3L) and (-5L, 4L) since, as shown above, the simulations from the starting point (-6L, 2L) have not had any successful performance for berthing operation in the limited times through the previous cases. As presented in table 5.10, the number of cases for successful berthing operation is decreasing as the step of heading angles is getting close to 0 degree. With heading angles between -30 and -15 degrees, only 22 cases are successful from the starting point (-5L, 4L) though all cases are successful from the starting points (-3L, 5L) and (-5L, 3L). Furthermore, with heading angles between -15 and 0 degrees, only 10 cases are successful from the starting point (-5L, 3L) and there is no successful case from the starting point (-5L, 4L). However, all cases from the starting point (-3L, 5L) are successful in whole range of heading angles between -90 and 0 degrees.

Table 5.8 Kose (heading step: 30 degrees, random initial heading: 10 cases for each)

Range of Initial Heading Angle (degree) Initial Position (L=Length of the ship)	[0, -30]	[-30, -60]	[-60, -90]	Sum
(-3L, 5L)	10	10	10	30
(-5L, 3L)	7	10	10	27
(-5L, 4L)	4	10	10	24
(-6L, 2L)	0	0	0	0
Sum	21	30	30	81

Table 5.9 Kose (heading step: 30 degrees, random initial heading: 30 cases for each)

Range of Initial Heading Angle (degree) Initial Position (L=Length of the ship)	[0, -30]	[-30, -60]	[-60, -90]	Sum
(-3L, 5L)	30	30	30	90
(-5L, 3L)	19	30	30	79
(-5L, 4L)	12	30	30	72
(-6L, 2L)	0	0	0	0
Sum	61	90	90	241

Table 5.10 Kose (heading step: 15 degrees, random initial heading: 30 cases for each)

Range of Initial Heading Angle (degree) Initial Position (L=Length of the ship)	[0, -15]	[-15, -30]	[-30, -45]	[-45, -60]	[-60, -75]	[-75, -90]	Sum
(-3L, 5L)	30	30	30	30	30	30	180
(-5L, 3L)	10	30	30	30	30	30	160
(-5L, 4L)	0	22	30	30	30	30	142
Sum	40	82	90	90	90	90	482

5.5 Berthing Simulation using Model Predictive Control

Using Model Predictive Control, the optimal trajectory of ship berthing operation is generated through path planning and the actual path to follow the optimal one is calculated through path tracking.

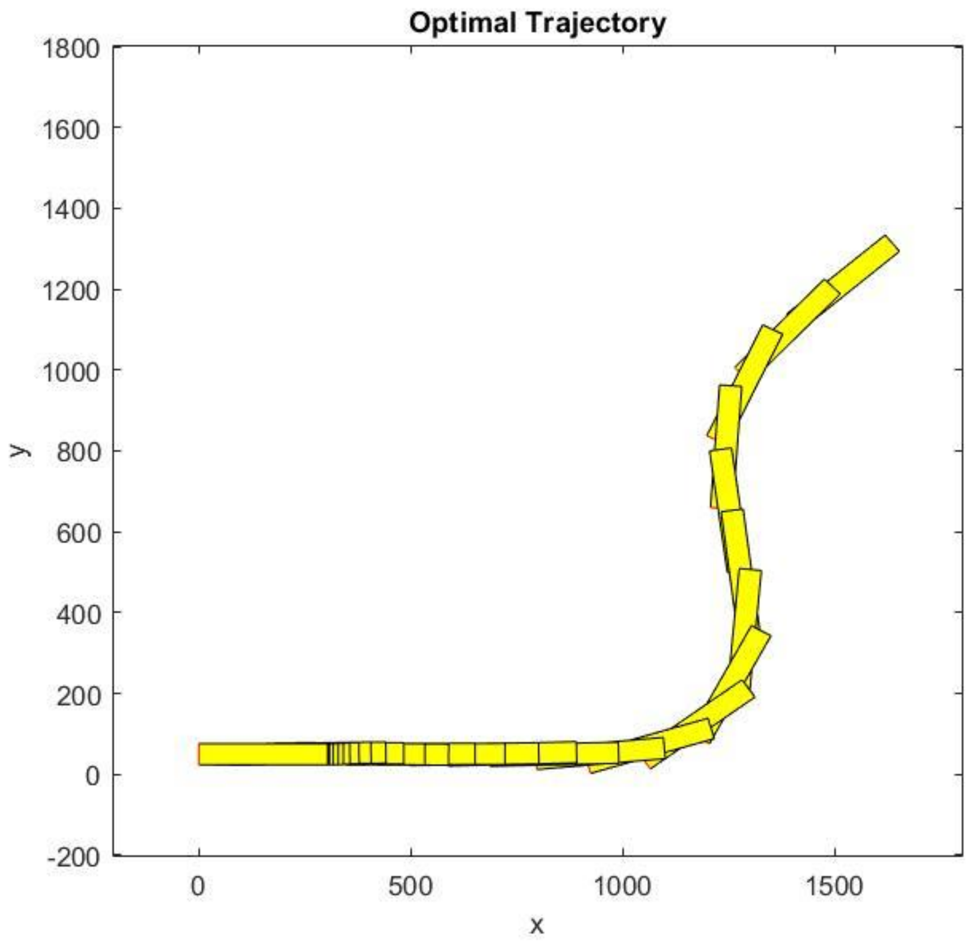

Figure 5.41 Trajectory for berthing simulation of tanker ship using MPC with Kose's mathematical model: initial position of ship (-5L, 4L), initial heading angle of ship -40 degrees and initial speed of ship 3 m/s

As shown in figure 5.41, the optimal trajectory for berthing operation of the model ship is generated by Model Predictive Control with the Kose's mathematical model in case where the initial position of the model ship is (-5L, 4L), the initial heading angle is - 40 degrees and the initial ship speed is 3 m/s. For the simulation case of this study, 12.94 m of rudder height and 98 m^2 of rudder area are applied. From the optimal trajectory, it shows the optimal path for the model ship to be berthed from the start point to the target point with 0 m/s of ship speed and 0 degree of ship heading angle to be stopped parallel to the quay at the end of the berthing operation.

Also, figure 5.42 presents the variations of X position X_G, Y position Y_G, heading angle psi, surge velocity u, sway velocity v and yaw rate r for path planning and path tracking with Model Predictive Control.

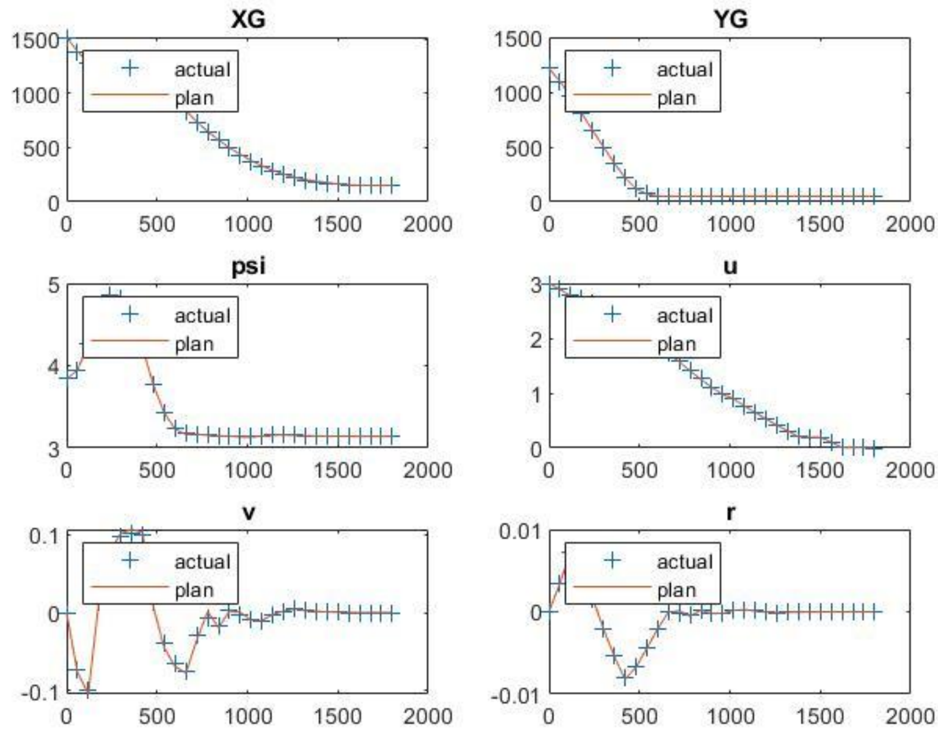

Figure 5.42 X position XG, Y position YG, heading angle psi, surge velocity u, sway velocity v and yaw rate r for berthing simulation of tanker using MPC with Kose's model: initial position of ship (-5L, 4L), initial heading angle -40 degrees and initial speed 3 m/s

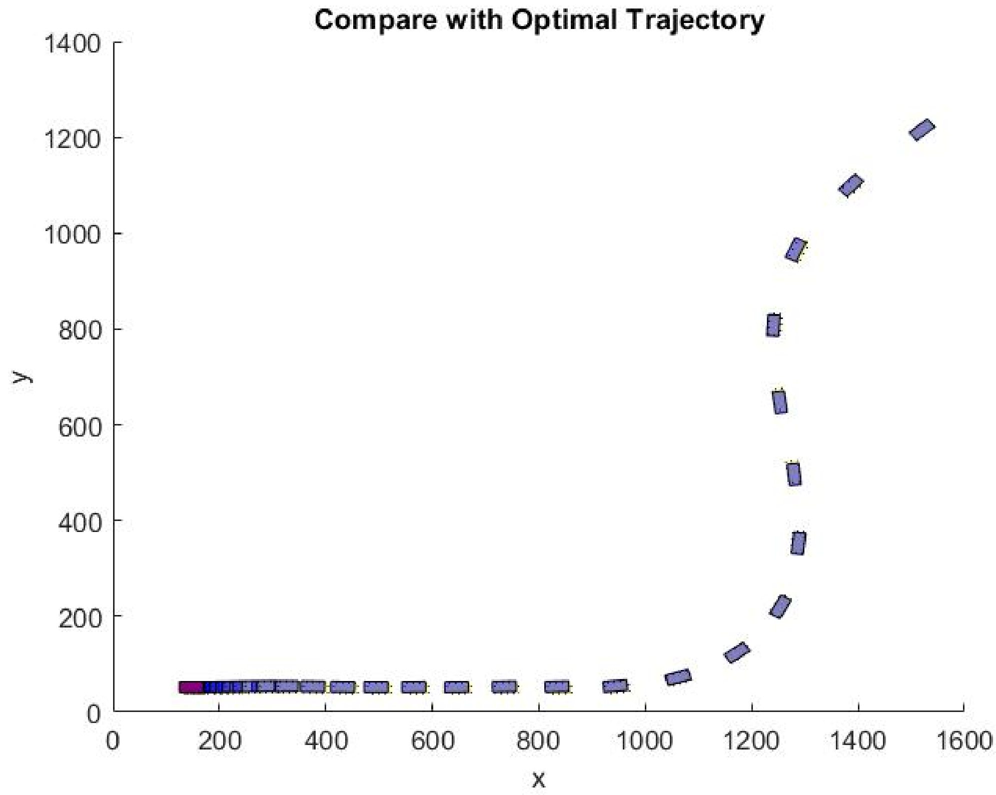

Figure 5.43 Actual and optimal trajectories for berthing simulation of tanker ship using MPC with Kose's mathematical model: initial position of ship (-5L, 4L), initial heading angle of ship -40 degrees and initial speed of ship 3 m/s

Furthermore, figure 5.43 presents the actual trajectory of the model ship compared with the optimal trajectory and it is found that the two trajectories are well matched. As shown in the results, the simulation of ship berthing operation with path planning and path tracking has been performed successfully with Model Predictive Control.

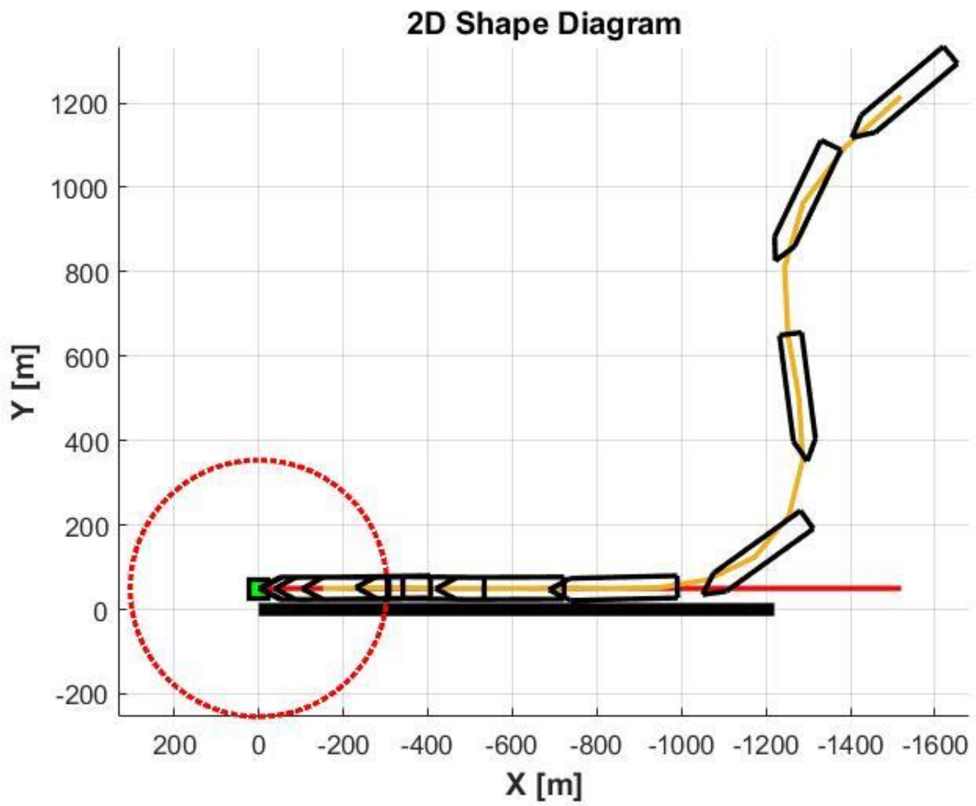

Figure 5.44 Diagram for berthing simulation of tanker ship using MPC with Kose's mathematical model: initial position of ship (-5L, 4L), initial heading angle of ship -40 degrees and initial speed of ship 3 m/s

Figure 5.44 presents the diagram of berthing operation by Model Predictive Control.

5.6 Closure

Development of automatic time-domain simulation program for ship berthing operation is performed and the simulation results are presented.

Firstly, simulations by the developed simulation programs using PD control with Kose's mathematical model and normal MMG are performed, and the results show stable berthing operations in both of mathematical models. However, it is recognised that the model ship moves in larger range of rudder and heading angle of the ship with longer time of berthing operation in the simulation with Kose's model compared with the simulation with normal MMG model.

Secondly, simulation result from the developed simulation program using PD control is well matched with the result of ANN by Hasegawa. Furthermore, the control of rudder angle is steadier in PD control than in ANN.

Thirdly, statistical analysis presents the initial conditions of ship berthing for successful operation.

Lastly, simulation result from the developed simulation program using MPC is presented and generating an optimal trajectory and following the path are performed successfully.

6. Discussion

6.1 Preamble

In this thesis, development of time-domain simulation program of berthing operation of ships has been presented, in particular, addressing control methodology and algorithm. Berthing operation is most difficult procedure on ship manoeuvring. Specially, control of ship speed and heading angle is highlighted issue for safe and time-saving berthing operation.

The fundamental design of the ship control system has remained virtually unchanged for several decades. Commercial autopilots found on the majority of vessels as sea still employ proportional, integral and derivative (PID) algorithms to control the heading in either course-keeping or course-changing mode. Such controllers are designed as single input-single output systems using Nomoto type transfer function models (Burns, 1995) (Nomoto, 1966).

This chapter elaborates on discussion of the major results of the thesis. Following a reference to the contribution of the thesis to the field in question, a general discussion is presented highlighting the difficulties encountered in the development of the various concepts, and the manner in which these difficulties were handled. The chapter concludes with recommendations for further research.

6.2 Own Contribution

Most of all, the research has been performed with entire review of control methodologies of ship manoeuvring, in particular, for berthing operation and also has been aiming to find the methodology for developing an effective simulation program for berthing procedure. In this respect, the fundamental idea for overcoming drawbacks from different approaches has been presented.

Secondly, the simulations have been performed with two different mathematical models, the normal MMG and Kose's, and this study gives the answer for how a simulation program works in low advance speed of a ship on berthing operation with different mathematical models and how it needs to be improved, particularly, in matter of simulating the control of ship heading and speed on ship motions.

As the third contribution, the project has been undertaken for developing the simulation program with a new control algorithm. In most updated control technologies, the fuzzy and the neural network controller have been expected for replacing traditional PID control system. However, these algorithms still need to be improved for overcoming their unstable performance. Through this thesis, a new control methodology with PD control and Model Predictive Control has been provided for aiming improved performance of ship berthing simulation.

Overall, this thesis proposed improved time-domain simulation program which is aiming to give more accurate result for ship berthing operation. Initial applications demonstrate the potential of the approach as an effective ship berthing simulation program. In this respect, the thesis has served its principal aim and objectives, as stated in Chapter 2.

6.3 Recommendations for Further Research

Berthing operation is the most important and difficult procedure in ship manoeuvring and gives many different questions to overcome. With reference to the points discussed above, a few recommendations for further research and development are as follows;

a) Improving control algorithm

b) Time and energy-saving control of berthing operation

c) Improved mathematical model considering bank effect and shallow water condition in harbour environment

6.4 Closure

In this chapter, the major results of the thesis have been discussed. Development of automatic time-domain simulation program of berthing operation of ships is the area of research that will develop in the future, demonstrating the benefits that can be gained by its application and exploitation. It is hoped that this thesis has contributed positively towards this scope.

7. Conclusion

Through the project performed, the main conclusions are drawn as follows.

a) To predict the berthing operations accurately, it is essential to have an improved mathematical model together with control algorithms with outputs which can be used by ship personnel.

b) The developed simulation program using PD control algorithm presents good performance for controlling rudder and heading angle of the model ship in both of Kose's mathematical model and normal MMG model and shows stabler control of rudder angle than the program using ANN by Hasegawa.

c) For successful berthing operations, the selection of the initial values of heading angle, position of ship and speed are critical.

d) It has been possible to simulate ship berthing operation using Model Predictive Control while incorporating path generating and path following features.

8. References

AHMED, Y. A. & KAZUHIKO, H. 2015. Consistently Trained Artificial Neural Network for Automatic Ship Berthing Control. *TransNav: International Journal on Marine Navigation and Safety of Sea Transportation,* 9**,** 417-426.

ÅSTRÖM, K. J. & WITTENMARK, B. 1973. On self tuning regulators. *Automatica,* 9**,** 185-199.

BURNS, R. S. 1995. The use of artificial neural networks for the intelligent optimal control of surface ships. *IEEE Journal of Oceanic Engineering,* 20**,** 65-72.

CHENG, J., YI, J. & ZHAO, D. 2006. A new fuzzy autopilot for way-point tracking control of ships. *IEEE International Conference on Fuzzy Systems*, Vancouver, BC, Canada.

DJOUANI, K. & HAMAM, Y. 1993. Optimal Constrained Multi-Criteria Trajectory Planning for Ship Maneuvering and Control. *Second IEEE Conference on Control Applications*, pp525-530, Vancouver.

DJOUANI, K. & HAMAM, Y. 1994. Ship Optimal Path Planning and Artificial Neural Nets for Berthing, *Oceans '94. 'Oceans Engineering for Today's Technology and Tomorrow's Preservation.'.*

DJOUANI, K. & HAMAM, Y. 1995. Minimum Time-Energy Trajectory Planning for Automatic Ship Berthing. *IEEE Journal of Oceanic Engineering*, Vol. 20, No. 1.

ERIKSEN, B.-O. H., BREIVIK, M., WILTHIL, E. F., FLÅTEN, A. L. & BREKKE, E. F. 2019. The branching-course model predictive control algorithm for maritime collision avoidance. *Journal of Field Robotics,* 36**,** 1222-1249.

FOSSEN, T.I., 1999. Guidance and control of ocean vehicles. *University of Trondheim, Norway, Printed by John Wiley & Sons, Chichester, England, ISBN: 0 471 94113 1, Doctors Thesis*.

FOSSEN, T.I., 2002. Marine control systems–guidance. navigation, and control of ships, rigs and underwater vehicles. *Marine Cybernetics, Trondheim, Norway, Org. Number NO 985 195 005 MVA, www. marinecybernetics. com, ISBN: 82 92356 00 2*.

GIERUSZ, W. & RYBCZAK, M. 2020. Effectiveness of Multidimensional Controllers Designated to Steering of the Motions of Ship at Low Speed. *Sensors (Basel, Switzerland),* 20.

GIERUSZ, W., CONG VINH, N. & RAK, A. 2007. Maneuvering control and trajectory tracking of very large crude carrier. *Ocean Engineering,* 34**,** 932-945.

HERMANNSEN, L., BEEDHOLM, K., TOUGAARD, J. & MADSEN, P. T. 2014. High frequency components of ship noise in shallow water with a discussion of implications for harbor porpoises (Phocoena phocoena). *The Journal of the Acoustical Society of America,* 136**,** 1640-1653.

HOLZHÜTER, T. 1997. LQG approach for the high-precision track control of ships. *IEE Proceedings: Control Theory and Applications,* 144**,** 121-127.

IM, N. & HASEGAWA, K. 2001. Automatic Ship Berthing Using Parallel Neural Controller. *IFAC Proceedings Volumes,* 34**,** 51-57.

KASASBEH, Y., POURZANJANI, M. & DOVE, M., 1993. Automatic berthing of ship. *Proc. of the Institute of Marine Engineers 3rd International Conference on Maritime Communications and Control,* pp.1993. 10-17.

KOSE, K., FUKUDO, J., SUGANO, K., AKAGI, S. & HARADA, M., 1986. On a computer aided maneuvering system in harbours. *Journal of the Society of Naval Architects of Japan,* 1986(160), pp.103-110.

LAYNE, J. R. & PASSINO, K. M. 1993. Fuzzy model reference learning control for cargo ship steering. *IEEE Control Systems*, vol. 13, no. 5, pp. 23-34.

LE, M.-D., NGUYEN, S.-H. & NGUYEN, L.-A. 2004. Study on a new and effective fuzzy PID ship autopilot.(Author abstract). *Artificial Life and Robotics,* 8**,** 197.

LEE, G., SURENDRAN, S. & KIM, S.-H. 2009. Algorithms to control the moving ship during harbour entry. *Applied Mathematical Modelling,* 33**,** 2474.

LIU, C., SUN, T. & HU, Q. 2021. Synchronization Control of Dynamic Positioning Ships Using Model Predictive Control. *Journal of Marine Science and Engineering,* 9**,** 1239.

MAKI, A., SAKAMOTO, N., AKIMOTO, Y., NISHIKAWA, H. & UMEDA, N. 2020. Application of optimal control theory based on the evolution strategy (CMA-ES) to automatic berthing. *Journal of Marine Science and Technology,* 25**,** 221-233.

MIZUNO, N., UCHIDA, Y. & OKAZAKI, T. 2015. Quasi Real-Time Optimal Control Scheme for Automatic Berthing. *IFAC PapersOnLine,* 48**,** 305-312.

MOSER, D., HOFSETH, K., HEISEY, S., MALES, R. & ROGERS, C., 2004. Harborsym: A data-driven Monte Carlo Simulation Model of Vessel Movement in Harbors. *Proceedings of HMS2004*.

MUCHA, P., EL MOCTAR, O., DETTMANN, T. & TENZER, M. 2017. Inland waterway ship test case for resistance and propulsion prediction in shallow water. *Ship Technology Research,* 64**,** 106-113.

NGUYEN, P. H. & Jung, Y. C. 2007. Automatic Berthing Control of Ship Using Adaptive Neural Network. *International Symposium on Electrical & Electronics Engineering*, HCM City, Vietnam, pp. 67-73.

OKAZAKI, T. & OHTSU, K., 2008, October. A study on ship berthing support system-Minimum time berthing control. In *2008 IEEE International Conference on Systems, Man and Cybernetics* (pp. 1522-1527). IEEE.

PAPADIMITRAKIS, M., STOGIANNOS, M., SARIMVEIS, H. & ALEXANDRIDIS, A. 2021. Multi-Ship Control and Collision Avoidance Using MPC and RBF-Based Trajectory Predictions. *Sensors (Basel, Switzerland),* 21.

PEREZ, T. 2005. *Ship motion control : course keeping and roll stabilisation using rudder and fins / [internet resource],* London, London : Springer.

PETTERSEN, K.Y. & LEFEBER, E., 2001, December. Way-point tracking control of ships. In *Proceedings of the 40th IEEE conference on decision and control (Cat. No. 01CH37228)* (Vol. 1, pp. 940-945). IEEE.

QIANG, Z., GUIBING, Z., XIN, H. & RENMING, Y. 2019. Adaptive neural network auto-berthing control of marine ships. *Ocean Engineering,* 177**,** 40-48.

ROGERS, C., WOELBELING, W., MALES, R., HOFSETH, K. & HEISEY, S., 2006. HSAM: An interactive, immersive animation of deep-draft maritime traffic simulations. In *Proceedings, 31st PIANC Congress*.

SERBAN, P. & PANAITESCU, V. 2015. SIMULATION OF SHIP TO SHORE INTERACTION IN SHALLOW AND NARROW WATERS. *Scientific Bulletin "Mircea cel Batran" Naval Academy,* 18**,** 112-116.

SUN, X., WANG, G., FAN, Y., MU, D. & QIU, B. 2018. Collision Avoidance Using Finite Control Set Model Predictive Control for Unmanned Surface Vehicle. *Applied Sciences,* 8**,** 926.

WANG, H., SHENG, X., WANG, S., CHEN, L., YUAN, Z. & WU, Q. 2017. Numerical study on water depth effects on hydrodynamic forces acting on berthing ships. *Journal of Shanghai Jiaotong University (Science),* 22**,** 198-205.

WULDER, J.H., HOEBEE, W., KOOREN, A.J., RAMSEY, D.G. & WENZ, R., 2000, May. Applications of Interactive Tug Simulation. In *Proceedings of the MARSIM 2000 Conference Proceedings: International Conference on Marine Simulation and Ship Maneuvering, Orlando, FL, USA* (pp. 8-12).

ZHANG, M., YU, S.R., CHUNG, K.S., CHEN, M.L. & YUAN, Z.M., 2023. Time-optimal path planning and tracking based on nonlinear model predictive control and its application on automatic berthing. *Ocean Engineering*, *286*, p.115228.

ZHANG, Y., HEARN, G.E. & SEN, P., 1997. A multivariable neural controller for automatic ship berthing. *IEEE Control Systems Magazine*, *17*(4), pp.31-45.

ZHAO, S., MAXIM, A., LIU, S., DE KEYSER, R. & IONESCU, C. 2018. Effect of Control Horizon in Model Predictive Control for Steam/Water Loop in Large-Scale Ships. *Processes,* 6**,** 265.

A. Appendix. Simulation Result

A.1 Application of Kose's Mathematical Model

(1) Initial speed of ship 3 m/s in Kose's model

(a) Initial position of ship (-5L, 4L), initial heading angle of ship -40 degrees and initial speed of ship 3 m/s

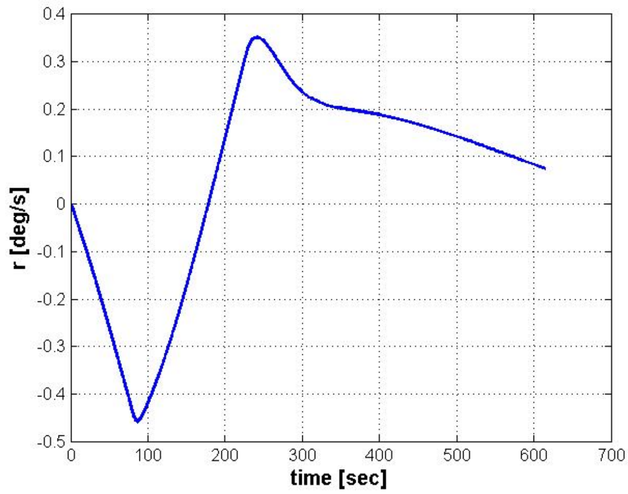

Figure A.1 Yaw rate r for berthing simulation of tanker ship using PD controller with Kose's mathematical model: initial position of ship (-5L, 4L), initial heading angle of ship -40 degrees and initial speed of ship 3 m/s

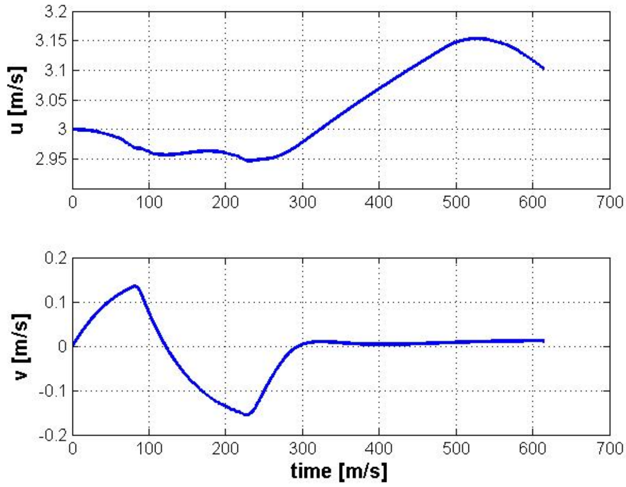

Figure A.2 Surge (u) and sway (v) velocity for berthing simulation of tanker ship using PD controller with Kose's mathematical model: initial position of ship (-5L, 4L), initial heading angle of ship -40 degrees and initial speed of ship 3 m/s

(b) Initial position of ship (-5L, 4L), initial heading angle of ship -70 degrees and initial speed of ship 3 m/s

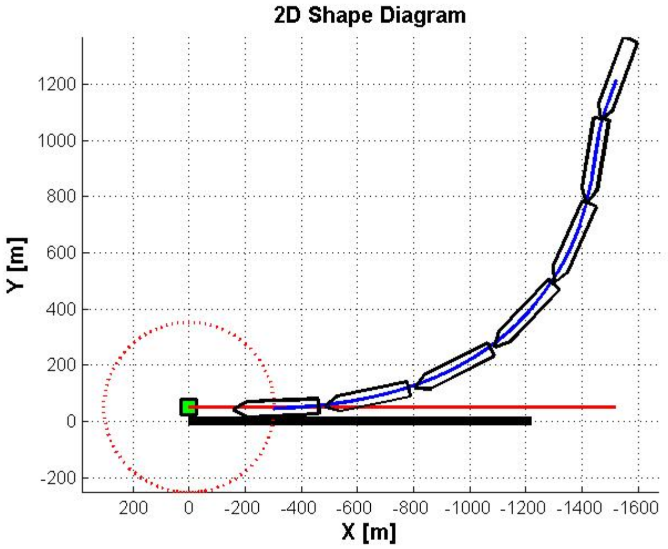

Figure A.3 Trajectory for berthing simulation of tanker ship using PD controller with Kose's mathematical model: initial position of ship (-5L, 4L), initial heading angle of ship -70 degrees and initial speed of ship 3 m/s

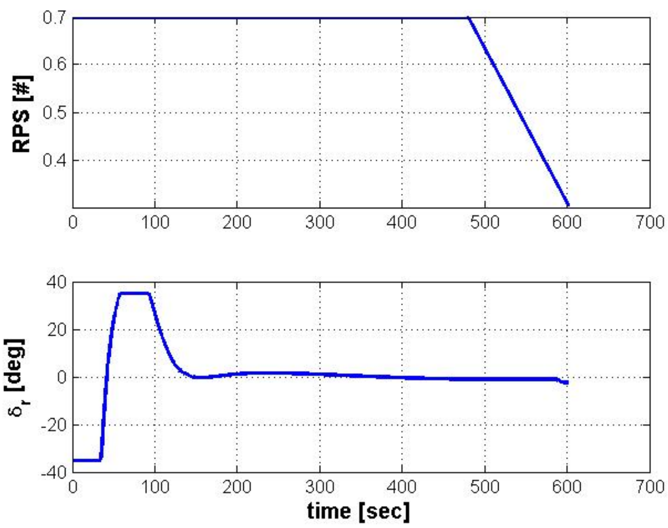

Figure A.4 RPS and δr for berthing simulation of tanker ship using PD controller with Kose's mathematical model: initial position of ship (-5L, 4L), initial heading angle of ship -70 degrees and initial speed of ship 3 m/s

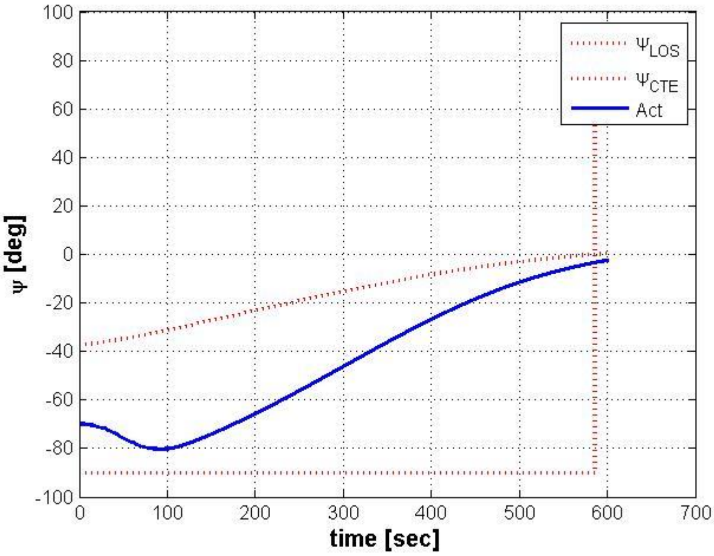

Figure A.5 Heading angle ψ for berthing simulation of tanker ship using PD controller with Kose's mathematical model: initial position of ship (-5L, 4L), initial heading angle of ship -70 degrees and initial speed of ship 3 m/s

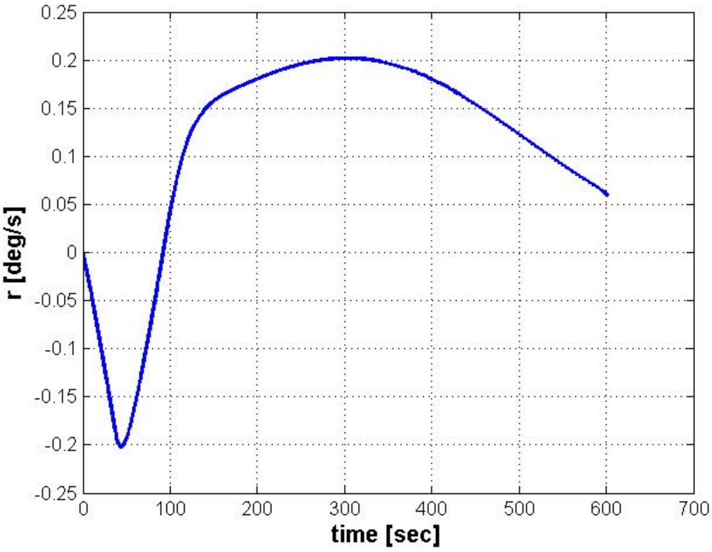

Figure A.6 Yaw rate r for berthing simulation of tanker ship using PD controller with Kose's mathematical model: initial position of ship (-5L, 4L), initial heading angle of ship -70 degrees and initial speed of ship 3 m/s

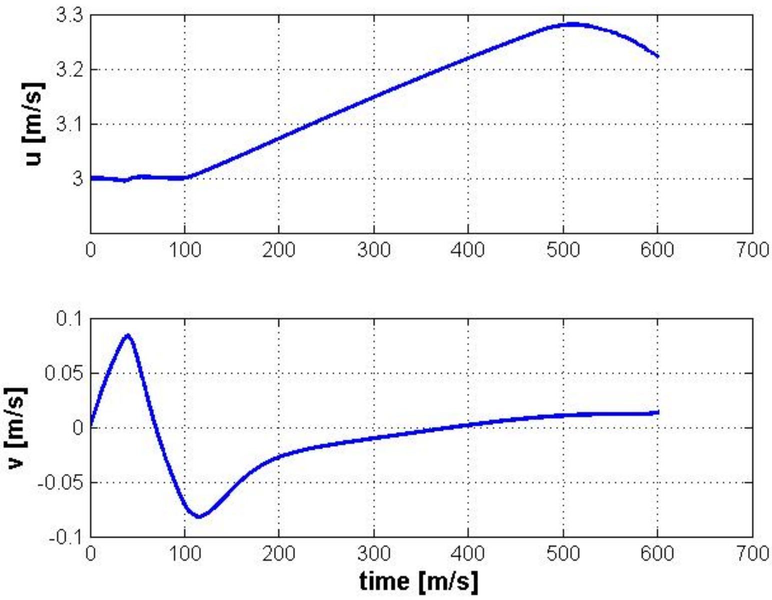

Figure A.7 Surge (u) and sway (v) velocity for berthing simulation of tanker ship using PD controller with Kose's mathematical model: initial position of ship (-5L, 4L), initial heading angle of ship -70 degrees and initial speed of ship 3 m/s

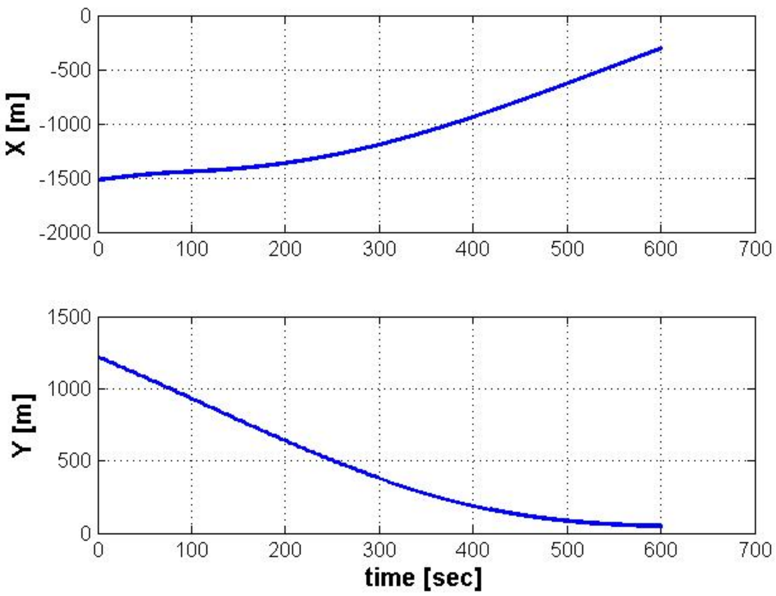

Figure A.8 X, Y variation for berthing simulation of tanker ship using PD controller with Kose's mathematical model: initial position of ship (-5L, 4L), initial heading angle of ship -70 degrees and initial speed of ship 3 m/s

(c) Initial position of ship (-5L, 3L), initial heading angle of ship -40 degrees and initial speed of ship 3 m/s

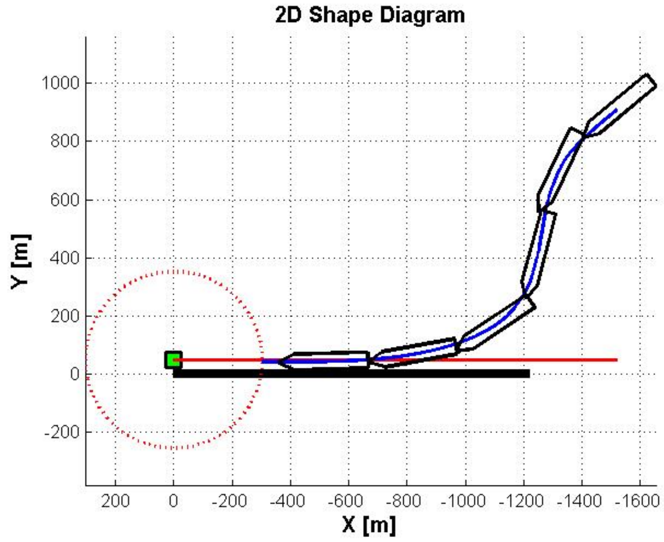

Figure A.9 Trajectory for berthing simulation of tanker ship using PD controller with Kose's mathematical model: initial position of ship (-5L, 3L), initial heading angle of ship -40 degrees and initial speed of ship 3 m/s

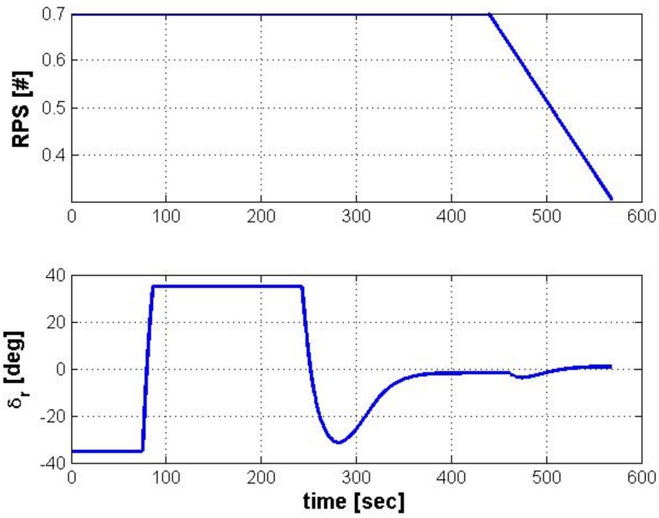

Figure A.10 RPS and δr for berthing simulation of tanker ship using PD controller with Kose's mathematical model: initial position of ship (-5L, 3L), initial heading angle of ship -40 degrees and initial speed of ship 3 m/s

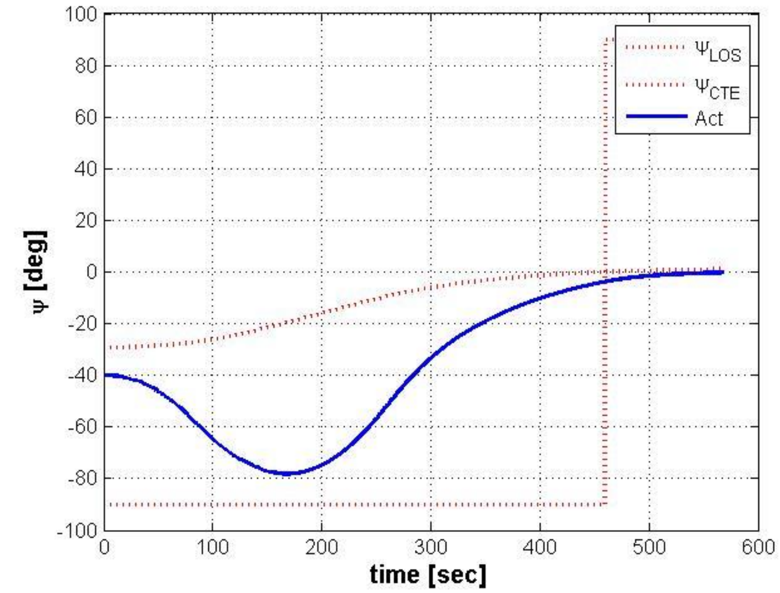

Figure A.11 Heading angle ψ for berthing simulation of tanker ship using PD controller with Kose's mathematical model: initial position of ship (-5L, 3L), initial heading angle of ship -40 degrees and initial speed of ship 3 m/s

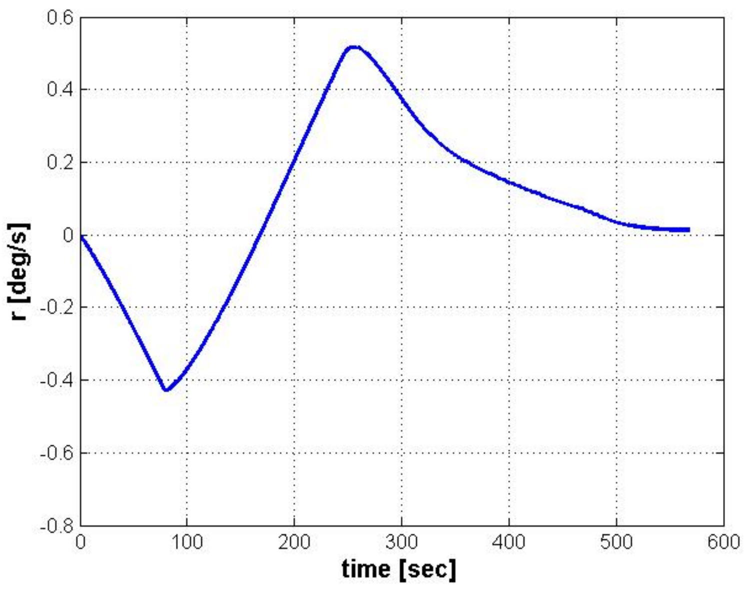

Figure A.12 Yaw rate r for berthing simulation of tanker ship using PD controller with Kose's mathematical model: initial position of ship (-5L, 3L), initial heading angle of ship -40 degrees and initial speed of ship 3 m/s

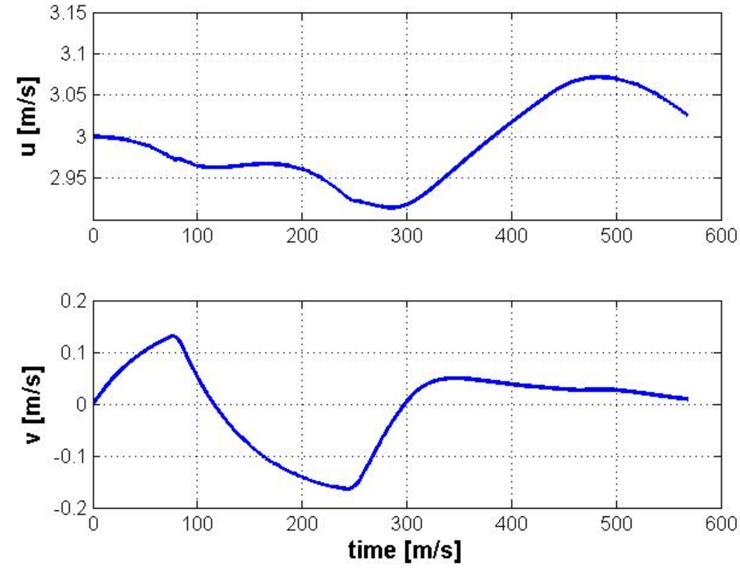

Figure A.13 Surge (u) and sway (v) velocity for berthing simulation of tanker ship using PD controller with Kose's mathematical model: initial position of ship (-5L, 3L), initial heading angle of ship -40 degrees and initial speed of ship 3 m/s

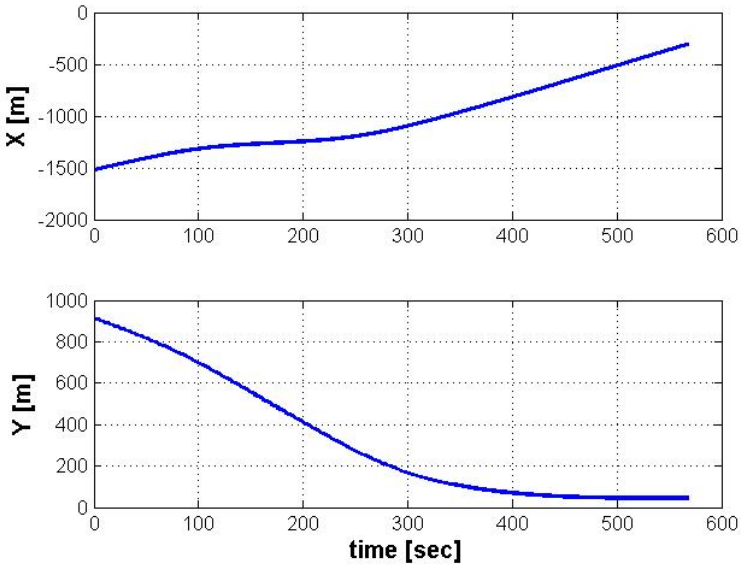

Figure A.14 X, Y variation for berthing simulation of tanker ship using PD controller with Kose's mathematical model: initial position of ship (-5L, 3L), initial heading angle of ship -40 degrees and initial speed of ship 3 m/s

(d) Initial position of ship (-6L, 2L), initial heading angle of ship -30 degrees and initial speed of ship 3 m/s

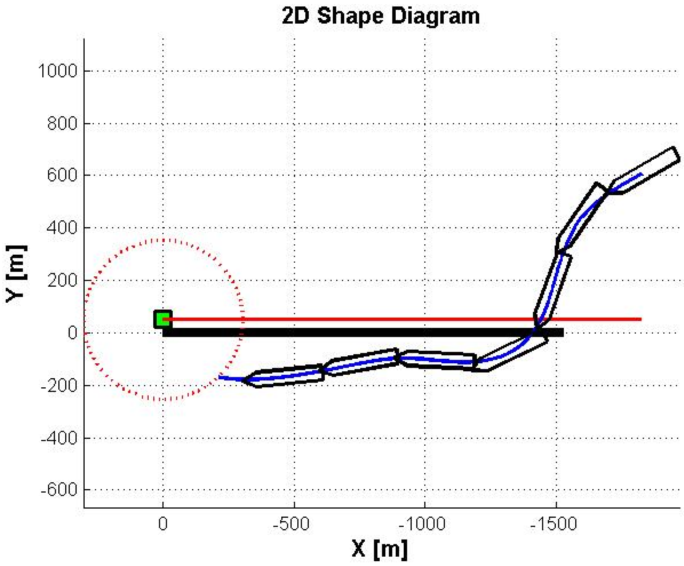

Figure A.15 Trajectory for berthing simulation of tanker ship using PD controller with Kose's mathematical model: initial position of ship (-6L, 2L), initial heading angle of ship -30 degrees and initial speed of ship 3 m/s

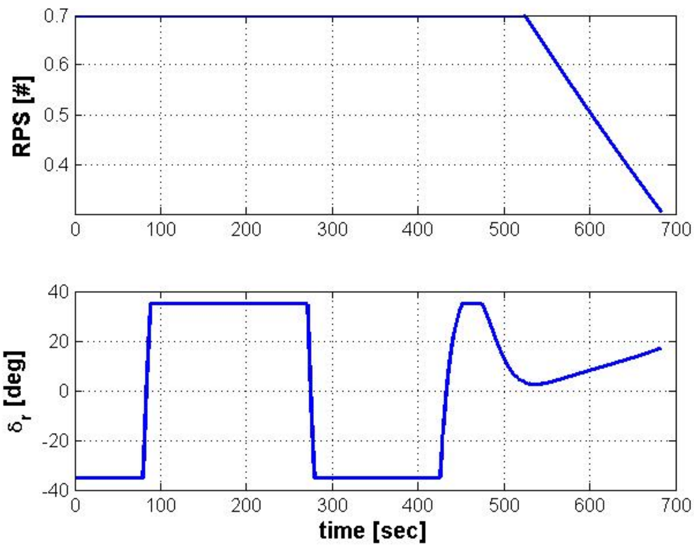

Figure A.16 RPS and δr for berthing simulation of tanker ship using PD controller with Kose's mathematical model: initial position of ship (-6L, 2L), initial heading angle of ship -30 degrees and initial speed of ship 3 m/s

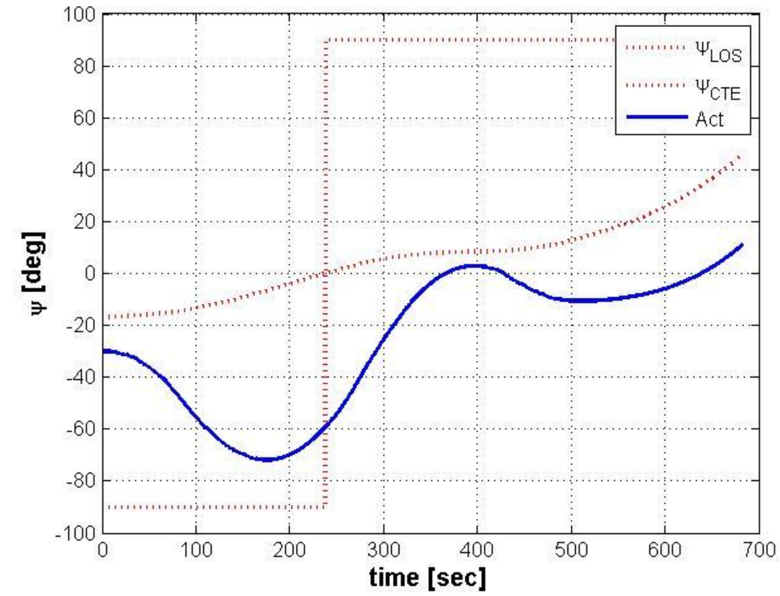

Figure A.17 Heading angle ψ for berthing simulation of tanker ship using PD controller with Kose's mathematical model: initial position of ship (-6L, 2L), initial heading angle of ship -30 degrees and initial speed of ship 3 m/s

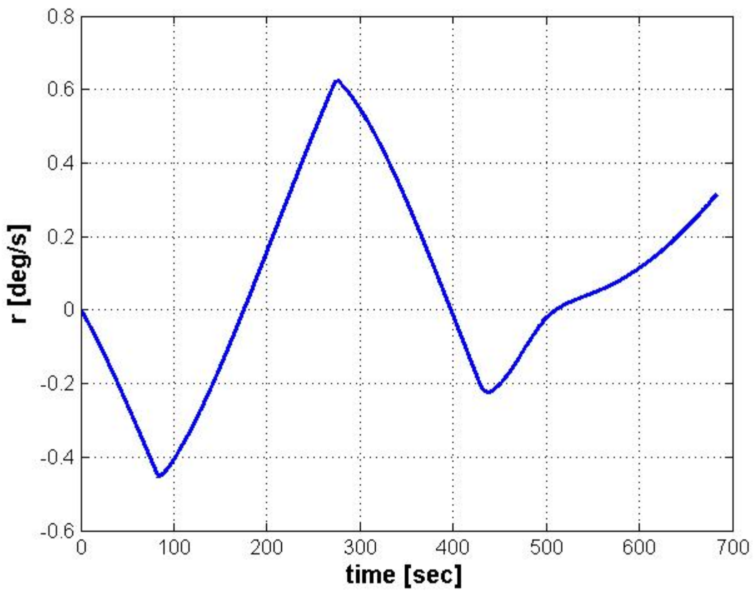

Figure A.18 Yaw rate r for berthing simulation of tanker ship using PD controller with Kose's mathematical model: initial position of ship (-6L, 2L), initial heading angle of ship -30 degrees and initial speed of ship 3 m/s

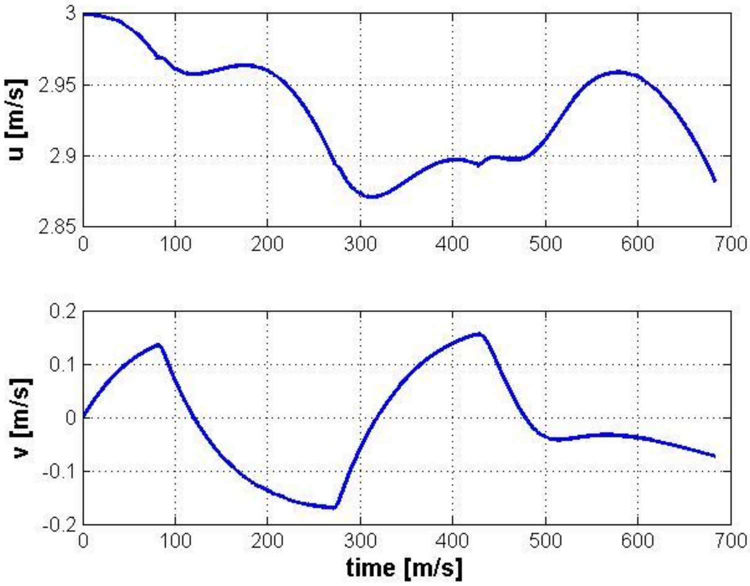

Figure A.19 Surge (u) and sway (v) velocity for berthing simulation of tanker ship using PD controller with Kose's mathematical model: initial position of ship (-6L, 2L), initial heading angle of ship -30 degrees and initial speed of ship 3 m/s

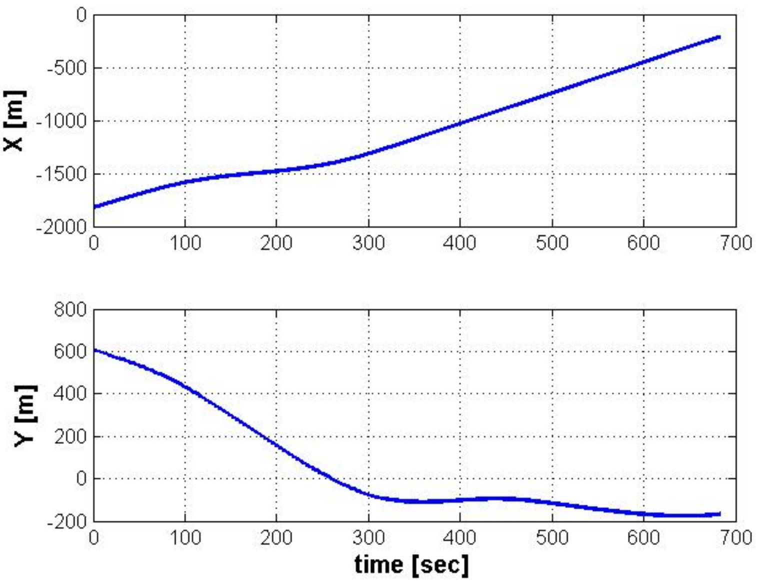

Figure A.20 X, Y variation for berthing simulation of tanker ship using PD controller with Kose's mathematical model: initial position of ship (-6L, 2L), initial heading angle of ship -30 degrees and initial speed of ship 3 m/s

(2) Initial speed of ship 4 m/s in Kose's model

(a) Initial position of ship (-5L, 4L), initial heading angle of ship -40 degrees and initial speed of ship 4 m/s

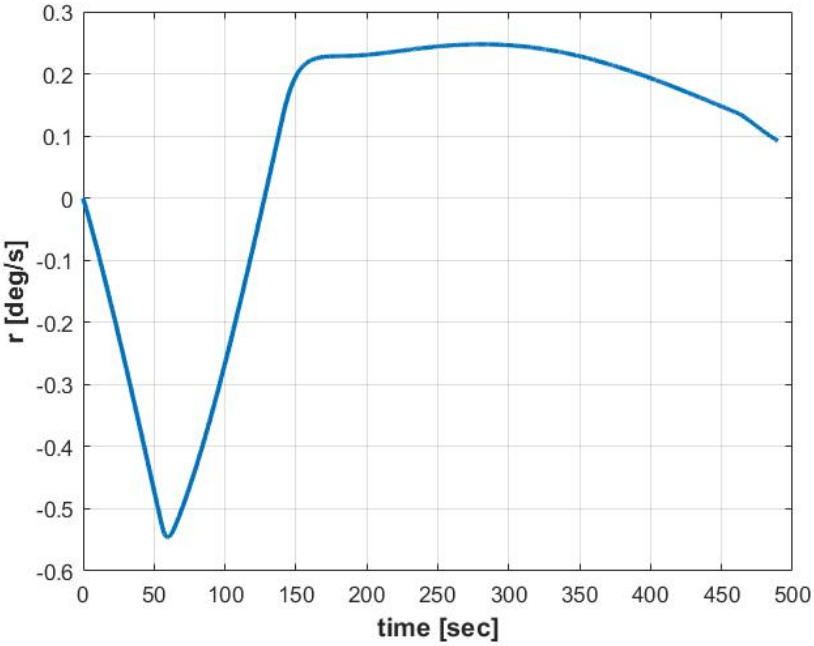

Figure A.21 Yaw rate r for berthing simulation of tanker ship using PD controller with Kose's mathematical model: initial position of ship (-5L, 4L), initial heading angle of ship -40 degrees and initial speed of ship 4 m/s

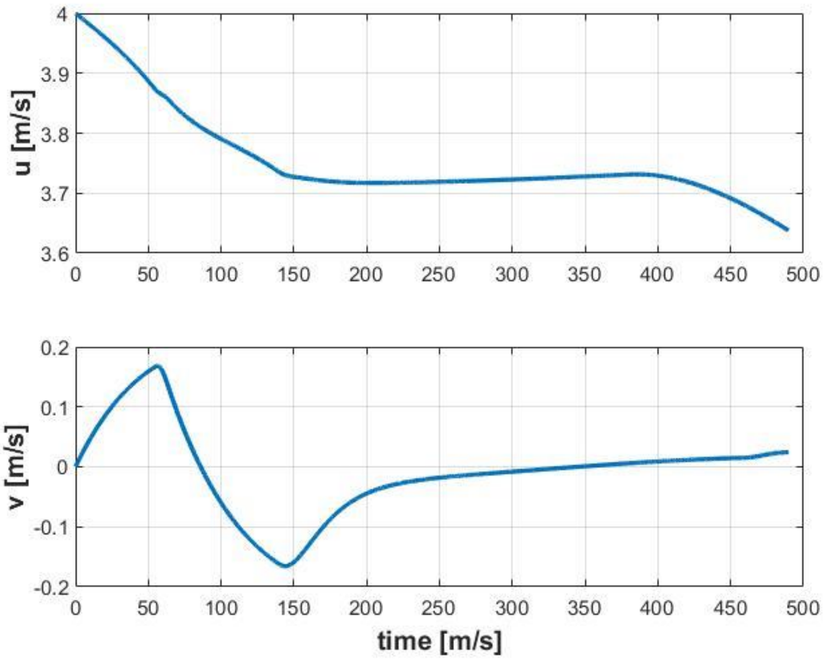

Figure A.22 Surge (u) and sway (v) velocity for berthing simulation of tanker ship using PD controller with Kose's mathematical model: initial position of ship (-5L, 4L), initial heading angle of ship -40 degrees and initial speed of ship 4 m/s

(b) Initial position of ship (-5L, 4L), initial heading angle of ship -70 degrees and initial speed of ship 4 m/s

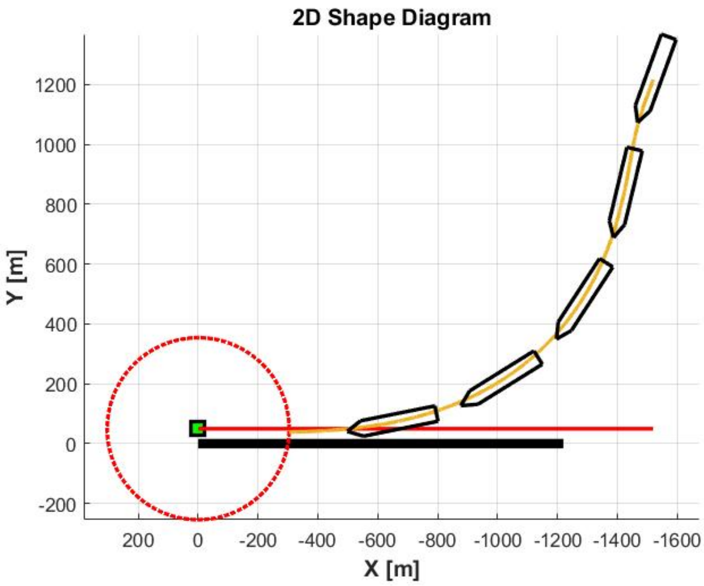

Figure A.23 Trajectory for berthing simulation of tanker ship using PD controller with Kose's mathematical model: initial position of ship (-5L, 4L), initial heading angle of ship -70 degrees and initial speed of ship 4 m/s

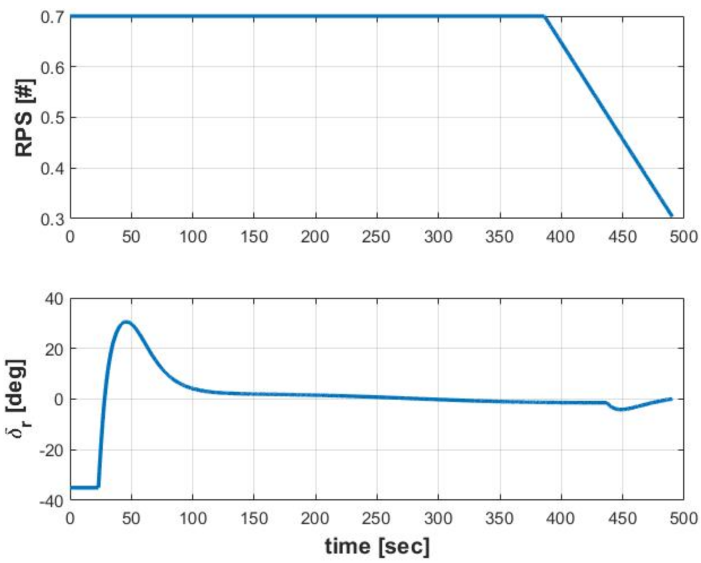

Figure A.24 RPS and δr for berthing simulation of tanker ship using PD controller with Kose's mathematical model: initial position of ship (-5L, 4L), initial heading angle of ship -70 degrees and initial speed of ship 4 m/s

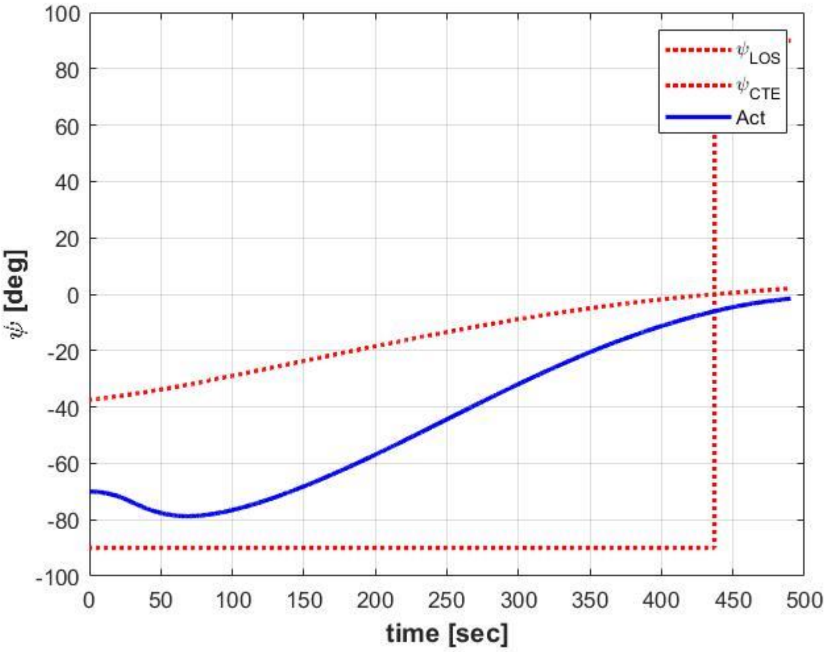

Figure A.25 Heading angle ψ for berthing simulation of tanker ship using PD controller with Kose's mathematical model: initial position of ship (-5L, 4L), initial heading angle of ship -70 degrees and initial speed of ship 4 m/s

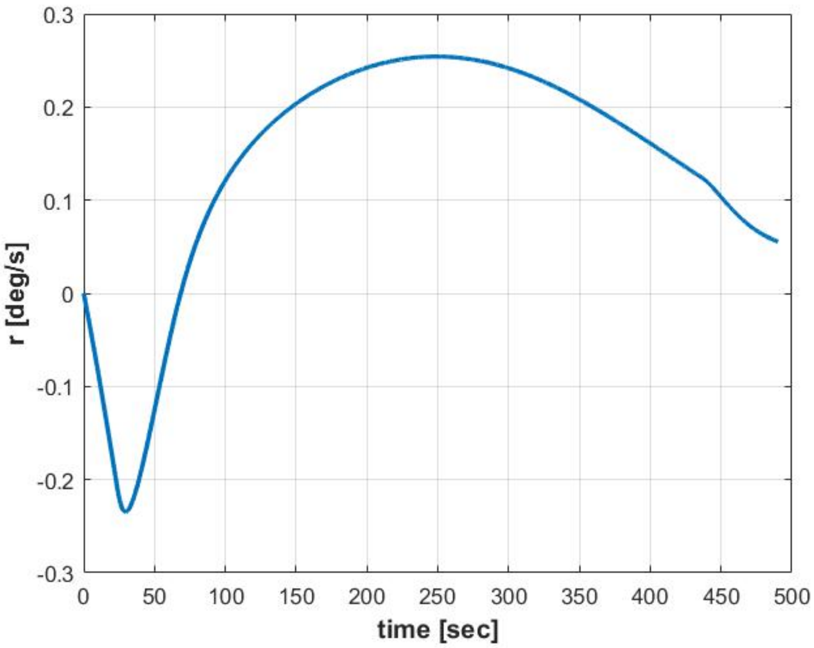

Figure A.26 Yaw rate r for berthing simulation of tanker ship using PD controller with Kose's mathematical model: initial position of ship (-5L, 4L), initial heading angle of ship -70 degrees and initial speed of ship 4 m/s

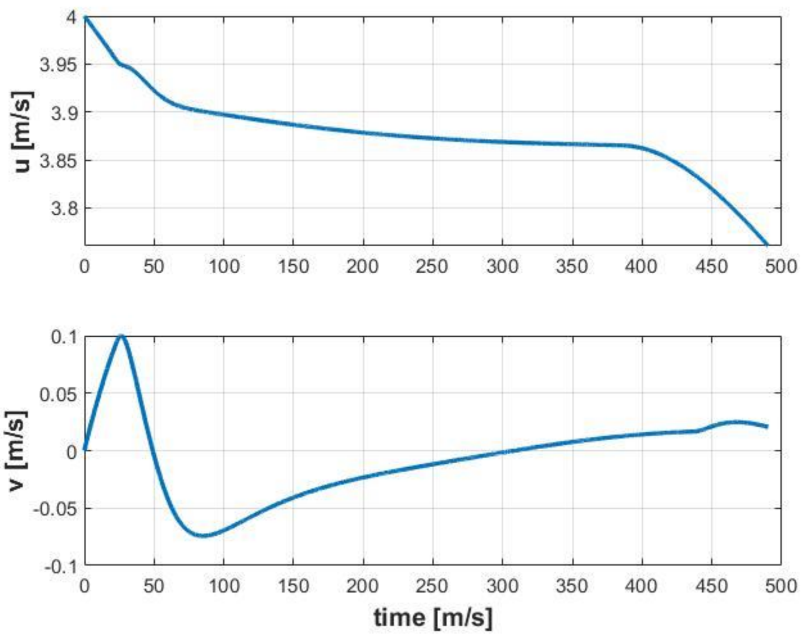

Figure A.27 Surge (u) and sway (v) velocity for berthing simulation of tanker ship using PD controller with Kose's mathematical model: initial position of ship (-5L, 4L), initial heading angle of ship -70 degrees and initial speed of ship 4 m/s

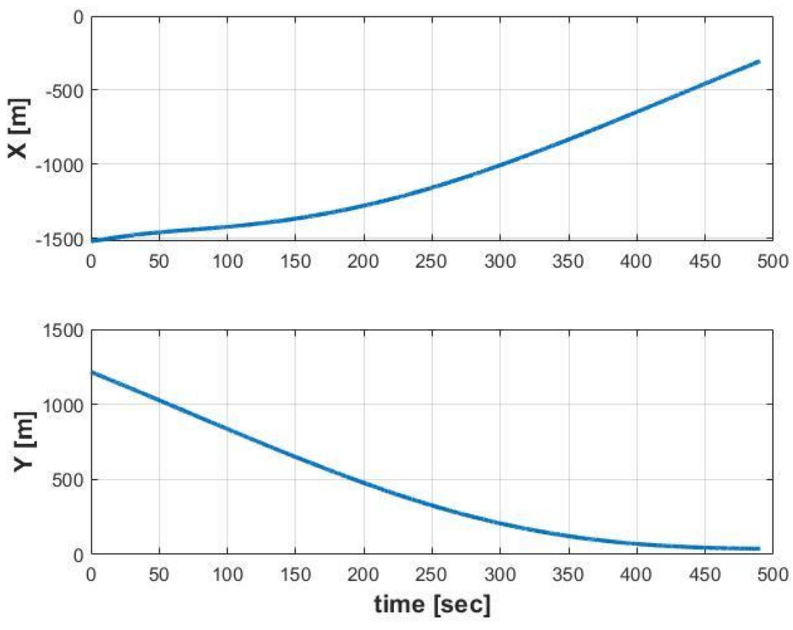

Figure A.28 X, Y variation for berthing simulation of tanker ship using PD controller with Kose's mathematical model: initial position of ship (-5L, 4L), initial heading angle of ship -70 degrees and initial speed of ship 4 m/s

(c) Initial position of ship (-5L, 3L), initial heading angle of ship -40 degrees and initial speed of ship 4 m/s

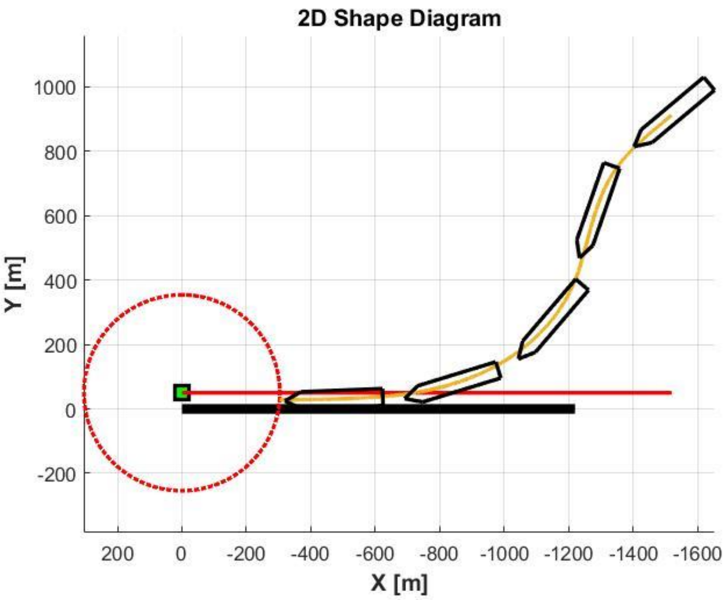

Figure A.29 Trajectory for berthing simulation of tanker ship using PD controller with Kose's mathematical model: initial position of ship (-5L, 3L), initial heading angle of ship -40 degrees and initial speed of ship 4 m/s

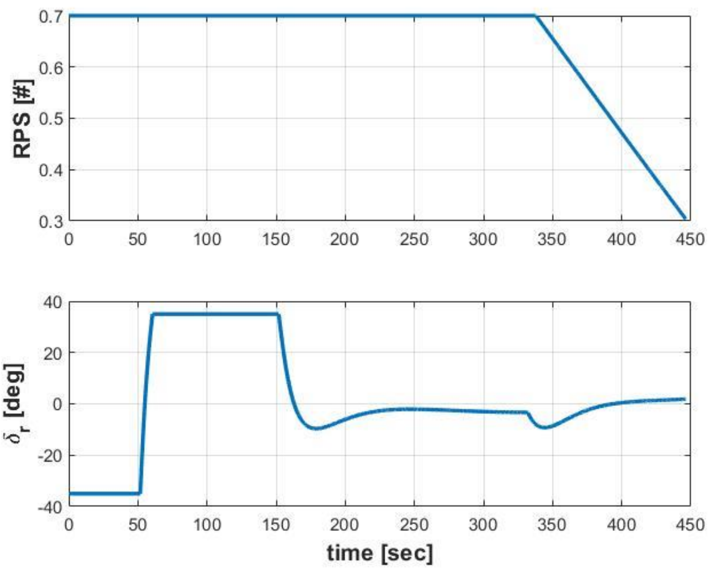

Figure A.30 RPS and δr for berthing simulation of tanker ship using PD controller with Kose's mathematical model: initial position of ship (-5L, 3L), initial heading angle of ship -40 degrees and initial speed of ship 4 m/s

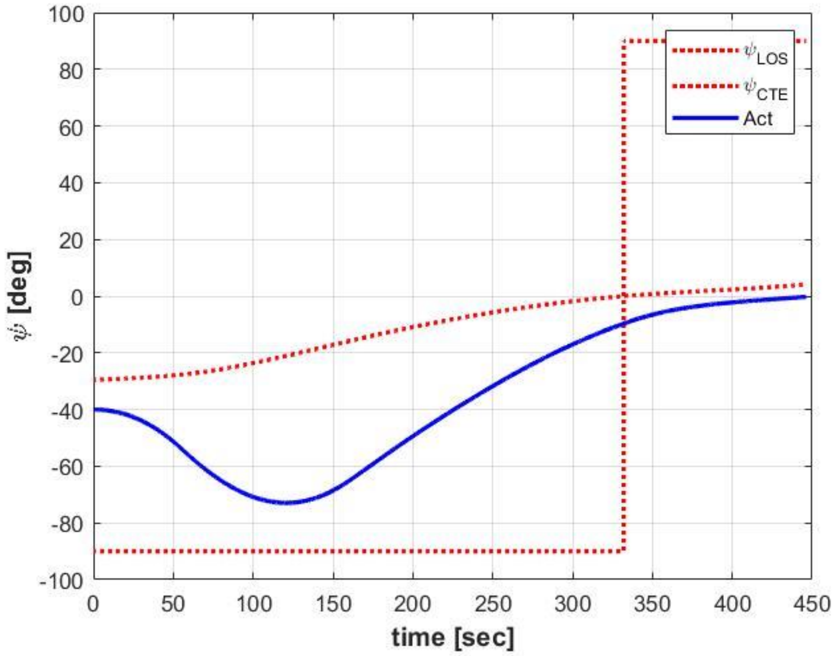

Figure A.31 Heading angle ψ for berthing simulation of tanker ship using PD controller with Kose's mathematical model: initial position of ship (-5L, 3L), initial heading angle of ship -40 degrees and initial speed of ship 4 m/s

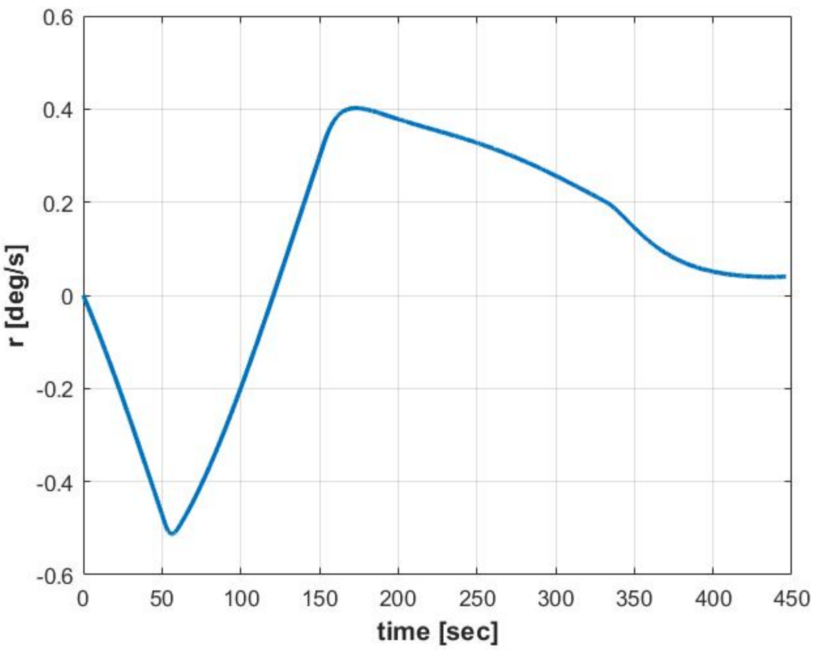

Figure A.32 Yaw rate r for berthing simulation of tanker ship using PD controller with Kose's mathematical model: initial position of ship (-5L, 3L), initial heading angle of ship -40 degrees and initial speed of ship 4 m/s

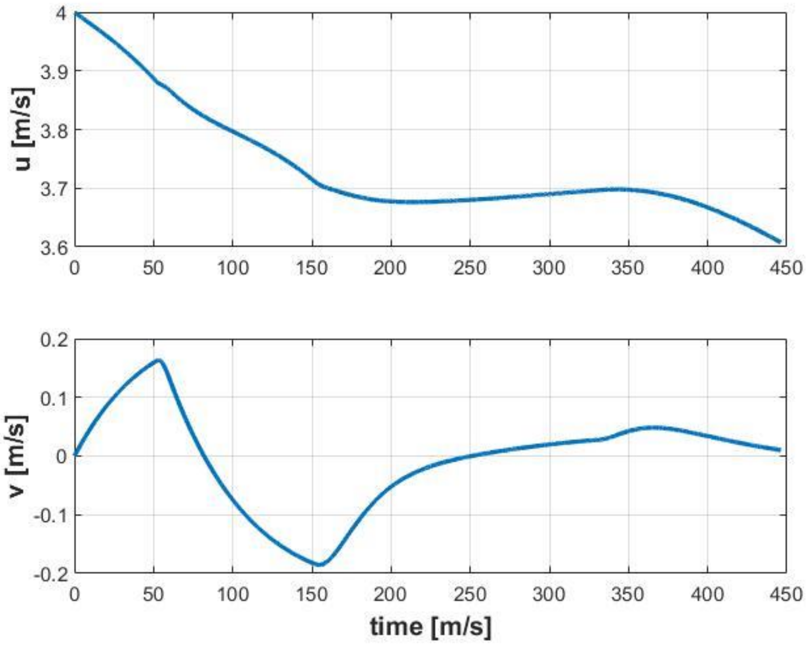

Figure A.33 Surge (u) and sway (v) velocity for berthing simulation of tanker ship using PD controller with Kose's mathematical model: initial position of ship (-5L, 3L), initial heading angle of ship -40 degrees and initial speed of ship 4 m/s

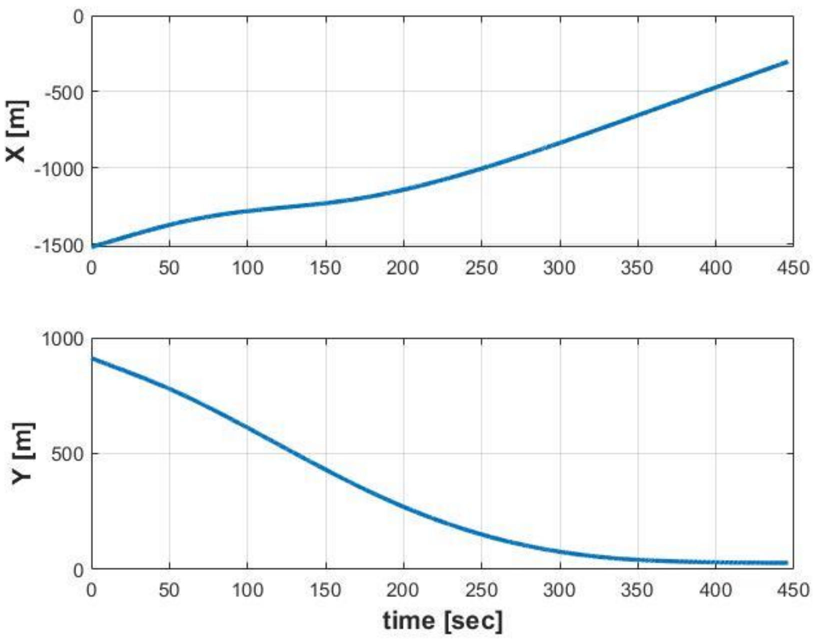

Figure A.34 X, Y variation for berthing simulation of tanker ship using PD controller with Kose's mathematical model: initial position of ship (-5L, 3L), initial heading angle of ship -40 degrees and initial speed of ship 4 m/s

A.2 Application of MMG Model

(1) Initial speed of ship 3 m/s in MMG model

(a) Initial position of ship (-5L, 4L), initial heading angle of ship -40 degrees and initial speed of ship 3 m/s

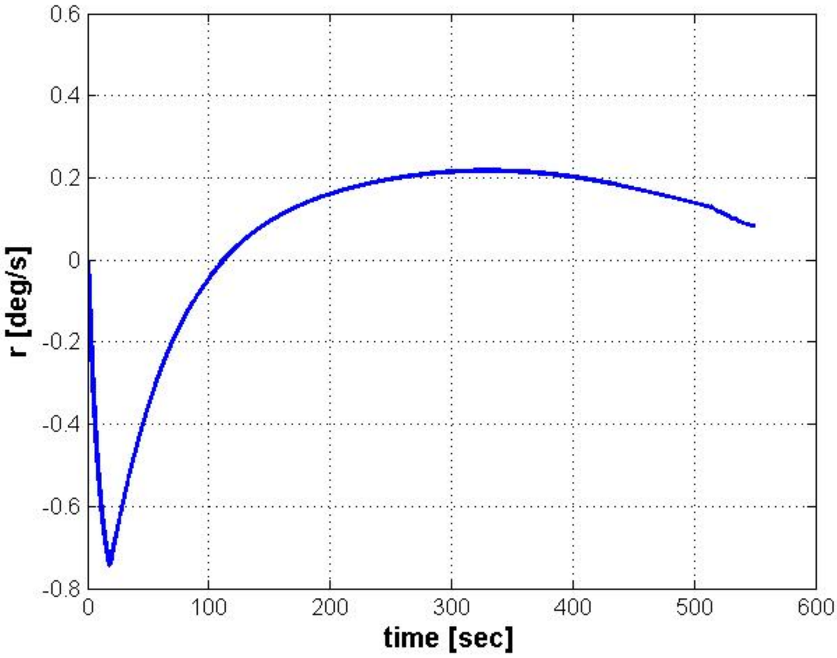

Figure A.35 Yaw rate r for berthing simulation of tanker ship using PD controller with normal MMG model: initial position of ship (-5L, 4L), initial heading angle of ship -40 degrees and initial speed of ship 3 m/s

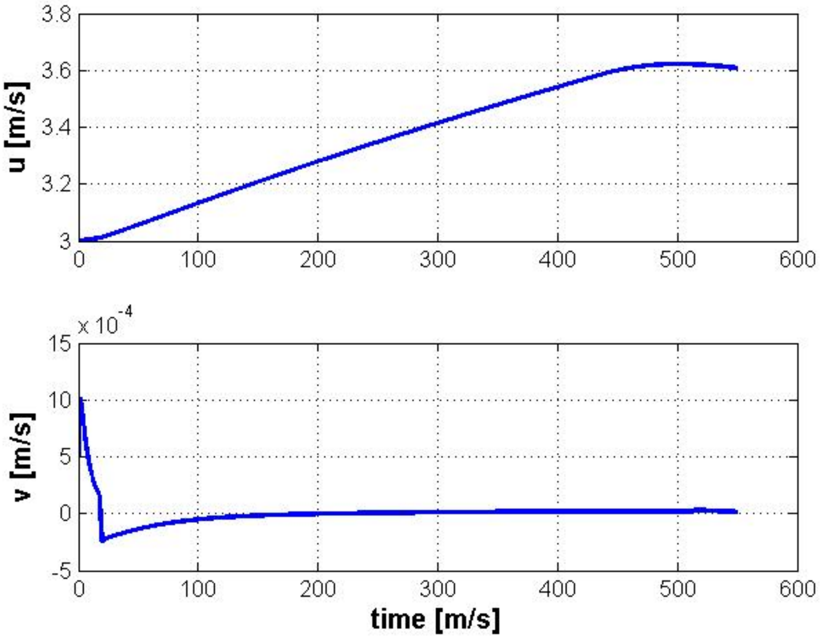

Figure A.36 Surge (u) and sway (v) velocity for berthing simulation of tanker ship using PD controller with normal MMG model: initial position of ship (-5L, 4L), initial heading angle of ship -40 degrees and initial speed of ship 3 m/s

(b) Initial position of ship (-5L, 4L), initial heading angle of ship -70 degrees and initial speed of ship 3 m/s

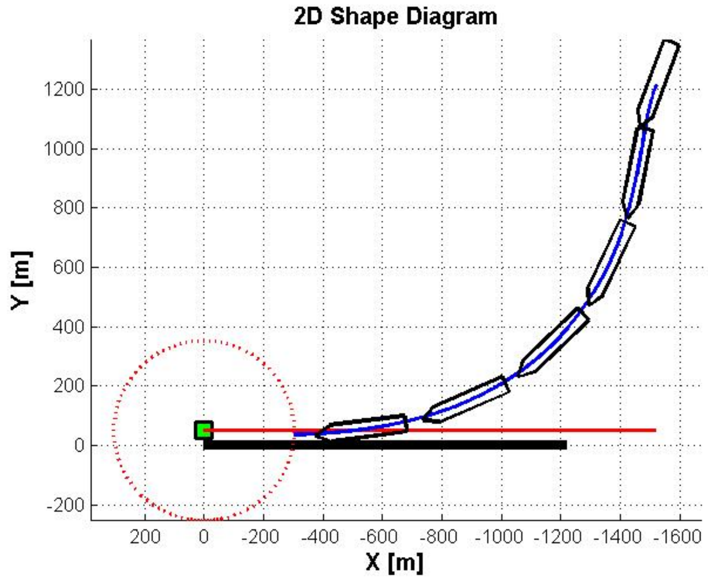

Figure A.37 Trajectory for berthing simulation of tanker ship using PD controller with normal MMG model: initial position of ship (-5L, 4L), initial heading angle of ship -70 degrees and initial speed of ship 3 m/s

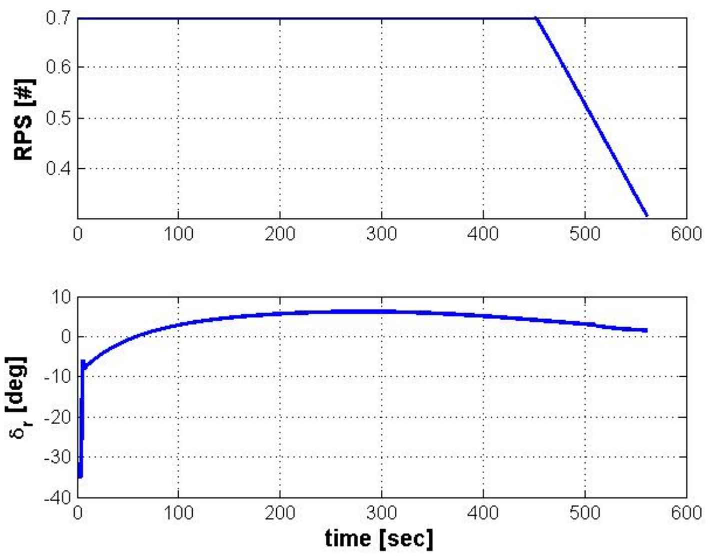

Figure A.38 RPS and δr for berthing simulation of tanker ship using PD controller with normal MMG model: initial position of ship (-5L, 4L), initial heading angle of ship -70 degrees and initial speed of ship 3 m/s

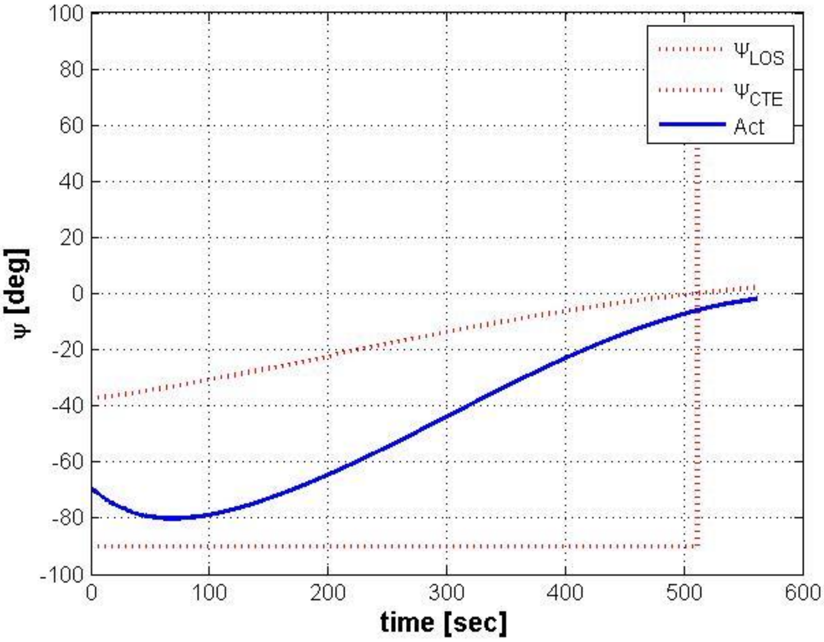

Figure A.39 Heading angle ψ for berthing simulation of tanker ship using PD controller with normal MMG model: initial position of ship (-5L, 4L), initial heading angle of ship -70 degrees and initial speed of ship 3 m/s

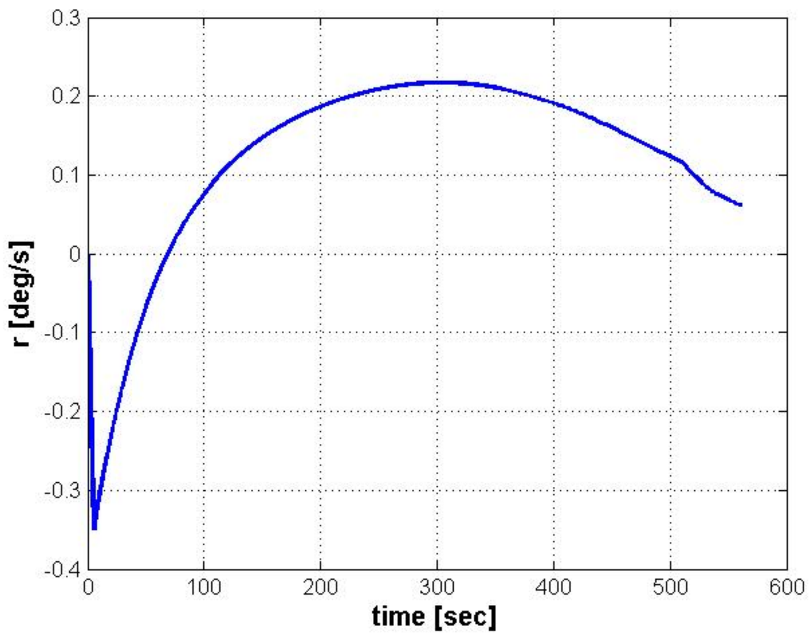

Figure A.40 Yaw rate r for berthing simulation of tanker ship using PD controller with normal MMG model: initial position of ship (-5L, 4L), initial heading angle of ship -70 degrees and initial speed of ship 3 m/s

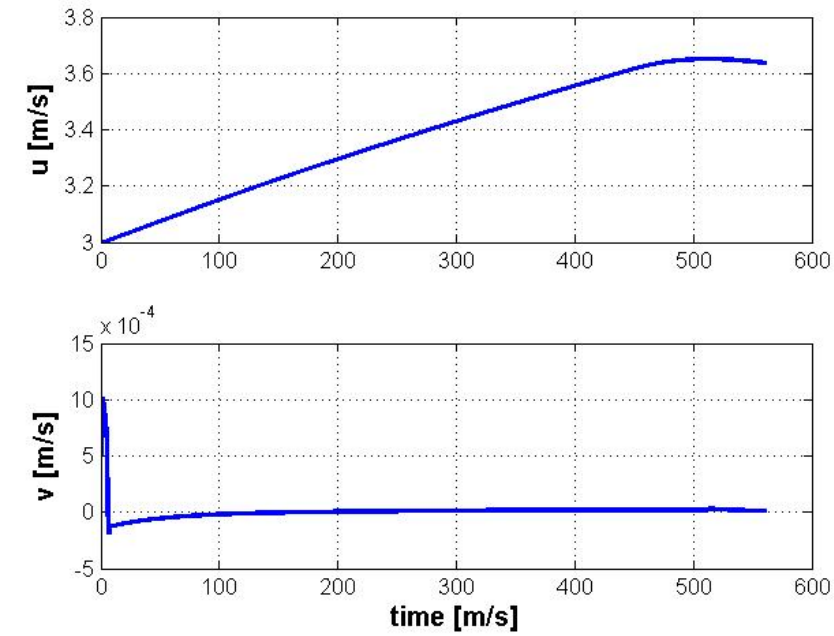

Figure A.41 Surge (u) and sway (v) velocity for berthing simulation of tanker ship using PD controller with normal MMG model: initial position of ship (-5L, 4L), initial heading angle of ship -70 degrees and initial speed of ship 3 m/s

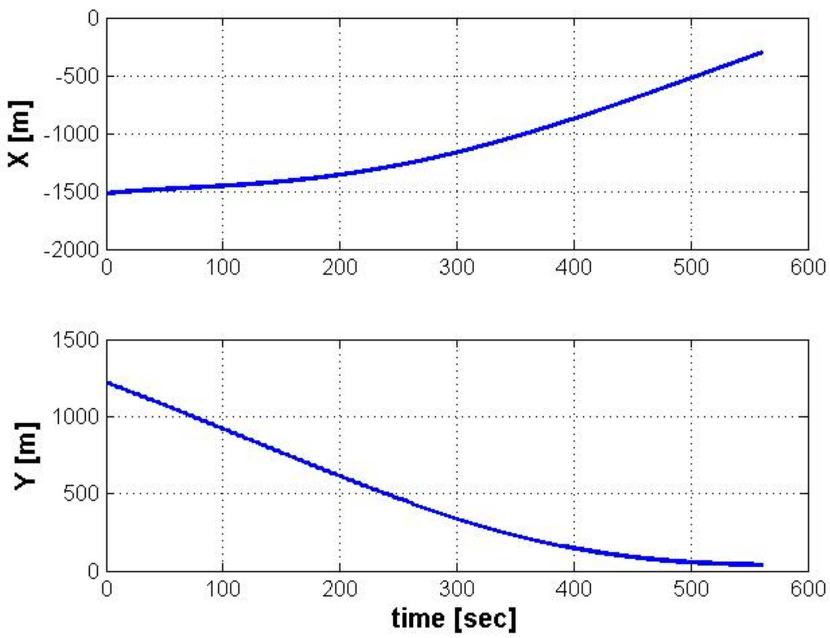

Figure A.42 X, Y variation for berthing simulation of tanker ship using PD controller with normal MMG model: initial position of ship (-5L, 4L), initial heading angle of ship -70 degrees and initial speed of ship 3 m/s

(c) Initial position of ship (-5L, 3L), initial heading angle of ship -40 degrees and initial speed of ship 3 m/s

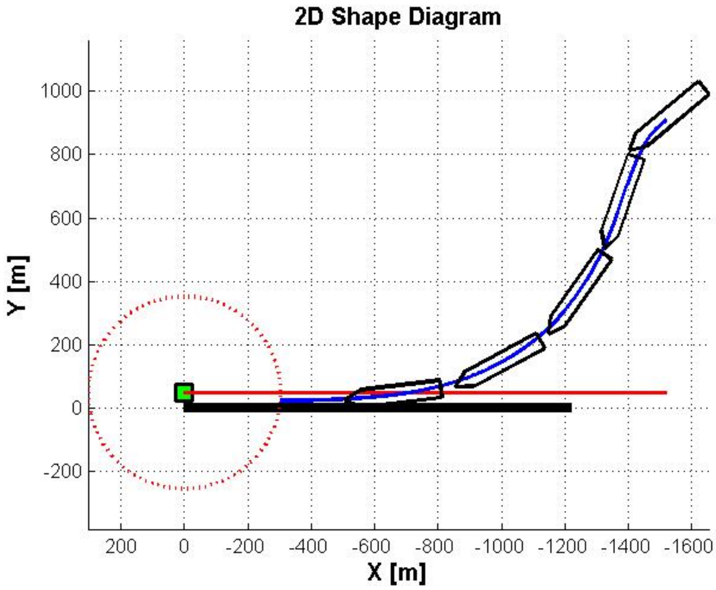

Figure A.43 Trajectory for berthing simulation of tanker ship using PD controller with normal MMG model: initial position of ship (-5L, 3L), initial heading angle of ship -40 degrees and initial speed of ship 3 m/s

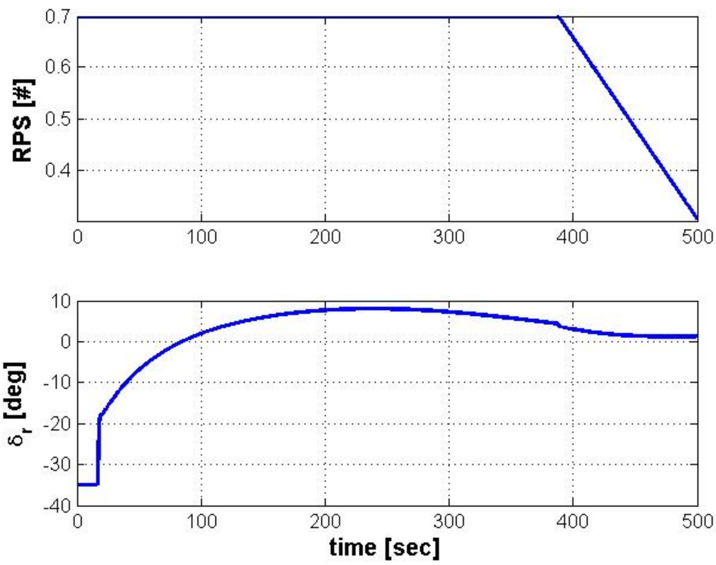

Figure A.44 RPS and δr for berthing simulation of tanker ship using PD controller with normal MMG model: initial position of ship (-5L, 3L), initial heading angle of ship -40 degrees and initial speed of ship 3 m/s

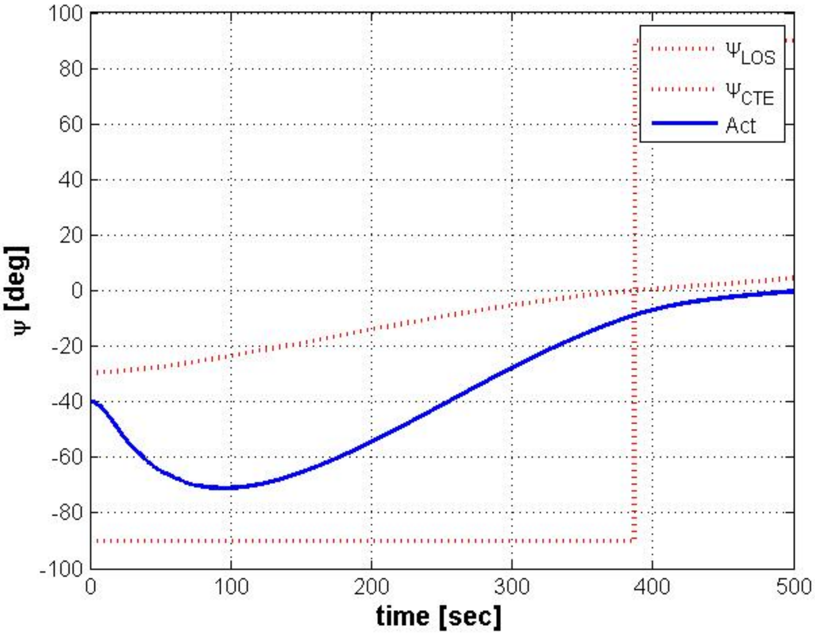

Figure A.45 Heading angle ψ for berthing simulation of tanker ship using PD controller with normal MMG model: initial position of ship (-5L, 3L), initial heading angle of ship -40 degrees and initial speed of ship 3 m/s

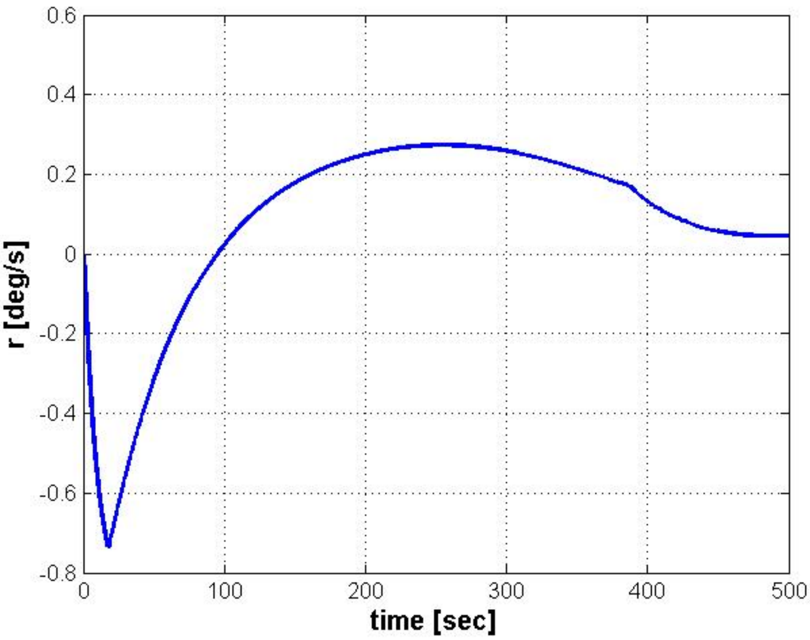

Figure A.46 Yaw rate r for berthing simulation of tanker ship using PD controller with normal MMG model: initial position of ship (-5L, 3L), initial heading angle of ship -40 degrees and initial speed of ship 3 m/s

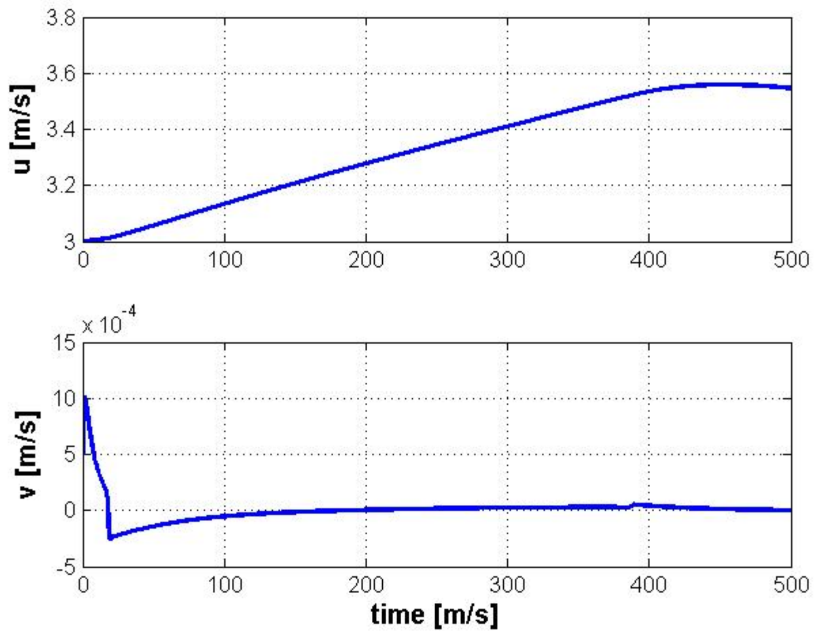

Figure A.47 Surge (u) and sway (v) velocity for berthing simulation of tanker ship using PD controller with normal MMG model: initial position of ship (-5L, 3L), initial heading angle of ship -40 degrees and initial speed of ship 3 m/s

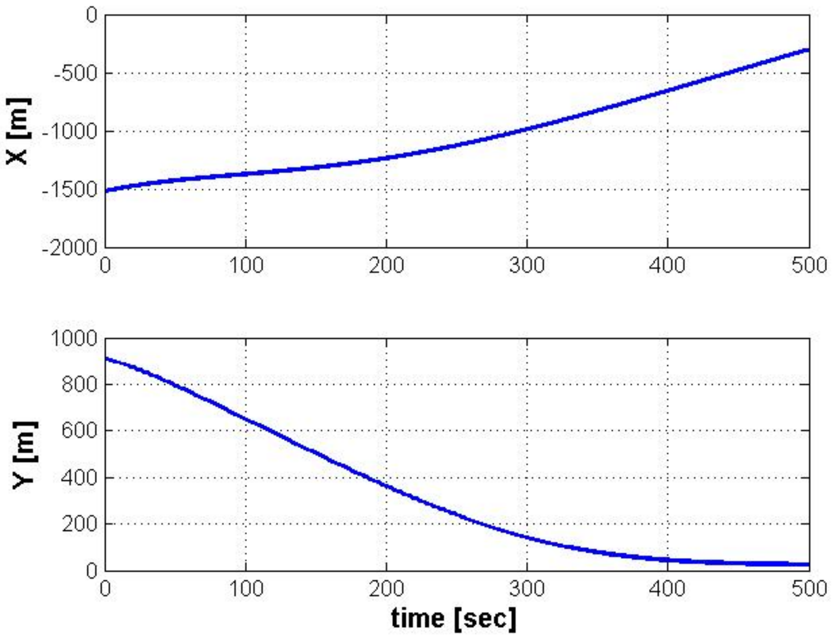

Figure A.48 X, Y variation for berthing simulation of tanker ship using PD controller with normal MMG model: initial position of ship (-5L, 3L), initial heading angle of ship -40 degrees and initial speed of ship 3 m/s

(d) Initial position of ship (-6L, 2L), initial heading angle of ship -30 degrees and initial speed of ship 3 m/s

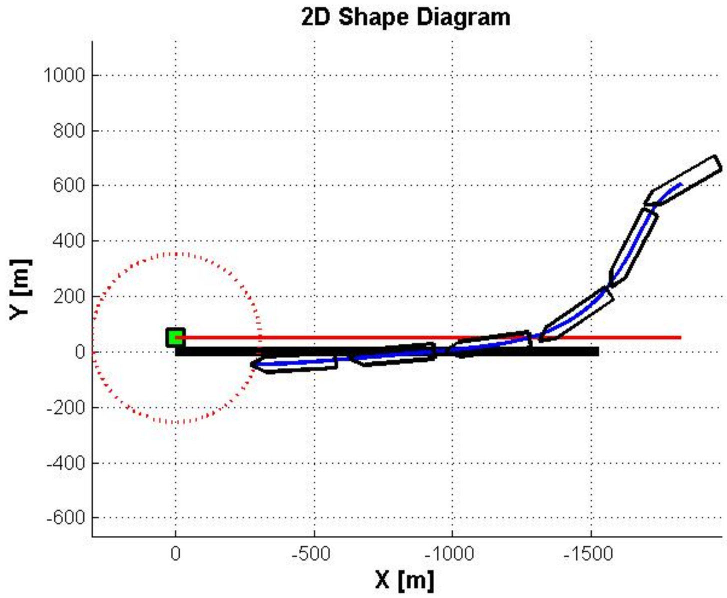

Figure A.49 Trajectory for berthing simulation of tanker ship using PD controller with normal MMG model: initial position of ship (-6L, 2L), initial heading angle of ship -30 degrees and initial speed of ship 3 m/s

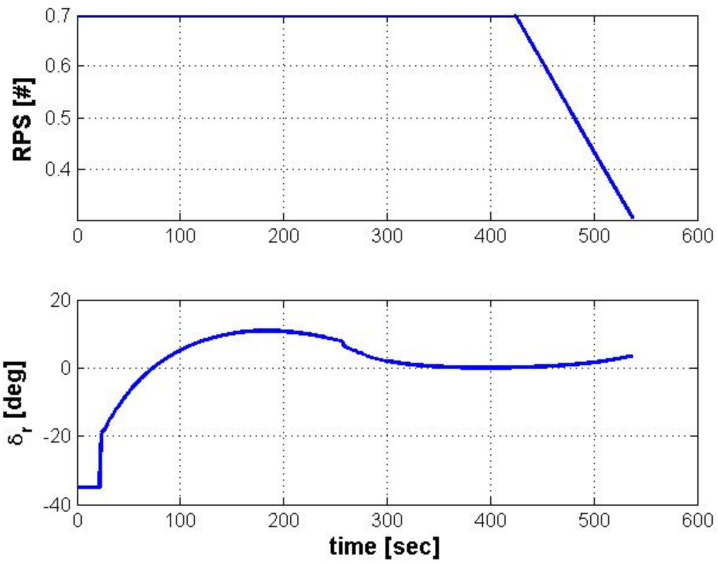

Figure A.50 RPS and δr for berthing simulation of tanker ship using PD controller with normal MMG model: initial position of ship (-6L, 2L), initial heading angle of ship -30 degrees and initial speed of ship 3 m/s

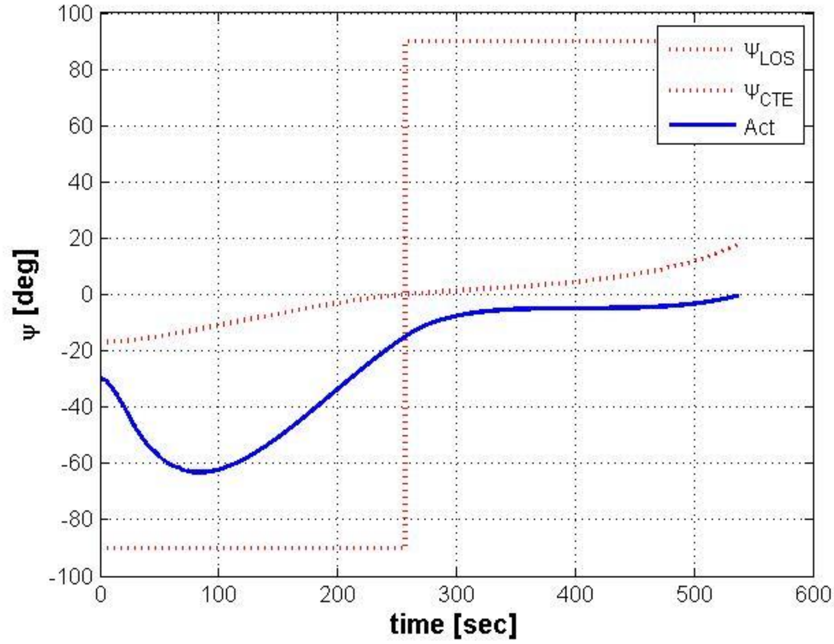

Figure A.51 Heading angle ψ for berthing simulation of tanker ship using PD controller with normal MMG model: initial position of ship (-6L, 2L), initial heading angle of ship -30 degrees and initial speed of ship 3 m/s

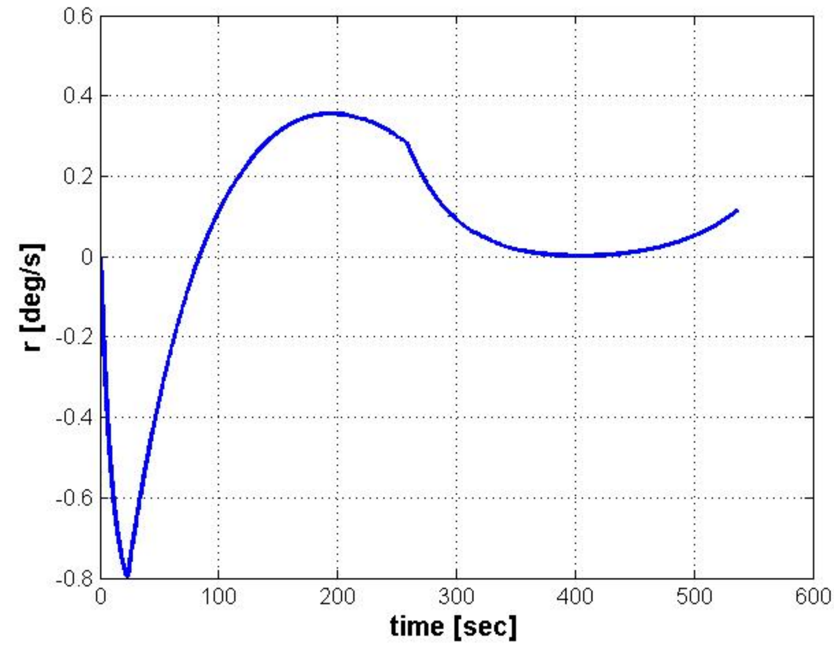

Figure A.52 Yaw rate r for berthing simulation of tanker ship using PD controller with normal MMG model: initial position of ship (-6L, 2L), initial heading angle of ship -30 degrees and initial speed of ship 3 m/s

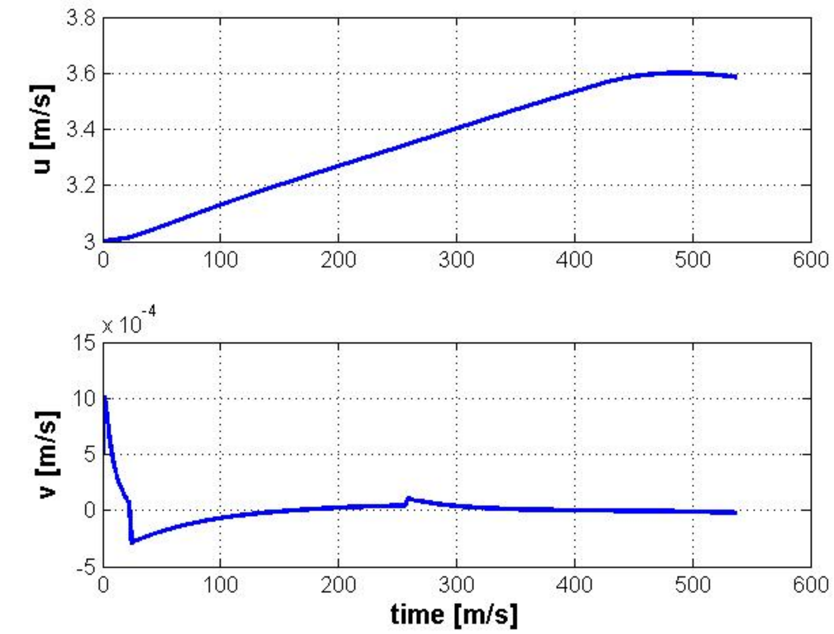

Figure A.53 Surge (u) and sway (v) velocity for berthing simulation of tanker ship using PD controller with normal MMG model: initial position of ship (-6L, 2L), initial heading angle of ship -30 degrees and initial speed of ship 3 m/s

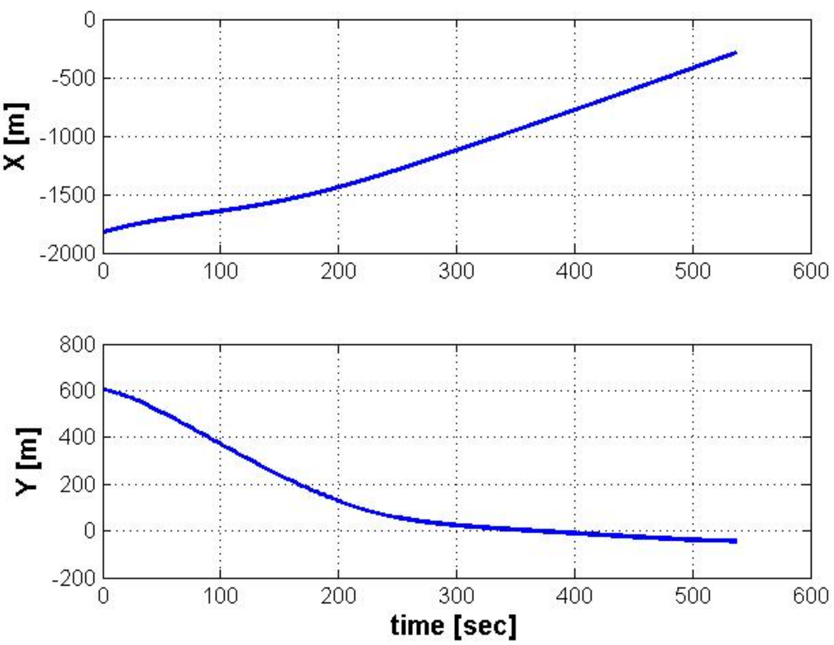

Figure A.54 X, Y variation for berthing simulation of tanker ship using PD controller with normal MMG model: initial position of ship (-6L, 2L), initial heading angle of ship -30 degrees and initial speed of ship 3 m/s

(2) Initial speed of ship 4 m/s in MMG model

(a) Initial position of ship (-5L, 4L), initial heading angle of ship -40 degrees and initial speed of ship 4 m/s

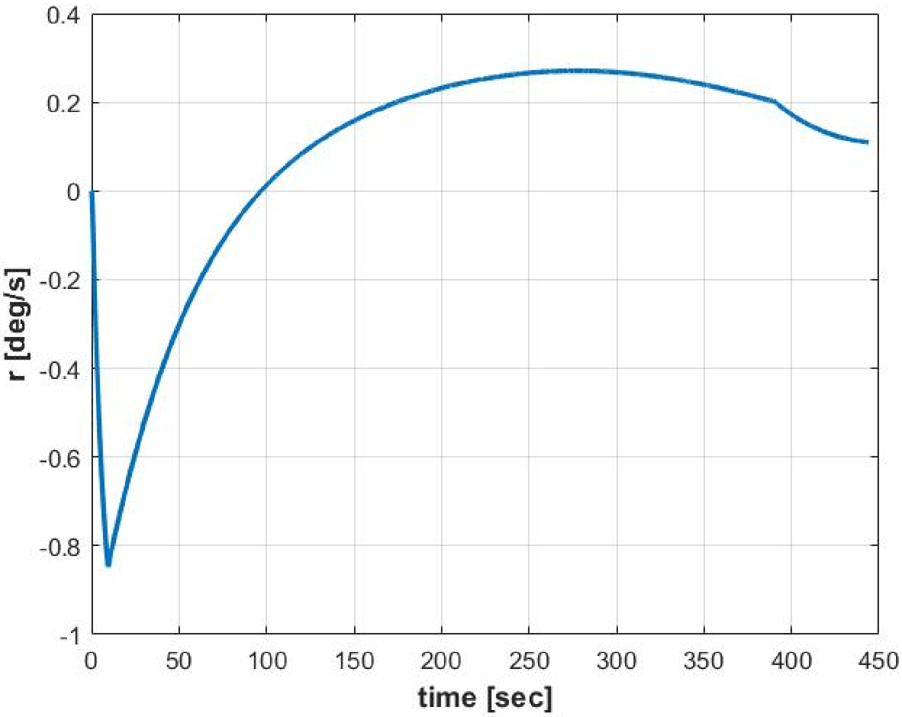

Figure A.55 Yaw rate r for berthing simulation of tanker ship using PD controller with normal MMG model: initial position of ship (-5L, 4L), initial heading angle of ship -40 degrees and initial speed of ship 4 m/s

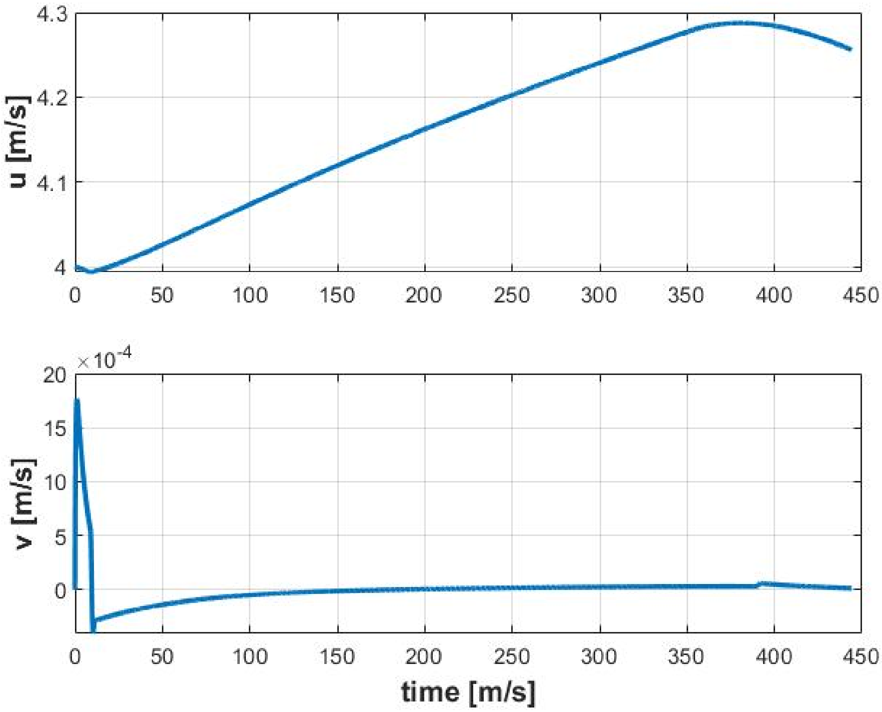

Figure A.56 Surge (u) and sway (v) velocity for berthing simulation of tanker ship using PD controller with normal MMG model: initial position of ship (-5L, 4L), initial heading angle of ship -40 degrees and initial speed of ship 4 m/s

(b) Initial position of ship (-5L, 4L), initial heading angle of ship -70 degrees and initial speed of ship 4 m/s

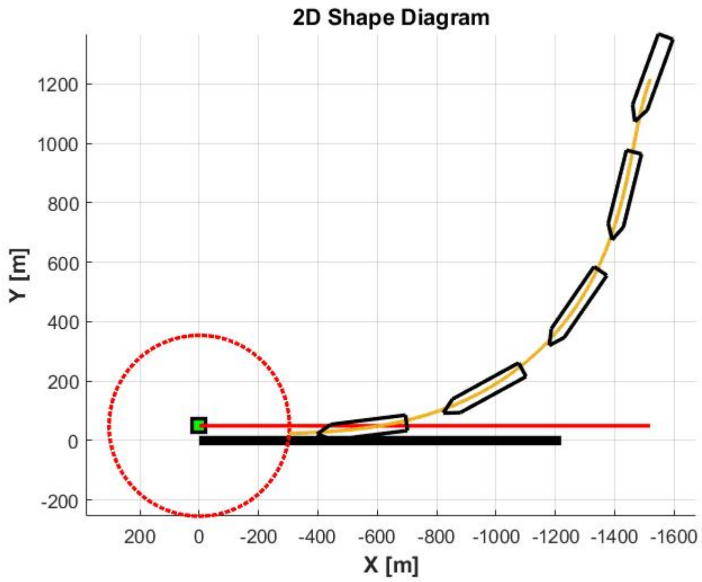

Figure A.57 Trajectory for berthing simulation of tanker ship using PD controller with normal MMG model: initial position of ship (-5L, 4L), initial heading angle of ship -70 degrees and initial speed of ship 4 m/s

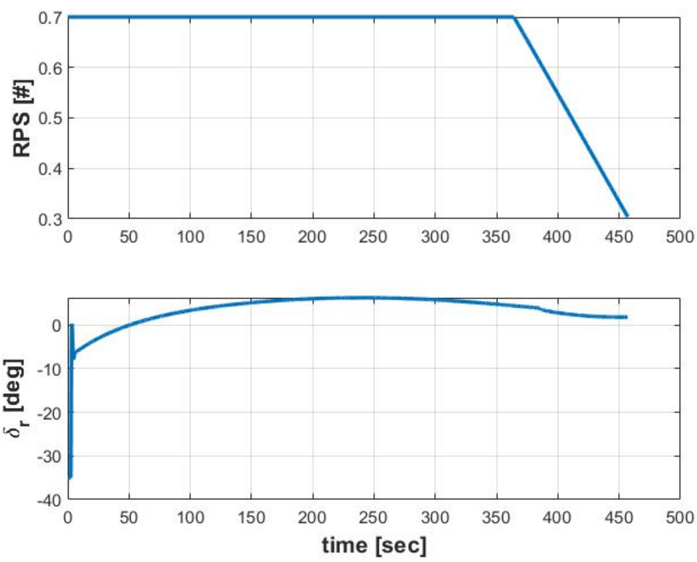

Figure A.58 RPS and δr for berthing simulation of tanker ship using PD controller with normal MMG model: initial position of ship (-5L, 4L), initial heading angle of ship -70 degrees and initial speed of ship 4 m/s

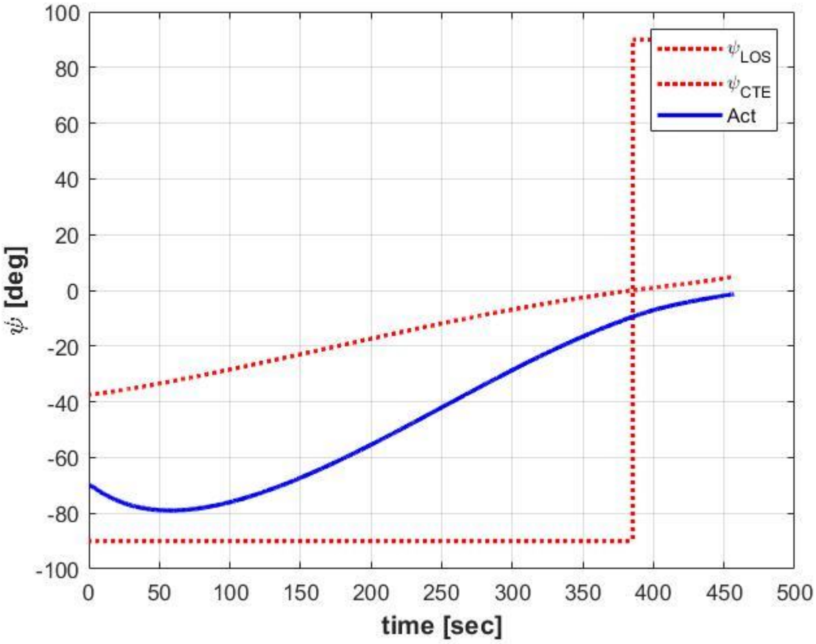

Figure A.59 Heading angle ψ for berthing simulation of tanker ship using PD controller with normal MMG model: initial position of ship (-5L, 4L), initial heading angle of ship -70 degrees and initial speed of ship 4 m/s

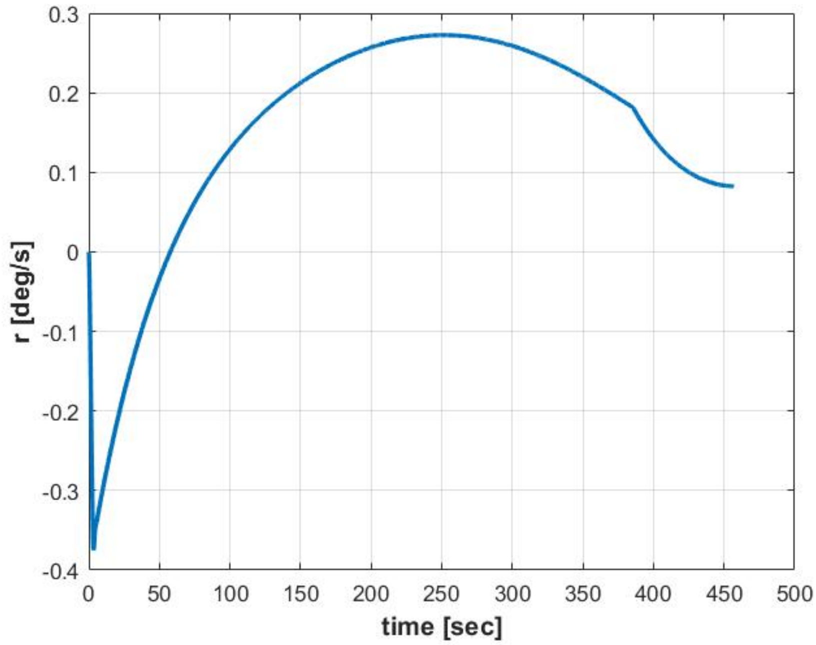

Figure A.60 Yaw rate r for berthing simulation of tanker ship using PD controller with normal MMG model: initial position of ship (-5L, 4L), initial heading angle of ship -70 degrees and initial speed of ship 4 m/s

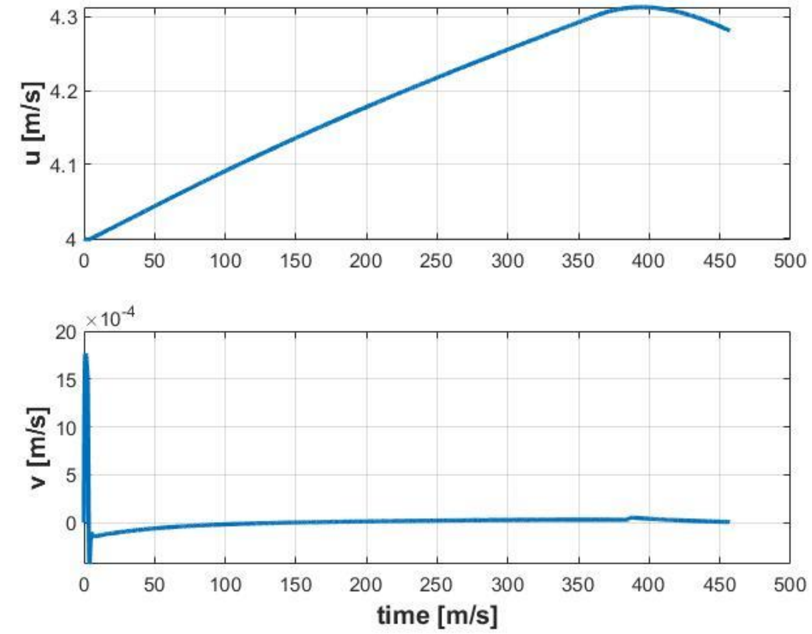

Figure A.61 Surge (u) and sway (v) velocity for berthing simulation of tanker ship using PD controller with normal MMG model: initial position of ship (-5L, 4L), initial heading angle of ship -70 degrees and initial speed of ship 4 m/s

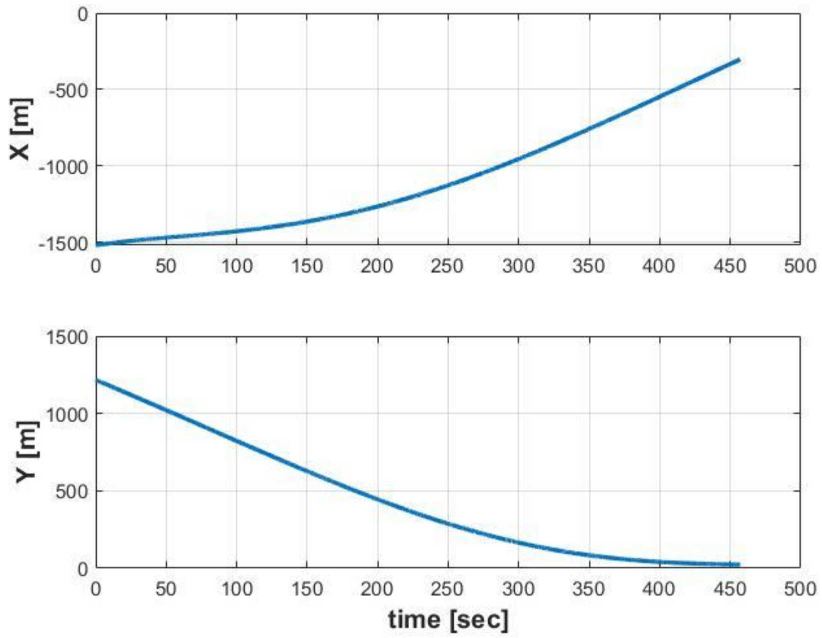

Figure A.62 X, Y variation for berthing simulation of tanker ship using PD controller with normal MMG model: initial position of ship (-5L, 4L), initial heading angle of ship -70 degrees and initial speed of ship 4 m/s

(c) Initial position of ship (-5L, 3L), initial heading angle of ship -40 degrees and initial speed of ship 4 m/s

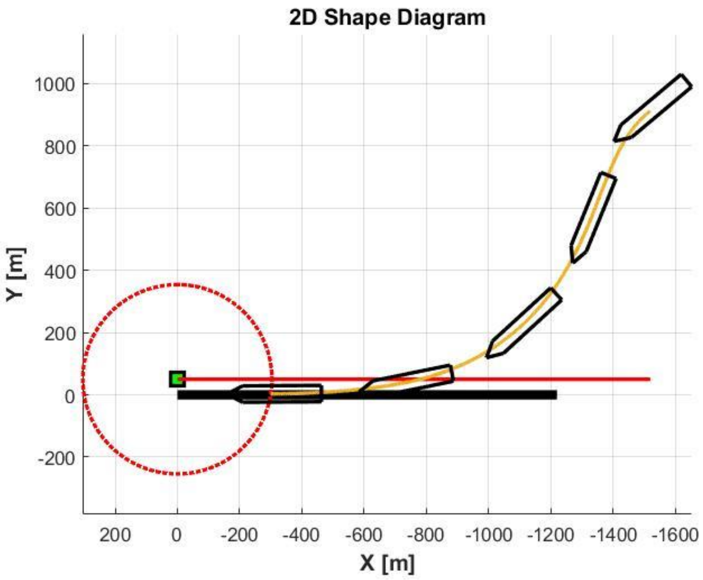

Figure A.63 Trajectory for berthing simulation of tanker ship using PD controller with normal MMG model: initial position of ship (-5L, 3L), initial heading angle of ship -40 degrees and initial speed of ship 4 m/s

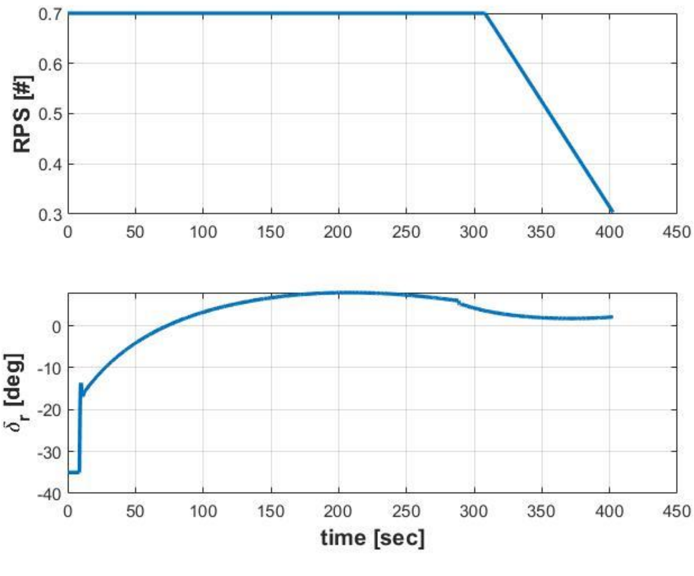

Figure A.64 RPS and δr for berthing simulation of tanker ship using PD controller with normal MMG model: initial position of ship (-5L, 3L), initial heading angle of ship -40 degrees and initial speed of ship 4 m/s

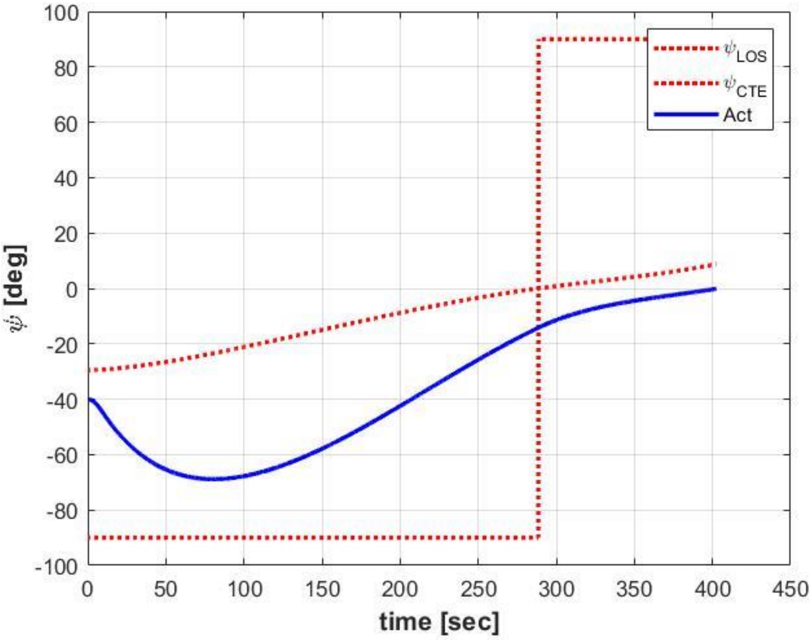

Figure A.65 Heading angle ψ for berthing simulation of tanker ship using PD controller with normal MMG model: initial position of ship (-5L, 3L), initial heading angle of ship -40 degrees and initial speed of ship 4 m/s

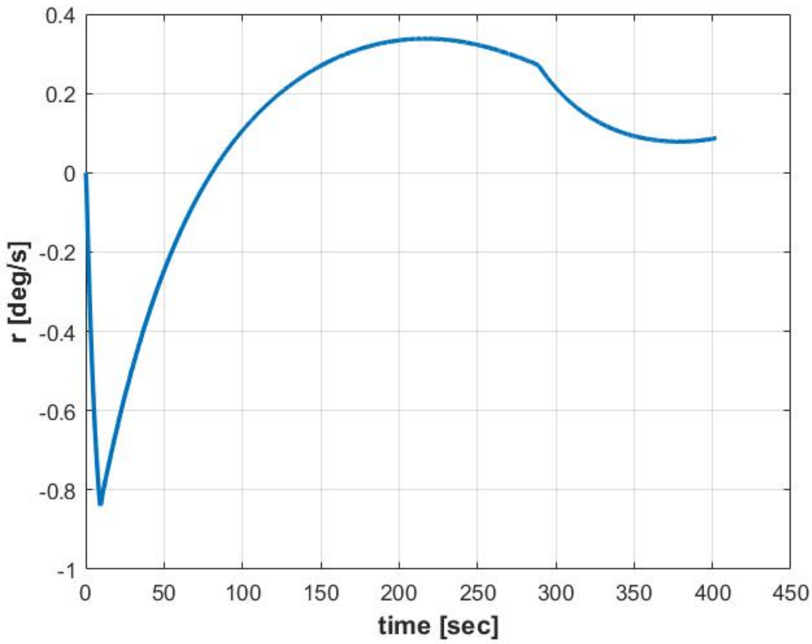

Figure A.66 Yaw rate r for berthing simulation of tanker ship using PD controller with normal MMG model: initial position of ship (-5L, 3L), initial heading angle of ship -40 degrees and initial speed of ship 4 m/s

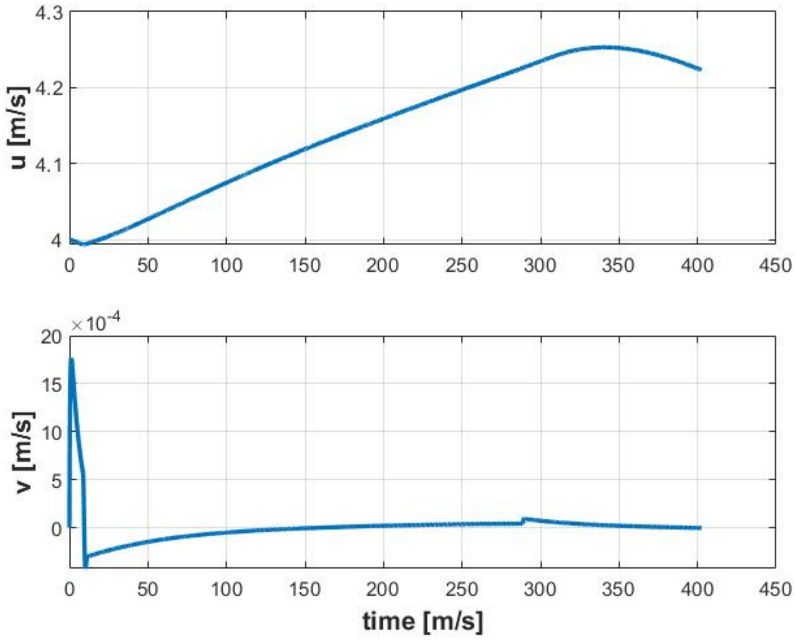

Figure A.67 Surge (u) and sway (v) velocity for berthing simulation of tanker ship using PD controller with normal MMG model: initial position of ship (-5L, 3L), initial heading angle of ship -40 degrees and initial speed of ship 4 m/s

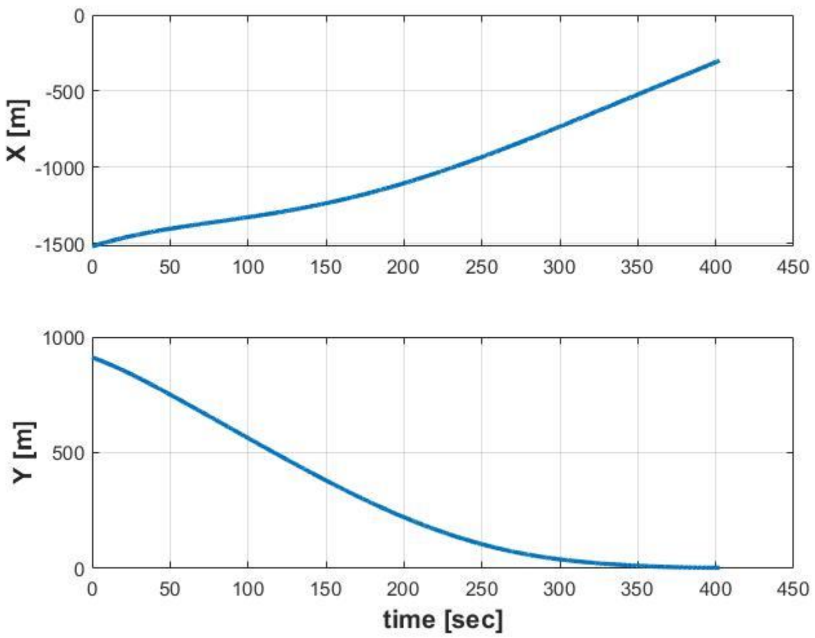

Figure A.68 X, Y variation for berthing simulation of tanker ship using PD controller with normal MMG model: initial position of ship (-5L, 3L), initial heading angle of ship -40 degrees and initial speed of ship 4 m/s

A.3 Comparative Analysis for Kose's Model and MMG Model

(1) Initial speed of ship 3 m/s

(a) Initial position of ship (-5L, 4L), initial heading angle of ship -40 degrees and initial speed of ship 3 m/s

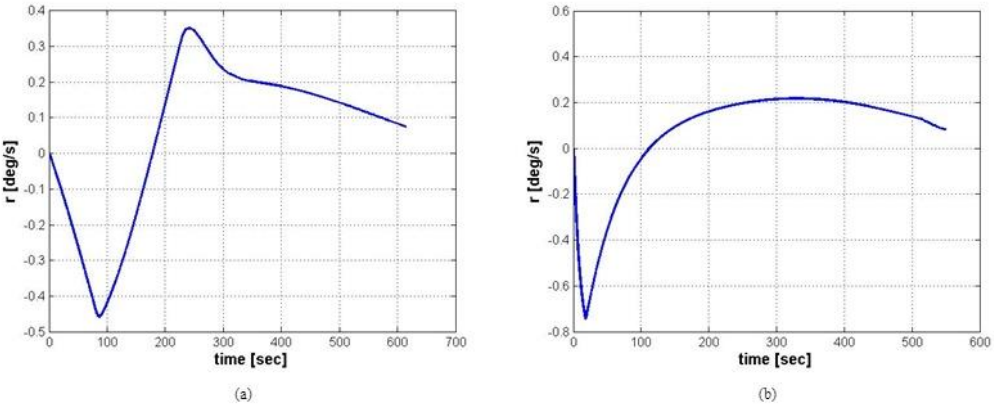

Figure A.69 Yaw rate r for berthing simulation of tanker ship using PD controller with (a) Kose's mathematical model and (b) normal MMG model: initial position of ship (-5L, 4L), initial heading angle of ship -40 degrees and initial speed of ship 3 m/s

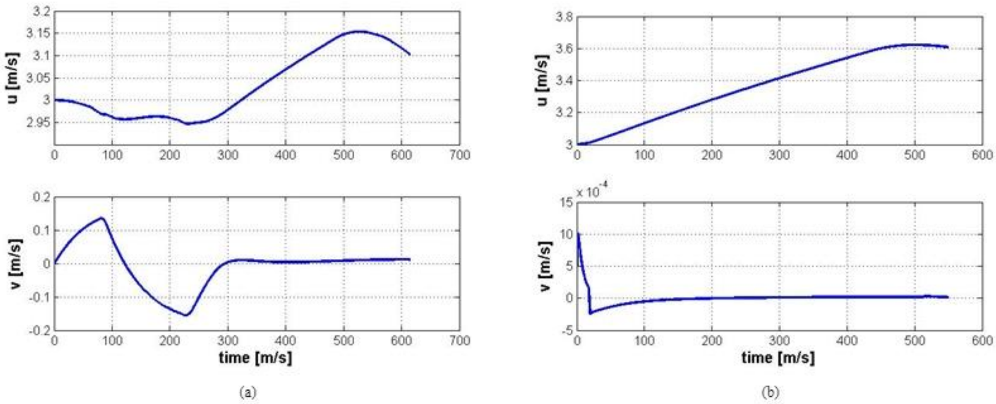

Figure A.70 Surge (u) and sway (v) velocity for berthing simulation of tanker ship using PD controller with (a) Kose's mathematical model and (b) normal MMG model: initial position of ship (-5L, 4L), initial heading angle -40 degrees and initial speed 3 m/s

(b) Initial position of ship (-5L, 4L), initial heading angle of ship -70 degrees and initial speed of ship 3 m/s

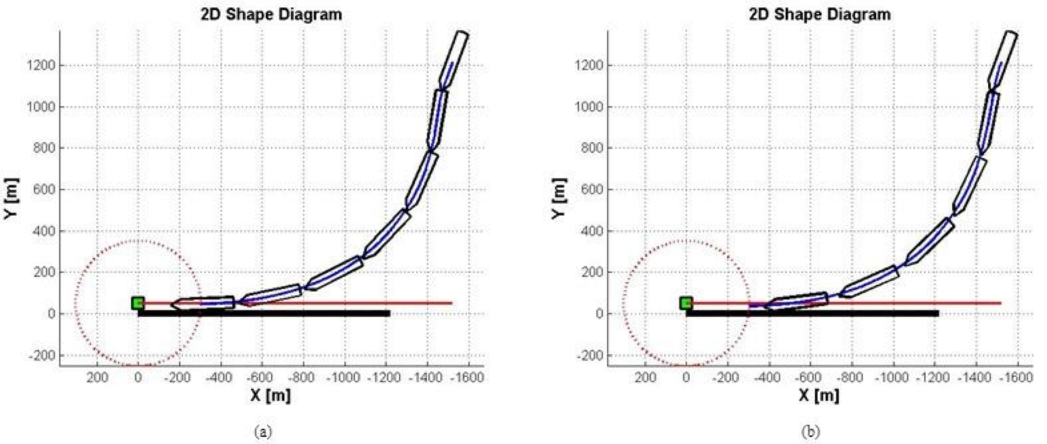

Figure A.71 Trajectory for berthing simulation of tanker ship using PD controller with (a) Kose's mathematical model and (b) normal MMG model: initial position of ship (-5L, 4L), initial heading angle -70 degrees and initial speed 3 m/s

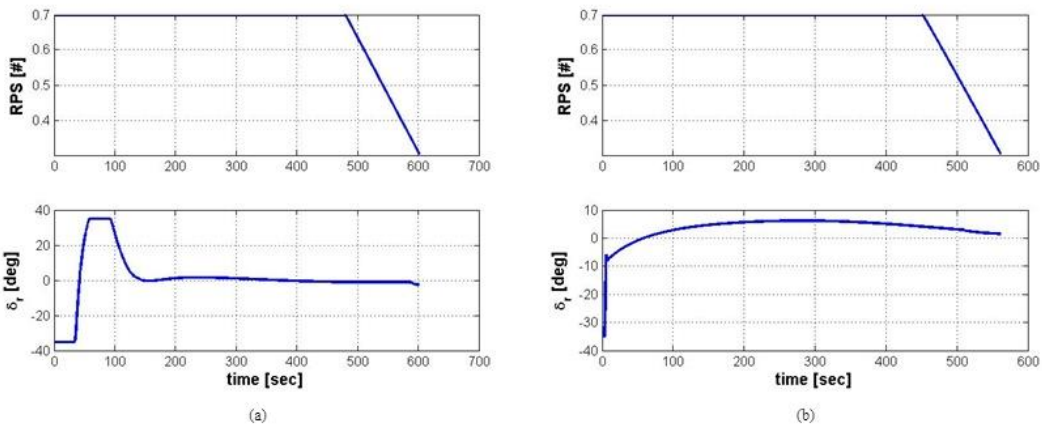

Figure A.72 RPS and δr for berthing simulation of tanker ship using PD controller with (a) Kose's mathematical model and (b) normal MMG model: initial position of ship (-5L, 4L), initial heading angle -70 degrees and initial speed 3 m/s

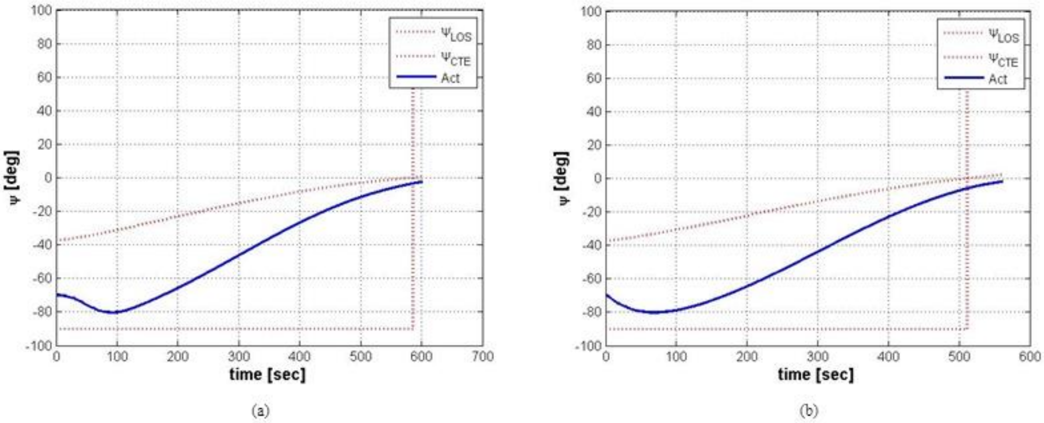

Figure A.73 Heading angle ψ for berthing simulation of tanker ship using PD controller with (a) Kose’s mathematical model and (b) normal MMG model: initial position of ship (-5L, 4L), initial heading angle -70 degrees and initial speed 3 m/s

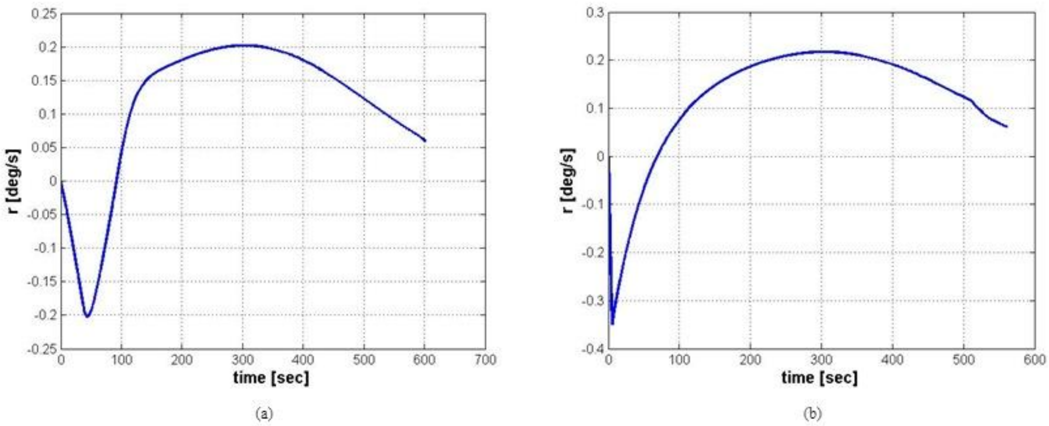

Figure A.74 Yaw rate r for berthing simulation of tanker ship using PD controller with (a) Kose’s mathematical model and (b) normal MMG model: initial position of ship (-5L, 4L), initial heading angle -70 degrees and initial speed 3 m/s

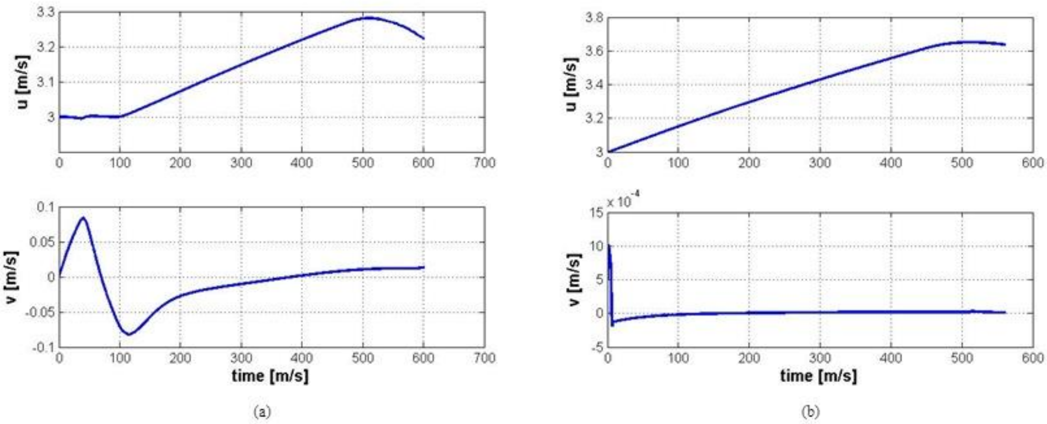

Figure A.75 Surge (u) and sway (v) velocity for berthing simulation of tanker ship using PD controller with (a) Kose’s mathematical model and (b) normal MMG model: initial position of ship (-5L, 4L), initial heading angle -70 degrees and initial speed 3 m/s

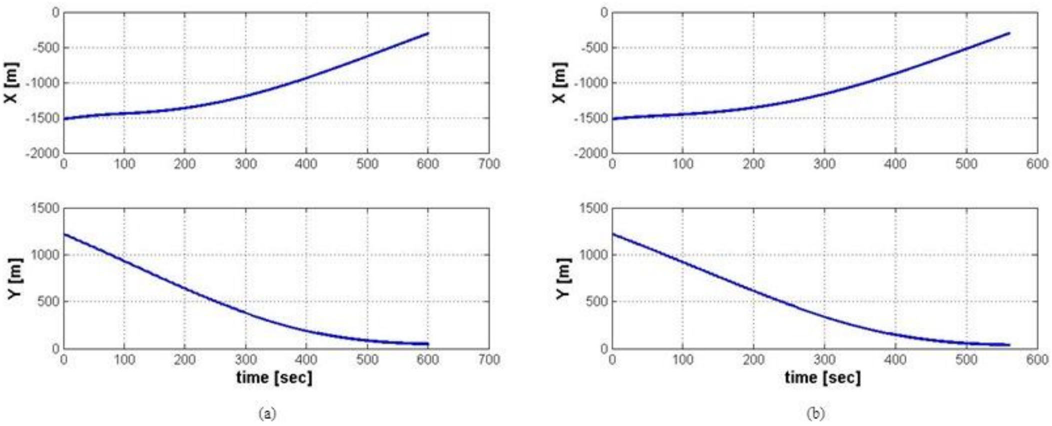

Figure A.76 X, Y variation for berthing simulation of tanker ship using PD controller with (a) Kose’s mathematical model and (b) normal MMG model: initial position of ship (-5L, 4L), initial heading angle -70 degrees and initial speed 3 m/s

(c) Initial position of ship (-5L, 3L), initial heading angle of ship -40 degrees and initial speed of ship 3 m/s

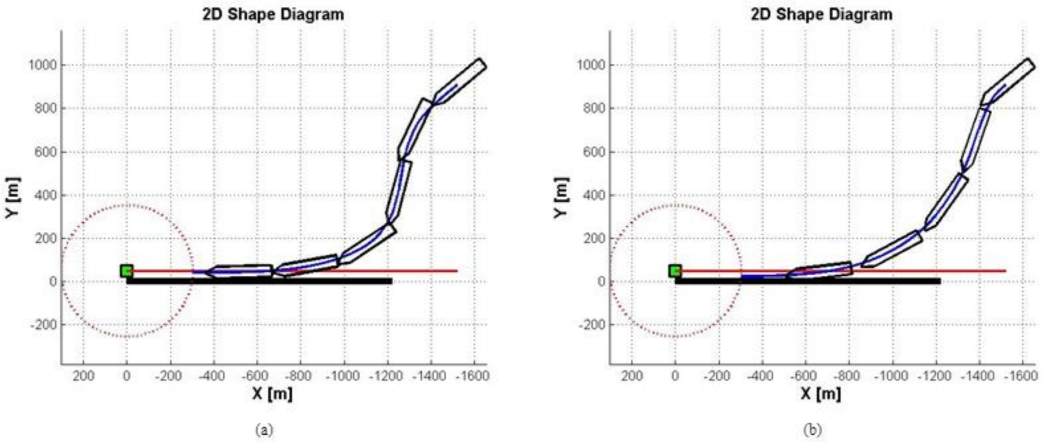

Figure A.77 Trajectory for berthing simulation of tanker ship using PD controller with (a) Kose's mathematical model and (b) normal MMG model: initial position of ship (-5L, 3L), initial heading angle -40 degrees and initial speed 3 m/s

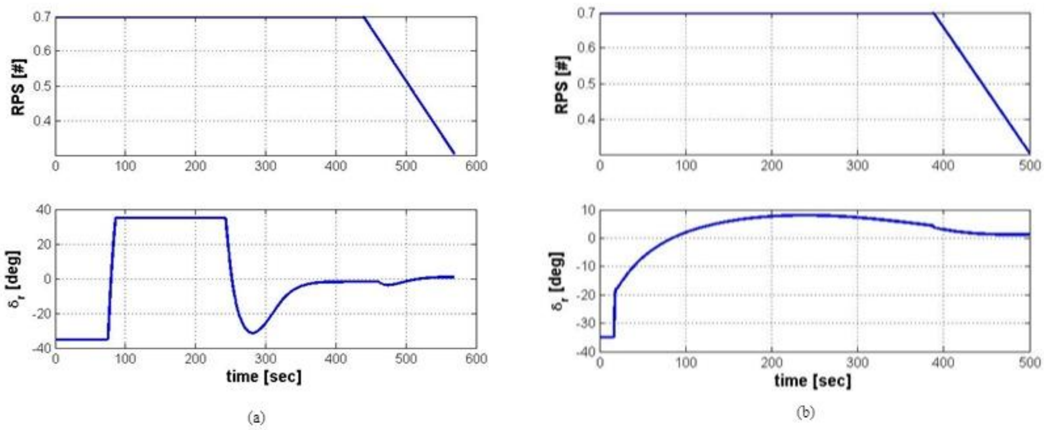

Figure A.78 RPS and δr for berthing simulation of tanker ship using PD controller with (a) Kose's mathematical model and (b) normal MMG model: initial position of ship (-5L, 3L), initial heading angle -40 degrees and initial speed 3 m/s

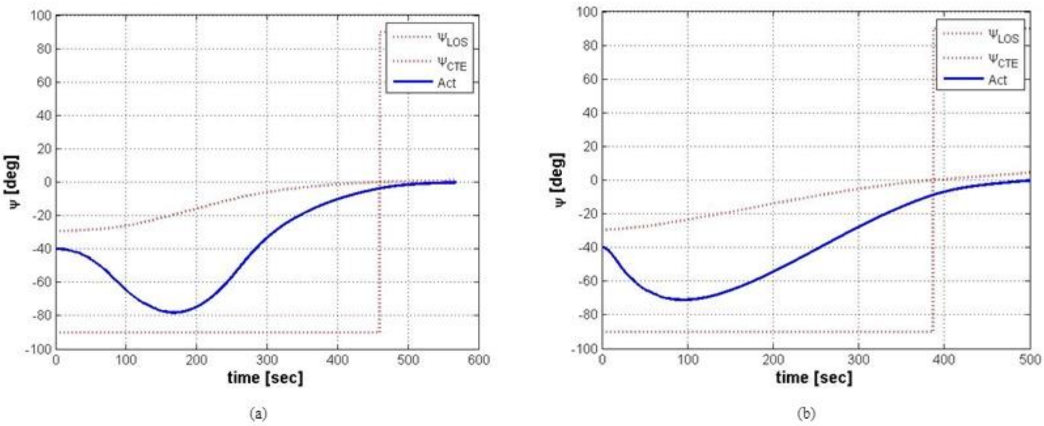

Figure A.79 Heading angle ψ for berthing simulation of tanker ship using PD controller with (a) Kose's mathematical model and (b) normal MMG model: initial position of ship (-5L, 3L), initial heading angle -40 degrees and initial speed 3 m/s

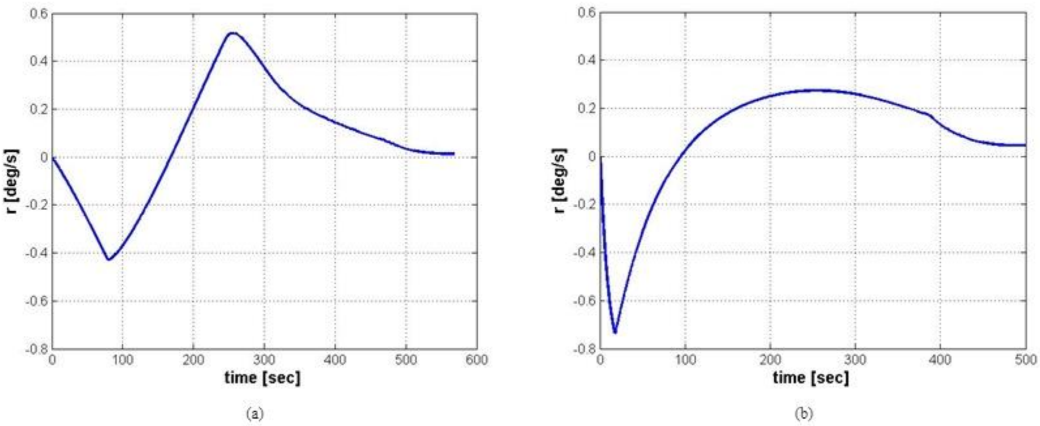

Figure A.80 Yaw rate r for berthing simulation of tanker ship using PD controller with (a) Kose's mathematical model and (b) normal MMG model: initial position of ship (-5L, 3L), initial heading angle -40 degrees and initial speed 3 m/s

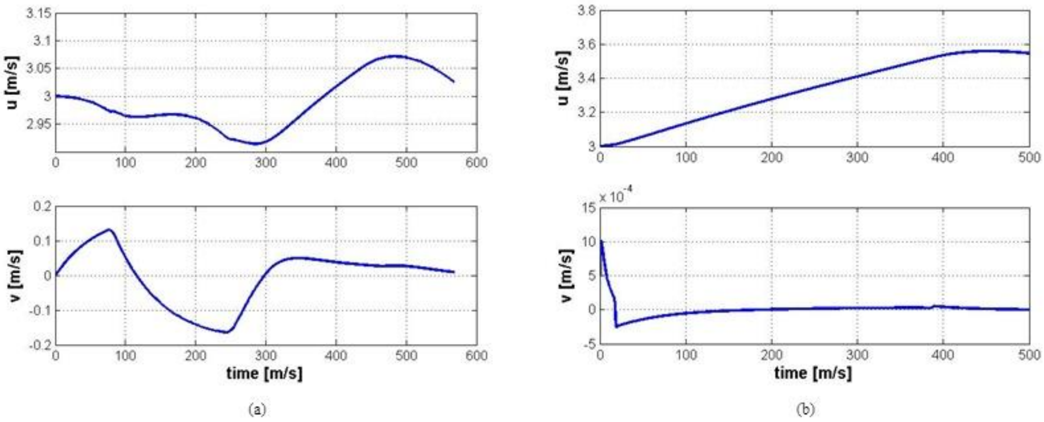

Figure A.81 Surge (u) and sway (v) velocity for berthing simulation of tanker ship using PD controller with (a) Kose's mathematical model and (b) normal MMG model: initial position of ship (-5L, 3L), initial heading angle -40 degrees and initial speed 3 m/s

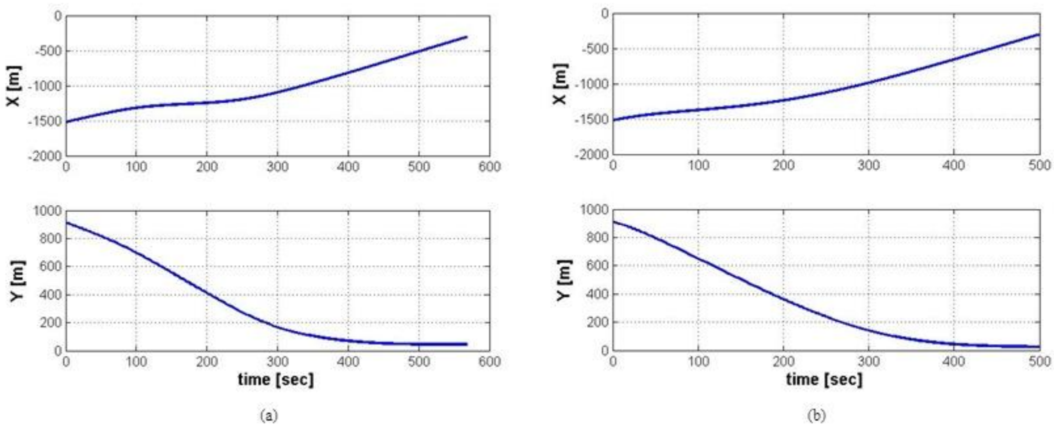

Figure A.82 X, Y variation for berthing simulation of tanker ship using PD controller with (a) Kose's mathematical model and (b) normal MMG model: initial position of ship (-5L, 3L), initial heading angle -40 degrees and initial speed 3 m/s

(2) Initial speed of ship 4 m/s

(a) Initial position of ship (-5L, 4L), initial heading angle of ship -40 degrees and initial speed of ship 4 m/s

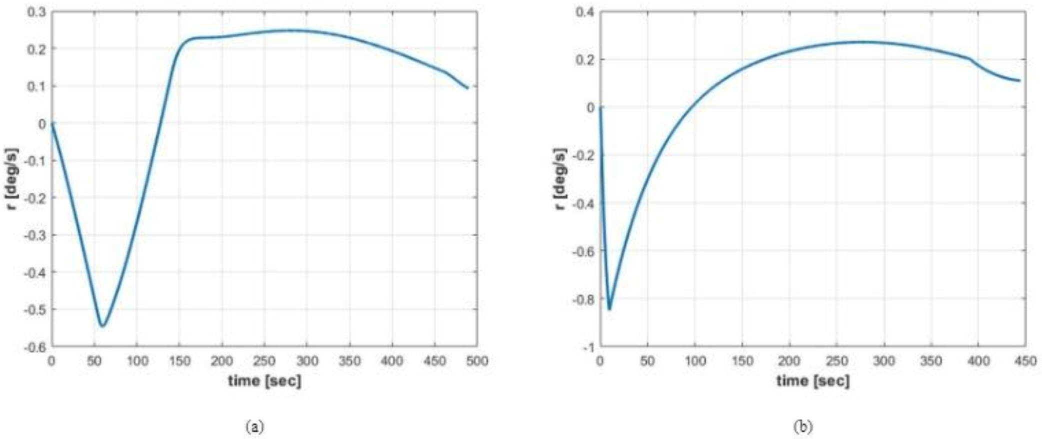

Figure A.83 Yaw rate r for berthing simulation of tanker ship using PD controller with (a) Kose's mathematical model and (b) normal MMG model: initial position of ship (-5L, 4L), initial heading angle of ship -40 degrees and initial speed of ship 4 m/s

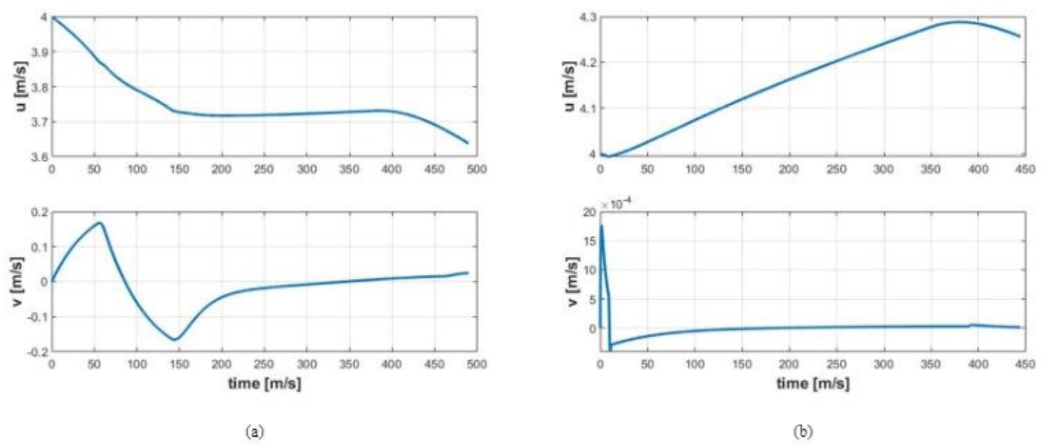

Figure A.84 Surge (u) and sway (v) velocity for berthing simulation of tanker ship using PD controller with (a) Kose's mathematical model and (b) normal MMG model: initial position of ship (-5L, 4L), initial heading angle -40 degrees and initial speed 4 m/s

(b) Initial position of ship (-5L, 4L), initial heading angle of ship -70 degrees and initial speed of ship 4 m/s

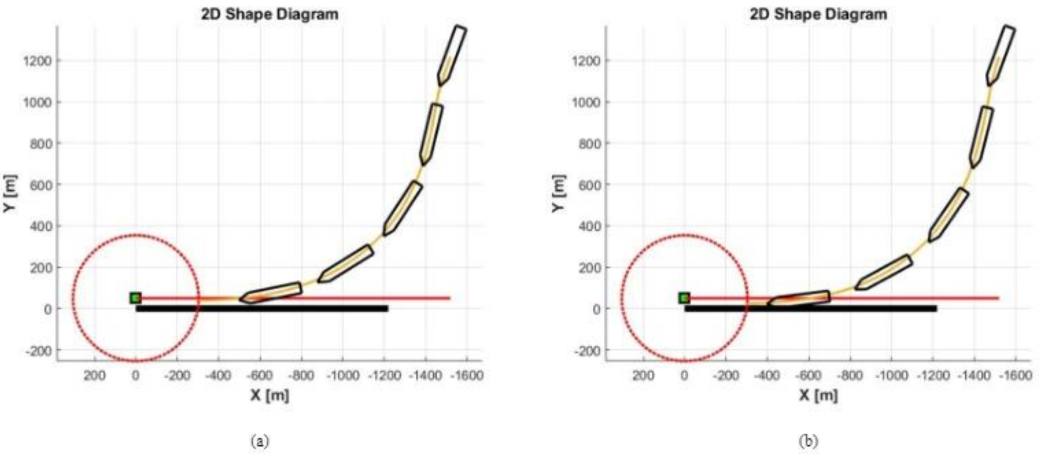

Figure A.85 Trajectory for berthing simulation of tanker ship using PD controller with (a) Kose's mathematical model and (b) normal MMG model: initial position of ship (-5L, 4L), initial heading angle -70 degrees and initial speed 4 m/s

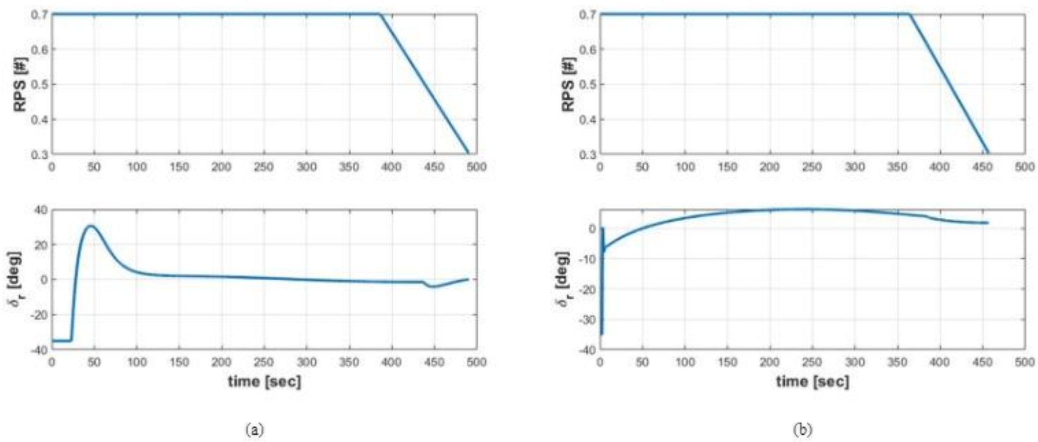

Figure A.86 RPS and δr for berthing simulation of tanker ship using PD controller with (a) Kose's mathematical model and (b) normal MMG model: initial position of ship (-5L, 4L), initial heading angle -70 degrees and initial speed 4 m/s

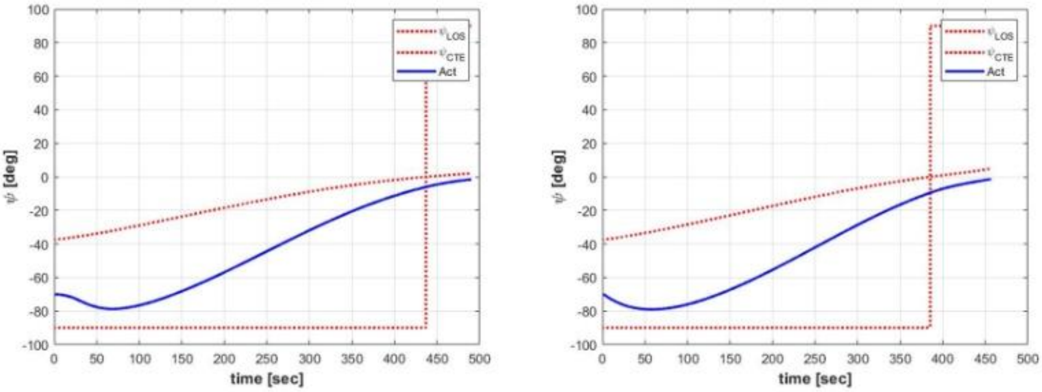

(a) (b)

Figure A.87 Heading angle ψ for berthing simulation of tanker ship using PD controller with (a) Kose's mathematical model and (b) normal MMG model: initial position of ship (-5L, 4L), initial heading angle -70 degrees and initial speed 4 m/s

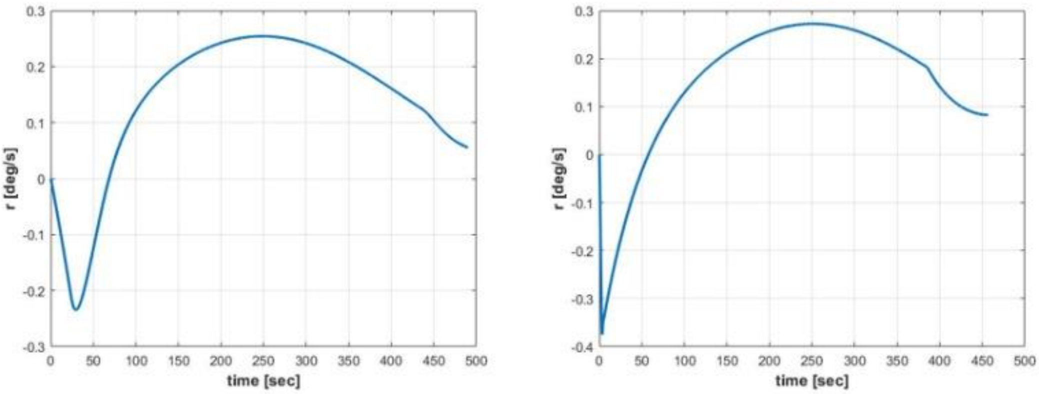

(a) (b)

Figure A.88 Yaw rate r for berthing simulation of tanker ship using PD controller with (a) Kose's mathematical model and (b) normal MMG model: initial position of ship (-5L, 4L), initial heading angle -70 degrees and initial speed 4 m/s

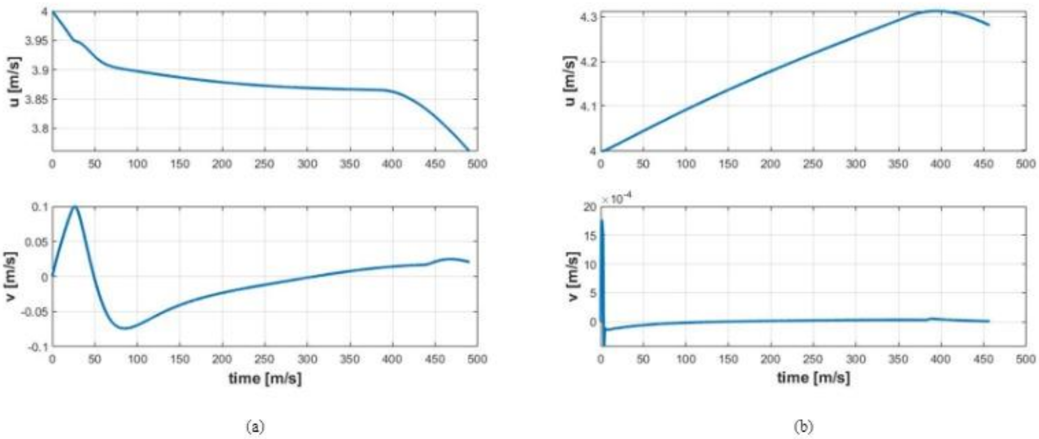

Figure A.89 Surge (u) and sway (v) velocity for berthing simulation of tanker ship using PD controller with (a) Kose's mathematical model and (b) normal MMG model: initial position of ship (-5L, 4L), initial heading angle -70 degrees and initial speed 4 m/s

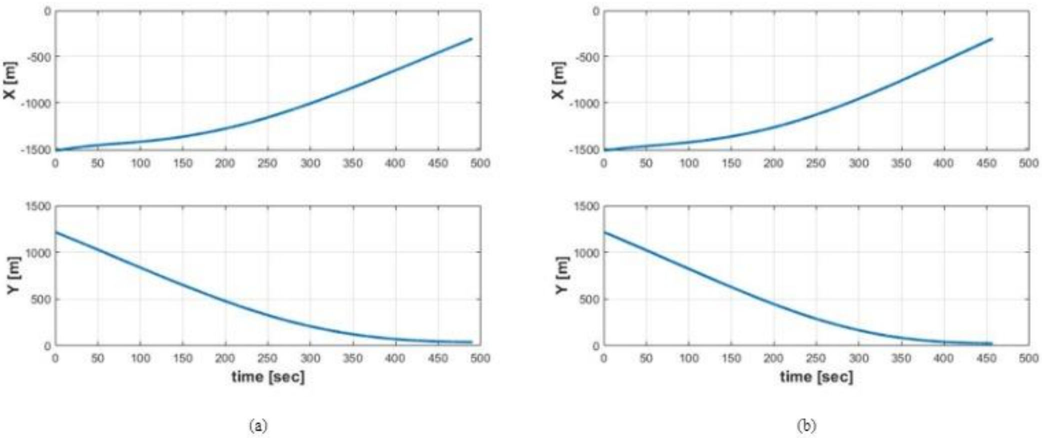

Figure A.90 X, Y variation for berthing simulation of tanker ship using PD controller with (a) Kose's mathematical model and (b) normal MMG model: initial position of ship (-5L, 4L), initial heading angle -70 degrees and initial speed 4 m/s

(c) Initial position of ship (-5L, 3L), initial heading angle of ship -40 degrees and initial speed of ship 4 m/s

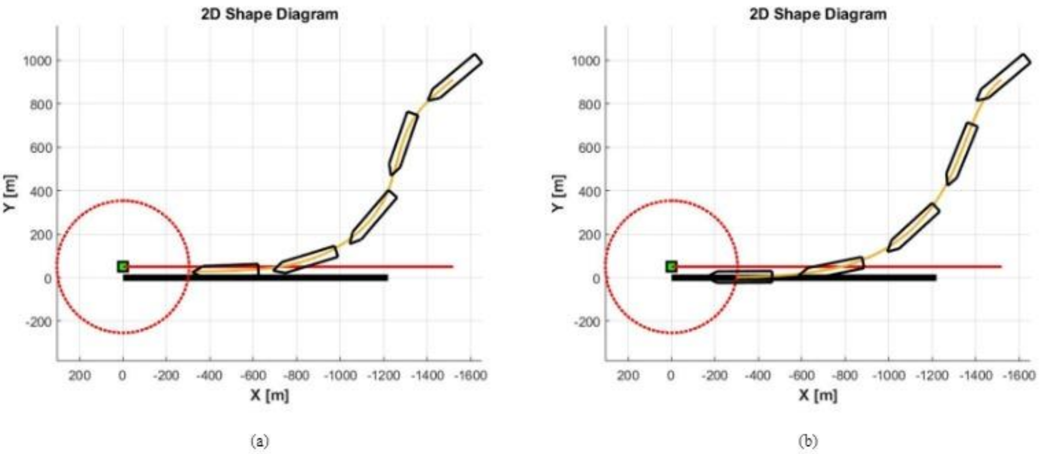

Figure A.91 Trajectory for berthing simulation of tanker ship using PD controller with (a) Kose's mathematical model and (b) normal MMG model: initial position of ship (-5L, 3L), initial heading angle -40 degrees and initial speed 4 m/s

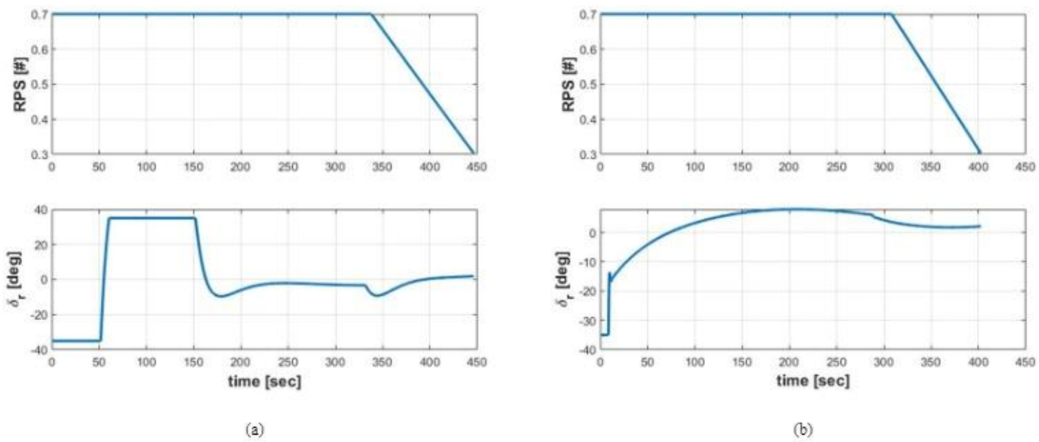

Figure A.92 RPS and δr for berthing simulation of tanker ship using PD controller with (a) Kose's mathematical model and (b) normal MMG model: initial position of ship (-5L, 3L), initial heading angle -40 degrees and initial speed 4 m/s

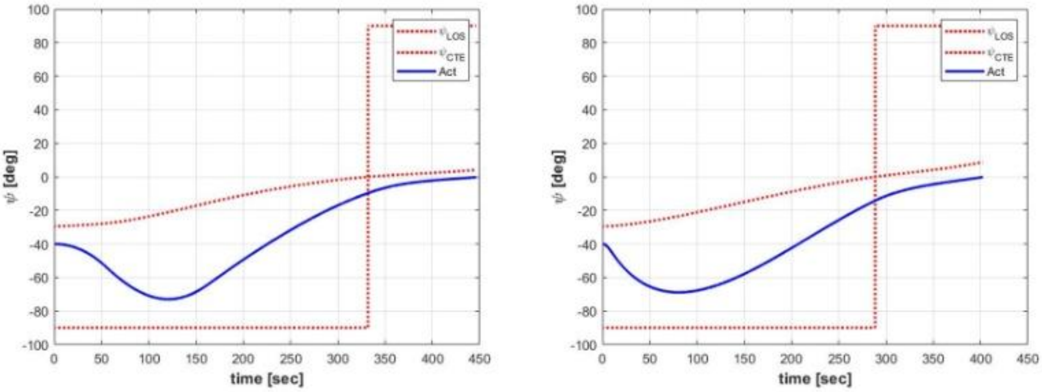

(a) (b)

Figure A.93 Heading angle ψ for berthing simulation of tanker ship using PD controller with (a) Kose's mathematical model and (b) normal MMG model: initial position of ship (-5L, 3L), initial heading angle -40 degrees and initial speed 4 m/s

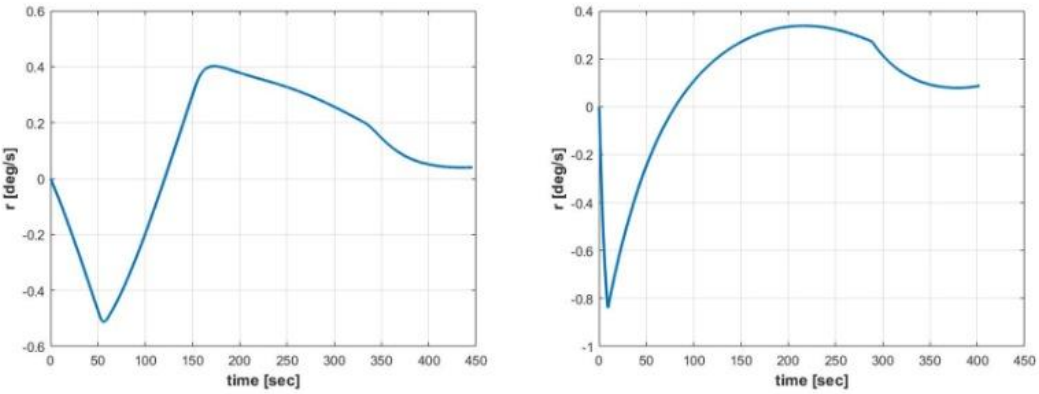

(a) (b)

Figure A.94 Yaw rate r for berthing simulation of tanker ship using PD controller with (a) Kose's mathematical model and (b) normal MMG model: initial position of ship (-5L, 3L), initial heading angle -40 degrees and initial speed 4 m/s

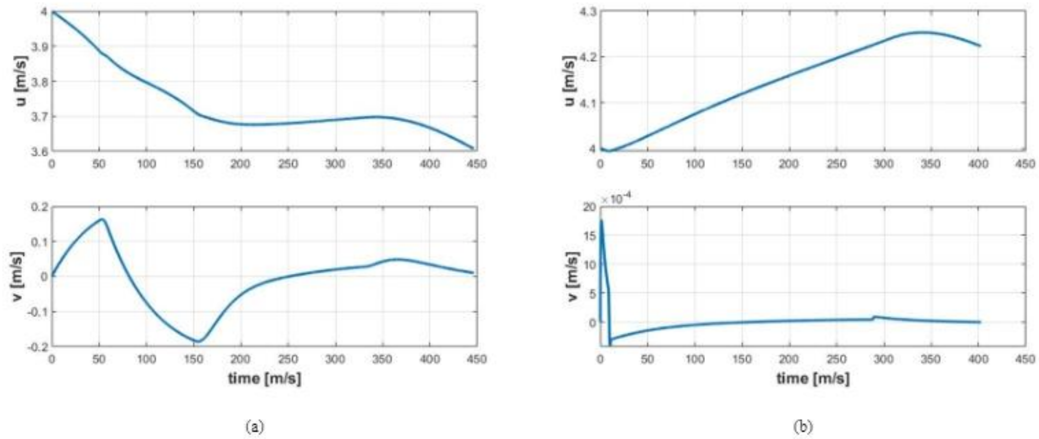

Figure A.95 Surge (u) and sway (v) velocity for berthing simulation of tanker ship using PD controller with (a) Kose's mathematical model and (b) normal MMG model: initial position of ship (-5L, 3L), initial heading angle -40 degrees and initial speed 4 m/s

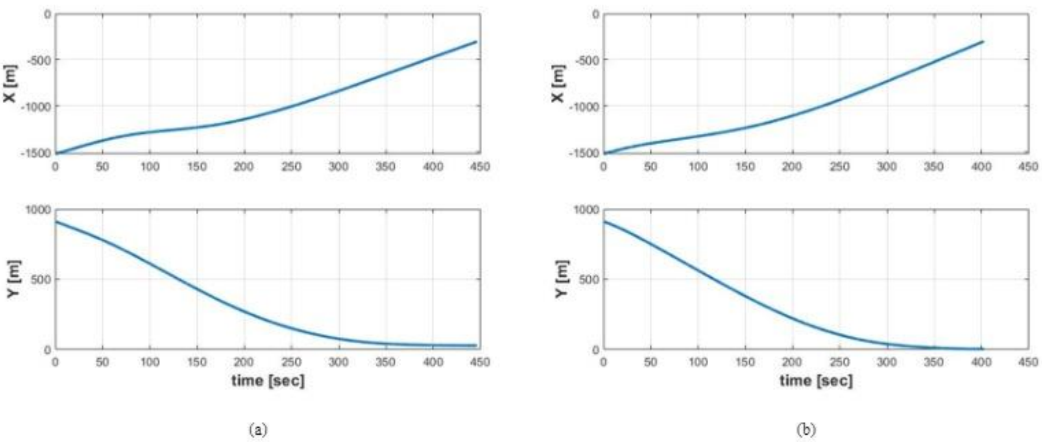

Figure A.96 X, Y variation for berthing simulation of tanker ship using PD controller with (a) Kose's mathematical model and (b) normal MMG model: initial position of ship (-5L, 3L), initial heading angle -40 degrees and initial speed 4 m/s

A.4 Comparative Analysis for Proportional Derivative (PD) Control and Artificial Neural Network (ANN)

(1) Initial position of ship (-5L, 4L), initial heading angle of ship -40 degrees and initial speed of ship 3 m/s

The result is shown and explained in Chapter 5.

(2) Initial position of ship (-5L, 4L), initial heading angle of ship -70 degrees and initial speed of ship 3 m/s

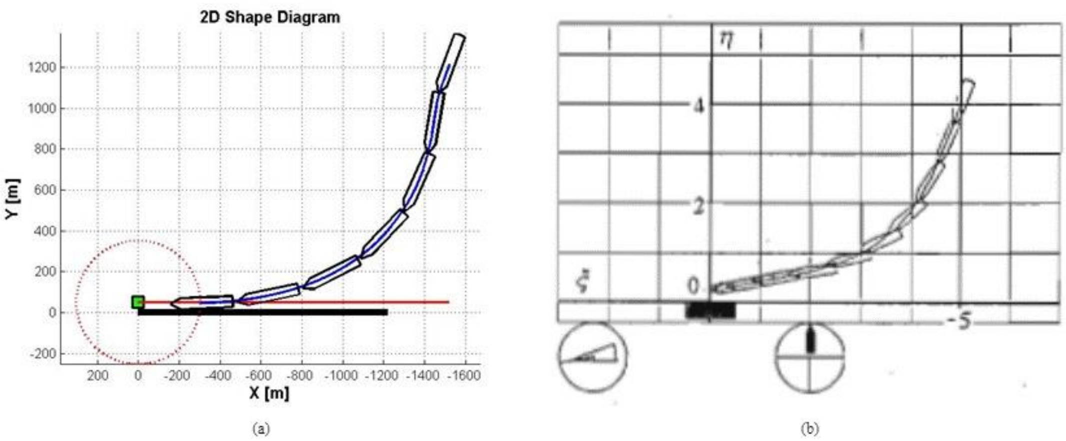

Figure A.97 Trajectory for berthing simulation of tanker ship using (a) PD controller and (b) ANN controller (Hasegawa and Kitera, 1993) with Kose's mathematical model: initial position of ship (-5L, 4L), initial heading angle -70 degrees and initial speed 3 m/s

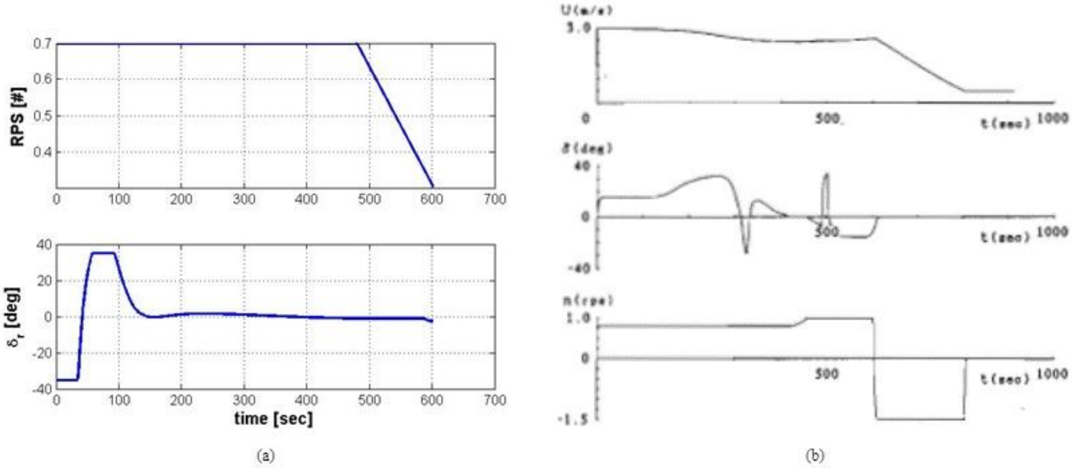

Figure A.98 RPS and δr for berthing simulation of tanker ship using (a) PD controller and (b) ANN controller (Hasegawa and Kitera, 1993) with Kose's mathematical model: initial position of ship (-5L, 4L), initial heading angle -70 degrees and initial speed 3 m/s

(3) Initial position of ship (-5L, 3L), initial heading angle of ship -40 degrees and initial speed of ship 3 m/s

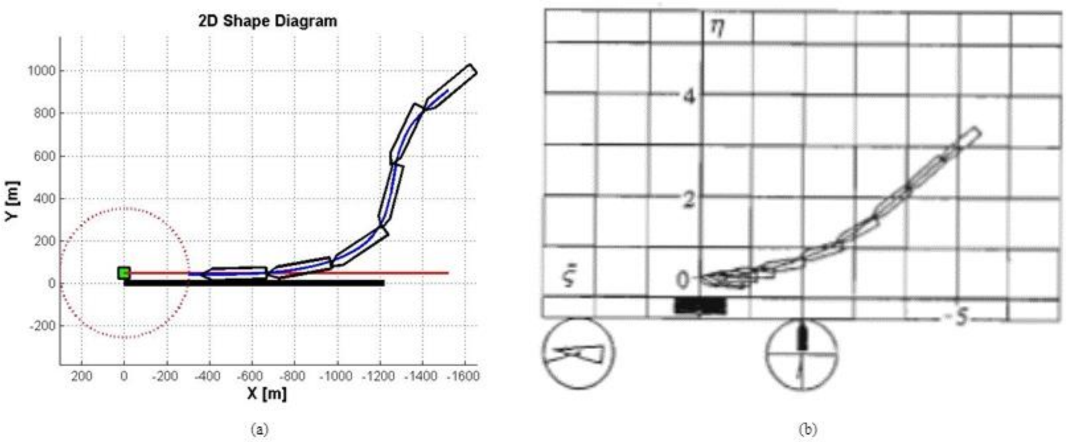

Figure A.99 Trajectory for berthing simulation of tanker ship using (a) PD controller and (b) ANN controller (Hasegawa and Kitera, 1993) with Kose's mathematical model: initial position of ship (-5L, 3L), initial heading angle -40 degrees and initial speed 3 m/s

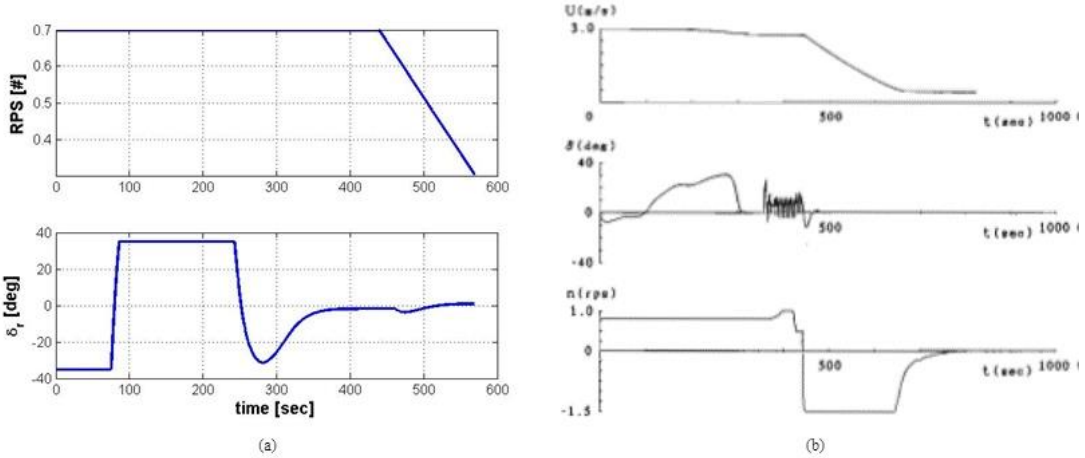

Figure A.100 RPS and δr for berthing simulation of tanker ship using (a) PD controller and (b) ANN controller (Hasegawa and Kitera, 1993) with Kose's mathematical model: initial position of ship (-5L, 3L), initial heading angle -40 degrees and initial speed 3 m/s

(4) Initial position of ship (-6L, 2L), initial heading angle of ship -30 degrees and initial speed of ship 3 m/s

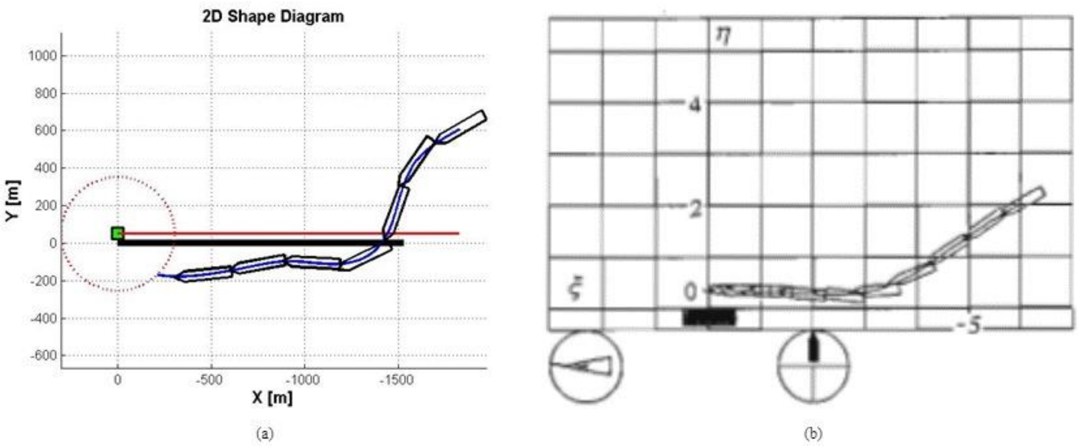

Figure A.101 Trajectory for berthing simulation of tanker ship using (a) PD controller and (b) ANN controller (Hasegawa and Kitera, 1993) with Kose's mathematical model: initial position of ship (-6L, 2L), initial heading angle -30 degrees and initial speed 3 m/s

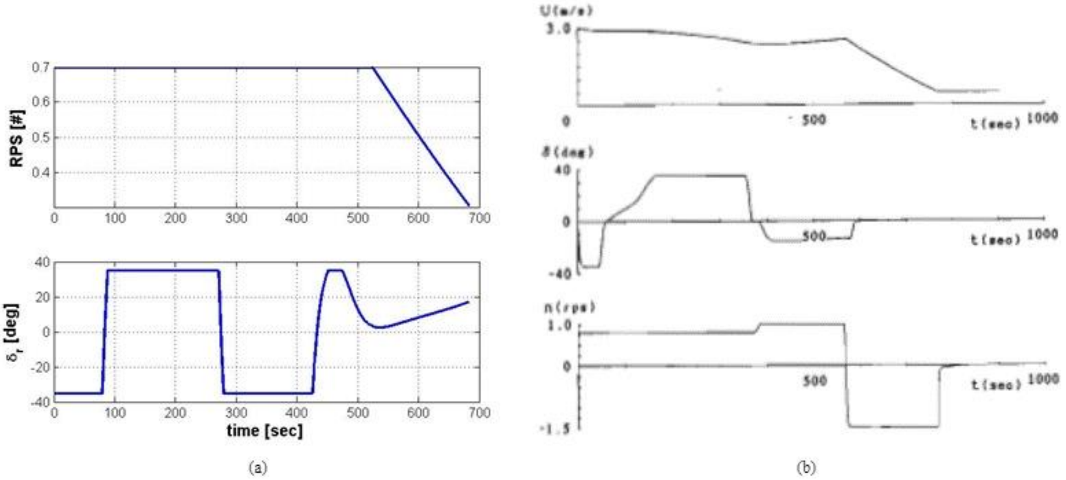

Figure A.102 RPS and δr for berthing simulation of tanker ship using (a) PD controller and (b) ANN controller (Hasegawa and Kitera, 1993) with Kose's mathematical model: initial position of ship (-6L, 2L), initial heading angle -30 degrees and initial speed 3 m/s

A.5 Berthing Simulation using Model Predictive Control

(1) Initial position of ship (-5L, 4L), initial heading angle of ship -40 degrees and initial speed of ship 3 m/s

The result is shown and explained in Chapter 5.

(2) Initial position of ship (-5L, 4L), initial heading angle of ship -70 degrees and initial speed of ship 3 m/s

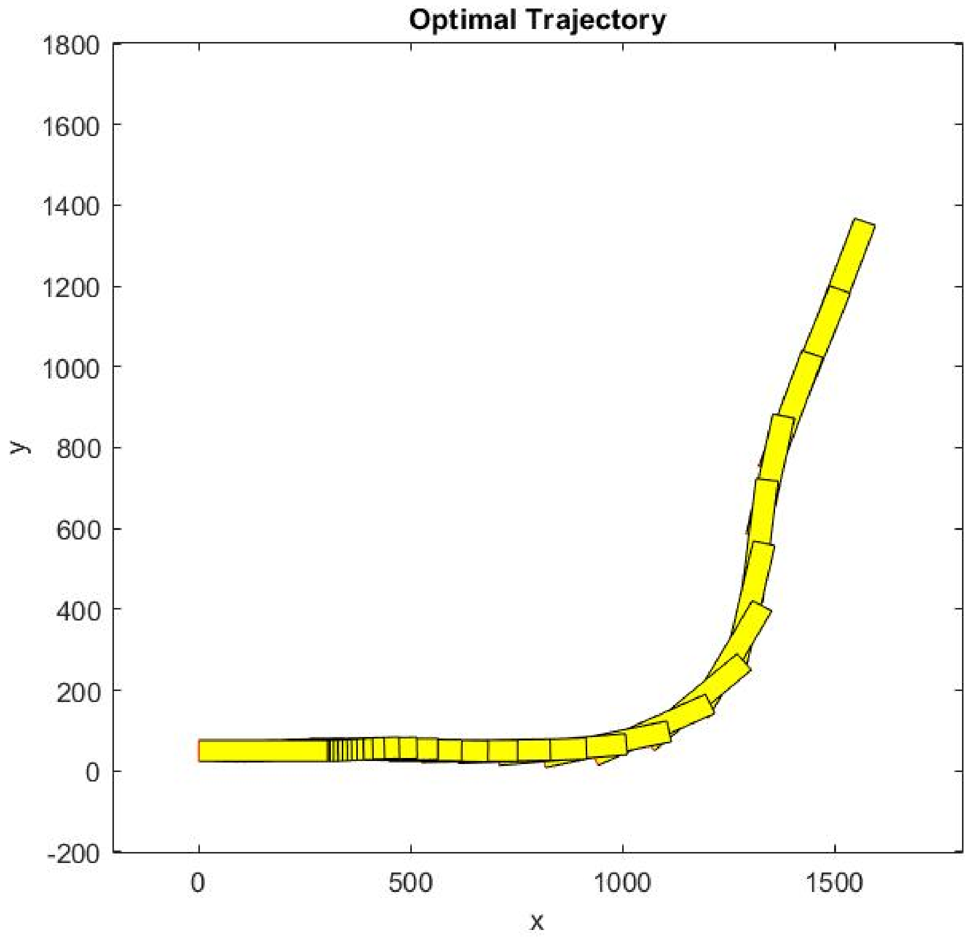

Figure A.103 Trajectory for berthing simulation of tanker ship using MPC with Kose's mathematical model: initial position of ship (-5L, 4L), initial heading angle of ship -70 degrees and initial speed of ship 3 m/s

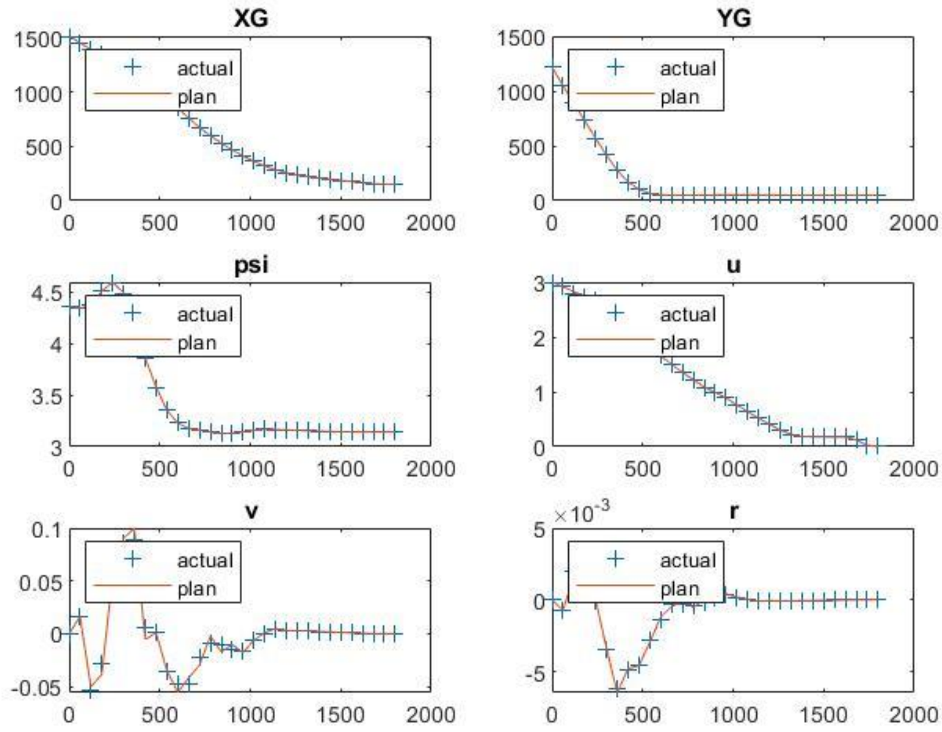

Figure A.104 X position XG, Y position YG, heading angle psi, surge velocity u, sway velocity v and yaw rate r for berthing simulation of tanker using MPC with Kose's model: initial position of ship (-5L, 4L), initial heading angle -70 degrees and initial speed 3 m/s

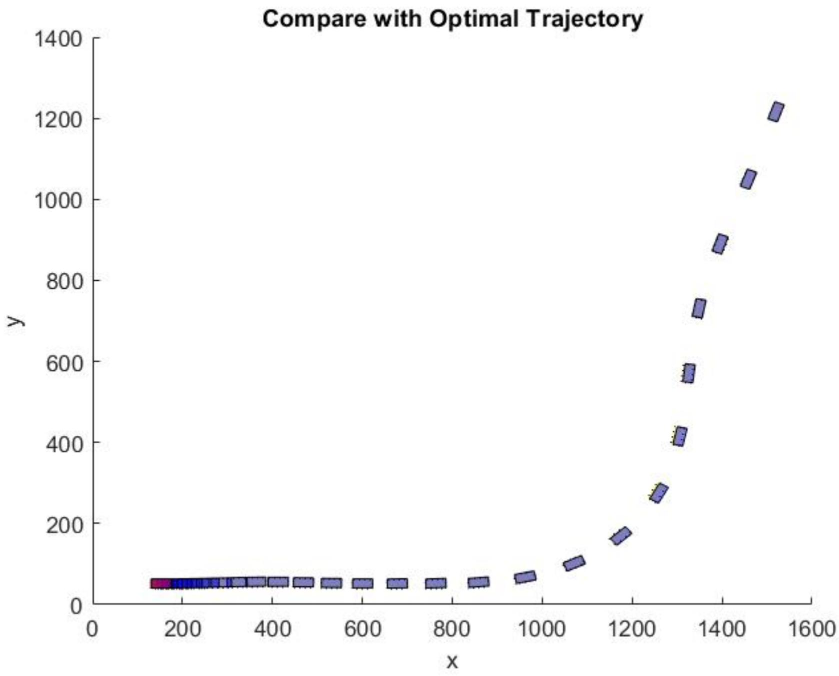

Figure A.105 Actual and optimal trajectories for berthing simulation of tanker ship using MPC with Kose's mathematical model: initial position of ship (-5L, 4L), initial heading angle of ship -70 degrees and initial speed of ship 3 m/s

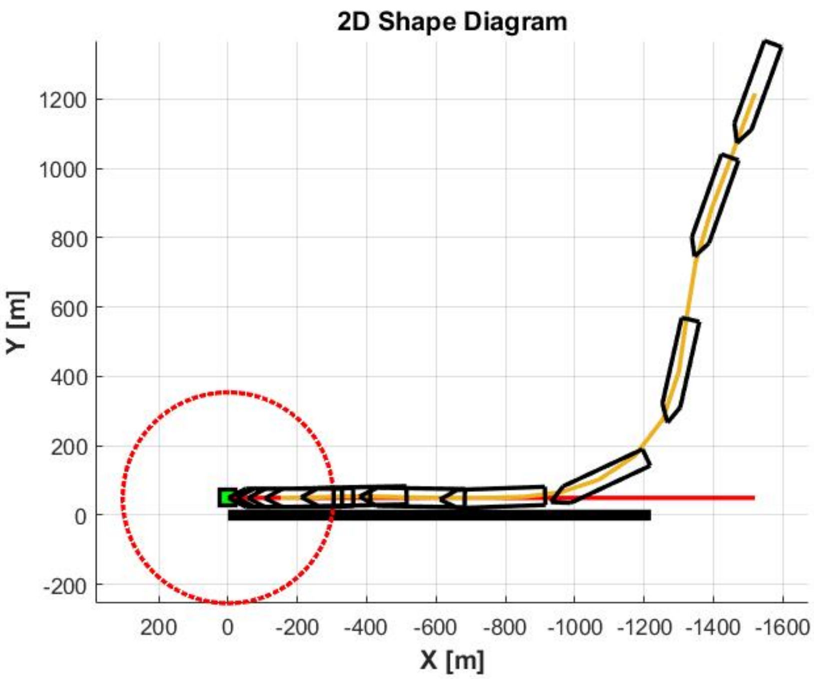

Figure A.106 Diagram for berthing simulation of tanker ship using MPC with Kose's mathematical model: initial position of ship (-5L, 4L), initial heading angle of ship -70 degrees and initial speed of ship 3 m/s

(3) Initial position of ship (-5L, 3L), initial heading angle of ship -40 degrees and initial speed of ship 3 m/s

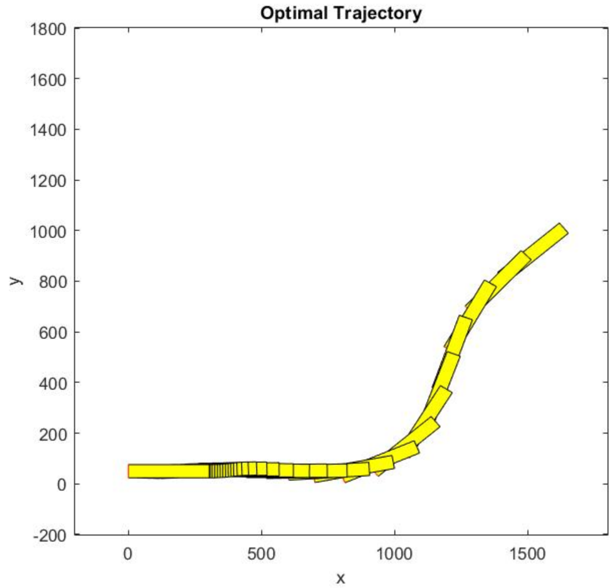

Figure A.107 Trajectory for berthing simulation of tanker ship using MPC with Kose's mathematical model: initial position of ship (-5L, 3L), initial heading angle of ship -40 degrees and initial speed of ship 3 m/s

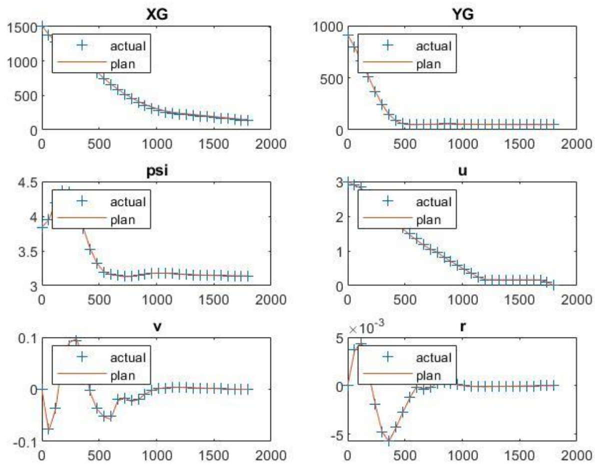

Figure A.108 X position XG, Y position YG, heading angle psi, surge velocity u, sway velocity v and yaw rate r for berthing simulation of tanker using MPC with Kose's model: initial position of ship (-5L, 3L), initial heading angle -40 degrees and initial speed 3 m/s

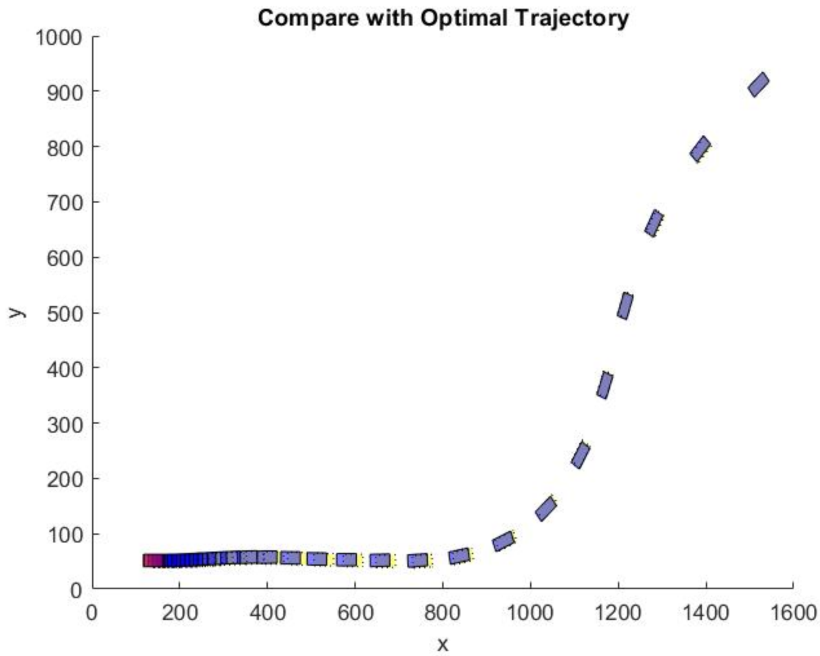

Figure A.109 Actual and optimal trajectories for berthing simulation of tanker ship using MPC with Kose's mathematical model: initial position of ship (-5L, 3L), initial heading angle of ship -40 degrees and initial speed of ship 3 m/s

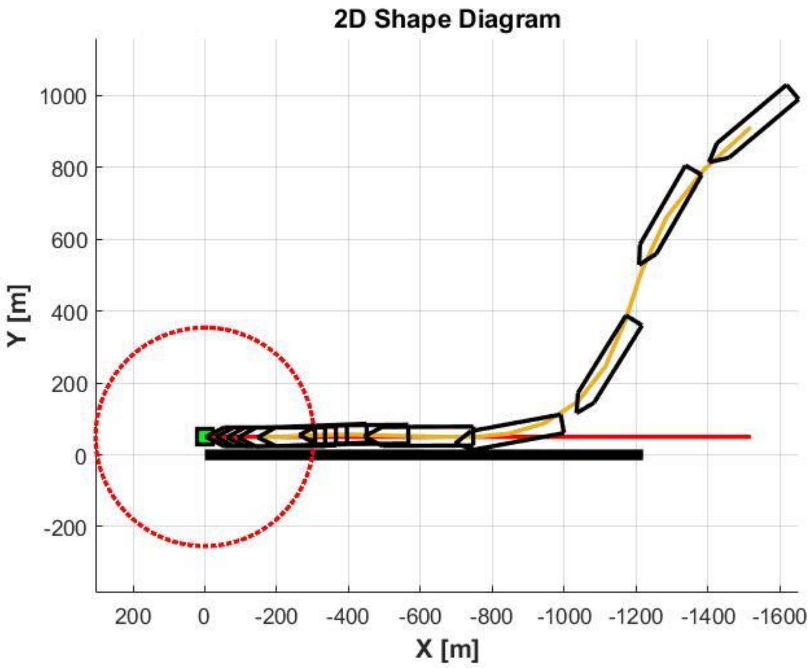

Figure A.110 Diagram for berthing simulation of tanker ship using MPC with Kose's mathematical model: initial position of ship (-5L, 3L), initial heading angle of ship -40 degrees and initial speed of ship 3 m/s